

STATE OF OREGON
DEPARTMENT OF GEOLOGY AND MINERAL INDUSTRIES
1005 State Office Building
Portland, Oregon 97201

OPEN-FILE REPORT O-83-3

SURVEY OF POTENTIAL GEOTHERMAL
EXPLORATION SITES AT
NEWBERRY VOLCANO, DESCHUTES COUNTY, OREGON

1983

edited by

George R. Priest, Beverly F. Vogt, and Gerald L. Black,
Oregon Department of Geology and Mineral Industries

This work was supported by the Bonneville Power Administration under
Cooperative Agreement No. DE-AC79-82BP36734.

Governing Board

Allen P. Stinchfield, Chairman, North Bend
Donald A. Haagensen, Portland
Sidney R. Johnson, Baker

State Geologist

Donald A. Hull

Deputy State Geologist

John D. Beaulieu

NOTICE

The views and opinions of authors expressed herein
do not necessarily state or reflect those
of the United States Government or any agency thereof.

Reference herein to any specific commercial product,
process, or service by trade name, mark, manufacturer, or otherwise,
does not necessarily constitute or imply its endorsement,
recommendation, or favoring by the United States Government
or any agency thereof.

NOTICE

The Oregon Department of Geology and Mineral Industries
is publishing this paper because the subject matter is
consistent with the mission of the Department.

To facilitate timely distribution of information,
this paper has not been edited to our usual standards.

CONTENTS

CHAPTER 1. EXECUTIVE SUMMARY, by George R. Priest	1
Introduction	1
Objectives	1
Methodology	1
Assumptions	2
Conclusions	2
Acknowledgments	4
CHAPTER 2. GEOLOGY OF THE NEWBERRY VOLCANO AREA, DESCHUTES COUNTY, OREGON, by George R. Priest	5
Introduction	5
General Geology	5
Results of USGS Drilling Program	10
Geophysical Evidence for a Shallow Intrusive	12
Distribution of Volcanic Centers: Implications for the Lateral Extent of a Silicic Intrusive Body	13
Caldera Geometry: Implications for Depths to Former Magma Chambers	14
Conclusions: Implications for Geothermal Exploration	18
CHAPTER 3. DISTRIBUTION OF VOLCANIC VENTS, by Gerald L. Black	21
Explanation	21
Distribution of Volcanic Vents	21
Interpretation Problems	23
Silicic Volcanic Centers Map	23
Causes of Vent Alignments	25
Map Interpretation	26
CHAPTER 4. NEWBERRY HYDROLOGY, by Gerald L. Black	28
Previous Work	28
Climate	28
Geology	29
Surface Hydrology	29
Ground-Water Hydrology	30
Summary	36

CHAPTER 5. THERMAL SPRINGS AND WELLS OF NEWBERRY VOLCANO, by Neil M. Woller	37
Introduction	37
Paulina Hot Springs	37
East Lake Hot Springs	37
Little Crater Campground Warm Well	39
Big Obsidian Flow Fumaroles	39
Geochemistry and Geothermometry of East Lake and Paulina Lake Hot Springs	39
Newberry 2 Drill Hole	42
 CHAPTER 6. PRELIMINARY SOIL-MERCURY SURVEY OF NEWBERRY VOLCANO, DESCHUTES COUNTY, OREGON, by George R. Priest, R. Mark Hadden, Neil M. Woller, and Chase B. Brand	 45
Introduction	45
Sampling Technique	45
Analytical Technique	49
Results	49
Interpretation	52
Introduction	52
Theoretical Geochemistry of Mercury at Newberry Volcano . . .	52
Effect of Shallow Ground-Water Circulation.	55
Background Concentrations of Mercury in Igneous Rock	56
Comparison with Mercury Data from Some Other Geothermal Resource Areas	58
Introduction	58
Concentrations of Mercury in Some Other Geothermal Resource Areas	60
Comparisons with Newberry	63
Conclusions	63
Influence of Bedrock Geology on Mercury Distribution	65
Conclusions	66
 CHAPTER 7. GRAVITY AND MAGNETIC INTERPRETATION OF NEWBERRY VOLCANO, by Andrew Griscom and Carter W. Roberts	 68
Introduction	68
Geology	68
Gravity Data	69
Magnetic Data	70

Densities of Samples from Newberry 1	70
Magnetic Properties of Samples from Newberry 1	71
Gravity Interpretation	72
General Magnetic Interpretation	77
Magnetic Interpretation of the Caldera Area	78
CHAPTER 8. THERMAL MODELS OF THE NEWBERRY VOLCANO, OREGON,	
by David D. Blackwell and John L. Steele	82
Introduction	82
Geology and Volcanic History	84
Geophysics	86
Characteristics of the Volcano	88
Thermal Models	92
Conduction Models	94
Convection Models	99
Discussion	111
CHAPTER 9. LAND USE AND REGULATION OF NEWBERRY VOLCANO,	
by Neil M. Woller	114
Introduction	114
National Forest Land Use Planning	114
Newberry Crater KGRA	115
Outside KGRA	115
Energy Facility Siting Council (ODOE)	117
Lease Applications	118
Private Lands	118
CHAPTER 10. RECOMMENDATIONS FOR GEOTHERMAL EXPLORATION,	
by George R. Priest, Gerald L. Black, and Neil M. Woller	119
Introduction	119
Exploration Strategy	119
Constraints on Possible Geothermal Models	120
Models that Meet the Constraints	123
General Considerations for a Drilling Program	124
Specific Drilling Recommendations	128
SELECTED REFERENCES	133

APPENDIX A. ANALYTICAL PROCEDURE FOR THE NEWBERRY MERCURY SURVEY	145
APPENDIX B. SOIL-MERCURY SURVEY ERROR ANALYSIS, by George R. Priest	150
APPENDIX C. DETAILED PLOTS OF CONVECTIVE HEAT-FLOW MODELS, by David D. Blackwell and John L. Steele	159

ILLUSTRATIONS

FIGURES

CHAPTER 2. Geology of the Newberry volcano area, Deschutes County, Oregon.	
2.1. Faults and volcanic vent alignments	6
2.2. Geologic map of Newberry caldera	8
2.3. Schematic cross section through Newberry volcano	9
2.4. Graph of vertical displacement caused by magmatic withdrawal from sill	15
CHAPTER 3. Explanation of the volcanic centers contour map	
3.1. Map of the distribution of volcanic centers, Newberry volcano, Deschutes, Klamath and Lake Counties, Oregon . .	22
3.2. Density distribution of silicic volcanic centers at Newberry volcano	24
CHAPTER 4. Newberry hydrology	
4.1. Elevation of the regional ground-water table in the Newberry volcano area.	33
4.2. Temperature-depth curve of the Newberry 2 drill hole	34
CHAPTER 5. Thermal springs and wells of Newberry volcano	
5.1. Locations of thermal springs and wells at Newberry caldera	38
CHAPTER 6. Preliminary soil-mercury survey of Newberry volcano, Deschutes County, Oregon	
6.1. Geologic structures and soil-mercury anomalies	46
6.2. Soil-mercury contour map	47
6.3. Histogram	50
6.4. Probability plot	51
6.5. Soil map of Newberry volcano	59
CHAPTER 7. Gravity and magnetic interpretation of Newberry volcano, Oregon	
7.1. Schematic cross section of Newberry volcano	72
7.2. Gravity profile A-A' across Newberry volcano showing possible form of regional gravity high	73
7.3. Aeromagnetic profile across Newberry volcano, Oregon	80

CHAPTER 8. Thermal modeling of the Newberry volcano	
8.1.	Generalized geology and topography of the Newberry volcano 83
8.2.	Topographic and hypothetical geologic section of Newberry volcano 89
8.3.	Temperature-depth curves for the Newberry volcano holes . 91
8.4.	Generalized topographic map of the Medicine Lake volcano in California 93
8.5.	True-scale cross section of the Newberry volcano showing various possible geometries for magma chambers . 94
8.6.	Normalized heat flow as a function of nondimensional length 96
8.7.	Surface heat flow generated by the conductive cooling of an instantaneous two-dimensional rectangular magma chamber 3 km wide, 3 km long, buried 3 km below the surface with an initial temperature of 800° C 97
8.8.	Isotherms corresponding to the times and heat-flow values shown in Figure 8.7. 98
8.9.	Heat flow generated by the instantaneous conductive cooling of a two-dimensional rectangular magma chamber 6 km wide, 3 km long, and buried at a depth of 3 km 100
8.10.	Isotherms corresponding to times and heat-flow values shown in Figure 8.9. 101
8.11.	Heat-flow values associated with the instantaneous conductive cooling of a two-dimensional rectangular magma chamber 10 km wide, 5 km thick, and buried at a depth of 5 km 102
8.12.	Isotherms corresponding to heat-flow values and times shown in Figure 8.11. 103
8.13.	Surface heat flow and subsurface temperatures for a two-dimensional rectangular magma chamber 3 km wide and buried 3 km deep 107
8.14.	Surface heat flow and subsurface temperatures for a two-dimensional rectangular magma chamber 6 km wide and buried 5 km deep 108
8.15.	Surface heat flow and subsurface temperatures for a two-dimensional rectangular magma chamber 10 km wide and buried 5 km deep 109
8.16.	Surface heat flow and subsurface temperatures for a two-dimensional rectangular magma chamber 10 km wide and buried 5 km deep 110
8.17.	Surface heat flow and subsurface temperatures for a two-dimensional rectangular magma chamber 15 km wide and buried 3 km deep 112

CHAPTER 10. Recommendations for geothermal exploration	
10.1. Schematic cross section through Newberry volcano	126
10.2. Suggested areas for four drill sites (A, B, C, and D) . .	130
10.3. Suggested sequence of drilling at four sites	132
APPENDIX A. Analytical procedure for the Newberry mercury survey	
A.1. Basic flow chart for Jerome 301 mercury testing	146
APPENDIX B. Soil-mercury survey error analysis	
B.1. Comparison of the low-temperature and high-temperature gold-film mercury measurements to atomic absorption determinations on the same samples	151
APPENDIX C. Detailed plots of convective heat-flow models	
C.1 through C.28 are untitled; see Table C.1 for parameters of each model	161

TABLES

CHAPTER 5. Thermal springs and wells of Newberry volcano

- 5.1. Chemical composition of thermal waters at Newberry volcano 40
- 5.2. Gas and isotopic composition of thermal waters of Newberry volcano 41
- 5.3. Geothermometer calculations 43
- 5.4. Preliminary flow test results on Newberry 2 drill hole . . 43

CHAPTER 6. Preliminary soil-mercury survey of Newberry volcano, Deschutes County, Oregon

- 6.1. Test pit data 48
- 6.2. Comparison of Newberry soil-mercury to mercury contents of some common igneous rocks 58
- 6.3. Comparison of mercury data from some geothermal resource areas 61

CHAPTER 8. Thermal modeling of the Newberry volcano, Oregon

- 8.1. Radiometrically dated volcanic units (data from MacLeod and others, 1982) 84

CHAPTER 9. Land use regulation of Newberry volcano

- 9.1. Summary of acreage by USFS leasing category 117

APPENDIX B

- B.1. Duplicate analyses of 50 Newberry volcano soil samples analyzed by atomic absorption spectrometry, utilizing total sample decomposition, by the low-temperature volatilization gold film method and by the high-temperature volatilization gold film method 152
- B.2. Regression data 154

APPENDIX C

- C.1. Parameters and ages for convective model results 160

PLATES

1. Map of the distribution of volcanic centers, Newberry volcano, Deschutes County, Oregon
2. Preliminary soil-mercury map of Newberry volcano, Deschutes County, Oregon
3. Generalized geologic map of Newberry volcano, Oregon
4. Complete Bouguer gravity anomaly map of Newberry volcano
5. Aeromagnetic map of Newberry volcano, Oregon
6. Interpretive geophysical map, Newberry volcano, Oregon
7. Calculated magnetic map of digital topographic model of Newberry volcano, Oregon
8. Newberry volcano lease plan map

CHAPTER 1
EXECUTIVE SUMMARY
by

George R. Priest,
Oregon Department of Geology and Mineral Industries

Introduction

Discovery of hydrothermal fluids at a temperature of 265° C at a depth of 932 m in the caldera of Newberry volcano (Sammel, 1981) has focused attention on this area as a potential producer of electrical energy from geothermal fluids. In order to gain a better understanding of the electrical power generation potential, Bonneville Power Administration (BPA) contracted with the Oregon Department of Geology and Mineral Industries (DOGAMI) for a study of the geothermal resources at Newberry volcano.

Objectives

The DOGAMI study was intended to summarize the current data, generate some new data, and recommend further steps which should be taken to investigate the electrical power production potential of the volcano. The Draft Land Management Plan for the Deschutes National Forest (see Chapter 9) designated the caldera and certain other areas off limits to geothermal leasing. It was therefore the objective of this study to concentrate on data from the developable flanks of the volcano.

Methodology

In order to investigate the potential for discovery of geothermal resources on the flanks of the volcano, the following steps were taken:

1. All previous data on the geology, hydrology, and geophysics were summarized.
2. A soil-mercury survey focused on the flanks of the volcano was conducted. Samples from 1,000 km² of the volcano were analyzed for mercury content.

3. All this information was utilized to evaluate (1) the likelihood of future discovery of electrical-quality geothermal fluids on the flanks, and (2) the most cost-effective means of improving the quality of available power generation estimates for the volcano.

Assumptions

The following basic assumptions were used in the report:

1. Faults, fractures, and volcanic rock units control the circulation of geothermal fluids in the volcano.
2. Shallow bodies of molten, partially molten, or solid but still hot rock are the heat sources for the geothermal system.
3. The above features have characteristic geophysical expressions (e.g., in seismic, gravity, magnetic, and heat-flow surveys).
4. Volatilization of mercury from geothermal (hydrothermal) systems can cause accumulation of anomalously high contents of adsorbed mercury in overlying soils. The mercury migrates upward through zones of high permeability and may be used as a guide to these zones.

Conclusions

Because no new drilling data are available, it is not possible to advance any new electrical power generation estimates for Newberry volcano from data examined in this study. On the basis of data from Newberry and other analogous areas, the USGS has estimated that the electrical power production potential of the caldera of the volcano is about 740 MWe for 30 years (Brook and others, 1979). The USGS discovery of fluids at 265° C (Sammel, 1981) prompted DOGAMI, at the request of the Pacific Northwest Utilities Conference Committee (PNUCC), to update the USGS estimate. Utilizing 265° C rather than the 230° C used in the 1979 USGS calculation, DOGAMI estimates that the electrical generation potential of the caldera is 1,116 MWe for 30 years (Black, 1982).

Both of the above estimates are very optimistic, because they assume that most of the caldera block is saturated with fluid. On the other hand, both are somewhat conservative in that neither considers the possibility of hydrothermal fluids outside of the caldera.

In order to put an upper limit on the potential resource at Newberry, Black (1982), utilizing the most optimistic estimate of the size of the underlying heat source, estimates that a maximum of 13,430 MWe for 30 years could be present at the volcano. This estimate includes the caldera and large areas on the flanks.

The present study investigated the source of heat for the geothermal systems at Newberry by analysis of geologic, teleseismic, gravity, aeromagnetic, and heat-flow data (Chapters 2, 7, and 8). These geologic and geophysical data indicate that a large, relatively shallow, mostly solidified magma body could underlie the summit of the volcano. However, none of these analyses conclusively proves this hypothesis. Under the most pessimistic interpretation of the data, only a few small silicic magma bodies may be present at shallow depths. These small bodies may have been the feeders to the Big Obsidian Flow and the young silicic domes on the uppermost southeast flank.

A soil-mercury survey conducted on the flanks and in the caldera of the volcano (Chapter 6) revealed that there is a very high probability that hydrothermal systems occur well outside of the caldera. The survey indicated that about 32 km² of the flanks and about 8 km² of the caldera possess anomalous soil mercury. The anomalies tend to correlate with concentrations of volcanic centers (Chapter 3) and major caldera faults and fracture zones. Soils near the discovery well in the caldera do not possess anomalous soil mercury, indicating that lack of a mercury anomaly does not preclude the presence of hydrothermal fluids at depth. Although the results of the mercury survey cannot yield quantitative estimates of the electrical generation potential of the volcano, they do indicate that thermal fluids may underlie large areas accessible to exploration on the east and south flanks of the volcano.

Utilizing a best and worst case argument for the geothermal model of the volcano, Priest (Chapter 10) concludes that the current data base puts very little real constraint on the electrical-generation potential of the volcano. With only one drill hole deep enough to directly test the system, the range of uncertainty reaches from a developable potential of essentially zero to a case approaching the 13,430 MWe estimate of Black (1982). Priest (Chapter 10) recommends further drilling as the only viable means of further constraining the estimates. An initial drilling program of three to four holes drilled to depths of about 1 km is recommended. The general areas for the sites and sequence of drilling are summarized on Figures 10.2 and 10.3 (see Chapter 10). The detailed arguments for this drilling program are given in Chapter 10.

Acknowledgments

This work was supported by the Bonneville Power Administration (Cooperative Agreement No. DE-AC79-82BP36734). The report would not have been possible without the invaluable advice and cooperation given by the U.S. Forest Service (USFS) and United States Geological Survey (USGS). Norman MacLeod of the USGS reviewed the report, provided extensive geological information, and led a field trip to the area. Edward A. Sammel of the USGS also reviewed the report. Larry Chitwood of the USFS graciously offered data on the hydrology and geology. We are particularly indebted to Andrew Griscom and Carter Roberts of the USGS, who provided the excellent paper on gravity and aeromagnetic measurements of Newberry volcano.

The USFS provided invaluable assistance by providing a base map for the soil-mercury survey, numerous other favors, and helpful advice. David Brown of the Oregon Department of Energy provided initial help with the mercury analytical technique. Al Waibel (Columbia Geoscience) and Eugene Ciancanelli (Cascadia Exploration Corporation) provided numerous references and advice for the soil-mercury survey.

CHAPTER 2
GEOLOGY OF THE NEWBERRY VOLCANO AREA,
DESCHUTES COUNTY, OREGON

by
George R. Priest,
Oregon Department of Geology and Mineral Industries

Introduction

Newberry volcano, about 40 km southeast of Bend, Oregon, is one of the largest volcanoes in the conterminous United States (Figure 2.1). The volcano covers an area of over 1,300 km² and has been the site of both silicic and mafic volcanism for many hundreds of thousands of years.

Recent mapping and drilling by the U.S. Geological Survey (USGS) at Newberry volcano have provided an excellent geological data base for this report. The volcanic and stratigraphic data in this report are abstracted entirely from MacLeod and others (1981, 1982) and MacLeod and Sammel (1982). Specific geological data mentioned here can be found in those papers. Radiometric data are from MacLeod and others (1982) and Fiebelkorn and others (1982). No attempt is made to duplicate the comprehensive geological reports; instead, structural and volcanic features relevant to geothermal resources are summarized along with current geophysical data. Geological data are taken from the above papers unless otherwise noted.

General Geology

Newberry volcano is located near the intersection of the Brothers fault zone and a broad, bow-shaped, northwest- to northeast-trending fault zone called the Tumalo-Walker Rim fault zone (Figure 2.1). The volcano is at the western end of a sequence of silicic volcanoes which began erupting about 10 m.y. B.P. in southeastern Oregon and which become younger to the west (see Figure 2 of MacLeod and others [1975]). The presence of intersecting faults and silicic volcanism should create ideal conditions for the production of high-temperature hydrothermal systems at Newberry. Because of their high viscosity, silicic magmas can form large, shallow plutonic bodies which can drive hydrothermal convection systems. Intersecting fault zones provide

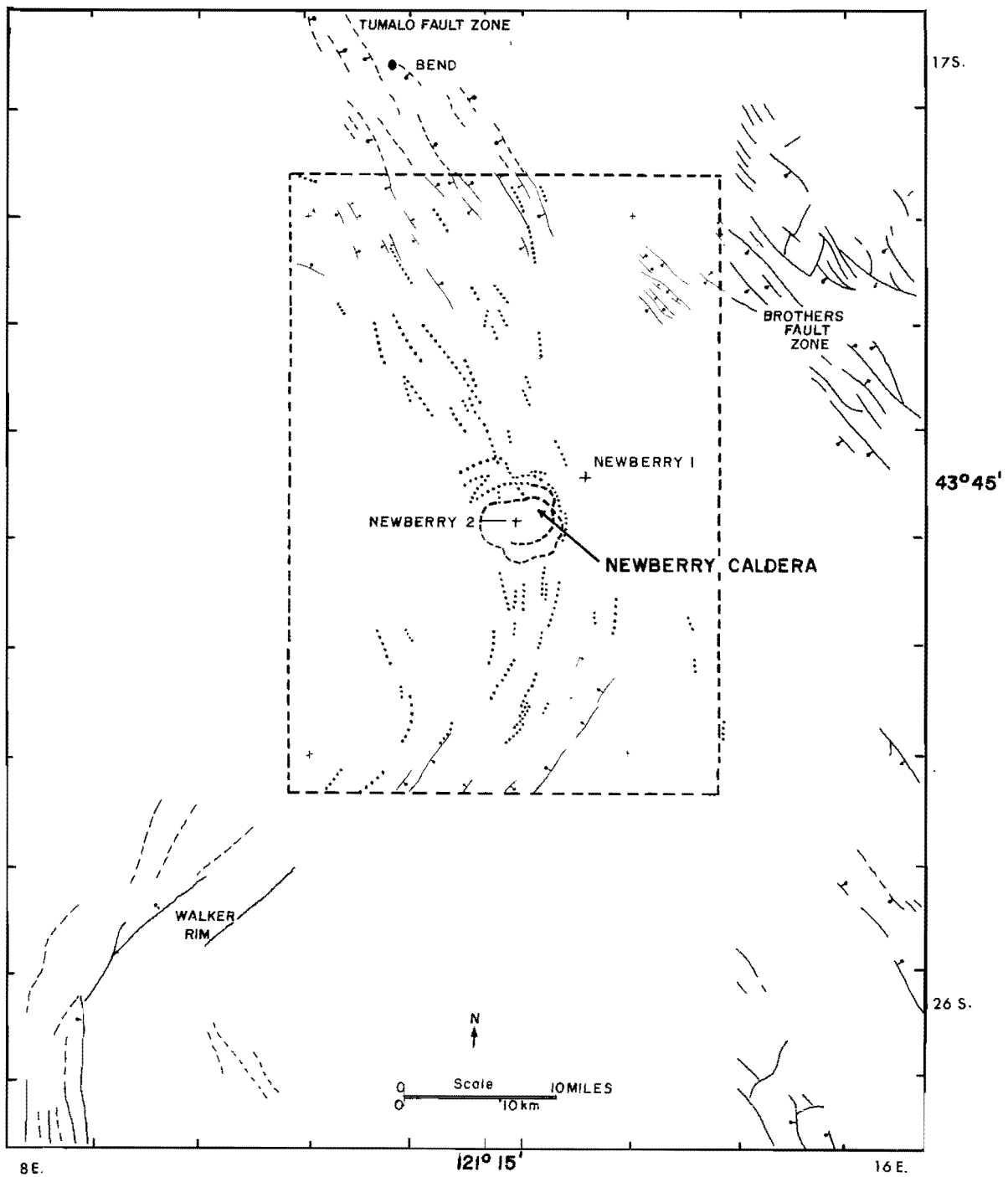


Figure 2.1. Faults and volcanic vent alignments. Crosses are USGS drill holes Newberry 1 and Newberry 2. Dashed rectangle outlines the geologic map of MacLeod and others (1982). Other data are from Wells and Peck (1961), Walker (1977), and Peterson and others (1976). Thin solid lines = faults; dotted lines = fissures and associated volcanic vent alignments.

enhanced permeability for thermal fluid circulation. The presence of fumaroles and hot springs in the caldera of the volcano and the recent USGS discovery (Sammel, 1981) of temperatures of 265° C at a depth of 932 m in a drill hole (Newberry 2) in the caldera confirm that the area has high geothermal potential (see Figure 4.2 of Black, this volume).

The volcano has a low shieldlike profile with a 6- to 8-km-wide summit caldera. The caldera was probably formed by repeated collapse of cylindrical blocks of crust into underlying shallow magma chambers following the explosive evacuation of silicic magmas. These eruptions produced large ash-flow and ash-fall deposits. The caldera-forming eruptions began about 510,000 yr B.P. and occurred repeatedly, with the most recent collapse event occurring several tens of thousands of years or more ago. Within the caldera, rhyolitic rocks dominate surface outcrops. These silicic rocks are chiefly younger than the Mazama ash layer which blankets the area. The Mazama ash has a carbon-14 date of 6,845 yr B.P. (Bacon, 1983), but carbon-14 dates of this magnitude are generally about 800 years younger than actual ages. The most recent eruption from the caldera occurred near the southern margin about 1,350 yr B.P. and produced the Big Obsidian Flow (Figure 2.2).

The flanks of the volcano include 95 percent of its total area and consist of basalt and basaltic andesite flows and andesite to rhyolite domes and flows. Rhyolites on the flanks have K-Ar dates of 100,000 to 600,000 yr B.P., although some may be younger. Small rhyolitic domes on the upper southeast flank may be less than 10,000 years old. The mafic volcanic rocks are probably all younger than 700,000 years, based on magnetic polarity; the youngest are about 6,000 years old.

Most of the volcanic vents cluster in a northwest- to northeast-trending arc which parallels the Tumalo and Walker Rim fault zones (Figures 2.1 and 3.1). The higher elevations of both the north and south flanks relative to the east and west flanks are caused by this clustering of vents and their related flows (Figure 2.3). A lesser clustering of somewhat older vents parallels the west-northwest-trending Brothers fault zone. The silicic vents are clustered in the caldera, with small lobes of vent complexes on the northeast, the south, and west-southwest flanks (see Black, Chapter 3, Figure 3.2). The distribution of mafic vent areas is thus much more strongly controlled by the regional fault zones than is the distribution of silicic centers.

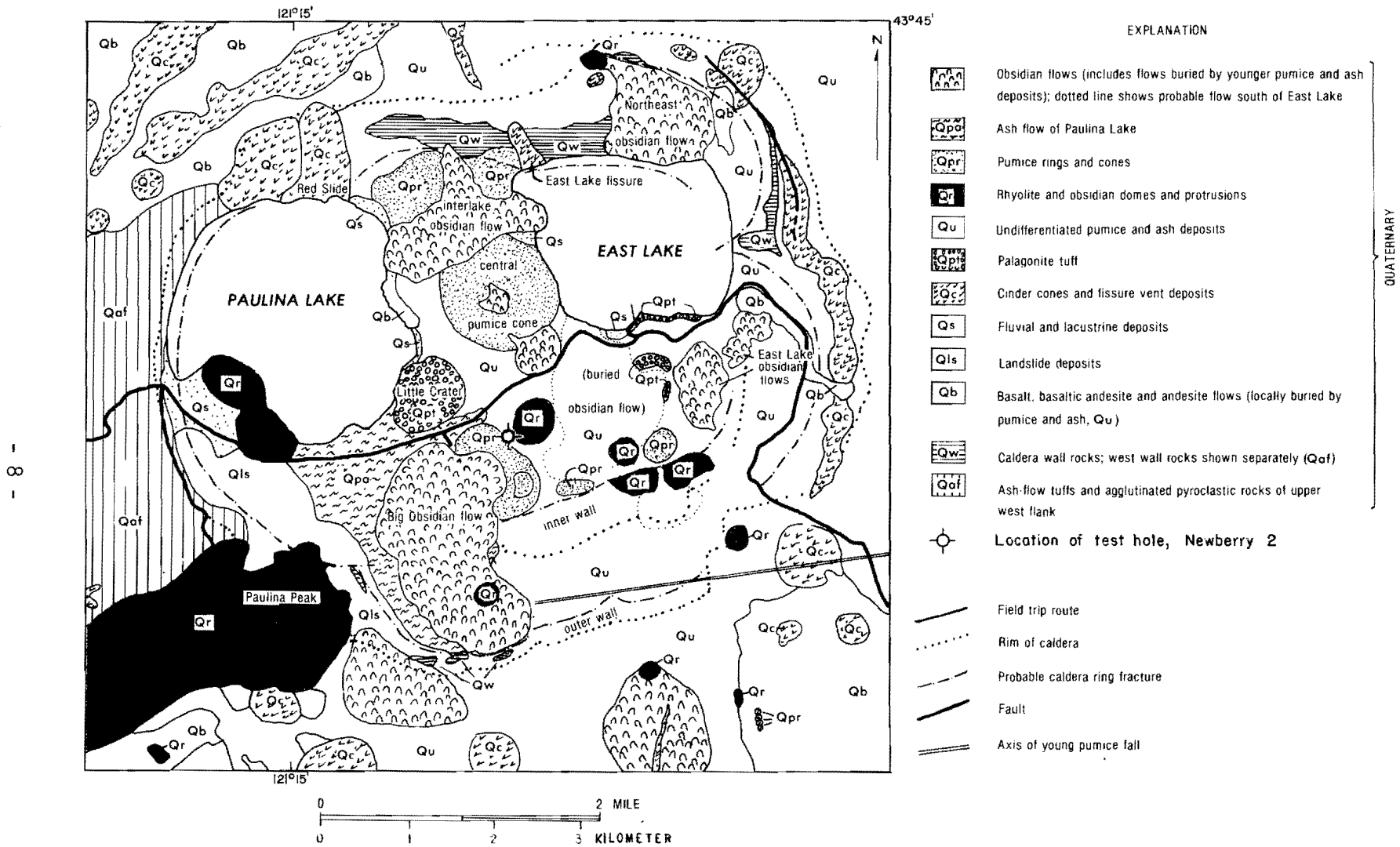


Figure 2.2. Geologic map of Newberry caldera (taken from MacLeod and Sammel, 1982).

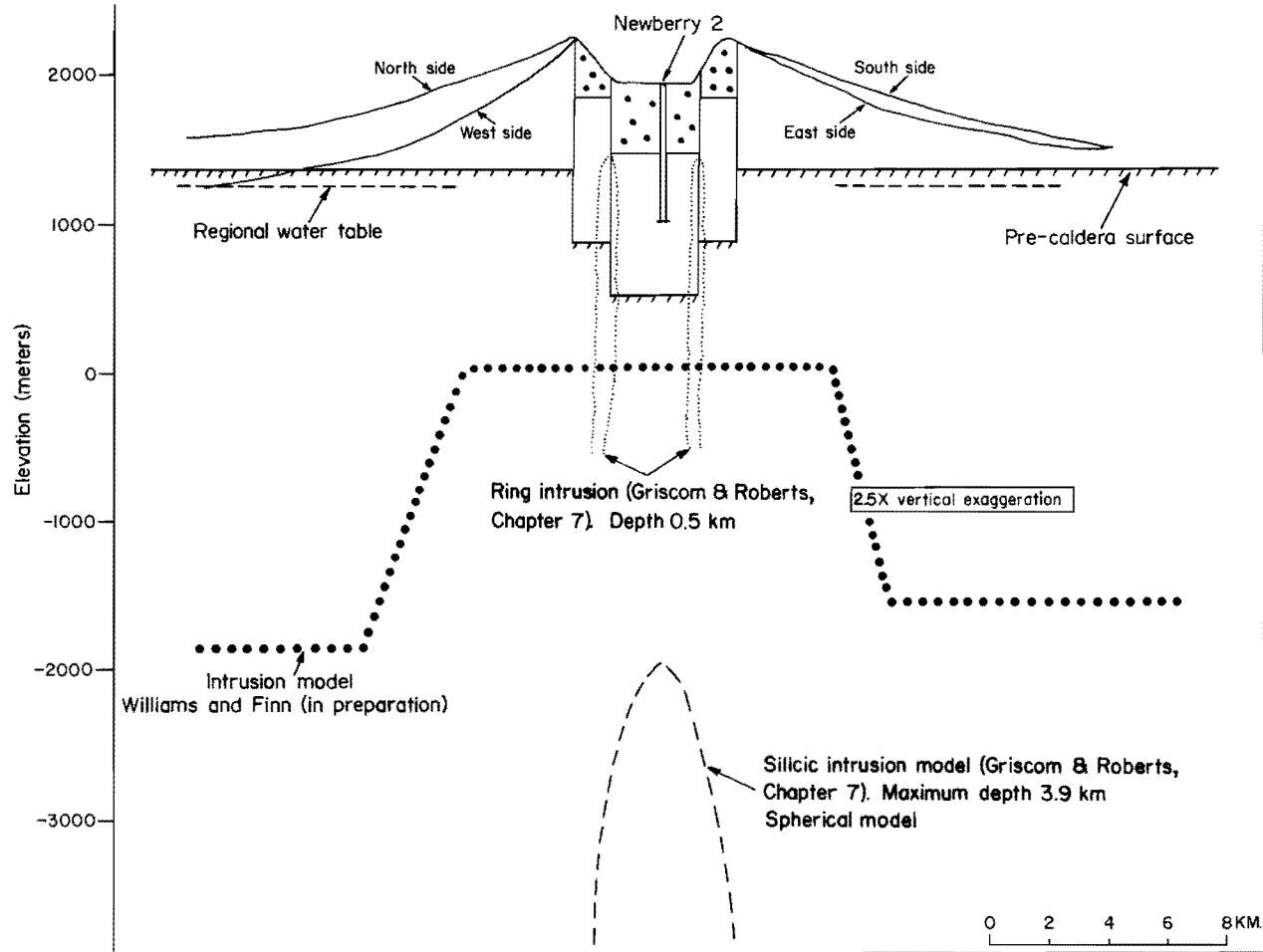


Figure 2.3. Schematic cross section through Newberry volcano. Topographic profiles taken from Blackwell and Steele (Chapter 8); geology taken from MacLeod and Sammel (1982); regional ground-water table inferred from data of L. Chitwood.

Results of the USGS Drilling Program

The USGS has drilled two diamond drill holes on Newberry volcano. The first, Newberry 1, was drilled in 1977 on the northeast flank to a depth of 386 m (Figure 2.1). A second hole, Newberry 2, was drilled during 1979 and 1981 to 932 m. It is located in the caldera near the vent of the Big Obsidian Flow (Figures 2.1 and 2.2). The Newberry 1 hole did not penetrate below shallow perched aquifers and encountered no thermal fluids. The Newberry 2 hole probably penetrated the regional ground-water table (Black, Chapter 4) and encountered high-temperature fluids (265° C) in the lowest 2 m of the hole (see Figure 8.3 for temperature logs of Newberry 1 and 2).

The lithologic data from Newberry 2 well indicate that the lacustrine sediments occur at a depth of 300 m, implying that fragmental rocks occurring above that depth are fill in a caldera which was once as deep as the Crater Lake caldera. Pumice lapilli and breccia 130 m thick occur below the lake sediments and above lavas which appear to be downdropped equivalents of flank flows. The lapilli and breccia probably represent some of the material erupted during the collapse of the caldera block. The thickness of the lavas below the lapilli and breccia is estimated to be at least 90 m, based on the thickness of the same flows in the surrounding volcanic edifice.

In their analysis of the fluids, temperatures, and rocks encountered in the test wells at Newberry, MacLeod and Sammel (1982) conclude the following:

1. Zones of high lateral permeability are common in the upper 758 m of the Newberry 2 caldera well and within many parts of the Newberry 1 flank well.
2. Below 758 m in the Newberry 2 well, permeable zones are few in number, although gas and hydrothermally altered strata were encountered. This section is dominated by mafic flows.
3. Fluids collected in a 20-hour flow test from the bottom 2 m of the hole (Sammel, 1981) were originally thought to be drilling fluids and volcanic gases (MacLeod and Sammel, 1982). Recent chemical and isotopic analyses of the recovered fluids indicate that they are definitely at least partly formation fluids (Ed Sammel, personal communication, 1983). For more detailed information on hydrology, see Chapter 4.
4. Vertical permeabilities are low in the caldera fill, as well as in the collapsed caldera block.

5. Vertical circulation of thermal and nonthermal waters is probably restricted to faults, ring fractures, and brecciated intrusion conduits.
6. Lateral circulation is probably confined to those stratigraphic layers with good hydraulic connections to water-bearing vertical fracture zones.
7. Preliminary analysis of the heat flow from the Newberry 2 well indicates that if the heat flux represents a widespread, long-lasting thermal regime, the magmatic heat source would likely have a diameter of several kilometers and would have been continuously supplied with magma for a period of thousands of years prior to the most recent (1,350 yr B.P.) eruption.
8. The most recent rhyolitic eruptions from within the caldera and on the upper southeast flank of the caldera form a chemical group which differs in composition from older silicic domes and flows on the flanks. The young rhyolites are essentially aphyric and have closely similar compositions. This suggests that they are from the same magma chamber, and that the chamber was at or above the liquidus (melting point of the most refractory mineral component) as recently as 1,350 yr B.P. Liquidus temperatures of rhyolites are typically in the vicinity of 800° C.
9. If the heat flux in the Newberry 2 well is representative of the flux over the caldera during the last 1,350 years, then much of the magma in a 3-km-wide chamber could have solidified.
10. If the high temperature gradient between 860 and 930 m in the Newberry 2 hole (505° C/km) can be projected to a depth of 1.4 km below the caldera floor (the base of the collapsed block), then temperatures at the base would be about 500° C.
11. Below the base of the collapsed caldera block, possible fracturing and faulting from intrusive activity in the pre-Newberry rocks may cause enhanced vertical permeability. This would promote hydrothermal convection in the older rocks.

Geophysical Evidence for a Shallow Intrusive

A large gravity anomaly centered on Newberry caldera has been modeled by Williams and Finn (1981b) and Griscom and Roberts (Chapter 7) as an intrusive mass lying 2 to 4 km beneath the surface (Figure 2.3). Teleseismic data indicate that individual molten bodies greater than 3 km in diameter do not exist within the pluton (Iyer, oral communication to MacLeod and Sammel, 1981, in MacLeod and Sammel [1982]), but Griscom (Chapter 7) suggests that because the pluton has no magnetic expression on an aeromagnetic map, it may be hotter than about 580° C (the Curie-point temperature for magnetite). Griscom (Chapter 7) also suggests that a ring-shaped intrusion may lie within the caldera ring faults (Figure 2.3). This intrusion also lacks magnetic expression and may be hotter than 580° C. It must be noted that an absence of magnetic expression might also be caused by alteration effects or, as in the case of the silicic dome at Paulina Peak, a lack of magnetic susceptibility rather than high temperature.

Whereas there is general agreement that a shallow plutonic body underlies Newberry caldera, the size and shape of the intrusion are not well constrained. Williams and Finn (1981b) estimate from gravity data that the body could be about 10 to 12 km in diameter at its top and about 2 km below the caldera floor. Their model assumes outward sloping sides of the body which, at a depth of about 4 km, has a diameter of about 17 to 22 km (Figure 2.3). Griscom and Roberts (Chapter 7) estimate that a spherical pluton could have a diameter of between 11.7 and 13.4 km, with a depth to the top of the body of 3 to 4 km (Figure 2.3). Griscom and Roberts (Chapter 7) point out that the assumption of a more tabular shape results in shallower calculated depth to the top of the pluton. In all models it is clear that, if a large plutonic body underlies the volcano, it is considerably wider than the 6- to 8 km-wide caldera.

It is important to point out that the gravity anomaly at the summit of the volcano could be caused by something other than a shallow silicic intrusion. The density contrasts assumed in the models (0.2 to 0.3 g/cm³) between the volcanic rocks and the intrusive rocks could be caused by loss of porosity associated with hydrothermal alteration. Likewise, the data could be modeled using a mafic rather than a silicic intrusion. However, regardless of these alternative models, the shallow silicic pluton hypothesis is strongly supported

by the abundant silicic volcanic rocks. A shallow pluton is also indicated by teleseismic data which indicate a "large compressional-wave velocity contrast in the area, with higher velocities localized under the caldera" (Mahadeva Iyer, oral communication, 1981, to MacLeod and Sammel, 1982).

Regional heat flow studies indicate that a zone of very hot to partially molten rock lies at depths of 7 to 10 km in the High Cascade Range (Blackwell and others, 1978, 1982b). Background heat flow at Newberry may approach the values measured adjacent to the High Cascade Range, which implies that a similar partially molten zone could occur at 7 to 10 km depth over wide areas around the volcano (Blackwell and Steele, Chapter 8). This interpretation is consistent with interpretations of the regional seismic data (Iyer and others, 1982), the Curie-point isotherm depth of 6 km estimated from aeromagnetic data (Couch, 1979), and regional magnetotelluric studies (Stanley, 1982). Blackwell and Steele (Chapter 8), in a more detailed discussion of these regional geophysical studies, conclude that a logical maximum depth to partially molten rocks at Newberry is about 10 km.

Distribution of Volcanic Centers: Implications for the Lateral Extent of a Silicic Intrusive Body

The distribution of silicic and mafic volcanic centers should provide clues about the lateral extent of the plutonic complex inferred from the geophysical evidence. The higher density of mafic magma relative to silicic magma should inhibit ascent of mafic magmas through silicic magma chambers. The concentration of mafic volcanic vents on the flanks of the volcano is much higher than at and immediately adjacent to the caldera (Figure 3.1). Silicic volcanic rocks ranging in age from about 6,700 to 1,350 years cover the eastern two-thirds of the caldera (MacLeod and Sammel, 1982). These youngest silicic rocks, together with some young (probably less than 10,000 years) silicic domes on the uppermost southeast flank, form a geochemical group significantly different from older rhyolites (MacLeod and Sammel, 1982). The most recent basaltic eruptions have occurred outside of the zone of recent silicic volcanism, probably because there is a shallow silicic magma preventing rise of the basalts to the surface. A roughly circular area about 3 to 4 km in diameter would enclose the youngest silicic vents, and this would be a logical diameter for a still-hot underlying silicic

magma body (e.g., see Blackwell and Steele, Chapter 8).

This diameter of 3 to 4 km is significantly smaller than has been inferred from the distribution of older silicic rocks on the flanks of the volcano. Six chemically distinct groups of silicic volcanic centers have been recognized, and the lateral separations between volcanic centers within each group is as much as 18 km (MacLeod and Sammel, 1982). This distance is similar to the diameter of the 4-km-deep plutonic body modeled from gravity data by Williams and Finn (1981b) and is similar to the diameter (11.7 km to 13.4 km) of the spherical silicic magma body modeled from the same data by Griscom and Roberts (Chapter 7). The diameter of the crudely circular area covered by the 5 centers/1 percent-area contour on the silicic volcanic center map (Figure 3.2) is about 10 km (Black, Chapter 3).

The above data are consistent with the presence of a composite silicic pluton about 18 km in diameter which has developed over the life of the volcanic center. The last intrusion of material into the composite pluton was probably about 3 to 4 km in diameter and probably occurred during the last 10,000 years under the southeastern part of the caldera.

Although the above discussion strongly suggests that a shallow plutonic complex underlies the volcano, there is no information in the data on the depth to the intrusives. The next section will explore some possible geologic constraints on the depth to caldera-forming magma chambers at Newberry.

Caldera Geometry: Implications for Depths to Former Magma Chambers

One question worth pursuing is whether the presence of a complex caldera with several overlapping ring fault systems at Newberry volcano suggests that magma bodies have ascended to relatively shallow crustal levels. Does the geometry of the caldera give clues about the depth and size of the underlying plutons which caused subsidence of the cauldron block? Answers to these questions might elucidate the nature of possible plutons which have been postulated from geophysical evidence.

The writers were not able to find an adequate quantitative, three-dimensional model for the cauldron subsidence process. Anderson's (1936) work shows the pattern of subsurface faults but does not give an adequate three-dimensional treatment. A three-dimensional model for surface deformation caused by magmatic withdrawal from a basaltic sill was worked out by Ryan and others (1983) for the Hawaiian volcano Kilauea (Figure 2.4). It is apparent

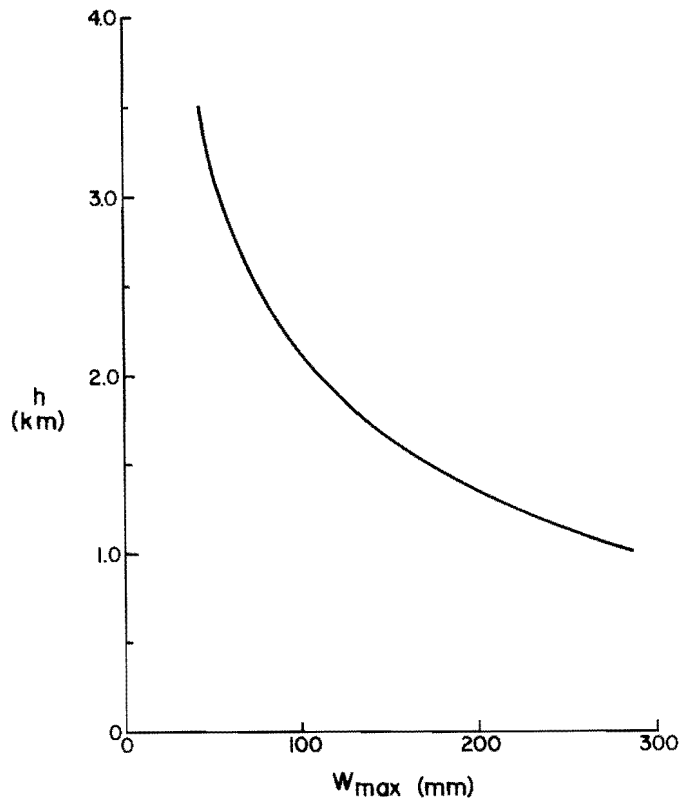


Figure 2.4. Graph of the maximum vertical displacement (W_{max}) caused at the surface by complete magmatic withdrawal from a basaltic sill 1 m thick at various depths (h). The sill has a half width of 500 m. Data are for Kilauea, Hawaii, and are from Table 2 of Ryan and others (1983).

from Figure 2.4 that the surface effects of magmatic withdrawal fall off very sharply with increasing depth. There should be, therefore, some limiting depth below which magmatic withdrawal cannot cause cauldron subsidence.

The width of a subsided cauldron block must also be directly related to the width of the underlying magma chamber. It also seems apparent that a large magma chamber could cause a large amount of subsidence at the surface, even if it were deeply buried, whereas the opposite is true of small chambers. An example would be the quantitative model of Ryan and others (1983) for Kilauea. In their model, a sill lying at a depth of 2.2 km, with a width of 1 km, a thickness of 1 m, and a length of 1.4 km, could cause a maximum of about 49 mm of vertical displacement if all magma were withdrawn. Leaving other dimensions the same, increasing the length of the sill from 1.4 km to 10 km caused a

maximum vertical displacement of about 145 mm, and the zone of surface deformation was spread over a much wider area than in the first case. These calculations suggest that the areal extent and vertical displacement of a cauldron block may give some indication of the depth of burial and size of the underlying magma chamber. However, the above models assume that subsidence occurs by small increments of deformation over a wide lateral extent rather than by caldera block faulting. They are not, therefore, completely applicable to calderas.

Another approach to the problem is to compare the depths of known magma chambers to their associated caldera dimensions. Unfortunately, only two calderas-- Long Valley in California and Yellowstone in Wyoming-- are sufficiently well studied to allow such comparisons.

Long Valley caldera is one of the only active volcanic centers for which relatively definitive data on the depth to the caldera-forming magma chamber are available. About 0.7 m.y. B.P., a 600-km³ ash-flow eruption caused a cauldron block 32 km long and 17 km wide to subside about 3,000 m (Bailey and others, 1976). Hildreth and Spera (1974), utilizing microprobe data, estimate that the top of the caldera-forming magma chamber lay at a depth of about 6 km. About 0.6 m.y. B.P., the magma moved upward to between 5 and 2 km (Bailey and others, 1976). Since that time the chamber has crystallized downward, and partially molten zones are now largely below about 7 to 8 km (Steeple and Iyer, 1976).

The Yellowstone caldera is a 70-km-long by 45-km-wide depression which formed as a result of three large ash-flow eruptions at 2 m.y. B.P., 1.2 m.y. B.P., and 0.6 m.y. B.P. (Christiansen and Blank, 1972). Iyer and others (1981), utilizing teleseismic data and the Curie-isotherm depth from Bhattacharyya and Leu (1975), estimate that the partially molten magma body currently underlying Yellowstone caldera is of about the same width as the caldera and lies at a depth of about 10 km.

If there is some relationship between depth to magma and the size of the overlying caldera, then the ratios of the caldera dimensions (length = ℓ ; width = w) to the depth (d) of the underlying magma chambers at Long Valley and Yellowstone may give clues to similar ratios at Newberry. For Yellowstone, the caldera dimensions give the ratios $\ell/d = 7.0$ and $w/d = 4.5$; for Long Valley the same ratios are $\ell/d = 5.3$ and $w/d = 2.8$. The aspect ratio (w/ℓ)

of Yellowstone is 0.64, and for Long Valley it is 0.53; for Newberry, however, it is close to 1.0 (circular). It is apparent that there is no constant ratio of the dimensions of the calderas to the depths to underlying magma chambers, but the smaller Long Valley chamber is shallower than the larger Yellowstone chamber. This may not be a legitimate comparison, because the greater depth of the Yellowstone chamber may be partly caused by downward crystallization since the last caldera-forming eruptions. No estimate is available for the depth of the Yellowstone chamber at the time of the last eruption 0.6 m.y. ago.

The Long Valley chamber congealed inward and downward about 4 km between 6.6 and 0.2 m.y. B.P. (Bailey and others, 1976). Assuming a similar crystallization and cooling rate at Yellowstone, the chamber top 0.6 m.y. ago could have been as shallow as 4 km. This cooling rate is, however, probably too high, and the estimated depth too shallow, because the Yellowstone pluton, because of its larger size, would have cooled more slowly than the Long Valley pluton (e.g., see heat-flow models of Blackwell and Steele, Chapter 8). The depths to the caldera-forming Yellowstone and Long Valley plutons could thus have been similar (about 6 km), although there is no definitive proof of this.

The above argument suggests that the depths to the caldera-forming silicic magma chambers at Yellowstone and Long Valley are dependent on some factor other than the size of the pluton. Assuming that silicic magmas are not far above their liquidus temperatures, the most important constraints on the final depth of intrusion are probably the density contrast between magma and country rock and the volatile content. A high density contrast would make the magma more buoyant, and a high volatile content would, as the magma rose, cause crystallization at great depth as the volatiles boiled off.

If the above speculations are correct, and if it is assumed that the density contrast and volatile content of the caldera-forming Newberry magma were similar to those of the silicic plutons at Yellowstone and Long Valley, then the depth to the caldera-forming magma chamber at Newberry could have been about 6 km. Using Long Valley as an analogue, a composite pluton at Newberry could have developed over the history of the volcano by repeated injections of silicic magma between about 6 and 2 km. These estimates are similar to the 2- to 4-km depths of the Newberry pluton inferred by Griscom and Roberts (Chapter 7)

and Williams and Finn (1982).

To summarize, it is clear from theoretical considerations that magmatic withdrawal is less able to cause surface displacements as the depth of burial becomes greater. Although no quantitative model for caldera-forming processes is available, it is probably reasonable to assume that there is some limiting depth below which the forces generated from magmatic withdrawal cannot cause ring faulting and cauldron subsidence at the surface. Without a quantitative model for cauldron subsidence, the limiting depth is unknown, although it must, as demonstrated by the Kilauea modeling, increase as the size of the magma body increases. For the large magma chambers at Long Valley and Yellowstone, which caused calderas over 2.5 times larger than the Newberry caldera, the estimated depth of 6 km to the underlying chambers was far less than the limiting depth. The small aspect ratios of these large calderas (0.53 to 0.64) also suggest that the depth to magma was very shallow relative to their capacity to cause deformation at the surface (according to Ryan and others, 1983, the aspect ratio of surface depressions is inversely proportional to the depth of the causative low-aspect magma bodies). Without an adequately studied caldera-magma chamber system of about the same dimensions as occur at Newberry, it is not possible to make convincing geometric arguments for the depth to the magma chamber. It may be that the depths of 2 to 6 km estimated by Bailey and others (1976) for the Long Valley chamber at various stages in its evolution are similar to what may be expected for silicic magmas at other ash-flow centers. If so, then the plutonic complex at Newberry may also lie at these depths.

Conclusions: Implications for Geothermal Exploration

The total area of silicic intrusive activity probably has a diameter of about 18 km and extends at least a few kilometers outside of the caldera. This large silicic intrusive complex probably lies at depths of about 2 to 6 km and has been emplaced chiefly during the last 510,000 years. Although no molten zones larger than about 3 km are probably present in the complex, repeated intrusions of magma could have kept the composite pluton at temperatures higher than the regional background heat flow would predict. The most likely location for intrusives which are still molten is in the southeast part of the caldera and uppermost southeast flank.

It is possible that faults, particularly the Tumalo-Walker Rim and Brothers zones, and caldera ring fractures may allow vertical circulation of geothermal fluids within Newberry volcanic rocks. Probable plutons beneath the caldera that are possibly still at high temperature (i.e., over 580° C) should provide the necessary heat to drive hydrothermal circulation.

Vertical circulation may also be possible in pre-Newberry rocks where intrusions have caused brecciation and faulting. Such systems would be limited to areas where extensive intrusion has taken place. If the distribution of surface silicic vents is a good guide to zones of extensive intrusion at depth, then the summit caldera and the small clusters of silicic volcanic centers which extend up to 4 km away from the caldera on its southwest, southeast, and northeast margins may be good exploration sites.

The intruded pre-Newberry rocks should be closer to the surface beyond the caldera than they are within the caldera. In the caldera about 500 m of intracaldera fill and 900 m of Newberry lavas in the collapsed block must be penetrated to reach pre-Newberry rock. Outside the caldera, a maximum of about 900 m of flank flows must be penetrated before encountering the older rocks.

Whereas vertical permeability may be locally higher in the pre-Newberry rocks, it is by no means certain that the overall permeability within the pre-Newberry rocks is greater than in the overlying rocks. Some factors which could lead to low permeability in the older rocks include the following:

1. Hydrothermal alteration from the current and older hydrothermal systems.
2. Resealing of fractures by continued magma injection.
3. High confining pressure which would tend to close open fractures.

It would probably be wise to aim exploration efforts at areas where there are both faulting and high density of young silicic volcanic centers. Domes and flows of youthful rhyolites (unit Qyr of MacLeod and others [1982]) occupy an area where the Walker Rim fault zone merges with or intersects the caldera ring-fracture system. This area may have an unusually high vertical permeability within drillable depths. Likewise, thermal waters may migrate laterally from this area toward the southwest along the dike and fault zones of the Walker Rim system. The large soil mercury anomalies over these zones may indicate the presence of both permeability and hydrothermal

circulation (Priest and others, Chapter 6).

The caldera ring-fracture systems should be excellent targets. These areas are probably the foci of both magmatic and hydrothermal circulation. Griscom and Roberts (Chapter 7) conclude from analysis of magnetic and gravity data that the ring-fracture/fault system may be intruded by plutonic rocks with temperatures of over 580° C. All of these faults, where not sealed by deposition of alteration minerals, should provide vertical conduits for circulation of thermal waters. These same waters could also spread out into shallow subhorizontal aquifers within and outside the caldera. The soil-mercury anomalies on the southeast and north caldera ring fractures may indicate the presence of zones of high vertical permeability (Priest and others, Chapter 6).

CHAPTER 3
DISTRIBUTION OF VOLCANIC VENTS

by

Gerald L. Black

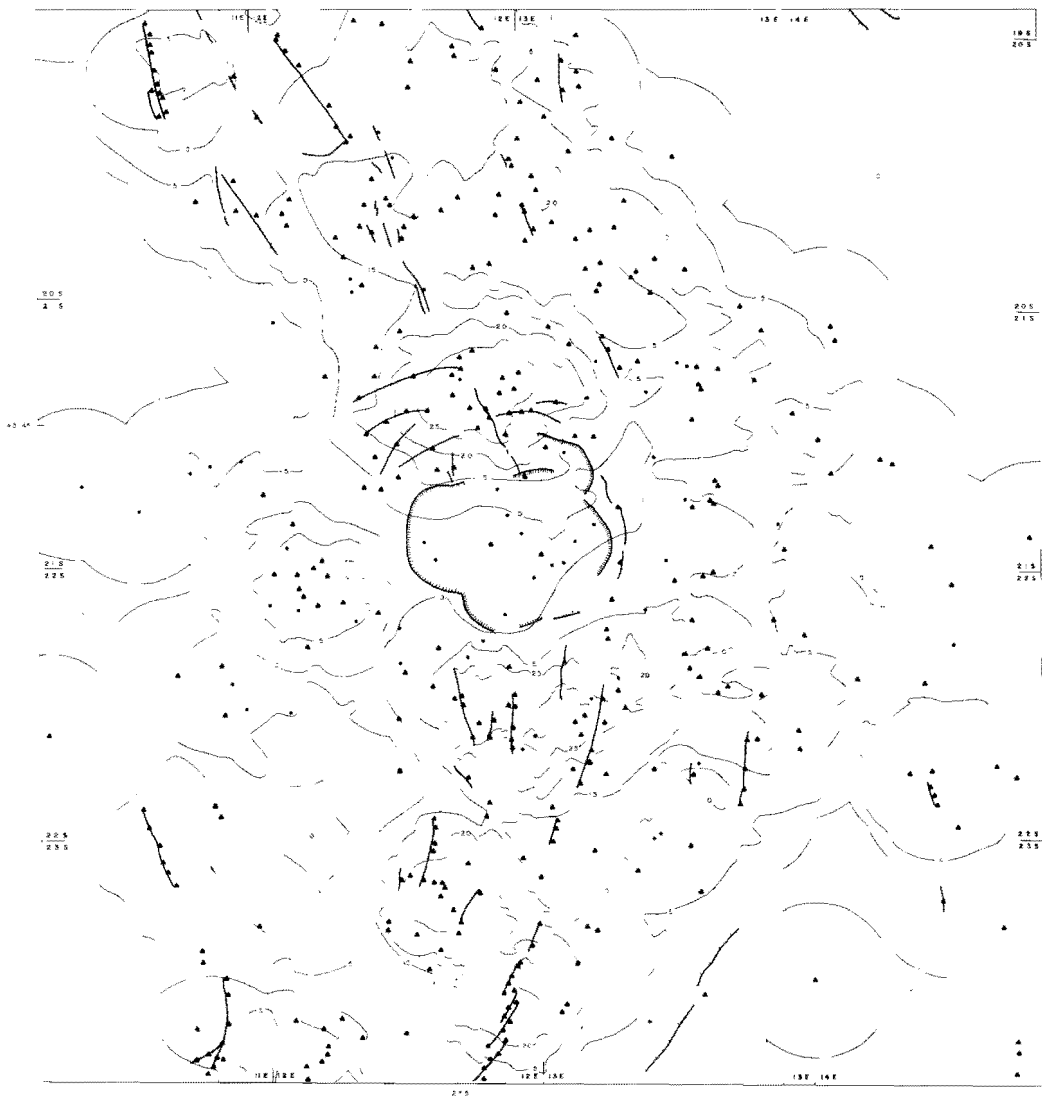
Oregon Department of Geology and Mineral Industries

Explanation

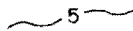
The volcanic centers map (Figure 3.1 and Plate 1) shows the density distribution of volcanic centers on Newberry volcano. Shown on the map are contours representing the numbers of volcanic centers/1-percent area and the locations of silicic volcanic centers, mafic volcanic centers, faults, ring fractures, and fissure vents. The contours are constructed so that a circle that encompasses an area equivalent to 1 percent of the total map area and that is centered on any point between the 20 and 25 volcanic centers/1-percent-area contours will enclose between 20 and 25 volcanic centers. Contours are drawn at 1, 5, 10, 15, 20, and 25 volcanic centers/1-percent area.

Distribution of Volcanic Vents

The volcanic centers map uses as a base the geologic map of MacLeod and others (1982) and was constructed using methods similar to those described by Turner and Weiss (1963) for contouring the distribution of points on equal-area nets. As a first step, the surface area covered by the geologic map was determined, and a circular template was constructed with the area of the circle representing 1 percent of the total area of the geologic map. A circle was inscribed around each volcanic center, and the resulting network of overlapping circles was contoured. Areas enclosed by five overlapping circles thus represent 5 centers/1-percent area, areas enclosed by 10 circles represent 10 centers/1-percent area, and so on. The very complex contours generated by the above process were then hand smoothed to simplify reading and interpretation of the resulting map.



Legend

- 
 Contours indicate numbers of volcanic centers per 1% area (of geologic map of MacLeod and others, 1982)
- 
 Mafic volcanic centers
- 
 Silicic volcanic centers
- 
 Ring fractures
- 
 Faults
- 
 Fissures

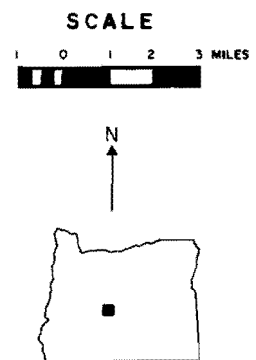


Figure 3.1. Map of the distribution of volcanic centers, Newberry volcano, Deschutes, Klamath, and Lake Counties, Oregon.

Interpretation Problems

Volcanic centers which occur outside the map at a distance of one radius (of the circular template) or less from the map edge were not used in the construction of the map. Therefore, there is a one-radius-wide band along the edge of the volcanic centers map which does not accurately represent the distribution of volcanic centers. The volcanic centers map has been cropped so that it covers the same area as the soil-mercury survey. The edge effect described above is therefore present only along the east and west edges.

Each center, regardless of size, was given equal weight. Where a series of vents was aligned along a fissure, a circle was drawn around each individual cinder cone. In the case of fissure-type eruptions where eruptions occurred simultaneously along the entire length of the fissure, only one circle centered on the middle of the fissure was drawn. Thus some fissures of a given length were considered to contain several vents, whereas others of identical length were considered as only one vent, and the map is weighted toward areas where discrete vents are located along fissures.

No attempt was made to take into account the periodicity of eruptions at any one center. As a result, the volcanic centers map does not accurately reflect the amount of volcanic activity that has occurred at some locations. This is particularly true for the summit caldera, which shows up as a low of only 10-15 centers/1-percent area on the volcanic centers map but which has obviously been the focus of volcanic activity for a considerable period of time, with younger deposits burying older vents.

Silicic Volcanic Centers Map

The density of silicic volcanic centers in the vicinity of Newberry volcano is shown on Figure 3.2. The same limitations which applied to the composite volcanic centers map also apply to the silicic volcanic centers map, though in the latter case, the edge effect is not a significant problem because the density of silicic centers is low near the map margins.

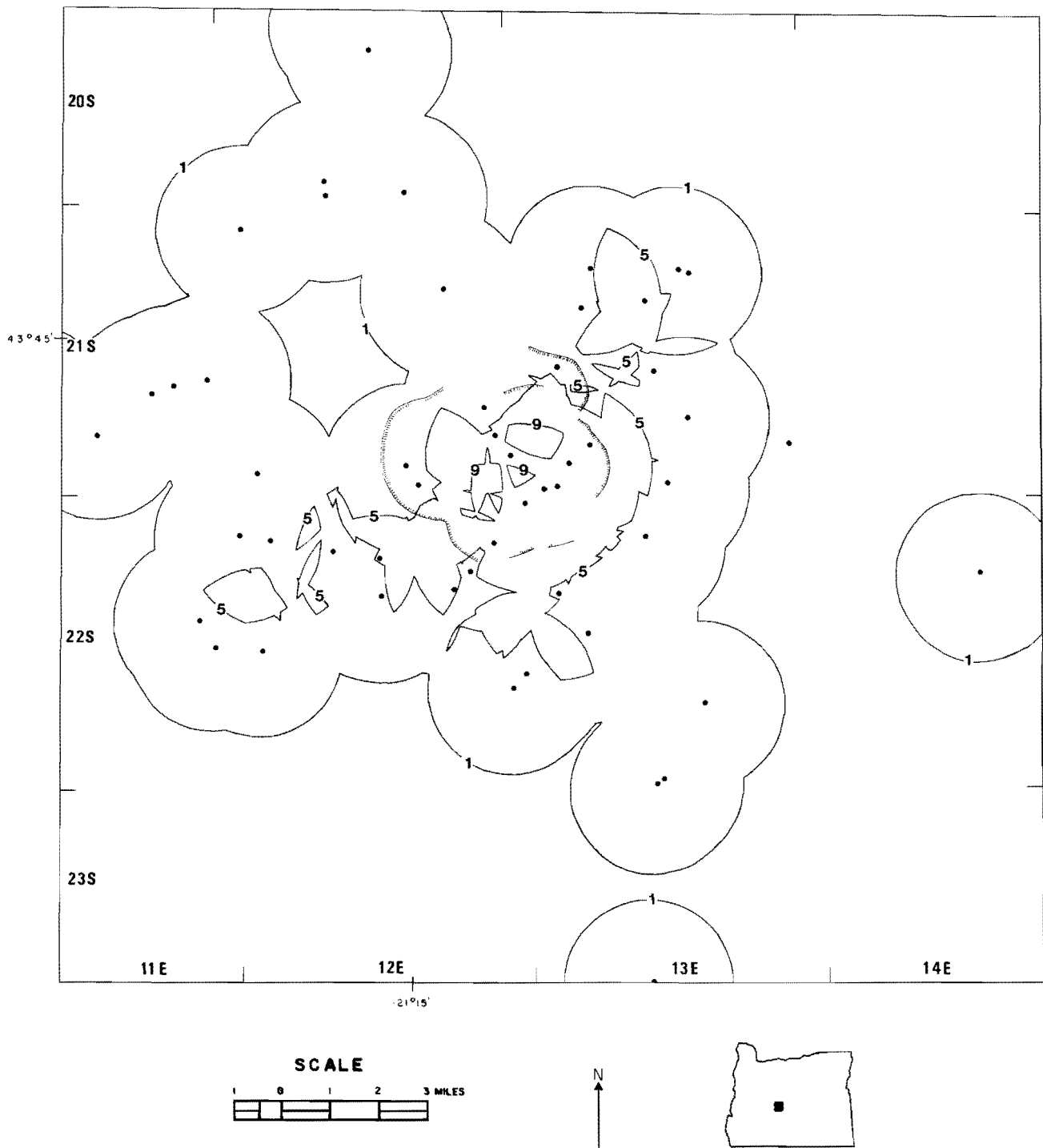


Figure 3.2. Density distribution of silicic volcanic centers at Newberry volcano. Contours at 1, 5, and 9 volcanic centers/1 percent area. Hachures represent caldera ring fractures. Dots represent silicic volcanic centers. Data base is from MacLeod and others (1982).

Causes of Vent Alignments

Normal faults, fissure eruptions, and vent alignments at Newberry show an obvious preferred orientation. All are a response to the local and regional stress field, but fissures do not necessarily imply the presence of faults and are therefore not necessarily good targets for geothermal drilling.

Monogenetic volcanoes are those that erupt only once from a fissure or vent, while polygenetic volcanoes erupt repeatedly from the same general vent or vents. Nakamura (1977) noted that monogenetic volcanoes commonly occur in groups as part of a polygenetic volcano, where they form flank volcanoes and post-caldera cones. He interpreted the flank eruptions of composite volcanoes in the following way: "Prior to the eruption, magmatic pressure in the central conduit increases to the sum of both the tensile strength of the surrounding rocks and the minimum compressional stress of external origin. If the magmatic pressure is not sufficiently relieved by an eruption from the summit, a radial vertical fracture develops laterally from the central pipe and is simultaneously filled with the source magma..... Flank eruptions occur where the dike first reaches the surface. If the available magma is of sufficient quantity and its viscosity is low enough, then the dike arrives at the surface causing a flank-fissure eruption."

Where the magmatic pressure in the central conduit predominates over other stresses or where the regional stress does not vary in azimuth, the resulting dike pattern is ideally radial. If, however, a regional stress field exists in the vicinity of the volcano, dikes which form will tend to curve and assume a preferred orientation with respect to that stress field. Dikes are planar features which are vertical in cross section, and the preferred orientation will be parallel to a plane defined by the maximum and intermediate principal stress axes. Because one of the principal stress axes is always vertical at the surface of the earth, the trend of zones of flank eruptions will be parallel either to the direction of maximum compressional stress (for compressional tectonics) or to the direction of intermediate stress (for extensional tectonics) (Nakamura, 1977).

From the above discussion, it is evident that fissures and vent alignments at Newberry are a response to the local and regional stress

field. Faults are a response to the same stresses and obviously represent zones of crustal weakness. In areas of extensional tectonics, such as at Newberry, it is to be expected that faults will occasionally act as conduits that channel magma to the surface, but fissures do not necessarily indicate the presence of faults, and vice versa.

Map Interpretation

In general, the distribution of maxima on the composite volcanic centers map (Figure 3.1) reflects the north-northeast trend of the Walker Rim fault zone south of the volcano and the northwesterly trend of the Tumalo fault zone north of the volcano (see Figure 2.1 of Priest, this volume). The concentration of volcanic centers indicates that the faults act as conduits for the ascent of basaltic magmas. The faults are a response to the regional stress field, and some vent alignments may also be (Nakamura, 1977). The close correspondence of greater than 90-ppb-mercury anomalies with volcanic center maxima on the south flank of Newberry indicates that there may be significant vertical permeability associated with many of the faults in that area (see Chapter 6).

The Brothers fault zone (see Figure 2.1 of Priest, this volume) does not influence the location of volcanic centers (Figures 3.1 and 3.2). The west-northwest-trending faults of this zone do not cut the older Newberry flank flows (MacLeod and others, 1982). The faults apparently do not act as conduits for basaltic magma, though some of the older rhyolitic intrusives east of Newberry are located on faults of the Brothers fault zone (Walker and others, 1967). A west-trending band of greater than 90-ppb-mercury anomalies appears to correlate more with the distribution of the Newberry pumice (see Priest and others, Chapter 6) than with any west-trending structure.

A small circular concentration of vents (15 centers/1-percent area) located just west of the summit caldera (Figure 3.1) corresponds to a low-level mercury anomaly of 50-70 ppb (see soil-mercury survey map). South of the caldera there is a hint of a northwesterly trend on the volcanic centers map which is caused by a series of en echelon fissures (Figure 3.1). The above-mentioned concentration of 15 centers/1-percent area lies at the northern end of that trend, although it is quite possible that the two areas are unrelated, as the vents on the upper west flank of the volcanoes are probably older than the vents of the south flank (Norm MacLeod, personal communication, 1983). A west-northwest-trending lobe on the large northeast-

trending mercury anomaly (90 ppb) is located south of the caldera, and a series of four closed anomalies (90 ppb) at the southern end of the soil-mercury survey map have a northwest trend (Priest and others, Chapter 6). No structures that correlate specifically to either trend have been mapped, and there is no concentration of volcanic centers corresponding to the more southerly trend. Although it is possible that these trends are of no significance, a few northwest-trending vent alignments have been identified in the southern portion of the study area. A more plausible explanation is that the mercury anomalies represent zones of vertical permeability on faults that have been buried by younger flank basalt flows.

Flows and intrusives of silicic composition tend to cluster around the summit caldera of Newberry volcano (Figure 3.2). The maximum concentrations of centers are located within the summit caldera, with lobes of lesser concentrations extending to the south, southwest, and northeast. The area covered by concentrations of silicic centers greater than 5 centers/1-percent area roughly coincides with an area inferred by Williams and Finn (1982) and Griscom and Roberts (Chapter 7) to be underlain by an intrusive mass at depths of 2 to 4 km.

CHAPTER 4
NEWBERRY HYDROLOGY

by
Gerald L. Black,
Oregon Department of Geology and Mineral Industries

Previous Work

No hydrologic studies have been completed on Newberry volcano, primarily because data are virtually nonexistent. An unpublished report on the groundwater resources of the Deschutes River basin by Jack Sceva of the (then) Oregon State Engineers Office provides some information, as does a report prepared by Cindy Gebhard for Central Oregon Project Energy (COPE) titled "Geothermal Development Issues: Recommendations to Deschutes County." A report titled "La Pine Aquifer Management Plan," which was prepared by Century West Engineering Corporation of Bend, Oregon, contains a considerable amount of hydrologic information. Unfortunately, the study area in this last report is restricted to the La Pine basin, and only the outermost edge of the western flank of the volcano is included. The most useful sources of information on general hydrologic conditions in the vicinity of Newberry volcano were personal communications with L.A. Chitwood, geologist with the Deschutes National Forest, and E.A. Sammel, USGS.

Climate

The climate in the Newberry volcano area is primarily influenced by the Cascade Mountains. The mountains cut off rainfall to the eastern part of the state and weaken the moderating effect of marine air masses on temperatures. As a result, the climate east of the Cascade Mountains is drier and temperature variations are more extreme (Loy and others, 1976) than in the western part of the state.

The temperature at Bend averages 8.6° C but varies from recorded extremes of 40.5° C in the summer to -22° C in the winter (Peterson and others, 1976).

Precipitation along the Cascade crest varies from 152 cm/yr to 254 cm/yr. The precipitation gradually decreases eastward until, at the western edge of

Newberry volcano, it averages about 38 cm/yr. On Newberry volcano proper, precipitation averages about 51 cm/yr at lower elevations and about 89 cm/yr at high elevations. Most of the precipitation is in the form of snow.

Geology

Newberry volcano is composed of young volcanic rocks of varying compositions. The rocks can be divided into two groups on the basis of their ages relative to the Mazama ash, which has a carbon-14 age of $6,845 \pm 50$ years. All of the mafic flows sampled that are older than the Mazama ash exhibit normal magnetic polarity, indicating that they are younger than about 700,000 years, although some of the silicic rocks are reversed (MacLeod and Sammel, 1982).

According to MacLeod and Sammel (1982), the oldest rocks associated with the volcano are a series of ash-flow tuffs, pumice-fall tuffs, mudflows, and other pyroclastic deposits which occur predominantly on the east and west flanks of the volcano. Their compositions range from rhyolite, through rhyodacite and andesite, to basaltic andesite. MacLeod and Sammel (1982) consider it likely that these older pyroclastic rocks extend completely around the volcano but are buried on the north and south flanks of the volcano by basalt to basaltic andesite flows. The flows range in thickness from a few meters to 30 m and cover areas from less than 1 km² to many tens of square kilometers. The more than 400 cinder cones and fissure vents which have been identified on the flanks of the volcano are concentrated in three zones on the northwest, southwest, and eastern sides of the volcano. Also common on the flanks are rhyolite domes, flows, and pumice rings.

The floor of the caldera at Newberry volcano is composed mostly of domes, flows, ash flows, pumice falls, and explosion-breccias of rhyolitic composition. Mafic rocks are uncommon, and those that are present are mostly older than the Mazama ash (MacLeod and Sammel, 1982). Newberry 2, a 932-m hole drilled by the USGS in the caldera floor, encountered fragmental rocks to a depth of 500 m and flows and associated breccias below 500 m (MacLeod and Sammel, 1982).

Surface Hydrology

Surface waters in the study area are limited to one creek and the two

lakes which occupy the caldera floor. East and Paulina Lakes cover areas of 409 and 567 hectares (Loy and others, 1976). They are interesting in that, although located less than 2 km apart, their surface elevations differ by about 15 m.

Flow rates in Paulina Creek, the only perennial stream in the area, are regulated by a dam and irrigation gates at its source at Paulina Lake. Flow in the creek is maintained at an average of 15 ft³/second (cfs) during the irrigation season. The flow rates range from more than 40 cfs during the spring snowmelt to 1-2 cfs during the winter, when the irrigation gates are closed for winter water storage in Paulina Lake (U.S. Forest Service, 1980).

Except for short periods during the spring runoff, the waters from Paulina Creek do not actually reach the Little Deschutes River. A private landowner adjacent to the Deschutes National Forest has water rights to nearly all of the water flowing in the creek, so most of it is diverted for pasture irrigation after the stream leaves USFS land (U.S. Forest Service, 1980).

The only springs which occur in the study area are two hot springs which occur along the margins of East and Paulina Lakes. Temperatures in the hot springs, which are interpreted to be drowned fumaroles (Mariner and others, 1980), range from 49° to 62° C (Mariner and others, 1980).

Ground-Water Hydrology

Ground water is water which fills void spaces in the rock beneath the land surface. The water table is defined as the upper surface of a body of unconfined ground water at which the pressure is equal to that of the atmosphere. The permeability of a rock body refers to the ease with which it transmits fluids, and an aquifer is a body of rock that can both transmit and store water in the pore spaces of the rock and yield significant quantities of water to wells and springs. Perched ground water is unconfined ground water that is separated from an underlying main body of ground water by an unsaturated or relatively impermeable rock unit.

The various types of volcanic rocks which are present on the flanks of Newberry volcano are expected to possess, for the most part, good lateral and vertical permeability. Beneath the regional water table, the autobreccias

which occur at the tops and bottoms of lava flows are good aquifers. Most of the flows at Newberry are the aa type of flows, which are characterized by rubbly flow margins. As was mentioned in the geology section, the individual flows of Newberry vary considerably in thickness and lateral extent, so that the deposits, when viewed as a whole, have a complex, overlapping "fishscale" appearance. This geometry should provide abundant complex paths for the downward percolation of precipitation. Perched aquifers likely are present in places, but they probably are small and local in nature. For example, Newberry 1, the USGS hole drilled on the upper northeast flank of the volcano, encountered small perched aquifers at 154 m and 280 m in rocks that were generally unsaturated (MacLeod and Sammel, 1982). Below the regional water table, good aquifers should be present, but their exact configuration will be extremely complex and impossible to predict.

Within the caldera at Newberry volcano, MacLeod and Sammel (1982) concluded (1) that vertical permeabilities are low both in the caldera fill (the fragmental material above 500 m in the Newberry 2 well) and in the collapsed caldera block (the flows deeper than 500 m in Newberry 2), and (2) that the vertical flow of both geothermal fluids and meteoric recharge water would be limited to faults, ring fractures, and brecciated intrusion conduits. They also concluded that lateral ground-water flow beneath the caldera would be restricted to permeable strata (e.g., breccias and brecciated flow contacts) with good hydrologic connections to water-bearing vertical conduits. Therefore, for that portion of the volcano above the regional water table, ground water may be present only in perched aquifers with good lateral connection to zones of high vertical permeability (e.g., ring fractures).

Essentially there are no well data from Newberry volcano on which to base a hydrologic interpretation. Numerous water wells have been drilled in the La Pine basin, just west of the volcano, but the vast majority of these wells produce from sedimentary deposits that overlie the volcanic rocks which are exposed on Newberry's flanks. Although these shallow wells provide no specific information on the hydrologic conditions at depth beneath Newberry, they can be used to make two very general observations: (1) The regional ground-water system is recharged in the Cascade Mountains to the west of the volcano and in the highlands south of the volcano. Some recharge surely occurs at Newberry itself, on the basis of topography alone, but is probably relatively minor. Vertical permeability appears limited in the caldera, where precipitation is highest, and precipitation is low on the flanks where there likely is significant vertical permeability. (2) The

direction of ground-water flow is to the east-northeast.

The elevation of the regional ground-water table in the vicinity of Newberry volcano is shown on Figure 4.1. The map was prepared by Larry Chitwood of the Deschutes National Forest and is based on data from wells located near population centers (e.g., Bend and La Pine), agricultural areas, and historic "land boom" areas. Because the contours are projected beneath the volcano from data from water wells outside the volcano, the mounding of ground water beneath the volcano is not taken into account. Because precipitation at Newberry is moderate and vertical permeability on the flanks is excellent, some rise in the ground-water table probably occurs beneath the volcano.

The regional water table was not encountered in Newberry 1, the USGS hole drilled to a depth of 386 m on the northeast flank of the volcano. The only water found in Newberry 1 was in small perched zones at 154 m and 280 m (MacLeod and Sammel, 1982). The bottom of the drill hole is at an elevation of approximately 1,500 m.

In Newberry 2, the USGS hole drilled within the caldera, the situation is more complex. The drilling logs and temperature-depth curves (Figure 4.2) indicate that cool perched aquifers were encountered at 280 m and 555 m and that warm perched aquifers were encountered at 350 m and 450 m (MacLeod and Sammel, 1982). Below 758 m there were very few permeable zones, and there was no evidence of water or steam, although gas was present in places (MacLeod and Sammel, 1982). Fluid that was recovered from the bottom 2 m of the hole during a 20-hour flow test was initially interpreted to have been a combination of formation gas and drilling fluid injected into the formation during the drilling process (Sammel, 1981; MacLeod and Sammel, 1982).

More recent information suggests that the regional water table was penetrated by the Newberry 2 drill hole. The elevation at the bottom of the hole is 1,024 m above sea level, well below the predicted water-table elevation of approximately 1,274 m (Figure 4.1). The temperature-depth curve from Newberry 2 (Figure 4.2) reveals that heat flow becomes conductive (a linear increase of temperature with depth) at about 680 m. This depth corresponds to an elevation of about 1,277 m, which is very close to the ground-water elevation predicted by Figure 4.1 (about 1,274 m).

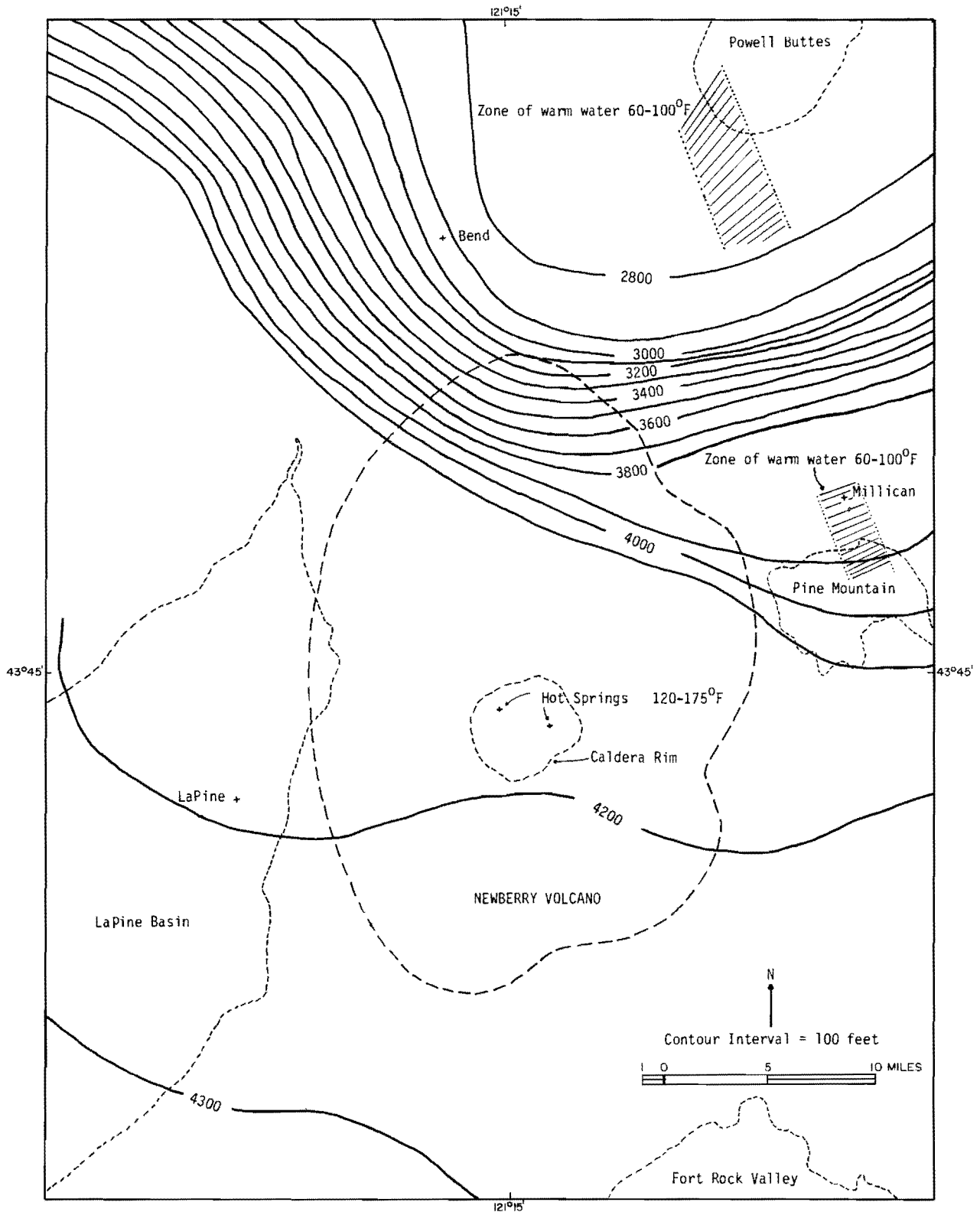


Figure 4.1. Elevation of the regional ground water table in the vicinity of Newberry volcano (by Larry Chitwood, Deschutes National Forest). Scale 1:250,000.

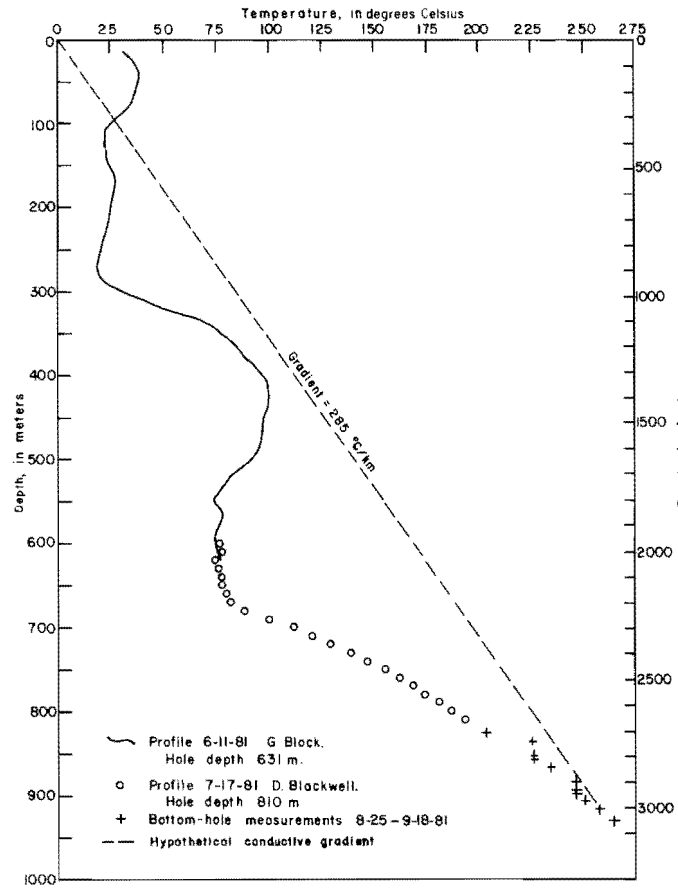


Figure 4.2. Temperature-depth curve for the Newberry 2 drill hole (taken from MacLeod and Sammel, 1982).

In addition to the close correlation between the predicted ground-water elevation and the onset of conductive heat flow in the Newberry 2 hole, the fact that the temperature-depth curve is linear tends to indicate that ground water is, or has been, present. The lithology in the bottom 250 m of Newberry 2 consists mostly of flows of dacite, andesite, basaltic andesite, and basalt with a few thin interbeds of tuffaceous sediments and pumice lapilli tuff (MacLeod and Sammel, 1982). Temperature-depth curves in these types of rocks are typically stair stepped in appearance, much like the upper portion of the Newberry 2 temperature-depth curve (Figure 4.2). This stair-step pattern is caused by intraborehole fluid movements and/or the rapid lateral movement of ground water (perched or otherwise) in zones of high permeability at flow contacts. Experience in similar rocks in

other parts of Oregon has shown that temperature-depth curves tend to be stair stepped whether water is present or not. The linearity of the temperature-depth curve indicates that most of the permeability in the lower part of the hole has been lost. MacLeod and Sammel (1982) note that alteration was more intense lower in the hole, that initially glassy rocks were locally altered to clays, sulfides, carbonates, and quartz along fractures, and that many of the breccias had a bleached appearance and were altered to clays, quartz, carbonates, epidote, chlorite, and sulfides. More recent work by Terry Keith of the USGS tends to confirm that alteration has very tightly sealed the rocks in the lower part of the hole (E.A. Sammel, personal communication, 1983). This alteration could have taken place only in the presence of fluids, though admittedly the fact that alteration has occurred does not necessarily indicate the presence (or absence) of the regional ground-water table now or in the past.

The apparent lack of fluids reported by MacLeod and Sammel (1982) in the lower part of the hole most probably resulted from the combination of negligible rock permeability (due to alteration) and the heavy muds used in the drilling process, which effectively sealed off the little permeability that was present. Griscom and Roberts of the USGS, while measuring the densities of cores from the Newberry 2 hole, noted that they appeared to be relatively saturated (see Chapter 7). The hole was drilled with mud, however, so that saturation could have occurred during the drilling process. In addition, some of the core bubbled when removed from the core barrel, suggesting that it contained a gas phase (N.S. MacLeod, personal communication, 1983). However, the nature of the core and the close correlation between the onset of conductive heat flow and the predicted regional ground-water table (Figure 4.1) suggest that the regional ground-water table may have been penetrated at an elevation of about 1,277 m in the Newberry 2 hole.

As previously mentioned, because of the impermeability in the lower part of Newberry 2 and the large pressure drop that occurred during a 20-hour flow test of the hole (Sammel, 1981), fluids recovered from the bottom 2 m of the hole were originally thought to be drilling fluids injected into the formation during the drilling process (Sammel, 1981; MacLeod and Sammel, 1982). Recent chemical and isotopic analyses of the fluids recovered during the flow test indicate that they are at least partly formation fluids, though at this point it is uncertain whether the aquifer contained steam or

whether it contained water which flashed to steam in the well bore during the flow test (E.A. Sammel, personal communication, 1983). The aquifer containing the fluids is very tightly confined vertically (E.A. Sammel, personal communication, 1983). Less is known about the lateral permeability, though the large pressure drop that occurred during the 20-hour flow test (Sammel, 1981) would seem to indicate that it might be limited.

Summary

To summarize, lateral and vertical permeability is expected to be excellent on the flanks of Newberry volcano. Within the caldera, vertical permeability is expected to be virtually nonexistent except in the vicinity of faults, ring fractures, and brecciated intrusion contacts. Lateral permeability will be confined to aquifers with good hydrologic connections to water-bearing vertical conduits. Below 758 m in the Newberry 2 drill hole there appears to be little permeability of any type, except in the bottom 2 m of the hole. Permeability conditions in the older rocks beneath the volcano are unknown, as the Newberry 2 hole did not penetrate through the base of the collapse block beneath the caldera. Most of the recharge for the ground water beneath the volcano occurs in the Cascade Mountains to the west and the highlands to the south. Limited recharge also occurs on the volcano.

The direction of the ground-water movement beneath the volcano is toward the north-northeast, and the regional water table may lie at an elevation of about 1,277 m beneath the caldera.

High-temperature fluids (265° C) are present beneath the caldera floor at at least one location (the Newberry 2 drill hole), although the amounts of the fluids present are unknown.

CHAPTER 5
THERMAL SPRINGS AND WELLS OF NEWBERRY VOLCANO
by
Neil M. Woller,
Oregon Department of Geology and Mineral Industries

Introduction

Paulina and East Lake Hot Springs are well known to both the scientific community and the public. Their presence within the geologically young caldera at Newberry volcano indicates that high temperatures exist beneath the floor of the crater.

Other thermal features within the caldera include fumaroles adjacent to the Big Obsidian Flow, a warm well at Little Crater Campground, drowned hot springs in East Lake, and the USGS Newberry 2 discovery well. All of the above locations are shown in Figure 5.1.

Paulina Hot Springs

Several springs occur on the northeast shore of Paulina Lake. Williams (1935) reported a temperature at one of the orifices around 43° C, but more recent publications (Berry and others, 1980; Bowen and others, 1978) indicate that the temperature is 21° C. The flow rate is very low. The orifices are in pumiceous tuffs and silicified lake sediments near the margin of the lake.

East Lake Hot Springs

Hot springs occur on the southeast shore of East Lake. They are commonly submerged during periods of high water. A zone of bubbling lake water extends from the shoreline-spring orifices northwestward into the lake. The springs are developed in palagonitic tuff which is fractured and altered over a wide area (Williams, 1935). Therefore, the total extent of the thermal area may formerly have been larger.

Several publications report the spring temperatures to be 62° C (Mariner and others, 1980; Berry and others, 1980), but MacLeod and others (1981) state that temperatures as high as 80° C have been measured at this location. The flow rate is very low.

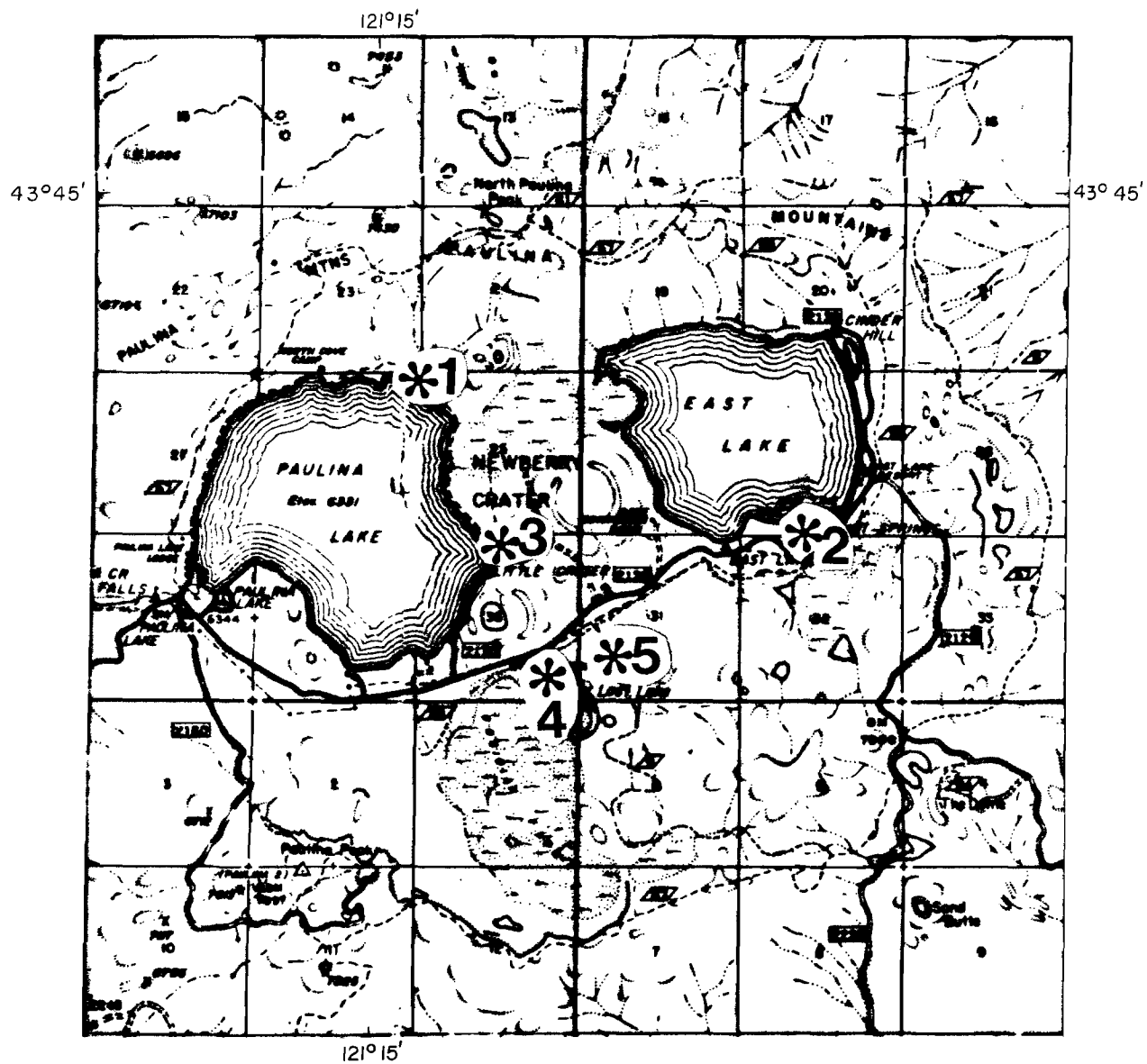


Figure 5.1. Locations of thermal springs and wells at Newberry caldera. 1 = Paulina Lake Hot Springs, 2 = East Lake Hot Springs, 3 = Little Crater Campground warm well, 4 = Big Obsidian Flow fumaroles, 5 = Newberry 2 drill hole.

Little Crater Campground Warm Well

The warm well at Little Crater Campground is 1.8 km southeast of the thermal springs at Paulina Lake (see Figure 5.1). The well was plugged and abandoned several years ago by the USFS because of concerns about its dissolved mineral content. The well was shallow, but its exact depth is not known. In a 1978 sampling program (Mariner and others, 1980), the fluids of the Little Crater Campground well were found to be similar chemically to those of Paulina Hot Springs (see Table 5.1). The obvious conclusion is that the well tapped the same system that feeds Paulina Hot Springs. Pumiceous sediments along the adjacent shore are silicified, suggesting that thermal waters were once more widespread.

Big Obsidian Flow Fumaroles

The fumaroles at the northern end of the Big Obsidian Flow issue from beneath the surface of a small ephemeral pond. Hydrogen sulfide odors can occasionally be detected in this area. Bubbles in the pond indicate the location of the fumaroles, but during dry periods when the pond level drops below the elevation of the fumaroles, they cannot be seen or smelled.

Geochemistry and Geothermometry of East Lake and Paulina Lake Hot Springs

The chemistry of the thermal waters of Newberry volcano is shown in Table 5.1. Sampling of the hot springs has been difficult due to their locations at lake margins. The high magnesium content is not common for thermal fluids and therefore suggests water-wall rock reactions at low temperatures. The silica, sodium, potassium, and calcium concentrations may also result from low-temperature fluid reactions with silicic pyroclastic wall rocks.

Table 5.2 shows the gas and isotopic data for the Newberry area. Mariner and others (1980) indicate that gas samples from the springs were contaminated by air and affected by gas-water reactions. The temperatures of the springs are directly proportional to the volumes of gas discharged and inversely proportional to the CO₂ content.

Mariner and others (1980) interpret the "hot springs" to be drowned fumaroles. Water from the springs is probably lake water that has been

Table 5.1. Chemical composition of thermal waters at Newberry volcano*
 (Source: Mariner and others, 1980)

	East Lake Hot Springs	East Lake Hot Springs	Paulina Hot Springs	Little Crater Campground Warm Well
Date of sampling	1973	8/1975	7/1977	8/1975
Specific conductivity	396	767	-	900
Temp°C	62.0	49.	-	35.5
pH	6.49	6.42	6.82	6.46
SiO ₂	36.	100.	205.	161.
Na	32.	53.	140.	83.
K	3.8	-	17.	10.
Ca	38.	70.	56.	54.
Mg	16.	34.	60.	48.
HCO ₃	184	547	856	679.
SO ₄	58.	28.	<1.	<1.
Cl	0.4	1.7	6.0	5.1
F	0.2	0.16	0.57	0.6
B	0.93	1.1	0.87	2.5
Li	0.01	0.04	0.22	0.12
Rb	<0.02	0.03	0.04	0.02
Cs	<0.1	<0.1	<0.1	<0.1
Sr	0.14	-	-	-
Al	-	0.008m	-	0.002m
Fe	<0.02	0.66	-	4.
Mn	0.10	0.90	-	0.25
Hg	0.0003	-	-	0.0001

* Concentrations in mg/l; m denotes monomeric aluminum.

Table 5.2. Gas and isotopic composition of thermal waters of Newberry volcano
(Source: Mariner and others, 1980)

	East Lake Hot Springs	East Lake Hot Springs	East Lake Hot Springs	Paulina Hot Springs	Paulina Hot Springs
Date sampled	1973	8/1975	7/1977	-	7/1977
Temperature° C	62.0	49.	-	-	-
%Ar	-	-	-	-	0.09
%CH ₄	9.	2.9	1.95	5.41	0.55
%CO ₂	56.	91.	95.55	71.37	93.45
%N ₂	30.	5.1	-	-	4.74
%O ₂	6*	0.9	2.72*	-	0.03
δ D of H ₂ O (0/00)	-76.2	-	-	-	-
δ O ¹⁸ of H ₂ O (0/00)	- 9.42	-	-	-	-
δ O ¹⁸ of SO ₄ (0/00)	-	-	-	-	-

Gas concentrations in volume percent; *Ar+O₂.

heated at shallow depths. Because the chemistry of the thermal waters does not represent fluid-wall rock equilibrium conditions at depth, geothermometric calculations of reservoir temperatures are probably not valid indicators of temperatures at depth. Table 5.3 gives the results of geothermometric calculations based on the chemical analyses of Table 5.1. Note that the bottom-hole temperature measured in the Newberry 2 drill hole (see below) is much higher than the calculated temperatures of Table 5.3. It is apparent that these estimated reservoir temperatures do not apply to any deep hydrothermal systems which may be present, in accord with the conclusion of Mariner and others (1980).

Newberry 2 Drill Hole

Newberry 2 was drilled to a total depth of 932 m. The mean thermal gradient was approximately 285° C/km, the heat flow was at least 3 W/m², and the bottom-hole temperature was 265° C (MacLeod and Sammel, 1982).

In 1981 a 20-hour flow test was performed on a 2-m interval of altered vesicular basalt at the bottom of the hole. The drill pipe (nx size) was swabbed to a depth of 427 m to initiate flow. Preliminary results of the test are listed in Table 5.4. Heavy mud used to control gas emissions and possible high downhole (formational) pressures during drilling may have affected the mass flow rates by coating some of the surface area of the 2-m test interval. However, the 84 percent decrease in wellhead pressure with the associated decrease in mass flow rate during the 20-hour flow test suggests that (1) there is low permeability and recharge of the tested interval, and/or (2) the zone tested was small in areal extent. There are insufficient data available to ascertain to what extent (1) and (2) (above) affect the test results.

The difference between the estimated formation pressure (62 bars, Table 5.4) and the calculated pressure of saturated steam at 265° C (52 bars) is probably due to the partial pressures of gases in the formation (Sammel, 1981; MacLeod and Sammel, 1982). Gas discharged during the test was predominantly steam. Other gases detected were CO₂ and minor H₂S and CH₄. The liquid fraction was extremely low in chloride, suggesting that it was derived almost entirely from condensed steam (Sammel, 1981). MacLeod and Sammel (1982) concluded that the fluids recovered during the test were

Table 5.3. Geothermometer calculations based upon the chemical data of Table 5.1 (source: Mariner and others, 1980). Calculated reservoir temperatures assume that (1) temperature-dependent fluid wall rock reactions reach equilibrium in the reservoir, (2) there is no mixing with nonthermal ground water, (3) there is an adequate supply of reactants in the reservoir, and (4) wall-rock reactions do not occur during fluid ascent. Note that the bottom-hole temperature of the Newberry 2 drill hole (265° C) is much greater than the temperatures predicted from the chemistry of the thermal waters. See text for explanation.

	East Lake Hot Springs	East Lake Hot Springs	Paulina Hot Springs	Little Crater Campground Warm Well
Date of sampling	1973	8/1975	7/1977	8/1975
Temperature ° C	62.0	49.0	-	35.5
Na-K	188	-	190	189
Na-K-Ca (1/3)	155	-	178	169
Na-K-Ca (4/3)	44	-	98	75
Na-K-Ca (Mg-corrected)	-	-	(cold)	(cold)
SiO ₂ conductive	87	180	182	166
SiO ₂ adiabatic	90	168	170	156
SiO ₂ chalcedony	56	158	161	142
SiO ₂ opal	-27	56	58	43

Table 5.4. Preliminary flow test results on Newberry 2 drill hole

Formation pressure (estimated)	62 bars (899 PSI)
Initial wellhead pressure	57 bars (826 PSI)
Initial mass flow rate	1.5 Kg/sec (approx.)
Final wellhead pressure (20 hours)	9 bars (130 PSI)
Final mass flow rate	0.7 Kg/sec (approx.)
Bottom-hole temperature (930 m)	265° C

(source: Sammel, 1981)

predominantly drilling fluids injected into the formation during drilling. However, new isotopic data from the recovered fluids indicate that at least a portion of the recovered fluids were indeed formational fluids (Sammel, personal communication, 1983). The new data are not yet available for inclusion in this report.

CHAPTER 6
PRELIMINARY SOIL-MERCURY SURVEY OF NEWBERRY VOLCANO,
DESCHUTES COUNTY, OREGON

by

George R. Priest, R. Mark Hadden, and Neil M. Woller,
Oregon Department of Geology and Mineral Industries,
and Chase B. Brand, Colorado College

Introduction

High concentrations of mercury are characteristically found in soils overlying active high-temperature hydrothermal systems (Matlick and Buseck, 1976; Phelps and Buseck, 1978; Capuano and Bamford, 1978). Because the mercury-exploration technique is relatively rapid and inexpensive, it was included as part of a very preliminary geothermal-resource assessment conducted during the summer and fall of 1982 on behalf of the Bonneville Power Administration.

For this study, 1,641 soil samples were collected in an area of about 1,000 km² of Newberry volcano (Figure 6.1). The results are summarized on Plate 2 and Figure 6.2. The areas of statistically anomalous soil-mercury concentrations at Newberry volcano warrant further research and exploration.

Sampling Technique

Samples were collected at 8- to 10-in. depths, chiefly from the Mazama ash layer, although some ash erupted from Newberry volcano and other soils were also sampled. Samples were dried, and the minus-80-mesh-size fraction was separated with a stainless steel sieve and split for analysis.

Samples were collected at 1,500-ft intervals mostly near roads but never in road material. Once anomalous samples were identified and where time permitted, a sample interval of 500 or 1,000 ft was utilized to delineate anomalies.

The sample depth was determined after analysis of vertical variations in mercury concentrations in test-pit sampling profiles from the Newberry area (Table 6.1) and from similar areas described in the literature (e.g., Klusman and Landress, 1978; Juncal, 1980). Vertical profiles within test pits show a

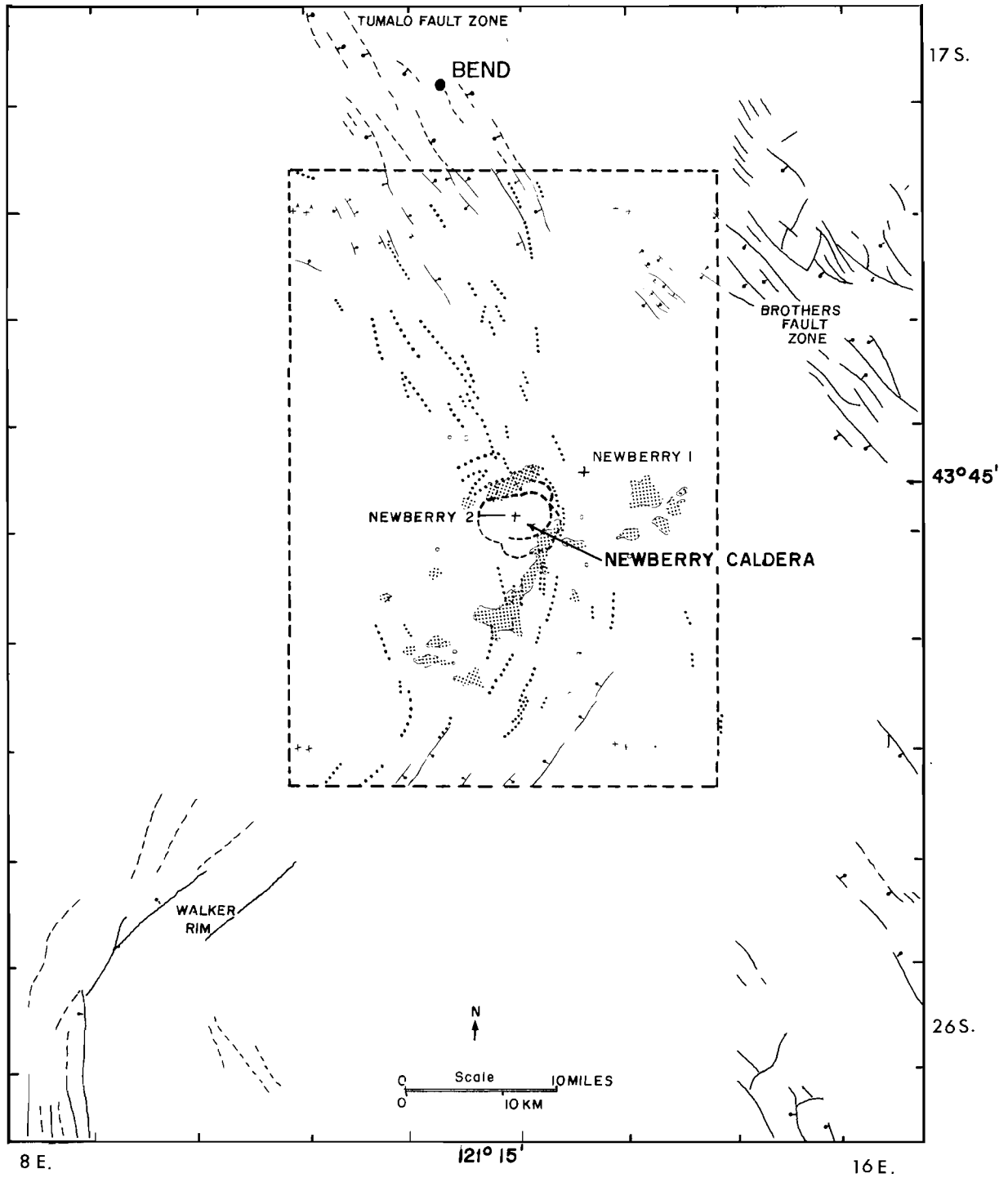


Figure 6.1. Geologic structures and soil-mercury anomalies; shaded areas are soil-mercury anomalies; the dashed rectangle outlines area covered by the geologic map of MacLeod and others (1982); thin solid lines represent faults; dotted lines are fissures and associated volcanic vent alignments. Data outside of the dashed rectangle were compiled from Wells and Peck (1961), Peterson and others (1976), and Walker (1977) by Priest (this volume). Areas with statistically anomalous soil mercury are shaded.

Table 6.1. Test-pit data. Mercury contents were determined by the low-temperature volatilization method.
Ppb = parts per billion.

Test pit no.	Location (T.(N).-R(E.)-sec.)	Primary material*	Date (mo.-day-yr.)	Hg at 3-4 in. (ppb)	Hg at 6 in. (ppb)	Hg at 9 in. (ppb)	Hg at 12 in. (ppb)	Hg at 18 in. (ppb)	Hg at 24 in. (ppb)
TP-1	21-13-25	Cinders	7-14-82	-**	39	-	76	-	111
TP-2	21-11-33	MA	7-21-82	-	19	-	21	19	-
TP-3	21-12-31	MA	7-21-82	-	21	-	28	30	-
TP-4	22-13-17	MA	7-21-82	-	17	-	24	35	-
TP-5	22-13-23	MA	7-21-82	-	32	-	34	26	-
TP-6	22-14-9	MA	7-21-82	-	28	-	260	-	-
TP-7	22-13-2	MA	7-21-82	-	39	-	83	-	-
TP-8	20-12-26	MA	7-21-82	-	46	-	37	-	-
TP-9	21-13-6	Cinders	7-21-82	-	57	450	-	-	-
TP-10	21-12-35	PA?	7-21-82	-	29	-	40	-	-
TP-10	21-12-35	PA?	9-23-82	30	31	31	36	-	-
TP-11	23-12-15	MA	9-14-82	35	28	36	38	-	-
TP-12	22-12-5	MA	9-23-82	51	46	33	64	-	-
TP-14	20-12-30	MA	10-6-82	40	48	38	36	-	-

*MA = Mazama ash

PA = Pre-Mazama ash from Newberry volcano

** = Not sampled

consistent increase in mercury with depth. This increase probably results from higher mercury sorption from increased clay and iron/manganese oxides in deeper soils (e.g., Fang, 1978; Horsnail and others, 1969). The 8- to 10-in. depth was chosen because it is easily reached with a shovel and does not contain large amounts of organic contaminants.

Organic contaminants, which can strongly concentrate mercury (Troost and Bisque, 1972; Fang, 1978), were avoided by clearing away the top inch of soil at each site and then "tunneling" into the side of each sample hole with a stainless steel spoon to avoid organic material which might fall onto the sides of the hole from above. Test pits TP-6 and TP-9 are examples of variations which can occur when this "tunneling" method is not followed.

Analytical Technique

The soil samples were analyzed utilizing the low-temperature volatilization method and a Jerome Gold Film Mercury Detector, Model 301. Sample aliquots were taken by volume by using the standard sample scoops provided with the detector. Samples were then heated to $327 \pm 5^{\circ}$ C on a hot plate to drive off a standard fraction of the mercury to the detector. Details of the analytical technique are summarized in Appendix A. A complete discussion of possible errors in the analysis are included in Appendix B along with regression equations for conversion of these data to corresponding atomic absorption and high-temperature-volatilization values.

Results

The total distribution of mercury concentration is log normal, with a range of 14 to 693 parts per billion (ppb) (low-T values), a median of 44 ppb, a mode of 37 ppb, and a threshold of 115 ppb (see Figures 6.3 and 6.4). About 30 percent of the data lie within 10 ppb of the mode (Figure 6.3).

The straight line through the data on the probability plot of Figure 6.4 represents the expected variation of a single log-normal sample population. Sharp deviations from this line represent statistically different population. A sharp positive deviation occurs at about 85 to 90 ppb (90 to 91 cumulative percent). The 9 percent of the total sample population with mercury above

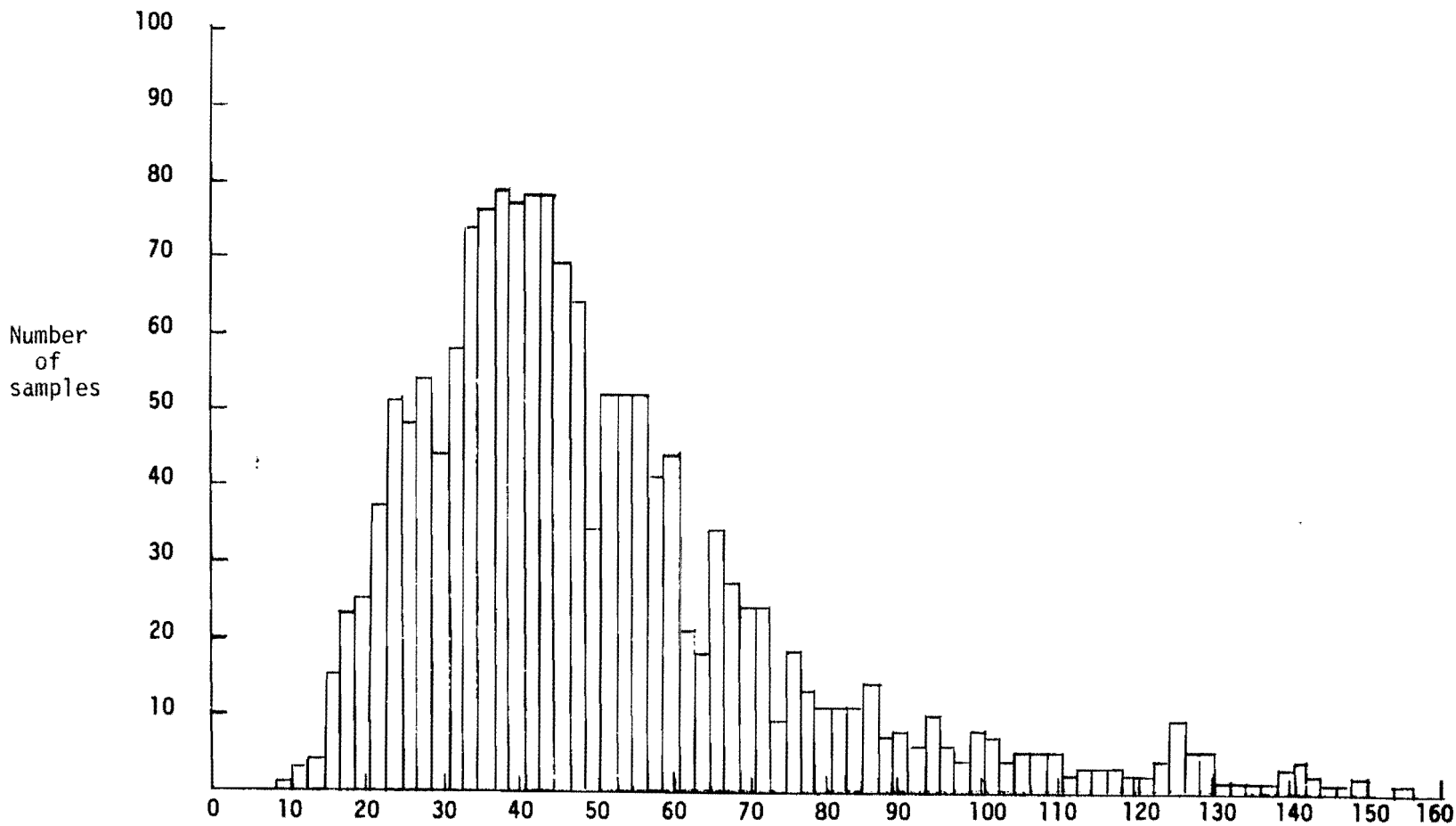


Figure 6.3. Histogram of parts per billion (ppb) Hg (low-temperature volatilization values); samples above 160 ppb Hg not included; 17 samples had Hg in excess of 160 ppb with a high of 693 ppb; see Appendix B for conversion to absolute values.

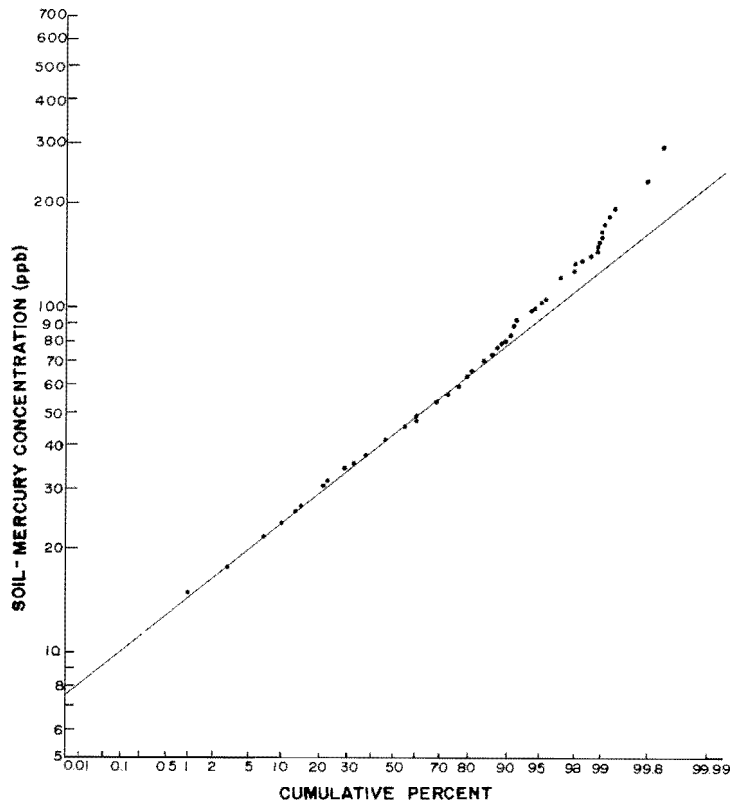


Figure 6.4. Probability plot of the cumulative percent of samples versus soil-mercury content (low-temperature volatilization values) for the entire data base.

90 ppb is truly anomalous in a statistical sense from the background population. These samples come from about 32 km² of the survey area. The 90-ppb contour was hachured on the contour map (Plate 2) to emphasize truly anomalous areas with soil-mercury contents above 90 ppb.

Using the atomic absorption values as a standard for absolute mercury (Appendix B), the 90-ppb contour would correspond to an absolute mercury content of about 157 ppb. The range of absolute mercury content would be from about 21 to 1,239 ppb, with a median of 75 ppb, a mode of 66 ppb, and a threshold of 202 ppb.

Areas with anomalously high mercury occur on the north and northwestern caldera ring fractures, the east flank of the volcano, and in a broad northeast-trending zone approximately coincident with northeast-trending faults and volcanic center alignments which dominate the southern flanks of the volcano (Figure 6.1; Plate 2). Small anomalies also occur locally on the west flank

of the volcano (Figure 6.2, Plate 2).

The northwest-trending band of anomalies on the south flank may continue farther to the southwest. The sample grid does not close all of those anomalies on their southwestern margins (Figure 6.2). It is quite possible that similar anomalous areas lie to the southwest where they are associated with the Walker Rim fault zone.

Interpretation

Introduction

Interpretation of the soil-mercury data must take into account numerous factors other than geothermal heat which can influence the distribution of mercury. Differing soil compositions, microclimate effects, transport of rising mercury vapor by ground water, decomposition of mercury sulfides and oxides from fossil hydrothermal systems, original mercury content of primary igneous material in the soil, and geologic barriers to vertical rise of mercury vapors can probably all influence the distribution of mercury.

Theoretical Geochemistry of Mercury at Newberry Volcano

Naturally occurring mercury is found in soils-- especially soils rich in organic matter-- and in sulfide ores. It can exist in the +2 and +1 oxidation states, and as the native metal (Hg^0). Cinnabar (HgS) is the principal ore of mercury, but mercury is also a significant trace element at the parts per million (ppm) level in many other sulfides (e.g., Hawkes and Williston, 1962).

Metallic mercury (Hg^0) is introduced into the atmosphere in volcanic gases (e.g., Eshelman and others, 1971), gases from geothermal fluids (e.g., Robertson and others, 1978), gases given off by ores containing mercury (e.g., Hawkes and Williston, 1962; McCarthy and others, 1970), and by various processes related to man's activities. In general, air in industrialized urban areas tends to contain more mercury vapor than other areas. For example, 0.003 to 0.009 $\mu\text{g Hg}^0/\text{m}^3$ was measured in air from nonmineralized, nonindustrial areas (McCarthy and others, 1970), whereas up to 4 $\mu\text{g Hg}^0/\text{m}^3$ has been found in air from selected U.S. urban areas (Jepson, 1973). Hopefully, the remoteness of Newberry volcano from urban areas precludes any effect from man's activities. The ease with which Hg^0

is transported as a vapor is a function of its low melting point (-38.9°C) and relatively high vapor pressure (10^{-3} mm Hg at 18°C and 1 mm Hg at 126°C) (Weast and others, 1965). Thus volatile mercury is available in nature from thermal and chemical decomposition of primary mercury-bearing sulfides and volatile streaming from magmas and hydrothermal systems. The mercury vapor probably leaks upward, following zones of high permeability.

Juncal (1980) gives a comprehensive summary of the various chemical parameters governing the transport of mercury; his conclusions are briefly summarized below, but the reader is referred to his text for complete references and documentation. In the zone of oxidation, HgS and other sulfides containing mercury will decompose, yielding both Hg^{+2} and Hg° . Both the mercury chlorides and HgS can undergo thermal decomposition to yield Hg° . Natural reducing agents such as iron may cause release of Hg° below the zone of oxidation. This elemental mercury will migrate to the surface through permeable zones where significant quantities are adsorbed on clay and organic matter or coprecipitated with hydrous oxides of iron and manganese.

In normal ground water, the solubility of the various forms of mercury is very low (i.e., less than 25 ppb), but significant mercury can dissolve and be carried by oxygenated high-chloride waters, if the waters are acidic. Mercury ore is precipitated at temperatures of 100°C to 200°C and pressures of 1 to 30 atmospheres from neutral to weakly alkaline waters of low salinity (Barnes, 1979). These moderate-temperature mineralizing fluids, especially where very rich in total sulfur (approximately 3,200 ppm), are thus also capable of transporting considerable dissolved mercury, probably as sulfide complexes. Above 200°C in sulfur-rich fluids, mercury strongly partitions into the steam phase and will precipitate at the surface as cinnabar from H_2S -bearing vapors.

A water sample taken from a probable drowned fumarole at East Lake in Newberry caldera contained only about 0.3 ppb Hg (0.003 mg/l), and water from a nearby hot well contained less than 0.1 ppb Hg (Mariner and others, 1980). It is difficult to make any observations about the probable mercury transport mechanism from these meager data, but it is probably reasonable to assume that most of the water at East Lake is not from a deep circulation system capable of carrying substantial mercury in solution. The low content of dissolved solids in the Newberry springs also tends to suggest that they are not representative of deep hydrothermal waters. The presence of probable fumaroles

suggests that mercury may be carried in volatiles streaming from cooling magma bodies and associated hydrothermal systems at depth.

The elemental mercury in volcanic gases in the caldera is, as previously mentioned, probably adsorbed onto soil particles, but some mercury may also be precipitated as HgS where H₂S-rich vapors have reached the surface. The presence of both sulfides (and possibly oxides) of mercury in addition to adsorbed elemental mercury is suggested in Appendix B as a cause for some of the erratic analytical results obtained for some Newberry caldera samples taken near the drowned fumaroles, and thus both forms of mercury could be present within the caldera.

Because of the very low solubility of mercury in normal surface waters and its tendency to adsorb onto soil once it is transported in either aqueous or volatile form to surface soils, it is not likely to be further dispersed by other than mechanical processes. Downslope movement of soils will, however, tend to widen the anomalies somewhat. This effect should be minimal in this survey because the slopes are very low in all areas sampled except the caldera rim. In any case, very little soil movement has probably had time to occur since deposition of the Mazama ash fall about 6,845 yr B.P. (C¹⁴ age from Bacon, 1983); as the Mazama ash or younger ash falls underlie most of the soils sampled, mechanical dispersion should be very minimal.

Another factor which could influence the shape and size of the mercury anomalies is the degree of adsorption of mercury in areas with high variation in the factors governing soil-mercury adsorption. A positive correlation between mercury content and soil organic content, pH, iron and manganese oxides, and aspect have been demonstrated by Klusman and others (1977) and Klusman and Landress (1978). Cox (1981) found a significant correlation between high clay content of young volcanic soils in Hawaii and the high soil mercury. The observations of all of these workers have been confirmed by experimental evidence of Fang (1978), Trost and Bisque (1971, 1972), Rogers and MacFarlane (1978), and Landa (1978), who demonstrated the ability of mercury to adsorb onto clays and, particularly, onto organic matter. Horsnail and others (1969), in detailed studies of the iron and manganese fractions of sediments, concluded that many of the transition metals similar to mercury are scavenged by coprecipitation with iron and manganese oxides.

The above-discussed factors are probably not significant controls on the mercury anomaly at Newberry. The sample type in most of the area consisted of weathered Mazama ash and was very uniform. As this ash is of the same age everywhere, there is little likelihood of great differences in soil development of clay or iron-manganese oxides, although local variations in climate may have some effect. There is, however, some correlation between high soil mercury and the distribution of post-Mazama Newberry ash falls on the east flank, although these ash deposits also have background mercury levels in many areas (Figure 6.2). Because more mature soils generally have higher clay and organic content and thus greater ability to scavenge mercury, it is unlikely that this high mercury in the youthful Newberry ash is caused by soil type. The possibility of primary igneous mercury is discussed in a later section. There is no other obvious relationship between the soil patterns mapped by the USFS in the study area and the mercury patterns. In any case, Klusman and others (1977) and Klusman and Landress (1978) found that soil parameters affecting mercury are overwhelmed in areas of active hydrothermal circulation and high heat flow.

It appears from an examination of the geochemistry of mercury that the mercury anomalies at Newberry volcano are not, in general, a function of surface factors such as soil type, but are caused by anomalously high influxes of mercury from depth, probably in volatile form. The source of the mercury vapor could be volcanic gases, hydrothermal gases, or gases derived from heating and/or oxidation of mercury-bearing minerals at depth. The vapors are probably concentrated in zones of high vertical permeability through which they migrate to the surface. The important influence of vertical permeability is demonstrated by the relatively low overall mercury content of soil above the Newberry 2 drill hole, where, according to MacLeod and Sammel (1982), high temperatures and abundant volatiles were encountered in several zones below relatively impermeable rock strata (see Figure 6.2).

Effect of Shallow Ground-Water Circulation

Whereas it is easy to see that hydrothermal fluids strongly control the path of mercury migration, at least until a vapor phase separates, it is more difficult to predict the effect the circulation of cooler overlying ground water might have on the distribution of mercury. The writers' extensive experience with temperature-gradient measurements in the La Pine basin-Bend

area has shown that large aquifers circulate water rapidly enough to wash out deep heat flow to depths of 600 m. Similar aquifers apparently strongly affected temperature gradients measured above the regional ground-water table in both the Newberry 1 and Newberry 2 drill holes (see Sammel, 1981; MacLeod and Sammel, 1982; Black, Chapter 4). It is not, at present, known what effect this ground-water circulation has on mercury migration, but it may well have some influence-- conceivably, a very large influence.

Quantitative data on the flow rates of the ground water and the diffusion rates of mercury in its various forms must be generated to evaluate the importance of this effect. If shallow ground-water flow proves to be important, the interpretation of mercury anomalies would have to be made within the context of an accurate hydrologic model for the area.

Background Concentrations of Mercury in Igneous Rocks

Most of the samples collected in this survey were from very youthful soils developed on ash falls younger than about 7,500 yr. An ash- and pumice-fall deposit blanketing much of the eastern part of the volcano has carbon-isotopic ages of $1,720 \pm 60$ (Higgins, 1969) and $1,550 \pm 120$ yr. B.P. (S.W. Robinson, written communication to MacLeod and others, 1982). Most of the rest of the area is covered by the Mazama ash (carbon 14 date = 6,845 yr B.P. = about 7,500 yr B.P.; Bacon, 1983). Much of the material analyzed was not soil clay but fine-grained ash from these ash falls. Because the samples are of primary igneous material, it is important to examine the possible initial mercury content of this source.

Table 6.2 shows the concentrations of mercury in some common igneous rocks compared to the probable absolute levels of mercury in soil samples collected here. Note that the absolute mercury values listed in the table for Newberry samples were calculated from the regression equations of Table B.2 (Appendix B), assuming that the atomic absorption method is accurate.

The highest mercury content for the common igneous rocks in the table (39 ppb in granite G-2) is about half of the mercury content of the median value (75 ppb) of the Newberry soil samples, and about 25 percent of the minimum level of mercury (157 ppb) which defines the boundaries of areas with statistically anomalous mercury on the contour map. It is improbable that

the pattern of mercury anomalies is strongly affected by variations in the amount of primary igneous material in the soil samples, if the Mazama and Newberry ash deposits have mercury similar to the rocks in Table 6.2.

Some mercury anomalies on the eastern part of the volcano are located in the same area as is the youthful Newberry ash fall (Figure 6.5). This implies that some of the mercury anomalies on the east flank could have been caused by primary mercury in the young pumice fall, although the correlation is far from perfect. Moreover, unlike the Newberry ash fall, none of the rocks of Table 6.2 are pumiceous. Pumiceous samples probably come from magmas more highly charged with volatile elements such as mercury than the nonvesiculated crystalline rocks of Table 6.2. On the other hand it seems unlikely that a large proportion of entrained mercury would be retained in magma erupted at temperatures probably approaching 800° C. The rapid quenching of the viscous rhyolitic glass during ejection and loss of fluxes such as H₂O would, however, probably significantly inhibit the ability of dissolved mercury to diffuse toward gas nucleation points during eruption. This important problem may be partially resolved by extensive analysis of a number of youthful pumice samples for mercury. Even after this type of experiment, the investigator would probably still be plagued with uncertainty about possible adsorbed mercury in the pumice from sources under the deposit. An additional experiment to evaluate the mercury-adsorbing ability of the pumice would also be necessary.

If original mercury content is a problem, then it may also affect the results from the older Mazama ash samples. If the youthful ash falls contained significant juvenile mercury, then the older ash falls may also have had high primary mercury. Original mercury seems less likely to be a factor for the Mazama samples, because large numbers of these samples contained very low mercury (this same argument could be made, albeit somewhat less convincingly, for the younger ash fall). Also, it is unlikely that the mercury anomalies would define broad patterns parallel to geologic structures in the area if the anomalies in Mazama ash were purely a function of original igneous mercury content (see Figures 6.1 and 6.2). The Mazama ash has also had a significantly longer time than the Newberry ash fall to develop clays and iron-manganese oxides which can scavenge mercury.

To summarize, the large east-west trending soil-mercury anomaly on the

Table 6.2. Comparison of Newberry soil mercury to mercury contents of some common igneous rocks. Newberry data are adjusted to equivalent absolute AA values using the calibration equations of Table B.2 (Appendix B). Values for BCR-1, GA-649, AGV-1, and G-2 are from Grdenic and others (1969); other igneous rock values are from Matlick and Buseck (1976).

Samples	Absolute Hg (ppb)
Newberry soils: Range	21-1,293
Median	75
Mode	66
Anomaly contour	157
Basalt BCR-1 (Columbia River Basalt Group)	7
Basalt GA-649 (Hawaii)	13
Basalt (Long Valley)	34.1
Andesite AGV-1	4
Rhyolite (Long Valley)	27.7-27.0
Obsidian (Long Valley)	27.3-27.6
Granite (Long Valley)	25.3-25.7
Granite G-2	39

east side of the volcano could be partly a function of primary igneous mercury in the underlying young pumice, but incomplete correlation of the anomaly with the distribution of the pumice casts doubt on this hypothesis. More analytical data on the pumice would be helpful in evaluating the east-flank anomaly. The large anomalies elsewhere on the volcano seem even less likely to be a function of original mercury content of pumice.

Comparison With Mercury Data from Some Other Geothermal Resource Areas

Introduction: It is important to compare the soil-mercury data from Newberry volcano with that from other areas underlain by known hydrothermal

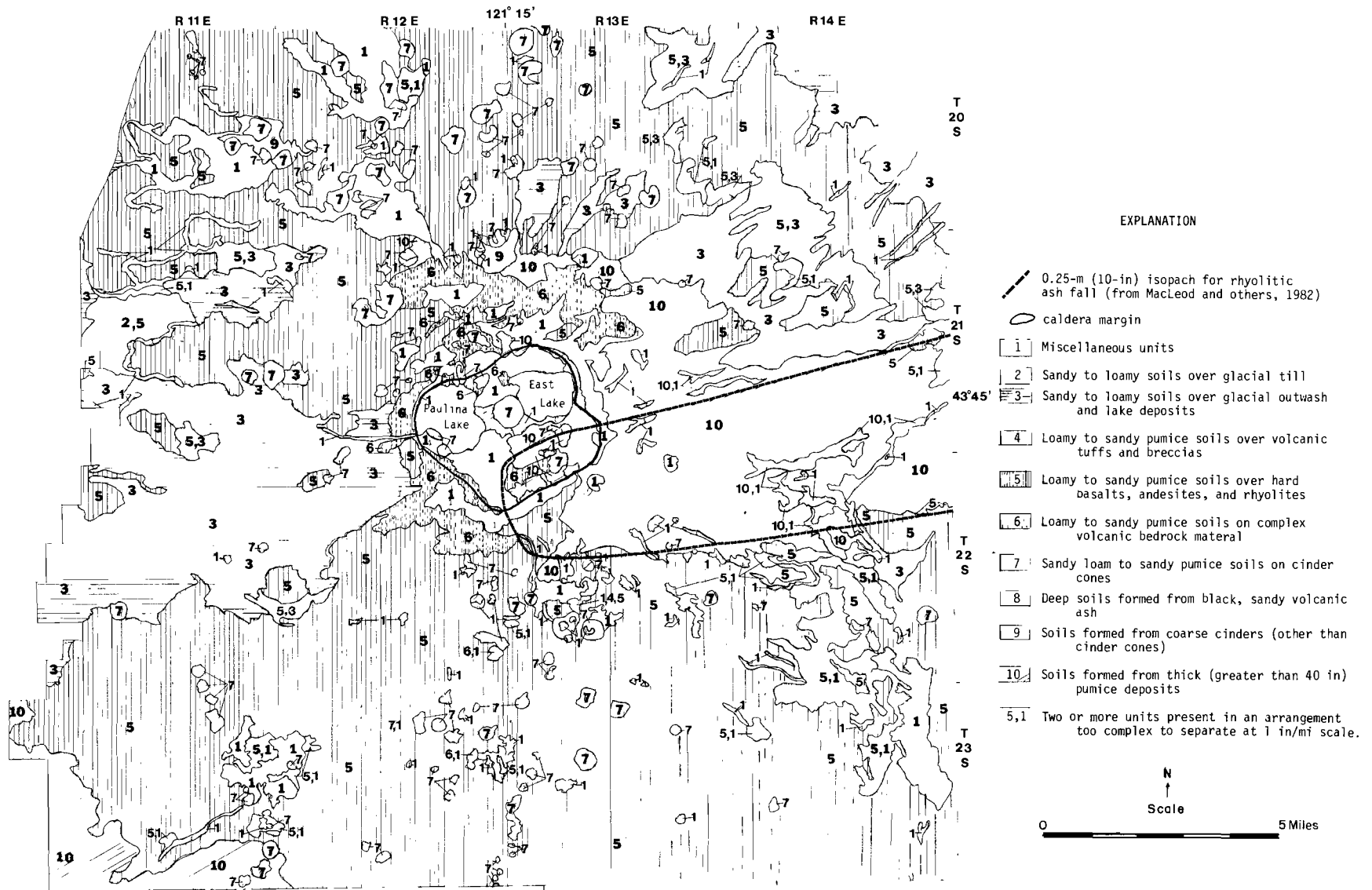


Figure 6.5. Soil map of Newberry volcano compiled from Larsen (1976).

systems so that the likelihood of similar resources at Newberry may be evaluated. Several different types of hydrothermal systems are examined. Some, such as Yellowstone caldera and Long Valley caldera, are geologic analogues of Newberry caldera, while others, such as Dixie Valley, Nevada, are analogues of the fault systems which occur on the north and south flanks of the volcano. Table 6.3 summarizes some pertinent data. All concentrations of mercury from the literature are from the high-temperature volatilization method. Comparative Newberry values are calibrated to corresponding atomic absorption values (Table B.2).

Concentrations of mercury in some other geothermal resource areas: The concentrations of mercury and the types of geothermal resources of other geothermal resource areas are discussed below:

1. Yellowstone geothermal area, Wyoming (abstracted from Phelps and Buseck, 1980). This is one of the largest silicic volcanic centers in the world with most recent eruptive activity about 70,000 years ago (see Christiansen and Blank, 1972). Eaton and others (1975) have proposed from geophysical evidence that a magma chamber exists at a depth of 6 km or more beneath the Yellowstone caldera.

Numerous hot springs within the area attest to very active hydrothermal systems. Estimated reservoir temperatures exceed 250° C in some cases (see chemical geothermometers of White and others, 1971, 1975; Fournier and others, 1976; Truesdell and Fournier, 1976).

Background mercury levels are 20 ppb with a threshold of 40 to 50 ppb and a maximum of greater than 100,000 ppb in one area. The anomalies were very narrow and did not extend more than 1 km beyond the thermal areas.

The areas interpreted to be water-dominated hydrothermal systems had poor correlation between mercury anomalies and specific hot springs, although there was an overall correlation between areas of thermal activity and high soil mercury. Areas thought to be underlain by vapor-dominated hydrothermal reservoirs had strong correlation between soil-mercury anomalies and intense vent activity. Because boiling frequently occurs as the hot-water-dominated fluids rise toward the surface, mercury vapor can partition into the vapor phase and follow paths independent of the paths followed by the mercury-depleted residual waters. Soil mercury in this area is thus a more

Table 6.3. Comparison of mercury data from some geothermal resource areas. References for study areas are given in text.

Area	Probable geologic controls of the hydrothermal systems	Reservoir temp. (°C)	Median or background Hg (ppb)	Lowest contour(s) which delineate the anomalies (ppb)	Threshold (ppb)	Range (ppb)
Newberry volcano, Oregon	Holocene silicic + faulting caldera	x>265 ²	75	157	202	21-1,239
Yellowstone, Wyoming	Pleistocene silicic caldera	267 ³	20	-	40-50	? - X>100,000
Long Valley, California	Holocene silicic caldera + Basin and Range faulting	227 ³	5.5	55	-	? - 3,125
Noya, Japan	Holocene volcanic field + graben faulting	X>177 ⁴	25	50-100	-	4-1,000
Roosevelt Hot Springs, Utah	Basin and Range + nearby silicic volcanism	265 ³	20	100-400	-	? - x>3,200
Northern Dixie Valley, Nevada	Basin and Range faulting	x>139 ⁵	20	120	-	8-1,720
Summer Lake, Oregon	Basin and Range faulting	118 ³	4	16	-	? - x>100 ppb
Klamath Falls, Oregon ⁶	Basin and Range faulting	124 ³	50-80? ⁶	150? ⁶	-	? - 512 ⁶

¹Newberry data are adjusted absolute mercury values from regressions through duplicate atomic absorption spectrometric analyses. Data for the other areas are from the high-temperature gold film technique.

²Temperature at the bottom of a 932-m drill hole (Sammel, 1981).

³Mean reservoir temperature estimated by Brook and others, (1979).

⁴Temperature at 701 m (Matlick and Shiraki, 1981).

⁵Mean reservoir temperature of Brook and others (1979), but the temperatures must be higher, because this area has been the site of a steam discovery well.

⁶Only 17 samples taken.

reliable guide to the vapor-dominated systems where boiling occurs from a very deep water table.

2. Long Valley caldera, California (abstracted from Matlick and Buseck, 1976). This is a silicic volcanic center with a large caldera. The last dated volcanic eruption was about 220 years ago. There are numerous hot springs, some with temperatures up to 93° C.

Soil within 27 km of the volcanic center has an average of 5.5 ppb Hg. The entire caldera showed a broad positive anomaly (7-22 ppb), with local anomalies up to 3,125 ppb Hg. The 55-ppb contour outlines most of the major anomalies.

Soil-mercury anomalies traverse different types of bed rock, showing little bedrock control of the mercury patterns. Most of the soil-mercury anomalies correlate with various geophysical anomalies (resistivity, AMT, aeromagnetic, and gravity), although some do not. Two of the major anomalies are correlated with hydrothermal mineralization.

3. Noya, Japan (abstracted from Matlick and Shiraki, 1981). Noya is on the island of Kyushu in a large graben where several recently active volcanoes occur. The area has a highest recorded temperature of 177° C at 2,300 ft and two 500-ft wells which vent steam. Mercury ranges from 4 to 1,000 ppb with a background of 25 ppb. The 50- to 100-ppb contours outline areas with anomalously high temperature gradients.
4. Roosevelt Hot Springs KGRA, Utah (summarized from Matlick and Shiraki, 1981). The liquid-dominated high-temperature (greater than 260° C) geothermal system is controlled by normal faults. The country rock is chiefly granitic plutons and Precambrian gneiss. Soil mercury exceeds 3,200 ppb in some areas, and the background is about 20 ppb. All of the mercury anomalies occur in areas with high temperature gradients along the major fault in the area. The boundaries of the anomalies are approximately outlined by the 100- to 400-ppb contours.
5. Northern Dixie Valley, Nevada (summarized from Matlick and Shiraki, 1981). This area is a complex graben bounded by horsts composed of basalt, tuff, gabbro, metasediments, and metavolcanic rocks. Active high-temperature hydrothermal systems have been verified, and a positive correlation between high temperature gradients and mercury content of soils has been demonstrated. Mercury ranges from 8 to 1,720 ppb, with a background of 20 ppb. The 120-ppb-mercury contour

outlines a major area of high temperature gradients with peak- to background-mercury anomalies of 43:1.

6. Summer Lake basin, Oregon (taken chiefly from Matlick and Buseck, 1976). Summer Lake occupies a basin within the Basin and Range province of southeastern Oregon. There is no local Holocene volcanism, but meteoric water can circulate to great depths along faults which occur in the area. All of the thermal springs and wells in the area are situated near large normal faults. A maximum temperature of 110° C was measured at a depth of 233 m in a well in the area (Blackwell and others, 1982a).

Soil-mercury concentrations range from background values of 4 to over 100 ppb. The 16-ppb contour outlines most of the major anomalies. Although some of the anomalies correlate with older hydrothermal mineralization, most tend to follow areas of known or probable geothermal activity.

7. Klamath Falls, Oregon (abstracted chiefly from Matlick and Buseck, 1976). This area is on the western edge of the Basin and Range province in southernmost Oregon. Thermal wells reach temperatures of 60° to 113° at depths of 30 to 550 m near major fault zones bounding grabens in the area.

Only 17 samples were analyzed for mercury by Matlick and Buseck (1976). They found that there was roughly a 10-fold increase in mercury concentrations in the areas of high heat flow relative to mercury values in adjacent areas. Samples taken in two traverses toward the thermal area varied in concentration between 50 and 80 ppb in the Klamath basin, whereas samples near fault zones along the margins of the basin had between 100 and 150 ppb mercury (estimated from their Figure 5). In the vicinity of the hot springs and hot wells, mercury concentrations ranged from 200 to somewhat over 500 ppb.

Comparisons with Newberry: The silicic Quaternary volcanic centers at Long Valley caldera and Yellowstone caldera are the areas most geologically analogous to Newberry volcano. Newberry also has a caldera probably formed during eruption of silicic ash flows, and it has also had Quaternary volcanic activity. Unfortunately, deep drilling data are not available for either

Long Valley or Yellowstone, although, like Newberry, those areas are considered to have very high potential for geothermal resources, and both have estimated reservoir temperatures in excess of 250° C (Table 6.3).

The mercury parameters for both Long Valley and Yellowstone do not look very similar to those of Newberry. The background values for the Long Valley and Yellowstone areas are lower than the minimum value at Newberry, whereas the highest values are three or more times those at Newberry. It follows that the peak-to-background ratios of the Newberry anomalies are much lower than anomalies at either Long Valley or Yellowstone.

With the possible exception of Klamath Falls, the Basin and Range hydrothermal systems also have background soil-mercury values lower than the minimum value measured at Newberry. The Roosevelt Hot Springs and Dixie Valley mercury anomalies-- which are also major thermal anomalies-- are outlined on their outer margins by mercury levels similar to those at Newberry. Although Roosevelt Hot Springs has a maximum mercury value that is about three times the Newberry maximum, the northern Dixie Valley maximum is similar to that of Newberry.

The other areas listed in Table 6.3 appear to have estimated reservoir temperatures somewhat lower than those at Newberry. They also have correspondingly lower mercury levels.

Mercury anomalies in the areas of Basin and Range faulting were closely controlled by the pattern of faulting which also controlled the hydrothermal systems. Mercury anomalies on the north margin of Newberry caldera and the south flank of the volcano also appear to be controlled by the pattern of faulting.

Conclusions: The background mercury values at Newberry are anomalously high compared to many other geothermal resource areas, with the possible exception of Klamath Falls. The high background and correspondingly high threshold values cause the peak-to-background ratio of the Newberry anomalies to also be somewhat lower than most of the other thermal areas. There is a slight possibility that the high background mercury at Newberry could be partly caused by high original mercury in the unweathered ash component of some of the samples, although the evidence for this is not at all compelling.

The high-temperature (greater than 250° C) Basin and Range hydrothermal systems at Roosevelt Hot Springs and Dixie Valley have soil-mercury anomalies

most similar to those of Newberry volcano.

The smaller maximum mercury value at Newberry relative to the Yellowstone and Long Valley maxima may be partly a function of hydrology. There are very few hot-spring orifices at Newberry, possibly because of rapid laterally flushing ground water. Long Valley and especially Yellowstone are characterized by many more hot springs and accompanying alteration halos than Newberry. It is well known that areas of hydrothermal alteration have anomalously concentrated mercury, commonly in the form of mercury sulfides or oxides. While it is only speculation, it seems likely that, were mercury data from intensely altered areas excluded from the Yellowstone and Long Valley data, the maxima would probably be much more similar to the Newberry maximum.

Anomaly patterns at Newberry, particularly on the southern flank of the volcano, appear to be aligned with regional fault patterns. This is strikingly similar to the mercury-anomaly distribution in areas with deeply circulating, fault-controlled hydrothermal systems of the Basin and Range province.

Influence of Bedrock Geology on Mercury Distribution

The two most compelling correlations between the distribution patterns of mercury and geologic structure are the anomalies on the north to west ring fractures and the zone of high mercury which follows the Walker Rim trend on the south flank (Figure 6.1). There is also a good correlation between an east-west trending ridge of high gravity and the east-west trending mercury high on the east flank of the volcano (see Plates 2 and 4). It seems likely that all of these areas are places of high vertical permeability where mercury vapors can migrate freely into surface soil units.

This may or may not mean that active hydrothermal systems underlie these areas. The demonstrated lack of vertical permeability within the intracaldera Newberry 2 well (Sammel, 1981; MacLeod and Sammel, 1982) suggests the possibility that mercury may migrate laterally or be absorbed by confining layers. Although high temperatures and volatiles were abundant in the Newberry 2 well, the mercury is low in overlying soils (Plate 2). If mercury is present in the gases at Newberry as it is in other volcanic fields, then the impermeable layers must affect its distribution in the same way that they affect the circulating hydrothermal fluids. If extensive lateral displacement

of mercury from its possible hydrothermal source areas has occurred, then the anomalies at the surface may not accurately reflect the location of the deep-seated circulation systems. Likewise, lack of mercury anomalies does not mean that there are no high-temperature fluids or heat sources at depth.

Another variable which must be considered is the possible presence of mercury sulfides and oxides deposited from old extinct hydrothermal systems. As previously explained, oxidation of ore minerals may cause mercury vapors to rise from these areas. These vapors could then migrate into the same zones of high vertical permeability as the vapors of hydrothermal systems. It is also quite possible that many of the faults which correlate with mercury anomalies have been active over a long period of geologic time and have localized ore minerals from earlier hydrothermal circulation.

In spite of the above-mentioned variables, (1) the presence of mercury anomalies following the caldera ring fractures, (2) the faults and volcanic center alignments of the Walker Rim trend, and (3) the east-west ridge of high gravity on the east flank are positive indicators for geothermal exploration. These anomalies strongly suggest that the underlying geologic structures are permeable. Vertical permeability is an important factor controlling hydrothermal circulation, as demonstrated by the previously mentioned Basin and Range hydrothermal systems. Given that the heat flow in this area is likely to be as high or higher than that in the Basin and Range (Blackwell and others, 1978; Blackwell and Steele, Chapter 8), all of the ingredients for active high-temperature hydrothermal circulation systems are present. A particularly attractive target is the area where the Walker Rim trend and associated mercury anomaly intercept the southeast part of the caldera ring-fracture system. This area is also the site of eruption of Holocene rhyolitic domes which may be indications of an underlying shallow magma body (see unit Qyr of MacLeod and others, 1982).

Conclusions

Mercury anomalies on the caldera ring faults, the Walker Rim trend, and the east flank of the volcano are highly favorable indications of high vertical permeability and possible hydrothermal circulation. The latter two anomalies indicate that the south and east flanks of Newberry volcano probably have high potential for geothermal resources. Intersection of the Walker Rim

trend on the southeast part of the caldera ring-fracture system is the site of a mercury anomaly which may be underlain by both high vertical permeability and a shallow silicic magma body. The mercury anomaly on the east flank may be partly the result of primary mercury in underlying pumice, but the evidence for this is not compelling. Some detailed analysis of the pumice may help to clarify the importance of primary mercury.

The ages of the Mazama ash (about 7,500 yr) and the young rhyolitic pumice fall (about $1,550 \pm 120$ to $1,720 \pm 60$ yr) provide maximum ages for the development of the mercury anomalies over most of the study area. High vertical permeability, sufficient to conduct mercury vapor into the overlying soils, must have been present in the areas of anomalous mercury within the last few thousand years. This is important, because zones of permeability can be quickly sealed from precipitation of minerals during hydrothermal circulation. If the source of the mercury vapor is a geothermal system, as seems likely, then the system must have been active very recently and is probably still active.

CHAPTER 7
GRAVITY AND MAGNETIC INTERPRETATION OF
NEWBERRY VOLCANO, OREGON

by
Andrew Griscom and Carter W. Roberts,
U.S. Geological Survey

Introduction

Gravity and magnetic investigations of Newberry volcano, Oregon, were initiated in 1975 as part of the Geothermal Research Program of the U.S. Geological Survey (USGS) with the expectation that these studies would provide useful information concerning the geothermal potential of the area. Analysis of the geophysical data is continuing, and detailed physical property measurements are still being acquired on core samples from two drill holes, Newberry 1 and Newberry 2, on the northeast flank of the volcano and within the caldera, respectively. This report is a summary of the present status of the geophysical study.

Geology

The geology of Newberry volcano has been summarized by MacLeod and Sammel (1982). The volcano "covers an area in excess of 1,200 km² and rises about 1,100 m above the surrounding terrain. The gently sloping flanks, studded with more than 400 cinder cones, consist of basalt and basaltic andesite flows, andesite to rhyolitic ash-flow and air-fall tuffs, dacite to rhyolite domes and flows, and alluvial sediments...The 6- to 8-km-wide caldera at Newberry's summit, which contains scenic Paulina and East Lakes, has been the site of numerous Holocene eruptions, the most recent of which occurred about 1,350 years ago." (MacLeod and Sammel, 1982, p. 236). The caldera is likely "the result of collapse following voluminous tephra eruptions of silicic to intermediate composition from one or more magma chambers below the summit" (MacLeod and Sammel, 1982, p. 237). "The young rhyolites in the caldera ... differ in chemical composition from older

caldera rhyolites ... [and] may be derived from the same magma chamber in as much as they are chemically closely similar and all are aphyric or nearly so. If so, parts of the chamber must have been at or above the liquidus as recently as 1,350 years ago and thus are probably still hot" (MacLeod and Sammel, 1982, p. 239). A generalized geologic map (Plate 3) depicts some of the geologic features that are relevant to the geophysical interpretation: cinder cones, dacite to rhyolite domes and flows, the caldera ring faults, small basalt shields, and older Tertiary volcanic rocks.

Gravity Data

The gravity map (Plate 4) was prepared from 397 gravity stations collected at Newberry volcano (Griscom and Roberts, 1982). The primary base station was California Division of Mines and Geology base station 173 (Chapman, 1966, p. 36) at Menlo Park, California, where the observed gravity is taken to be 979,958.74 mgal. Free-air anomalies were calculated using the International Gravity Formula of 1930, and terrain corrections for all stations to a radial distance of 166.7 km were calculated using a procedure developed by Plouff (1977). Only 15 terrain corrections are in excess of 8 mgal (using a reduction density of 2.67 g/cm^3 , so that the complete Bouguer anomaly values are for the most part accurate to much better than 1 mgal, assuming the maximum error in the terrain corrections to be about 10 percent.

The Bouguer reduction density for volcanic topography of this sort is a matter for concern (Williams and Finn, 1981a,b) in order to ensure that the actual topography of the mountain does not contribute to or distort the Bouguer anomaly. Williams and Finn (1981a,b), using visual comparison of topographic and Bouguer gravity profiles with various reduction densities, arrived at an average density of $2.2 \pm 0.1 \text{ g/cm}^3$ for the volcanic edifice. We have prepared contoured complete Bouguer gravity anomaly maps using reduction (and terrain correction) densities of 2.2, 2.3, 2.5, and 2.67 g/cm^3 and find that the map using 2.2 g/cm^3 shows the least correlation with topography. Hence a density of 2.2 g/cm^3 best represents the higher topography of the mountain, although the flatter shield portion of Newberry volcano may have a somewhat higher density if composed predominantly of lava flows. Measurements on core samples from the hole, Newberry 1, drilled to a depth of 386 m on the upper northeast flank of the volcano (MacLeod and Sammel, 1982), also

yield an average density of about 2.2 g/cm³ (see below).

Because of the above considerations, the gravity map presented in this report (Plate 4) was prepared using a Bouguer reduction density and a terrain correction density of 2.2 g/cm³. The datum level of this map is not directly comparable with other gravity maps of this region that have been prepared using other reduction densities.

Magnetic Data

An aeromagnetic map of Newberry volcano (U.S. Geological Survey, 1979) was flown in 1975 by Aerial Surveys of Salt Lake City, Utah, for the U.S. Geological Survey. East-west flight traverses were flown at an altitude of 2,440 m, and flight spacing is 0.8 km over the higher portions of the volcano and 1.6 km elsewhere. The contour interval of the 1979 publication is 20 gammas, but this map has been generalized to a 50-gamma contour interval (Plate 5) so that it can be compared with a calculated magnetic map (Plate 7) having a 50-gamma contour interval. A somewhat similar map was prepared in 1978 by the Geophysics Group of Oregon State University under the direction of Richard Couch and is illustrated at a scale of 1:500,000 by Connard (1979) and also published in Connard and others (1983). This other map was flown at a flight elevation of 2,740 m and is thus not as detailed as the map by Aerial Surveys.

Densities of Samples from Newberry 1

Dry-density measurements were performed by Robert Sikora on 193 samples taken, where available, at intervals of 1.5 m from the core of Newberry 1. These results have been weighted visually according to the detailed stratigraphy of the core as observed in the core boxes, taking into account the likely low density of the missing portions of the core. Major flows range in density from 2.3 to 2.75 g/cm³. Some of the pyroclastic rocks have densities below 1.5 g/cm³, even at depths below 300 m, and a few samples are as low as 1.1 g/cm³. The resulting average dry density is 2.22 g/cm³ with an unknown but significant uncertainty owing to poor recovery of low-density pyroclastic material. The dry-density measurements were obtained by weighing the samples dry and then, after waxing the surfaces of the core pieces, weighing them both dry and in water and correcting for the added

weight of wax. Dry densities are preferred because although "small amounts of perched water were found in Newberry 1, ...the rocks appeared to be generally unsaturated" (MacLeod and Sammel, 1982, p. 240). The density of 2.22 g/cm^3 then may represent the density of the upper portions of Newberry volcano if the hole is a truly representative sample of the heterogeneous rocks comprising the volcano.

Magnetic Properties of Samples from Newberry 1

Magnetic properties were measured by Katherine Freeman on 135 samples using a magnetic susceptibility bridge and a superconducting magnetometer. The samples were taken, where possible, at intervals of 1.5 m from the core of Newberry 1. Most very friable, low-density pyroclastic rocks were not measured because of the difficulty of drilling the small, 2.5-cm cores from the larger core samples.

The average remanent magnetization is between 3×10^{-3} and $5 \times 10^{-3} \text{ emu/cm}^3$ and is in a normal direction, although information on declination is not available. At least 16 samples are of pyroclastic rocks, and these in general also appear to possess a substantial coherent normal magnetization in agreement with studies by Duane Champion (personal communication, 1983) at Crater Lake, Oregon, which suggest that most pumice and ash-flow deposits have a coherent thermoremanent magnetization. The average magnetic susceptibility is in the range of 0.9 to $1.1 \times 10^{-3} \text{ emu}$ and, after multiplying by the local magnetic field (assumed to be 54,700 gammas), yields an induced magnetization of 0.5 to $0.6 \times 10^{-3} \text{ emu/cm}^3$.

The Koenigsberger ratio (Q) between the remanent and the induced magnetizations provides a measure of the relative importance of the two properties for causing magnetic anomalies. The value for Q for Newberry 1 samples is in the range 6 to 10, so that the susceptibility of the rocks is not especially important. The deepest flows, below 300 m, average about 10, whereas the lowest Q values (averaging 3) are in the lower half of a massive, 60-m-thick flow whose top is at a depth of 200 m. The values of Q do not change with depth, an observation relevant to geothermal exploration, because relatively low-temperature thermal effects can weaken and eventually destroy the thermoremanent magnetization of volcanic rocks while the induced magnetization is less affected, thus lowering the Q .

To summarize the average magnetic properties of the rocks in Newberry 1, about half the rocks are lava flows with normal remanent magnetization and about 60 percent of the remaining rocks possess a normal coherent remanent magnetization. On this basis, the average total magnetization of the rocks sampled by the core is about 3 to 4×10^{-3} emu/cm³.

Gravity Interpretation

Newberry volcano is characterized by a circular gravity high, about 18 mgal in amplitude, concentric with the caldera and approximately 19 km in diameter, measured at the steepest gradients, or approximately 15 km in diameter, measured at the half-amplitude points (located at the -104 mgal contour on the southwest side and the -102 mgal contour on the northeast). These dimensions imply a causative mass substantially larger in diameter than the caldera, and an approximate outline is shown on Plate 6. One possible cause of this gravity high (and the cause of the caldera) is a pluton intruding the older Tertiary volcanic rocks that underlie the volcano, the base of which is believed to be at an altitude of approximately 1,350 m above sea level (Figure 7.1). If the pluton is silicic and at least partly

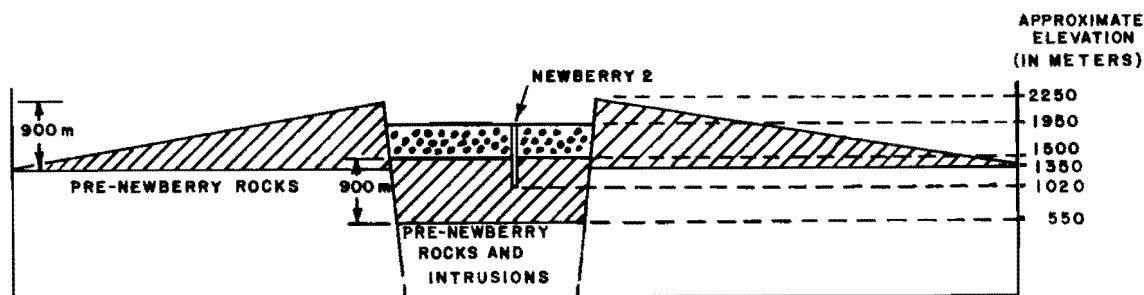


Figure 7.1. Schematic cross section of Newberry volcano, Oregon, showing dimensions in meters and probable position of collapsed central block (from MacLeod and Sammel, 1982, Figure 8).

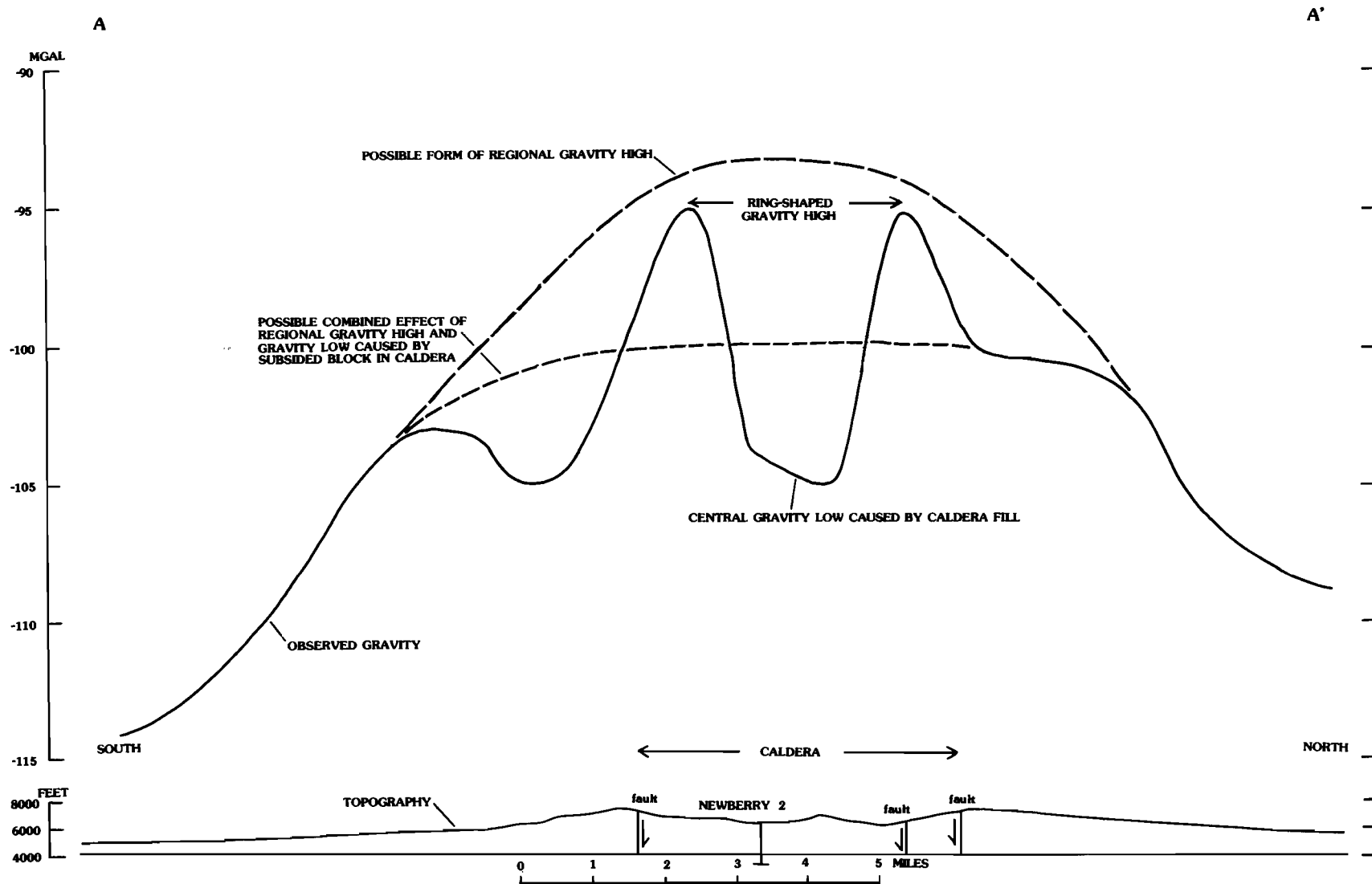


Figure 7.2. Gravity profile A-A' across Newberry volcano, Oregon, showing possible form of regional gravity high and possible gravity effect of subsided central block in the caldera. Profile is located on Plate 4.

molten, its density may be in the range of 2.55 to 2.70 g/cm³; the older underlying volcanic rocks have a bulk density estimated to be in the range of 2.40 to 2.50 g/cm³. Thus the density contrast between this inferred pluton and the older underlying volcanic rocks may be in the range of 0.2 to 0.3 g/cm³. Assuming a spherical shape for the intrusion allows one to calculate some simple constraints on the depth to the top. The following calculations assume a shape for the anomaly that is similar to the upper dashed curve in Figure 7.2.

The depth to the center of a spherical source is 1.305 times the half-width of the associated gravity anomaly measured at the half-amplitude; the resulting depth to the center of the assumed source at Newberry is 9.8 km and is a maximum value. The radius of the sphere depends upon the density contrast between it and the surrounding country rocks. For density contrasts of 0.2 and 0.3 g/cm³, the source sphere radii are 6.7 km and 5.85 km, respectively, and the corresponding depths to the top are accordingly 3.1 km and 3.9 km. Using flatter, more tabular shapes for the causative mass will result in substantially smaller calculated depths to the top, and it should be kept in mind that the actual density distribution of material within the pluton or the country rocks is certainly more complex than the simple models assumed here. If the pluton is partly mafic, its density contrast is probably larger than 0.3 g/cm³, its radius accordingly is smaller than 5.9 km, and its top is deeper than 3.9 km.

The gravity anomaly associated with Newberry volcano has additional shorter wavelength gravity features superimposed upon it that are caused by density variations directly associated with the caldera. A ring- or doughnut-shaped gravity high is located near the inner fault scarps of the caldera (Plate 4). The high has a local amplitude of about 4 to 6 mgal and is about 1.5 km wide. Models calculated for the anomaly indicate high-density masses with widths of 1 to 1.5 km at depths of less than 0.5 km, the models having steeply sloping sides and density contrasts of about 0.3 g/cm³. The approximate boundaries of the sides of this feature are shown as dashed lines A and B on the interpretation map (Plate 6). These results are interpreted to indicate a ring-shaped intrusion lying within the caldera faults; the intrusion could be the source for many of the rhyolite and obsidian domes and flows. Alternatively, some of the higher density material could be the result of hydrothermal mineralization that has reduced the porosity of the volcanic rocks in the vicinity of the faults.

Lying within the circular ring high is a gravity low with a probable

amplitude of about 5 mgal. The low extends from the southeast corner of Paulina Lake to the southwest half of East Lake, and the test hole, Newberry 2, is located near the south border of the low. The lithologic log of the hole (MacLeod and Sammel, 1982) indicates that the first 500 m is composed mostly of low-density pyroclastic rocks that fill the caldera. Density measurements on 109 core samples from this test hole yield an average wet density of $1.96 \pm 0.26 \text{ g/cm}^3$ (1σ) for the interval 313-500 m, and the lithologic description of the upper 300 m of the hole indicates that here the average wet density is probably no greater than 1.9 g/cm^3 . Wet densities are used because much of the core appeared to be relatively saturated when collected, and the lakes imply a shallow water table. Many of the core pieces were bubbling or giving off gas (MacLeod, written communication, 1983), suggesting that water at hydrostatic pressures was in the vesicles and compressing the gases therein. If the density contrast of the caldera fill with respect to the rim rocks is about -0.4 g/cm^3 , then a slab of this material only 300 m thick will produce a gravity low of 5 mgal. The steep marginal gradients on this feature and its subcircular form suggest it is bounded by caldera faults, the approximate locations of which are shown as dashed line B on Plate 6.

Analysis of the above-mentioned smaller gravity features associated with the caldera is hampered by uncertainty of the form of the larger gravity high associated with Newberry volcano. This high is a regional feature that more properly should be removed from the data in order to isolate the smaller features for analysis. The crudely circular forms of the concentric contours (-100, -98, -96 mgal), where located adjacent to the caldera on the west side, show that this larger high attains peak values of at least -95 mgal and that within the caldera such peak values are possible but uncertain because of the superimposed lows caused by different sources. An additional problem is created by the uncertain gravity expression of the collapsed block that occupies the floor of the caldera (Figure 7.1). This block of material may have a wet density of 2.34 g/cm^3 (equivalent to the dry density of 2.22 g/cm^3 from Newberry 1) and has subsided a minimum of 800 m into the older pre-Newberry volcanic rocks. The density of these older rocks is unknown but may be in the range 2.40 to 2.50 g/cm^3 , or approximately 0.1 to 0.2 g/cm^3 more than the Newberry rocks. Assuming a slab of subsided material 800 m thick, these density contrasts yield a gravity low of about 3 to 7 mgal, the marginal gradients of which would

extend about 2 to 3 km beyond the caldera faults. This anomaly, if present, would be approximately superimposed upon the top of the larger gravity high, and a pair of these possible anomaly shapes is illustrated by dashed lines in Figure 7.2, a gravity profile (Plate 4) trending northeast across the caldera. Note that the difference between these two dashed lines is about 6.5 mgal, a reasonable value for the hypothetical gravity low associated with the subsided central block. It seems likely that this observed gravity profile is indeed some combination of the large high with a superimposed low caused by a subsided block, but the available data certainly do not prove this interpretation.

Other gravity features on the map (Plate 4) include the following:

1. A broad gravity ridge, about 10 mgal in amplitude, extending N. 20° W. from the caldera. This ridge is generally associated with the northwest-trending rift zone and the field of cinder cones on this side of the volcano. The anomaly source may be mafic intrusive rocks, perhaps a swarm of dikes. The feature extends (Pitts, 1979) all the way to the Three Sisters volcanic area, a distance of more than 60 km.
2. Small, closed gravity lows associated with individual gravity stations on cinder cones and caused by the low density of the material. Four examples (Plate 6, feature D) occur on the north flanks of the volcano.
3. Gravity anomalies probably caused by density variations within the older volcanic rocks upon which Newberry volcano is constructed. For example, a circular gravity nose (also with an associated magnetic high) is located at lat. 43°39'N. long. 121°23'W. and is probably caused by an older mafic intrusion beneath the southwest flank of the volcano.
4. A gravity gradient sloping down to the west border of the map and probably caused by the low-density fluvial and lacustrine deposits in the Deschutes River valley.
5. A gravity nose at least 13 km long extending to the southwest corner of the map and caused by buried volcanic rocks that are faulted along northeast trends parallel to the Walker Rim fault system (faults shown on Plate 3).

General Magnetic Interpretation

The magnetic map (Plate 5) displays an irregular pattern of magnetic highs and lows that is typical of volcanic terranes. The area of more intense shorter wavelength anomalies in the center of the map correlates with the higher portions of Newberry volcano above 1,830 m and in general is caused by the relative proximity of this area to the aircraft performing the survey. The interpretation of this area associated with the caldera is deferred to the subsequent section.

The base of the Newberry volcanic edifice (Figure 7.1) is at or below an approximate elevation of 1,350 m. Inspection of the magnetic map indicates that most magnetic anomalies on the outer slopes of the volcano below about 1,830 m (this contour is shown generalized on Plate 6) are of relatively long wavelength and are thus probably not produced by the volcanic rocks of Newberry volcano, which here must be less than 480 m thick. Most of these longer wavelength magnetic features are probably produced by the older rocks, mostly volcanic, that underlie the volcano. Only four magnetic features are clearly correlated with rocks exposed at the surface (see geologic map, Plate 3). Two rhyolite domes (anomalies 1 and 2, Plate 6) cause magnetic lows and thus may possess reverse remanent magnetization. Measurements on rocks from the dome of anomaly 2 indicate it is reversed (MacLeod and others, 1982). These two domes may therefore be more than 700,000 years old, the time of the most recent reversal of the earth's magnetic field. A K-Ar age for McKay Butte (anomaly 1) is 0.60 ± 0.10 m.y. (MacLeod and others, 1982). A third dome (anomaly 3) has a weak magnetic high. Anomaly 4 is caused by a small basaltic shield volcano. The chains of cinder cones and the associated rifts do not appear to cause magnetic features on the map.

One circular magnetic high (anomaly 5) is associated with a local gravity high and has a concealed source, probably a small older intrusion 3 to 5 km in diameter. The linear magnetic high (anomaly 6) extending south from the caldera for a distance of about 8 km is caused most likely by rocks older than the caldera, although the local circular high at the north end of the feature is probably the superimposed effect of the topographic high at the caldera rim.

In the section on gravity interpretation, a substantial 18-mgal gravity high associated with Newberry volcano is interpreted as a large, relatively shallow pluton, centered beneath and substantially larger in diameter than

the caldera (see Plate 6). After comparing the gravity map (Plate 4) with the aeromagnetic map (Plate 5), there is little evidence that this large inferred pluton has any magnetic expression, even though the pluton has in the past erupted magnetic volcanic rocks with compositions ranging from silicic to mafic. The southwest quadrant of the gravity feature is associated with a general magnetic field of perhaps 200 gammas, which may be caused by the source of the gravity anomaly but which could also be caused by older rocks. A reasonable conclusion is that most of the inferred pluton is still too hot (above the Curie temperature of magnetite, 580° C) to display any magnetization. Alternative conclusions that are less convincing to the writers include the following possibilities: (1) the pluton is simply not magnetic; (2) alteration has destroyed the magnetite in the pluton; and (3) no pluton exists, and the gravity high has a different cause, such as filling of the pore spaces by hydrothermal alteration in the volcanic rocks beneath the caldera.

Magnetic Interpretation of the Caldera Area

The topographic depression within the caldera plus the magnetic volcanic rocks rimming it can be expected to cause a local magnetic low surrounded by a crescentic magnetic high. Accordingly, we digitized the topography of the mountain at ¼-minute intervals (i.e., rectangles approximately 500 by 300 m) and calculated the magnetic expression of the volcanic topography at an altitude of 2,440 m, using a program written by Blakely (1981) and assuming a magnetization of 4×10^{-3} emu/cm³ in the direction of the present earth's magnetic field. The assumed magnetization is based upon the results measured on samples from Newberry 1 and upon comparison of the calculated anomalies with the observed magnetic anomalies associated with the caldera rim; the assumed magnetization is deliberately chosen to be a maximum value. The results of the calculation (Plate 7) indicate a ring-shaped magnetic high, open to the west and ranging from about 250 to 750 gammas in amplitude along the anomaly crest. The calculated central low has an amplitude of -50 gammas. The calculation is in reasonable agreement with the average magnetic anomalies caused by the caldera rim but fails to produce a central low of sufficient amplitude to match that of the aeromagnetic map (anomaly 7, below -300 gammas). The observed central magnetic low, anomaly 7, extends well beyond the central gravity low so that nonmagnetic caldera fill is not a sufficient explanation for the magnetic low. An approximate two-dimensional

calculation (Figure 7.3) along a northeast-trending profile (A-A') on the magnetic map (Plate 5) indicates that beneath the central magnetic low the volcanic rocks within the caldera are less than half as magnetic as the rim rocks down to depths of at least 600 m below the surface. Results measured by Katherine Freeman on magnetic properties of 169 samples from Newberry 2 indicate an average total magnetization of about 1×10^{-3} emu/cm³ for the interval 314 to 502 m and about 2.3×10^{-3} emu/cm³ for the predominantly massive flows in the interval 502 to 630 m. These measured physical properties confirm the magnetic calculations and are significantly smaller than the magnetizations of 3 to 4×10^{-3} emu/cm³ both measured and calculated for the higher portions of the volcano. The major difference between the magnetic properties of the two groups of rocks is that the remanent magnetizations are substantially less within the caldera than are those of the rim rocks. In other words, the average Q for the interval 314 to 502 m is only about 2 for Newberry 2, compared to the value of 6 to 10 for Newberry 1. This difference may be caused by low-temperature alteration of the rocks in this thermally active area that has partially destroyed the relatively sensitive remanent magnetization. Thus, the magnetic low within the caldera is certainly in part due to the fact that the rocks have weaker magnetic properties, probably due to thermal alteration. However, the magnetic calculations along the northeast-trending magnetic profile identified one area as having nearly nil magnetization, and thus it is possible that some of the rocks may, in addition, be heated above their Curie temperature, although rock alteration may be a sufficient explanation.

Three minor magnetic highs or ridges within the caldera (anomalies 8 to 10) are outlined on the interpretation map (Plate 6) and are associated with three of the major obsidian flows. The large central pumice cone which has local relief of 185 m produces little, if any, anomaly. Anomaly 11 is caused by the domes on the southwest side of Paulina Lake.

The southern half of the ring gravity high, previously described as possibly being caused by a shallow intrusion in the caldera border faults, lies within the magnetic low of the caldera and does not appear to cause a magnetic anomaly. This gravity feature lies beneath the source vents of several young flows and domes, so perhaps its source is still hot and above the Curie temperature of magnetite, thus causing no magnetization.

Local magnetic irregularities, short-wavelength highs and lows, are found at and outside of the topographic rim of the caldera. These are typical

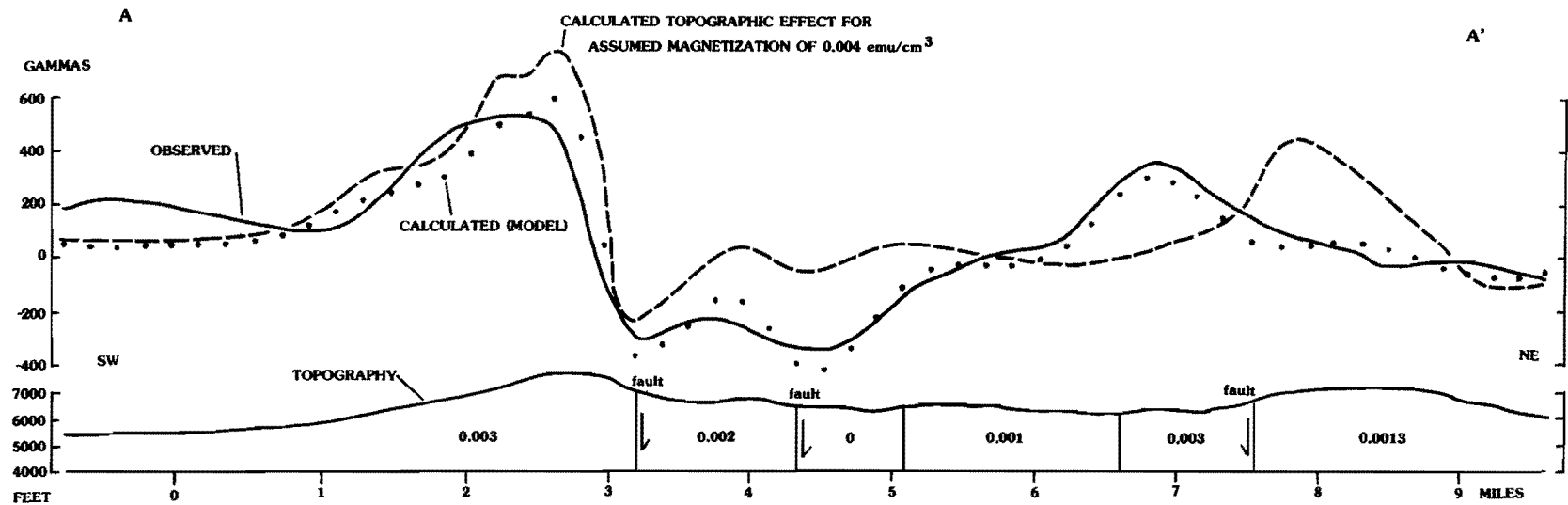


Figure 7.3. Aeromagnetic profile across Newberry volcano, Oregon. Shows observed profile, calculated two-dimensional profile from topography alone for an assumed magnetization of 4×10^{-3} emu/cm³, and a profile calculated from an assumed two-dimensional model of the volcano containing different blocks bounded in part by caldera ring faults and having different magnetizations, all in the direction of the earth's present field. Profile is located on Plate 5.

features of volcanic terranes and express the substantial local variations in average magnetic properties of the individual rock units. Many of the magnetic lows are explained as the usual polarization features observed on the north side of magnetic highs as a result of the inclination of the earth's field at these magnetic latitudes. However, at least six magnetic lows on the caldera rim are not easily explained as associated with magnetic highs and are numbered from 12 to 17 on the interpretive map (Plate 6) for purposes of discussion. Lows 12, 13, and 14 are probably caused by reversed remanent magnetization of rocks at or near the surface. Low 15 is associated with a topographic high, the flat-topped nose of a ridge, and is therefore probably also due to reverse remanent magnetization. However, lows 15 and 16 are colinear with a northeast-striking low within the caldera (Plate 5) and low 12 is similarly colinear with a northwest-striking low within the caldera, so these magnetic-low features may possibly be from alteration associated with fractures radiating from the caldera that has caused the rocks to become nonmagnetic. Newberry 1 is near anomaly 16 and detected no high temperatures. Also, core samples from Newberry 1 (described earlier) have significantly higher Q values than the samples from Newberry 2, indicating that the rocks of Newberry 1 may never have been exposed to heating. If some of these magnetic features are indeed caused by reversed remanent magnetization, then they imply the presence of rocks older than 700,000 years in the upper edifice of the volcano. Magnetic low 17 is of possible geothermal interest because it is associated with a relatively young volcanic area of the northwest rift zone and so may well be caused by a local mass of relatively nonmagnetic rocks, presumably either altered rocks or rocks perhaps at present heated above their Curie temperature (580° C for pure magnetite). A small gravity high (gravity anomaly C, unfortunately defined by only one station) appears to correlate with the magnetic low and may be caused by a local intrusion associated with the vents.

CHAPTER 8
THERMAL MODELS OF THE NEWBERRY VOLCANO, OREGON

by

David D. Blackwell and John L. Steele,
Department of Geological Sciences,
Southern Methodist University

Introduction

Newberry volcano is a major, young volcanic feature in central Oregon, approximately 40 km south of Bend. It is located approximately 30 to 40 km east of the axis of the High Cascade Range and near the west end of the Brothers fault zone, a major northwest-southeast-trending zone of normal faulting and young volcanism in central Oregon. Various people have related the Newberry volcano to either or both of these tectonic and volcanic trends. The volcano has been studied by several people, including Williams (1935) and Higgins (1973). More recently, an extensive mapping project has been completed (MacLeod and others, 1982). The overall results and some preliminary conclusions have been discussed by MacLeod and Sammel (1982). The geologic summary in this report is based on the work of MacLeod and others (1982). During the last several years, two holes have been drilled on the volcano. One on the northeast slope of the volcano was drilled to a depth of 386 m, and one near the center of the caldera was drilled to a depth of 392 m. These holes give us some information on the thermal structure of the volcano.

The shape of the volcano is a broad shield with low-angle slopes (see Figure 8.1). An elliptical caldera caps the volcano. The radius of the caldera is 6 to 8 km, and the typical relief between the caldera floor and rim is 200 to 250 m. Two lakes (Paulina Lake and East Lake) are located in the caldera, divided by a septum of young volcanic rocks. The latter are about 100 m deep, so that the total relief of the caldera is about 300 to 350 m. Most of the cone is covered by basaltic volcanic rocks and cinder cones, and Newberry has been referred to as a basaltic shield volcano. However, detailed mapping indicates that a significant amount of the volcano is composed of domes, flows, and pyroclastic rocks of intermediate and silicic composition. Andesites and dacites are also locally exposed.

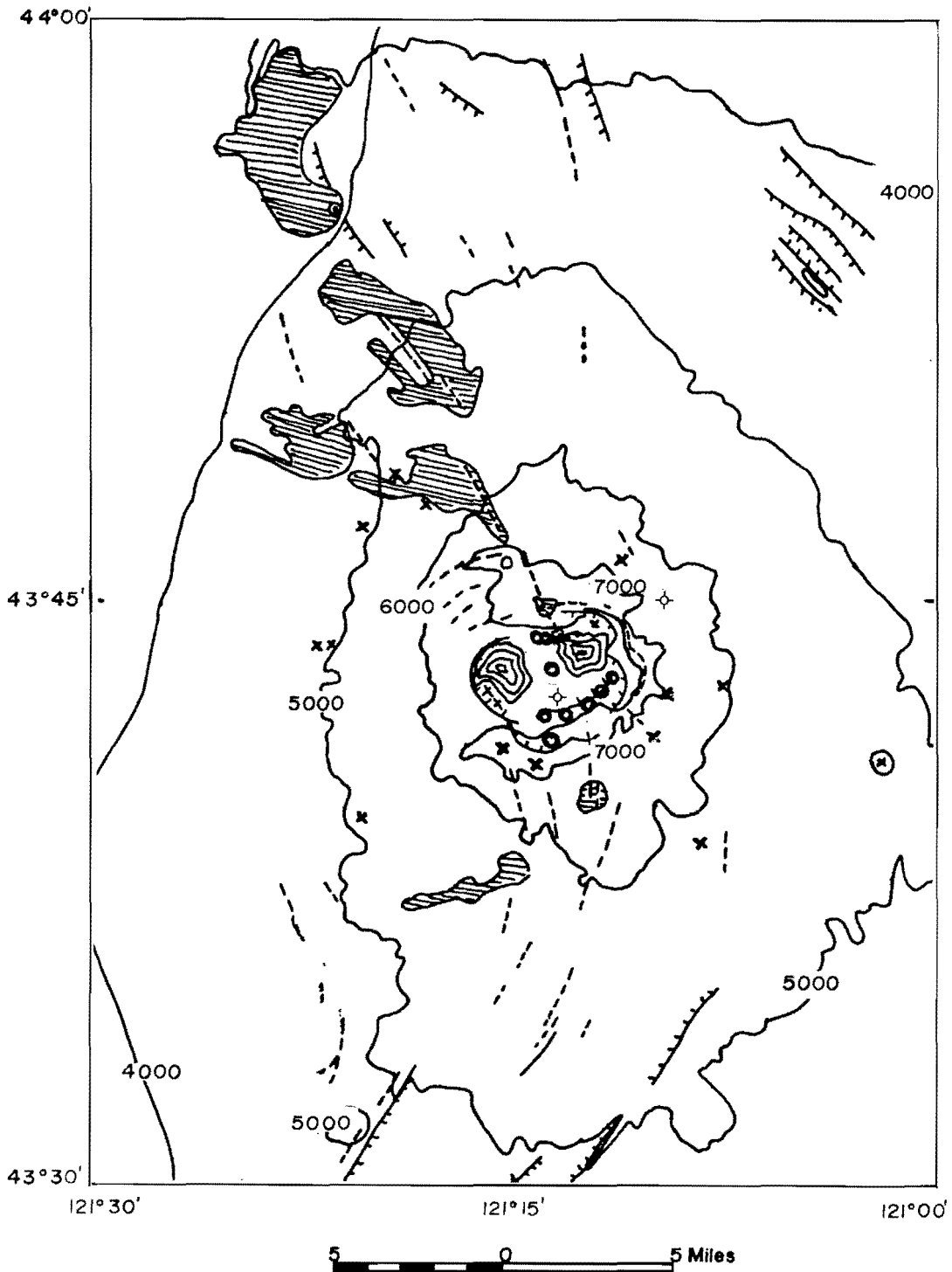


Figure 8.1. Generalized geology and topography of the Newberry volcano (contours in feet above sea level). The topography is from the 1:250,000-scale topographic map. Geology is generalized from MacLeod and others (1982). Hatched lines are normal faults; dotted lines are lineaments of basaltic volcanic centers; areas with parallel lines are basalts associated with the 6,000-year-old extrusive episode; silicic sources older than the 6,000-year-old basalts are shown as X's; silicic centers younger than 6,000 years are shown as circles. The locations of the two drill holes on Newberry volcano are shown by a dry-hole symbol (\oplus).

Table 8.1. Radiometrically dated volcanic units (taken from MacLeod and others, 1982).

Age(yr)	Composition	No. of units	Type	Location
1,300	Rhyolite	2	Flow and air-fall tuff	Caldera
1,600	Rhyolite	1	Pumice	Caldera
3,500	Rhyolite	1	Flow	Caldera
4,500(6,700)	Rhyolite	1	Flow	Caldera
5,800-6,200	Basalt	14	Flows and cinder cones	North and south flanks
6,700	Rhyolite	5 or 6	Flows and pumice	Caldera
6,800	Rhyolite	3 or 4	Pumice deposit	Caldera
<6,850	Rhyolite	-	Tephra	Extensive
- - - - - (MAZAMA ASH - 6,845 ± 50 yr) - - - - -				
8,000-15,000	Basalt	-	-	North and south flanks
"Lower Holocene"	Rhyolite	-	Domes and flows	Caldera and southeast flank
70,000 ± 120,000	Rhyodacite	1	Tephra	-
	Rhyolite	-	Flow	-
0.20-0.57 m.y.	Rhyodacite	-	Domes and flows	-
0.5 m.y.	Rhyolite	-	Ash flow	Teepee Draw
0.6-0.87 m.y.	Rhyolite	-	Domes	China Hat, East Butte, McKay Butte

Geology and Volcanic History

The geology and volcanic history will be briefly discussed in order to present the basis for the thermal modeling. The volcanic history is summarized, based on the work of MacLeod and others (1982) as shown on Table 8.1. Numerous carbon-14 dates have proven that the volcano has been very active in the last

7,000 years. About 6,000 years ago, there was a major episode of basalt extrusion represented by 14 different flows and many cinder cones and vent areas. These basaltic extrusives were primarily located north-northwest and south-southwest of the caldera, although one of the vents extended almost to East Lake. Just predating the 6,000-year-old basalts was an episode of silicic volcanism represented by six pumice deposits and three rhyolite obsidian flows. Beneath all these units and above all the older units is the marker bed of the Mazama ash from the eruption of Crater Lake (carbon-14 age of approximately $6,845 \pm 50$ years).

For the purpose of this discussion, the most significant features are the presence of five discrete rhyolite obsidian domes, flows, and ash falls which are younger than 5,000 years. The youngest of these are the Big Obsidian Flow and the Paulina Lake ash-flow and air-fall tuff, which have carbon-14 dates of 1,350 to 1,750 yr B.P. The vent areas of the youngest rhyolitic rocks are inside the caldera.

The eruption of the basalts was associated with an extensive set of volcanic vents and faults along the northern and southern flanks of the mountain. These features are shown in Figure 8.1. Solid lines are fault zones, and dashed lines are lineaments of basaltic cinder cones and vent areas. The basalt flows associated with the 6,000-year-old extrusive episode are shown. Young silicic vents, where identified, are shown as X's (>6,000 years) and circles (<6,000 years).

There are several rhyolite domes that have been dated at 50,000 to 250,000 and more years in age. Several of these domes are in the caldera, but many of them are outside the caldera. Somewhat older ash-flow tuffs are exposed on the east side of the caldera and rhyolite domes on the periphery of the volcano such as China Hat, East Butte, and McKay Butte. The ages of these rocks range from 0.5 to 0.9 m.y. Based on the results of mapping, MacLeod and others (1982) suggested that initial caldera formation may have been associated with the ash flow of Teepee Draw and with other as yet undated ash flows. The Teepee Draw ash flow has an age of 0.5 m.y.

The Newberry volcano sits at a very interesting structural location. It appears to be more or less in the corner of, or the intersection of, two major trends of extensional faulting. One of these is the Brothers fault zone, which trends northwest-southeast through central Oregon, rotating to a north-northwest, south-southeast trend as it approaches the Cascade Range. The second is a less prominent north-northeast, south-southwest trend extending from Newberry to

Crater Lake (see Figure 8.1). It is possible that this structural intersection has had a major influence on the location of the Newberry volcano either by localizing the source of the magma intrusion in the crust or by localizing the spot where magma is able to reach the surface from a deep, large magma chamber.

It seems clear from the volcanic history that there has been a significant amount of silicic magma present beneath the volcano for at least the past 7,000 years. Whether this is the same magma that was tapped by earlier extrusive episodes has not yet been determined. At the present time, because no geothermometry or geobarometry has been done on the volcanic rocks, we have no petrologic estimates of the possible depth to any magma chamber that might exist.

Geophysics

The regional geophysics of the Newberry area has been extensively studied and is briefly reviewed here. Some detailed information has been published on the Newberry volcano itself but, in terms of the nature of the heat source beneath the volcano, the results are inconclusive. Some of the results of regional gravity studies have been published by Pitts and Couch (1978). Analysis of the data has been discussed by Couch (1979) and by Murphey (1982). On a regional basis, the Newberry area is underlain by relative positive anomaly with the amplitude of approximately 10 mgal. The center of the positive anomaly is 2 or 3 km west of the western edge of the caldera, and the diameter is about 10 km. The positive gravity anomaly is part of a trend that is elongated in a north-northwest to south-southeast direction and that can be followed as far as the area immediately west of Green Ridge. The Three Sisters volcanic complex is along this gravity trend. The trend ends south of Newberry volcano, where the trends in the gravity field are more northeast-southwest, and thus may reflect the change in structural setting indicated by mapped faults.

Williams and Finn (1982; see also Finn and Williams, 1982) and Griscom and Roberts (Chapter 7) have discussed the gravity data for the Newberry volcano. The data have been interpreted by Williams and Finn (1982) in terms of a mass with a depth extent of approximately 2 km, a diameter of approximately 15 km, and a top on the order of 2 km deep at its shallowest point. Griscom and Roberts (Chapter 7) interpret the high as being due to a magma chamber with a density contrast of +0.2 to 0.3 g/cm³ and, if spherical, a depth to the top of 3 to 4 km, a radius of 5.9 to 6.7 km, and a depth to the center of 9.8 km

(maximum value). They further suggest that the temperature of the chamber is above 580° C, because of the lack of an associated magnetic anomaly. There is no evidence from the gravity data of a large, low-density body at depth beneath the volcano. But because of the complexity of the gravity pattern, such an anomaly cannot be ruled out.

Iyer and others (1982) discussed a study of regional P-wave travel-time residuals for the Cascade Range and the results of a detailed study around Newberry volcano. They found a slightly higher average velocity along the west flank of the volcano, approximately near the peak of the gravity anomaly. Elsewhere, very low-amplitude, slightly slow arrivals extend in a ring around the volcano, except on the west-southwest sides. The interpretation of the seismic data is consistent with the interpretation of the gravity data by Williams and Finn (1982). On a regional basis, Iyer and others (1982) observed P-wave delays associated with the region of the volcano which are consistent with existence of a regional zone of high temperature or partial melting in the upper crust, similar to interpretations of Blackwell and others (1978, 1982b).

Couch (1978) carried out a gravity and aeromagnetic study of the Newberry volcano, and interpretation of this aeromagnetic study was discussed in a subsequent paper (Couch, 1979). In general, high-amplitude magnetic anomalies are associated with the Newberry volcano and are caused by relatively shallow sources. A Curie-point depth analysis in the vicinity of the Newberry volcano suggested a depth to the Curie temperature of 6 km below sea level. Couch (1979) also suggested that the Curie temperature might be 580° and pointed out that the results of that study are consistent with the regional interpretations of the heat-flow data.

Regional magnetotelluric studies (Stanley, 1982) are consistent with the results of the heat-flow and the Curie-point determinations. Unusually low resistivity values are located near the station that was closest to the Newberry volcano. The data were not interpreted as suggesting the presence of a large-scale magma chamber, however.

Heat-flow data on or near the volcano are sparse. Regional data indicate that the Brothers fault zone has a high heat flow (averaging about 1.9 HFU) based on the work of Hull and others (1977). The heat flow in the Cascade Range is even higher (2.5 HFU, with gradients of 65° C/km) as discussed by Blackwell and others (1978, 1982b). The lack of water wells in the area and the great depth necessary for useful heat-flow measurements result in a lack of data near the important thermal/tectonic intersections at the Newberry

volcano. Background heat flow and gradients can be expected to be 1.9 to 2.5 HFU and 40° to 65° C/km.

Characteristics of the Volcano

A summary of some of the information known about the volcano is shown in Figure 8.2, a cross section with vertical exaggeration through the volcano. Included are somewhat generalized north-south and east-west cross sections. The volcano slope is more gentle to the north and to the south, where the buildup of volcanic rock associated with the basaltic extrusive activity has been more pronounced. The west slope is the steepest of all the sides and is also the only side that has no significant covering of basalt. The surface there is composed almost exclusively of pyroclastic rocks. Based on geologic mapping, MacLeod and others (1982) have located the base of the volcano (the pre-existing surface) at an elevation of approximately 1,350 m. This contact is shown on Figure 8.2. In the caldera, this horizon has been downdropped to approximately 550 m, and there is approximately 500 m of caldera fill. The approximate position and depth of the two drill holes on the volcano are also shown on Figure 8.2. The closest approach to the caldera of the 6,000-year-old basaltic activity is also shown on the cross section, as are the locations of the silicic extrusive activity within the last 6,000 years. The caldera is slightly ellipsoidal, but a circle with a diameter of 3 to 4 km (much smaller than the caldera) includes the sources of all of the youngest rhyolite vents. A circle with a radius of 5 to 7 km would include the caldera and the closest vents associated with the young basaltic activity. As noted above, at the north rim, basaltic volcanic activity extended almost to the floor of the caldera.

Away from the volcano, near the regional background elevation, the ground-water table is at an elevation of approximately 1,300 m (Black, Chapter 4). A local perched water table in the caldera is near the surface, as indicated by the existence of East Lake and Paulina Lake. The water-table configuration between the caldera and the flanks is unknown and is likely to be very complex. There are probably many perched water zones, and the flow pattern cannot be inferred from the data that are now available except in a very general way. The regional trend of the water table is from south to north toward Bend and toward the valley of the Deschutes River (Black, Chapter 4). Regional data show that there is significant lateral flow of ground water through the porous, young basalts characteristic of the Deschutes River valley and that the underlying geothermal character of the rocks is completely masked in holes 100 to 300 m

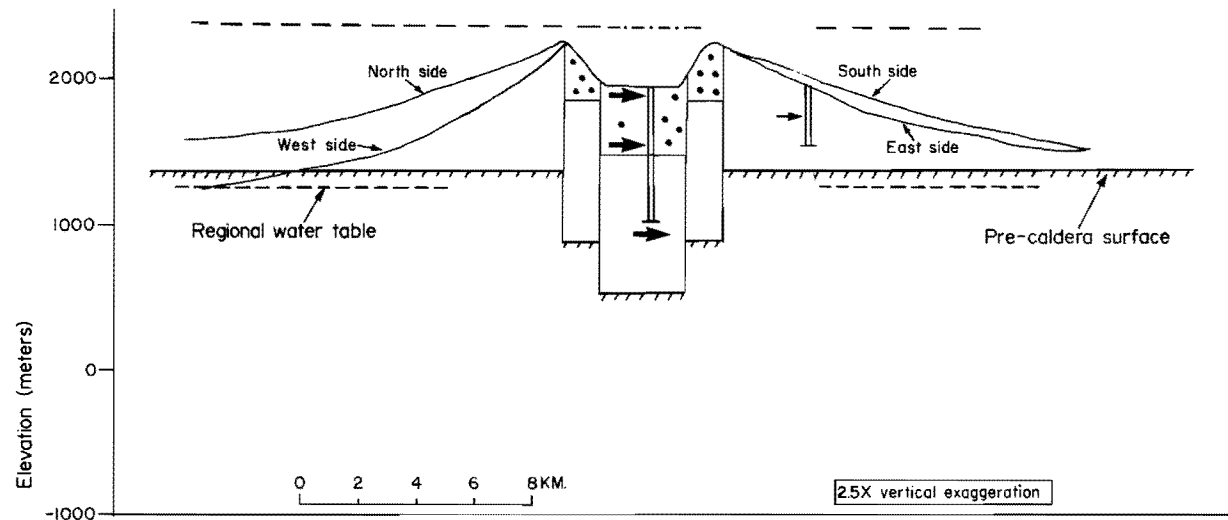


Figure 8.2. Topographic and hypothetical geologic section of Newberry volcano. Generalized topography of each side is shown. The geologic section is generalized from MacLeod and Sammel (1962). Location and approximate thicknesses of the caldera-fill volcanic rocks associated with volcano and prevolcano rocks, the regional water table (Black, Chapter 4), and the position and depth of the drill holes on the volcano are shown. Possible laterally flowing hot aquifers, as indicated by the drilling, are shown by arrows. Dotted horizontal lines above the sides of the volcano show the lateral extent of 6,000-year-old basaltic rocks. The dash-dot line above the caldera shows the extent of silicic volcanic centers younger than 6,000 years.

deep (DOMAGI and SMU, unpublished data). Because the flanks of the volcano are composed of extensive pyroclastic flows and interbedded basaltic volcanic rocks, the volcano is extremely porous. The horizontal permeability is probably much greater than the vertical permeability, as is typical of volcanic rocks. Lateral fluid flow away from the caldera might be more uniform in the eastern and western sides of the mountain than on the complexly intruded and faulted northern and southern sides.

The locations of major aquifers intersected by the drill holes are shown by small arrows at appropriate depths in each drill hole. The temperature data from the two drill holes are shown in Figure 8.3 (see Sammel, 1981). The hole on the east flank of the volcano (Newberry 1) indicates general regional downflow or lateral flow of water. It is not clear if the water table was ever actually penetrated by the hole. There is evidence for lateral flow of slightly warm water, as indicated by the spike on the temperature curve at a depth of 150 m. The overall gradient is quite low, and the gradient in the bottom of the hole (about 50° C/km, MacLeod and Sammel, 1982) is at or below the regional average.

The temperature pattern for the caldera hole is very complicated. The hole passes through shallow lateral flow of warm water at a depth of only 40 m. This warm water is undoubtedly associated with the flow system causing the hot springs along the banks of East Lake and Paulina Lake with the reported fumarole approximately 1 km from the drill hole at the edge of the Big Obsidian flow. Another major aquifer occurs in the hole in the depth range 400 to 460 m. In that aquifer, the water has a temperature of approximately 100° C, and either the aquifer is closely bounded on either side by cold aquifers or the warm water in the aquifer has only very recently been injected into this aquifer and the shape of the curve is due to transient heating (see the model discussed by Ziagos and Blackwell, 1980a). Below 640 m, temperatures increase rapidly to 265° C at the bottom of the hole (930 m). MacLeod and Sammel (1982) have interpreted these data to indicate an overall geothermal gradient for the caldera of approximately 285° C/km and projected a temperature of about 500° C at the base of the collapsed caldera block. It is likely that geothermal-fluid circulation is responsible for the high temperatures at the bottom of the hole and that temperatures will become nearly constant when the geothermal system is encountered. Typical temperatures are less than 350° C. Once the geothermal system is penetrated, the temperatures may remain isothermal at depths of 3 or 4 or more kilometers. MacLeod and Sammel (1982) concluded that a hydrothermal convection system probably lies below

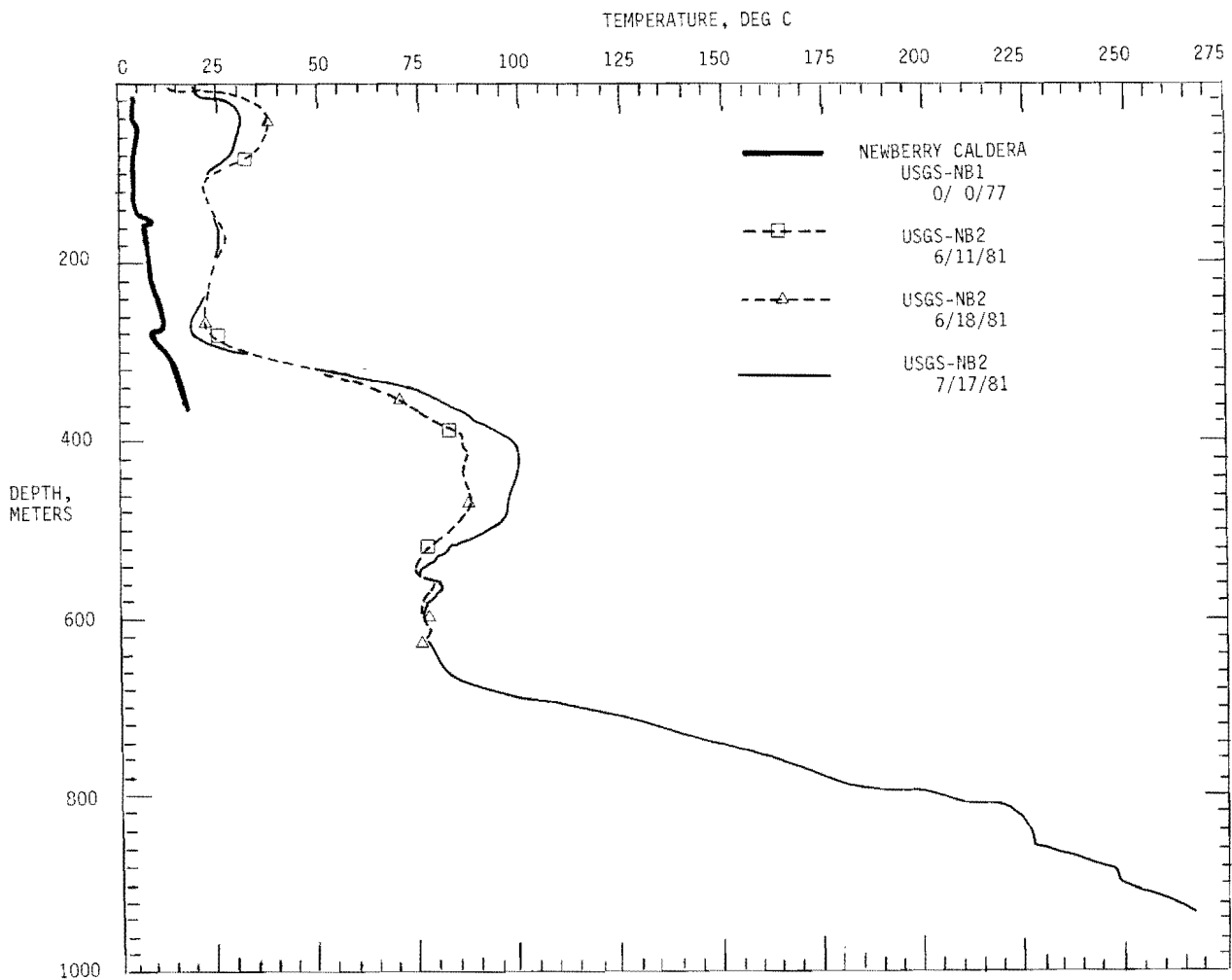


Figure 8.3. Temperature-depth curves for the Newberry volcano holes. The hole on the flank of the volcano is indicated as NB-1. Three logs for the hole in the volcano are shown. The temperature data above 800 m were collected by Jerry Black, David Blackwell, and Robert Spafford. The temperature data in the bottom of the hole are bottom-hole temperature measurements (Sammel, 1981; MacLeod and Sammel, 1982). The upper part of the curve on 7/17/81 is somewhat disturbed by drilling and has less relief than the equilibrium curves measured just before drilling started in 1981 (6/11/81 and 6/18/81).

the base of the collapsed block.

We do not yet know how to interpret the rate of heat loss from a geothermal system in terms of the depth of the magma chamber or heat source which powers the geothermal system. If, for the moment, we ignore the probability that the high gradient at Newberry 2 is caused by a convection system, and if we assume that the magma chamber behaves as an instantaneous heat source, then the depth to the source based on an assumed gradient of 285° C/km (MacLeod and Sammel, 1982) could be as shallow as 1.7 to 2 km, because the maximum contact temperature of such a magma chamber is only one-half of the melting temperature (Lachenbruch and others, 1976). Hence, we would need to extrapolate the overall geothermal gradient of 285° C/km only to a temperature of about 400° to 500° C. If the magma chamber were old enough to have cooled off significantly, then it could be even shallower. Definite evidence of emplacement of a significant volume of shallow magma does not exist, however. For example, no pistonlike uplift of the caldera associated with the recent silicic volcanic activity has been documented, although relaxation of magmatic forces following this activity could have removed any evidence of uplift.

Thermal Models

Because there are only weak constraints on the location and size of potential magma chambers associated with the Newberry volcano, we are forced to reason by analogy with other types of systems. However, Newberry is a somewhat unusual type of volcano, and there are few examples that are directly relevant to this particular volcano. Medicine Lake Highlands in northern California is a nearly identical topographic feature with similar compositions of extrusive volcanic rocks. However, not much more is known about the Medicine Lake volcano than is known about the Newberry volcano. For comparison, a topographic map of Medicine Lake Highlands at the same scale as Figure 8.1 is shown in Figure 8.4. Geothermal-gradient drilling associated with the geothermal exploration efforts of several companies is currently proceeding at that volcano. However, these data have not been released and cannot be used in attempting to constrain possible magma chambers associated with the Newberry volcano. A cross section through the Newberry volcano with no vertical exaggeration is shown in Figure 8.5. The same information is shown as was shown in Figure 8.2, but there is no vertical exaggeration in Figure 8.5.

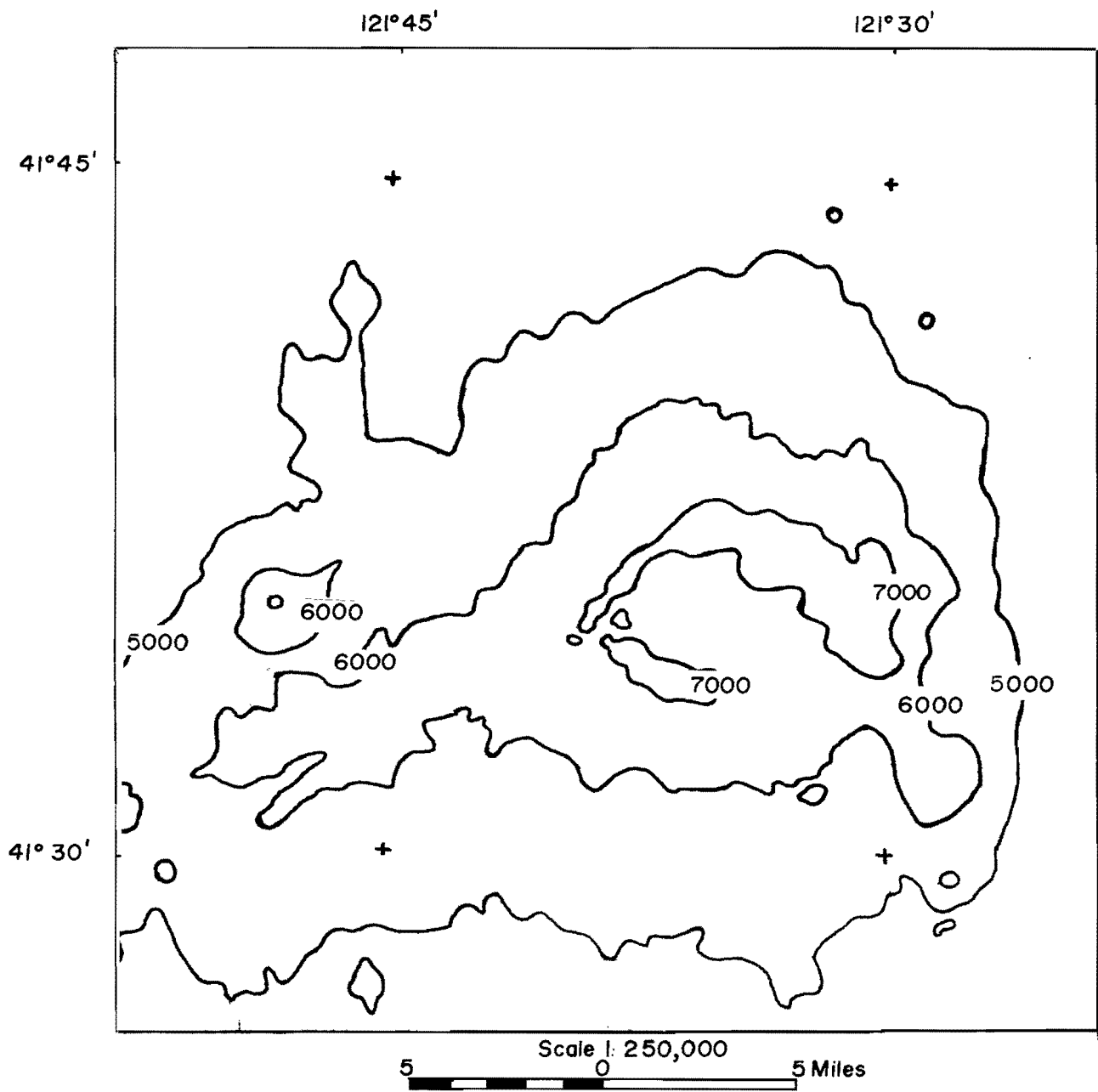


Figure 8.4. Generalized topographic map of the Medicine Lake volcano in California. This map is at the same scale as the map of Newberry volcano shown in Figure 8.1, and the contours (in feet above sea level) have also been generalized from the 1:250,000-scale topographic maps.

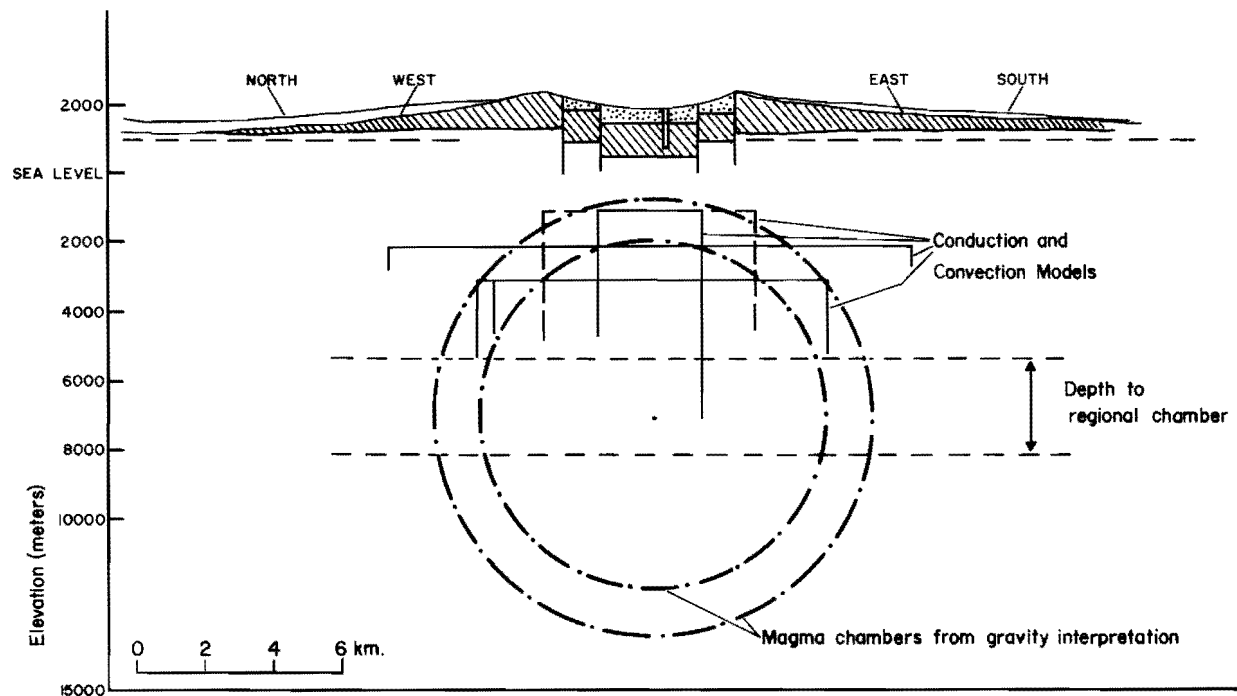


Figure 8.5. True-scale cross section of Newberry volcano showing various possible geometries for magma chambers. The parallelepiped models used in this study are indicated, as are the chambers interpreted by Griscom (Chapter 7) and Finn and Williams (1982) on the basis of gravity data.

Several different magma geometries were modeled, as indicated in Figure 8.5. The assumed magma chambers were as shallow as 3 km and as deep as 5 km. Heat-flow data from Blackwell and others (1978, 1982b) suggested that the High Cascade Range is underlain by a large regional heat source at a depth of 7 to 10 km. Thus 10 km would be the maximum depth to any large magma chamber that might occur beneath the Newberry volcano. The minimum diameter is assumed to be constrained by the size of the subsided block that formed the caldera. However, this assumption is complicated by the fact that several different events may be recorded by the caldera structure (MacLeod and others, 1982).

Conduction Models

The cooling of a possible magma chamber associated with the Newberry volcano was investigated using both conductive and convective heat-transfer models. The emphasis in the modeling is on the temperatures in the volcano edifice as they might influence the development of geothermal systems, not the details of the solidification of an actual chamber. The conductive models are discussed first. There are two limiting models which may be considered. The first of these models is referred to as a "continuous" magma chamber. In this case, the magma chamber might be actively convecting with no plating on

the top of the chamber, or the resupply rate would be high enough to maintain the top of the chamber at approximately magmatic temperatures. In this model, the temperature gradient above the magma chamber would rather rapidly reach the temperature of the magma chamber divided by the depth of the magma chamber. For example, a magma chamber at a depth of 10 km composed of dacite at a temperature of approximately 800° C would, if it existed long enough, generate a temperature gradient of 80° C/km. The time constant for the lid above the magma chamber to reach a steady state linear gradient would be a function of $\sqrt{4kt}$, where k is thermal diffusivity and has a value of approximately 0.01 cm²/sec. For a depth of 10 km, the characteristic time for steady state would be approximately 1 m.y. If the depth were 3.2 km, then the corresponding time would be approximately 0.1 m.y. Thus for magma chambers in the depth range likely to be encountered at Newberry volcano, a magma chamber would have to exist for a period of 100,000 yr to 1 m.y. for conditions to approach steady state above the magma chamber. Volcanism in the vicinity of Newberry volcano has certainly existed for several hundred thousand years; however, whether a single magma chamber has existed for this long a period of time (except at regional depths of perhaps 10 km) is unknown.

The second type of conduction model considers the cooling of a magma chamber which is "instantaneously" emplaced and cooled without resupply or convection. If this magma chamber is approximated as a large sill of variable thickness and infinite extent in the horizontal dimension, the surface heat flow is given by Figure 8.6. This model assumes that an infinitely wide sheet of magma is emplaced very quickly at a constant temperature and that this magma then cools by conduction alone. Shown in Figure 8.6 is the ratio of surface heat flow (Q) as a function of time (t) to the heat flow (Q_0) that would exist if the steady state temperature at depth (H equal to depth of burial) was equal to T_0 : i.e., $Q_0 = T_0 K/H$. Nondimensional scale parameters are shown on the left and bottom sides of the figure.

If the depth of burial is 5 km, then heat-flow values are as shown on right-hand and upper axes in Figure 8.6. In this case maximum heat flow will be reached approximately 200,000 years following emplacement and will drop slowly over a period of 1 to 2 m.y. following emplacement. This result holds approximately as long as the magma chamber is at least 5 km thick. If the magma chamber is much less than 5 km thick, then the peak heat flow is reduced considerably, but the shape of the cooling curve does not change significantly. The heat flow for this "instantaneous" model never exceeds half of that of the steady state "continuous" model, and cooling times are relatively short in a geologic sense, even for an infinitely thick magma. From this analysis, it is clear that heat-flow values in excess of 5 to 10 HFU commonly observed near volcanoes

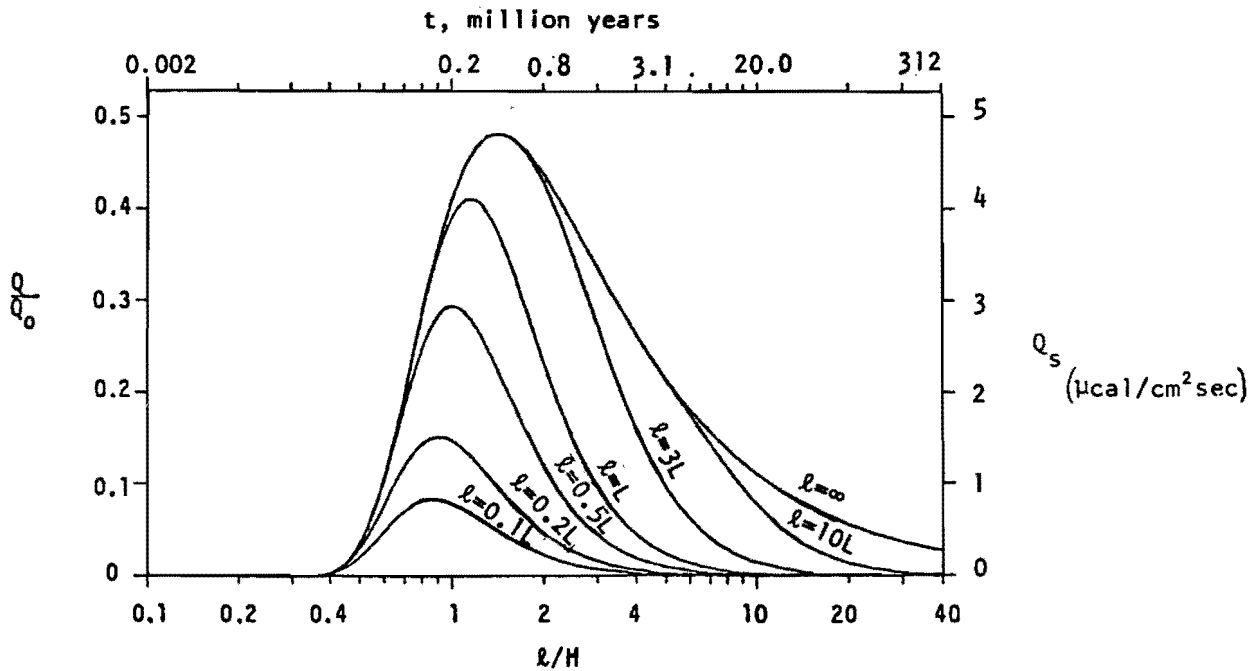


Figure 8.6. Normalized heat flow as a function of nondimensional length (l is conduction length, $\sqrt{4k\tau}$) for a one-dimensional instantaneous magma chamber cooling conductively (after Lachenbruch and others, 1976). Values of the curve for a thermal diffusivity of $0.01 \text{ cm}^2/\text{sec}$, depth of burial of 5 km , intrusion temperature of 800° C , and a thermal conductivity of $6 \text{ mcal/cm sec } ^\circ\text{C}$ are shown on the top and right sides.

must be related to hydrothermal convective systems associated with the cooling process.

The instantaneous cooling of magma chambers which are finite in a horizontal dimension are illustrated in Figures 8.7 through 8.12. The temperatures and heat-flow values are shown without any superposition of background values. The background effects would increase the surface heat flow by 1.5 to 2.5 HFU. A magma temperature of 800° C is assumed in all cases. The actual temperature would be the ambient background temperature plus 800° C . In all models, a diffusivity of $0.01 \text{ cm}^2/\text{sec}$ and a thermal conductivity of $6 \text{ mcal/cm sec } ^\circ\text{C}$ have been assumed.

Figures 8.7 and 8.8 show the surface heat flow and the subsurface temperatures, respectively, for a magma chamber 3 km by 3 km and buried at a depth of 3 km .

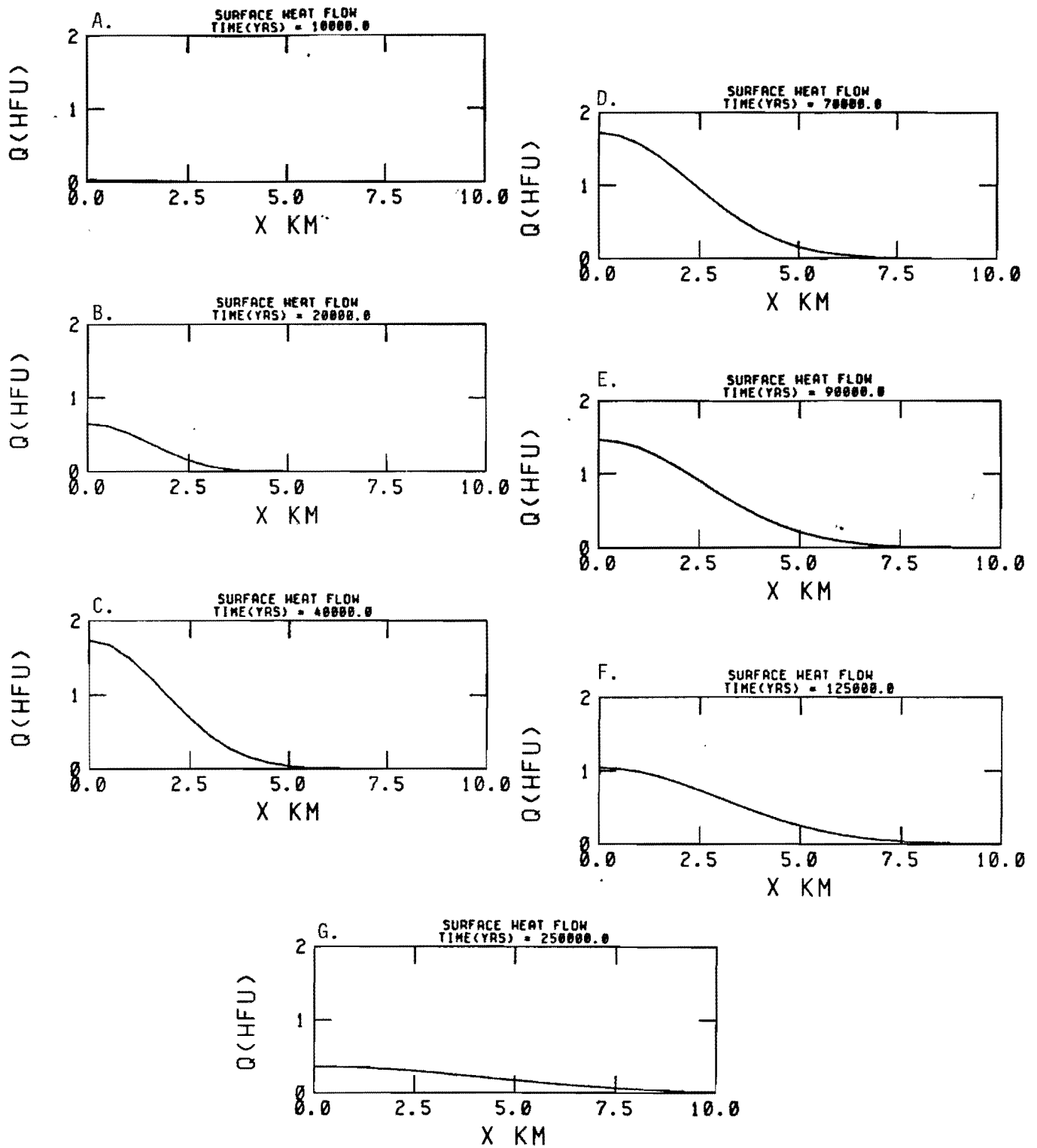


Figure 8.7. Surface heat flow generated by the conductive cooling on an instantaneous two-dimensional rectangular magma chamber 3 km wide and 3 km long, buried 3 km below the surface with an initial temperature of 800°C and a diffusivity of $0.01\text{ cm}^2/\text{sec}$. The thermal conductivity is $6\text{ mcal/cm sec }^{\circ}\text{C}$.

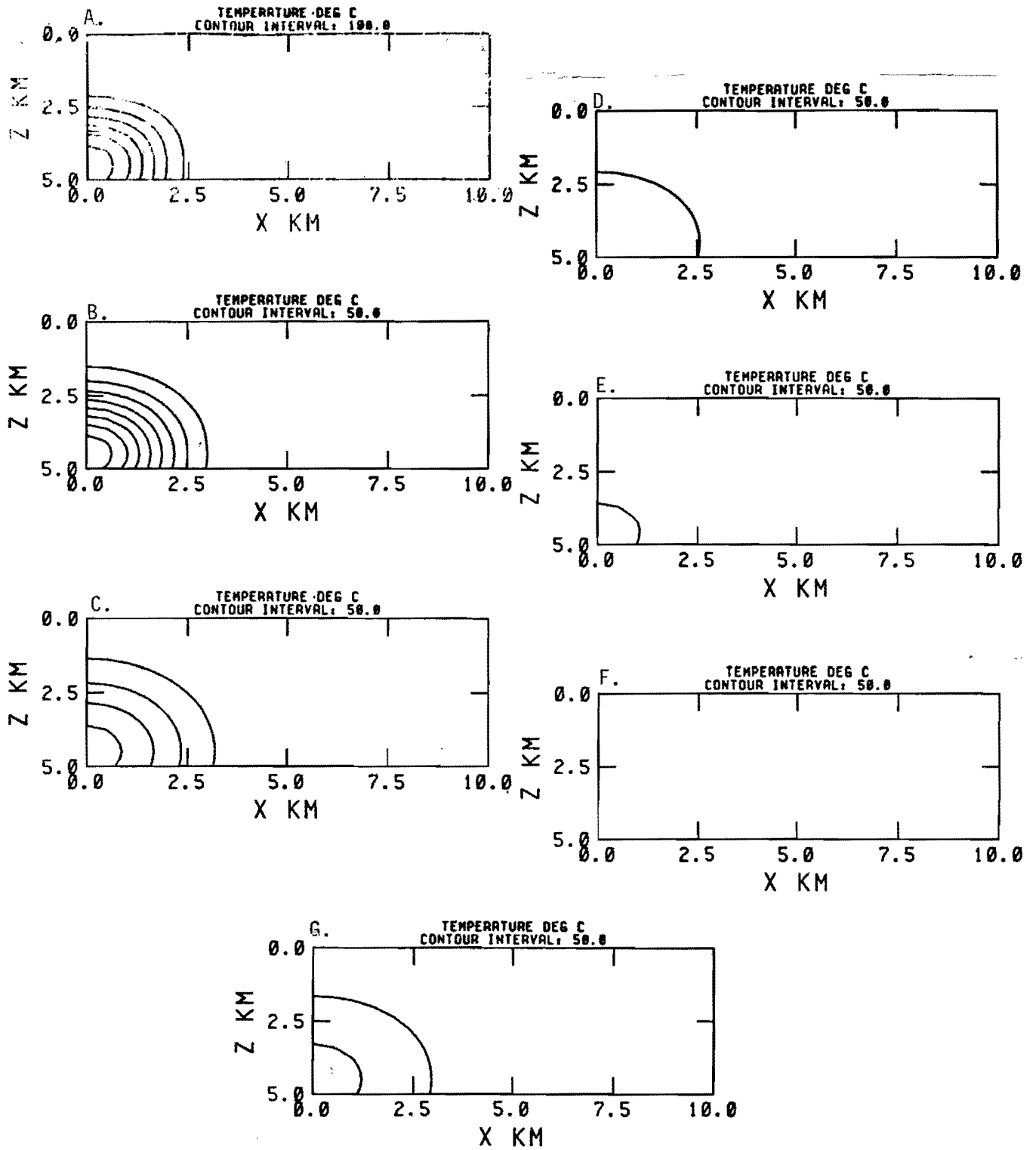


Figure 8.8. Isotherms corresponding to the times and heat-flow values shown in Figure 8.7. Note the change in contour interval from 100°C to 50°C between the 10,000-year and the 20,000-year solution.

The magma chamber is assumed to be a parallelepiped and so is infinitely extended in the direction perpendicular to the paper. The results show that the heat flow rises to a peak of just less than 2 HFU (above background) between 70,000 and 40,000 years. Temperatures in this size magma chamber drop very rapidly to less than 400° C 20,000 years after emplacement, while the surface heat flow has not yet reached its peak. Therefore, for a chamber this size to appear as a continuous heat source, resupply of magma would have to occur on the order of every few thousand years. On the other hand, if a "one-shot" magma chamber of this size were emplaced within the last 6,000 years, then temperatures could still be relatively high within and above the magma chamber.

Figures 8.9 and 8.10 show the conductive cooling of a magma chamber 6 km wide, 3 km thick, and buried at a depth of 3 km. Heat flow for this model rises much more dramatically than for the smaller magma chamber, and peak heat-flow values are approximately 4 HFU at about 70,000 years. The temperatures remain significantly higher in the magma chamber as well and exceed 450° C 40,000 years after emplacement. Recurrence times on the order of 50,000 to 100,000 years would be required to keep such a chamber near the melting temperature.

The final conductive model considered has a width of 10 km, a thickness of 5 km, and a depth to the top of 5 km. The results are shown in Figures 8.11 and 8.12. Heat-flow values reach a peak of approximately 3 HFU after about 100,000 years. Temperatures remain quite high for much longer period of time than for the smaller magma chambers. However, none of these conductive models will explain the high temperatures presently observed at shallow depths in the caldera.

Convection Models

Of course, most magma chambers do not cool in a completely conductive fashion, and convection is often a major part of the cooling. Numerical studies by Ribando and others (1978) and Norton and Taylor (1979) indicated that convective processes associated with magma chambers are typically two to 30 times more efficient in removing heat than conduction, with the exact response depending on details of permeability distribution, depth of emplacement, and so forth. Ziagos and Blackwell (1980b) evaluated the cooling behavior of a number of large granitic batholiths such as those beneath Yellowstone,

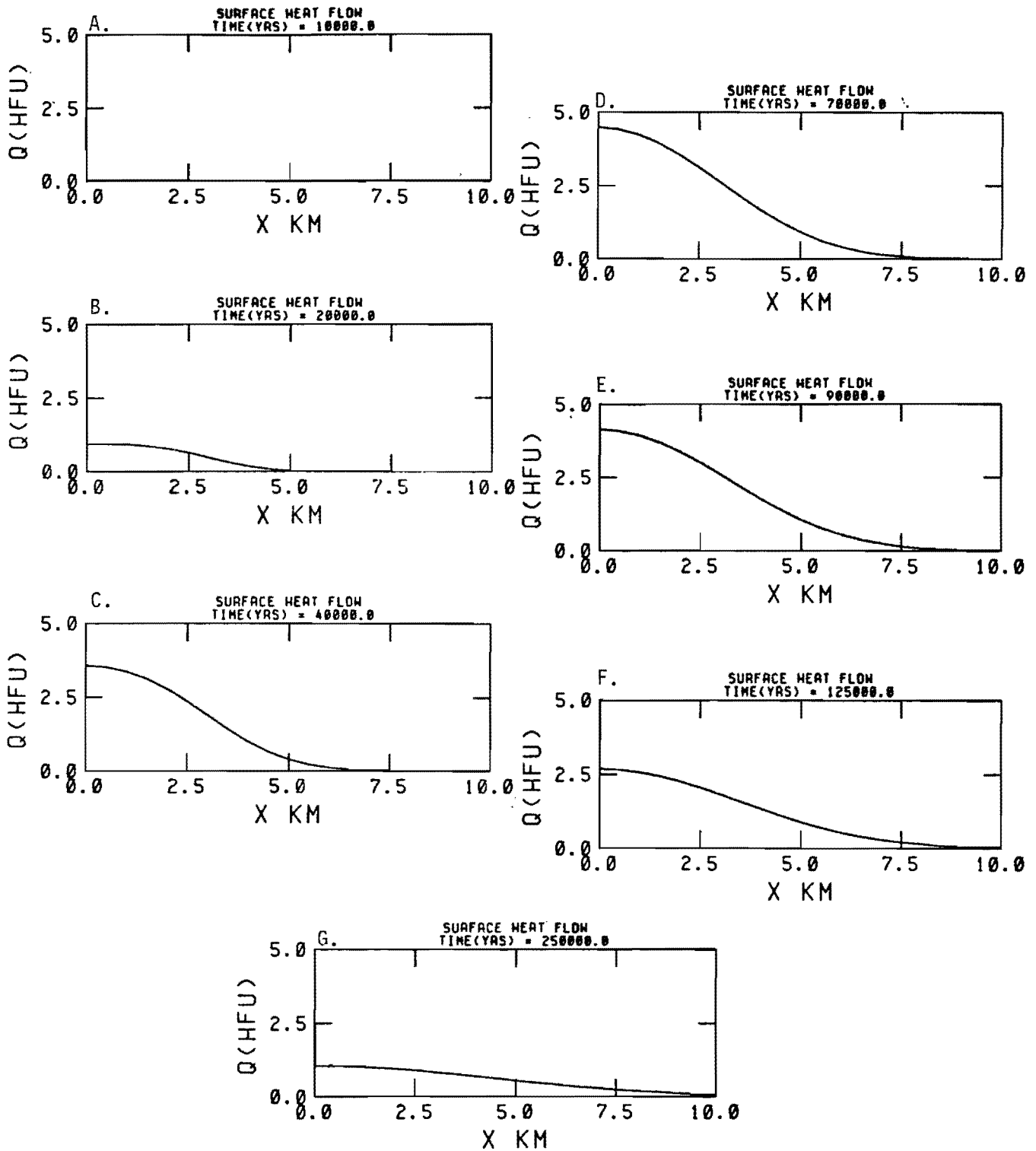


Figure 8.9. Heat flow generated by the instantaneous conductive cooling of a two-dimensional rectangular magma chamber 6 km wide and 3 km long, buried at a depth of 3 km. Other properties are the same as those in the model shown in Figures 8.7 and 8.8.

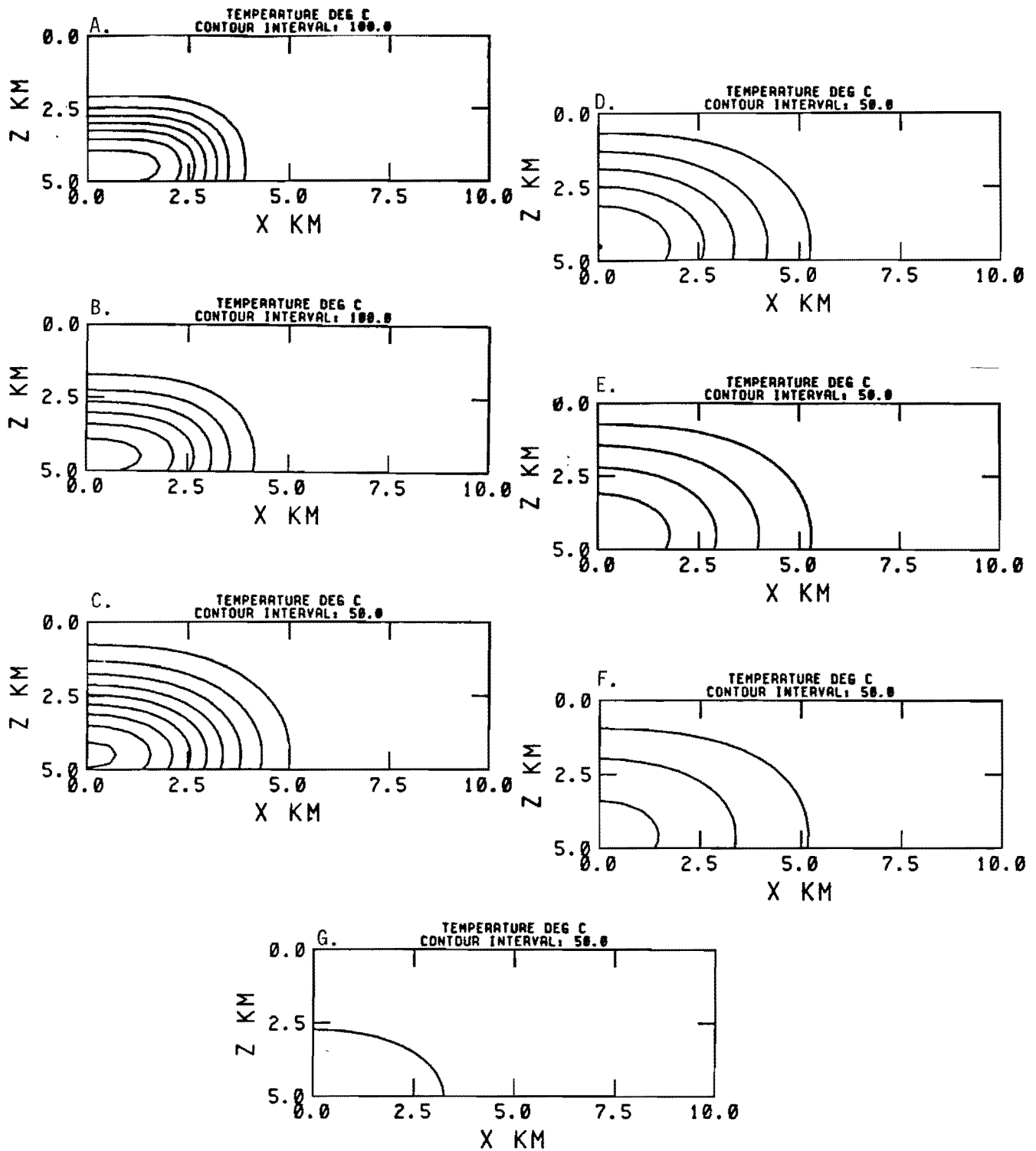


Figure 8.10. Isotherms corresponding to times and heat-flow values shown in Figure 8.9. Note the change in temperature contour interval from 100°C to 50°C between the isothermal sections corresponding to the 20,000-year solution and the 40,000-year solution.

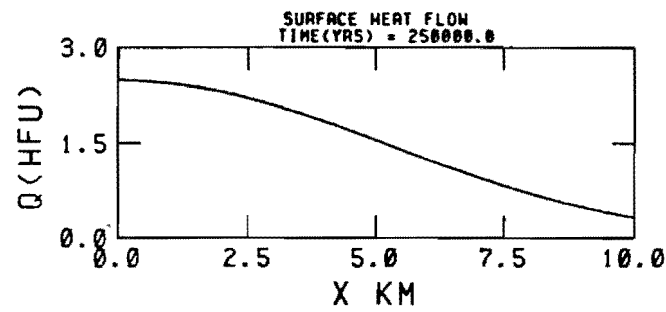
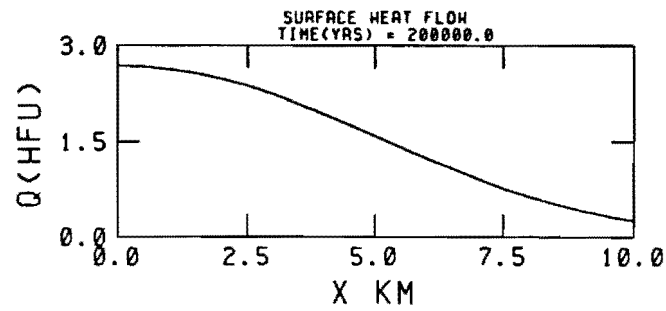
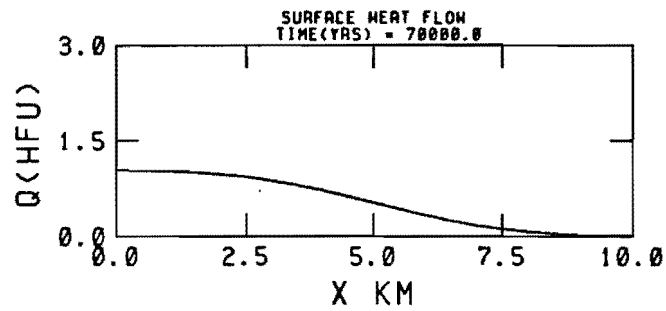
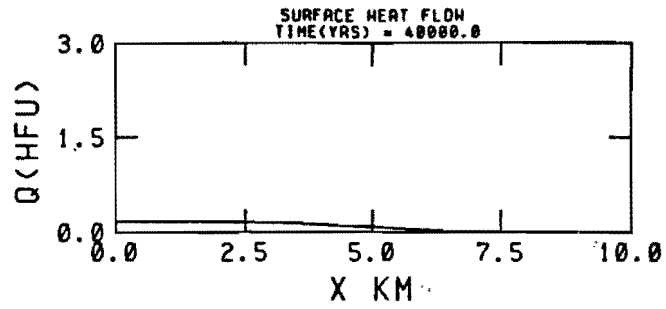


Figure 8.11. Heat-flow values associated with the instantaneous conductive cooling of a two-dimensional rectangular magma chamber 10 km wide and 5 km thick, buried at a depth of 5 km. Other properties are the same as those for the model shown in Figure 8.7.

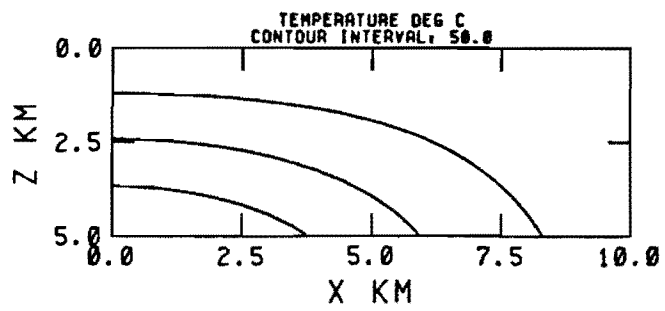
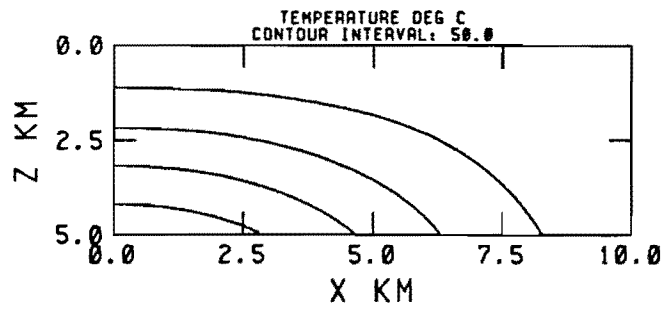
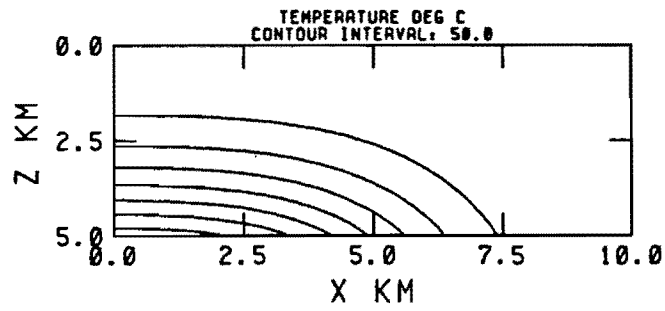
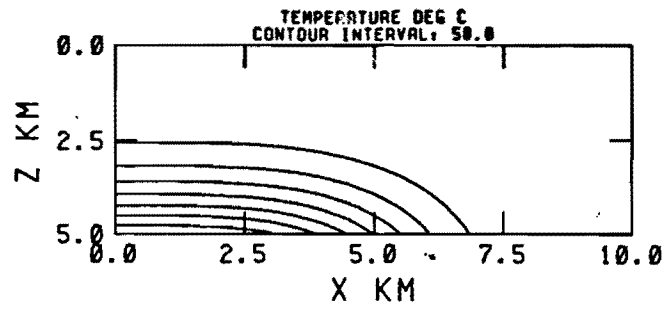


Figure 8.12. Isotherms corresponding to heat-flow values and times shown in Figure 8.11.

The Geysers, the Taupo graben, and Roosevelt Hot Springs. They concluded that the convective enhancements of heat transfer range from zero to a factor of approximately 15 to 20, with a typical value of 5 to 10.

It is difficult to construct a model for the magma chamber which might underlie Newberry volcano because of the unknown geology, hydrology, magma-chamber shape, and magma-chamber depth. For the purposes of developing a qualitative feeling for the effects of vigorous convection on the system, we utilized a model discussed by Lau (1980). This model assumes emplacement of an instantaneous two-dimensional dike of rectangular cross section into a permeable material. The magma chamber itself cools conductively; however, convection is allowed to take place in the material outside the magma chamber. A conduction-only layer caps the system. The ratio of the horizontal to vertical permeability and different values of Rayleigh number can be included in the model. The ratio of horizontal to vertical permeability is a very important parameter. It is certain that horizontal and vertical permeabilities in the rocks at Newberry volcano are very different, with the typical horizontal permeabilities being much greater than the overall mean vertical permeability (see MacLeod and others, 1982).

Lau (1980) applied his model to a simulation of the cooling of a magma chamber emplaced in a porous medium which might generate a geothermal system such as the Salton Sea geothermal system in the Imperial Valley of California. He noted that as the horizontal permeability increased with respect to the vertical permeability, more flattened convective patterns developed. In some of the models, temperature overturns were generated at certain periods of time by convective processes associated with the models which had higher horizontal than vertical permeabilities.

In order to investigate the Newberry volcano, calculations were carried out using the model of Lau (1980) for geometries similar to those used for the conductive models in the previous section, based on the cross section shown in Figure 8.5. The results of these calculations are shown in Figures 8.13 to 8.17 (p. 107-110 and p. 112). For each model, there are two separate figures, a space plot of the 100°, 200°, and 300° C isotherms at different times and a plot of surface heat flow. Thus, only a summary of the total results is shown in figures accompanying this discussion. A more complete display of results including plots of temperatures, stream function values, velocity, and surface heat flow for each time is shown in Appendix C. In all the convective models, a thermal diffusivity of 0.01 cm²/sec was assumed, and in all models

but one, a horizontal to vertical permeability ratio of 2 was assumed. This assumption represents an attempt to model somewhat realistically the inhomogeneity in the flow which would be induced by the observed properties of the volcano. That anisotropic permeability is an important part of the solutions has been emphasized by MacLeod and Sammel (1982). In all models, the Rayleigh number was assumed equal to 200. This is a typical average Rayleigh number associated with many types of magma chambers (Ziagos and Blackwell, 1980a). A 100-m impermeable layer was assumed to cap the top of the system, so that the heat loss at the surface is conductive even though the mechanism of heat transfer to the near surface is convection. The models are two-dimensional parallelepipeds and geometrically similar to those used for the instantaneous conductive cooling models. Models were run for magma chambers 3 km wide and buried at a depth of 3 km, 6 km wide and buried at a depth of 3 km, and 10 km wide and buried at a depth of 5 km. Because of the symmetry, only half of the solution is displayed. In addition, for a comparison, a model was run with a horizontal to vertical permeability ratio of 0.5 for a magma chamber 10 km wide and buried at a depth of 5 km. Finally, in order to model a broad but shallow magma chamber or hot zone as suggested by one interpretation of the gravity data, a model was run with a magma-chamber width of 15 km and depth of burial of 4 km.

In all cases, the models show an overturn in temperatures above the magma chamber. The direction of water flow is in toward the magma chamber at the bottom of the circulation system and up the side of the magma chamber; then part of the flow either crosses the magma chamber or moves directly away from the magma chamber. At the surface of the system, rapid flow takes place away from the magma chamber. The horizontal flow of cooler water is fast enough along the top of the chamber in most cases to induce an overturn in temperature that extends beyond the margins of the magma chamber for at least some time periods. Under the model conditions, the chambers cool on the order of two or three times faster than they would based on conduction alone. During approximately the first third of the cooling time of the conductive solution, the heat-flow values in the convective solution are significantly higher because of fluid transport to the near surface. For example, the results from the 3-km-wide, 3-km-deep magma chamber are shown in Figure 8.13. High temperatures are constrained to exist at or directly above the magma chamber. Heat-flow values are shown for various times, as are the 100°, 200°, and 300° isotherms for four different times, so that some idea of the change in the flow pattern and temperatures in the geothermal system with time can be developed. A strong, relatively shallow overturn occurs in both the 40,000- and

70,000-year models, although relatively high temperatures at shallow depths (greater than 200° C, less than 2 km) exist only for a period of a few tens of thousands of years.

The results for the 6-km-wide magma chamber are shown in Figure 8.14. The results are similar to those in Figure 8.13, except the cooling times are extended almost twice as long, and there is much more dramatic and long continued overturn of temperature. The flow system carries the geothermal anomaly at least some distance outside the edges of the magma chamber, although the high temperatures are constrained to occur only inside the edge of the magma chamber. The pattern is complicated by the water flow across the top of the magma chamber, which causes an overturn in temperatures for much of the cooling time of the model. A phenomenon which occurs in the remainder of the models shows up in this model. In the broader models, convective heat flow over the center of the magma chamber is initially suppressed by the active circulation induced by the corner of the magma chamber, and it is only somewhat later in the cooling period that heat-flow values in the center of the magma chamber become high. Eventually, they actually exceed the heat-flow values on the margins related to the rapid initial fluid circulation up the hot side of the magma chamber. Cathles (1977) also discussed this phenomenon.

Results for the deeper and broader magma chamber (10 km wide, 5 km deep) are shown in Figure 8.15. In this case, the reservoir was extended to a depth of 10 km. The heat-flow values are significantly lower than those generated by the shallower magma chambers except very early in the history of the system, but the anomaly is much broader. Figure 8.16 shows the same model with a greater vertical than horizontal permeability. The significant difference is that the temperature overturn is significantly reduced. The convective cooling is suppressed, as it is more difficult to pull colder water in from the margins through the geothermal system. The highest heat flows are still generated at early times along the margins of the pluton, but the heat-flow values are significantly depressed with respect to the model with the greater horizontal permeability. This result is somewhat counter to intuition because it appears that greater horizontal than vertical permeability enhances fluid circulation. Of course above any actual magma chamber, there may be very high permeability along steeply dipping faults that would allow very effective vertical circulation, so that this result is not necessarily directly applicable to all magma chambers.

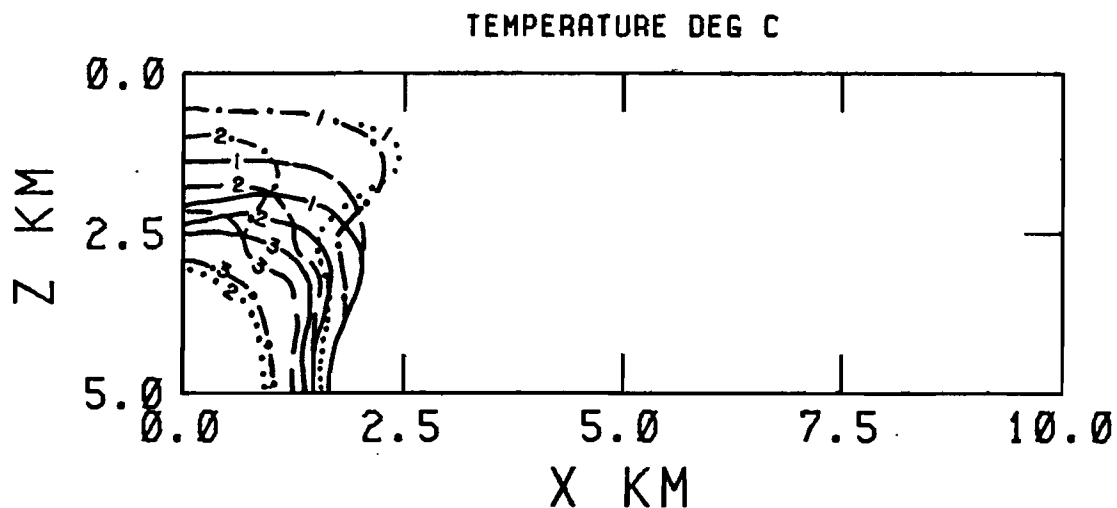
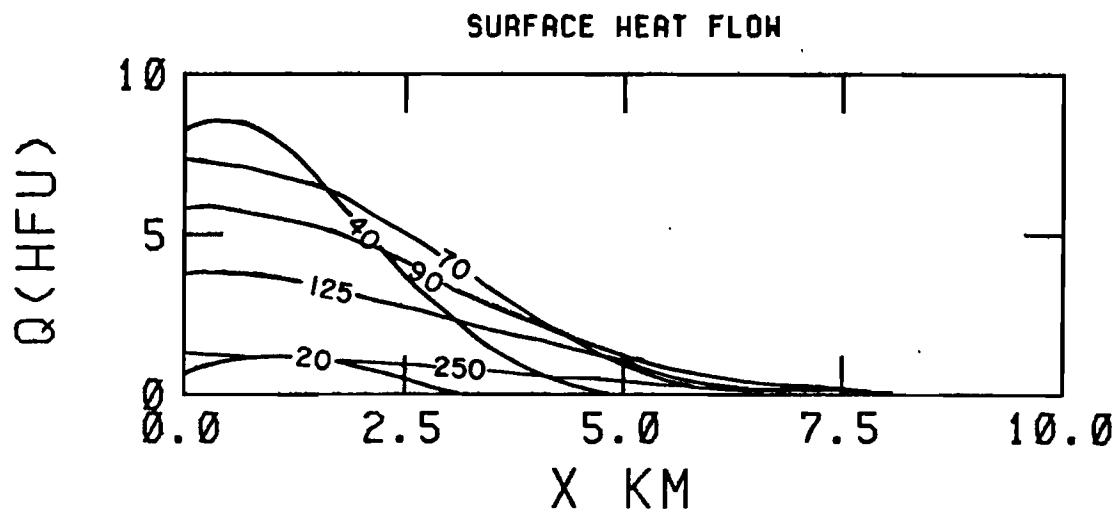


Figure 8.13. Surface heat flow and subsurface temperatures for a two-dimensional rectangular magma chamber 3 km wide, buried 3 km deep, cooling convectively. The initial temperature is 800°C , the Rayleigh number is 200 and the ratio of horizontal to vertical permeability is 2.0. 1 HFU = $10^{-6}\text{cal/cm}^2\text{ sec}$. The numbers shown on the surface heat-flow figure are thousands of years. Numbers shown on the temperature cross sections are hundreds of degrees C. The isotherms on the subsurface cross section are for cooling ages of 10,000 years (solid line), 20,000 years (dashed line), 40,000 years (dot-dash line), and 70,000 years (dotted line).

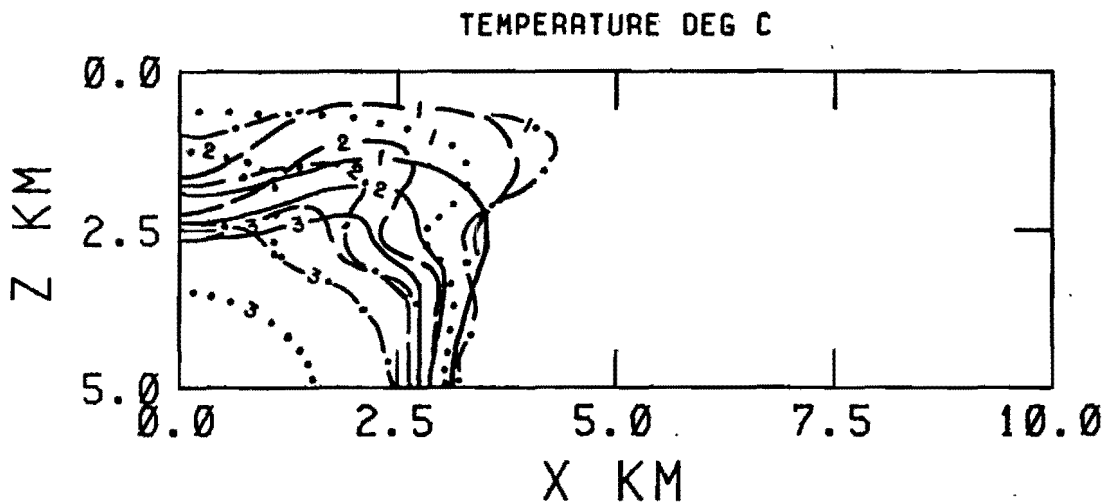
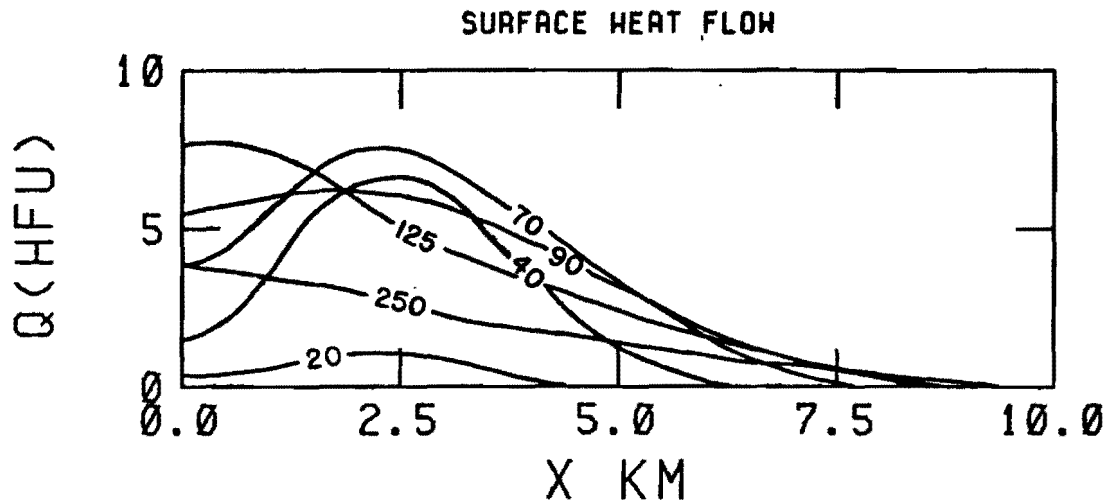


Figure 8.14. Surface heat flow and subsurface temperatures for a two-dimensional rectangular magma chamber 6 km wide, buried 3 km deep, cooling convectively. The initial temperature is 800°C , the Rayleigh number is 200, and the ratio of horizontal to vertical permeability is 2.0. $1\text{ HFU} = 10^{-6}\text{ cal/cm}^2\text{ sec}$. The numbers shown on the surface heat-flow figure are thousands of years. Numbers shown on the temperature cross sections are hundreds of degrees C. The isotherms on the subsurface cross section are for cooling ages of 20,000 years (solid line), 40,000 years (dashed line), 70,000 years (dot-dash line), and 125,000 years (dotted line).

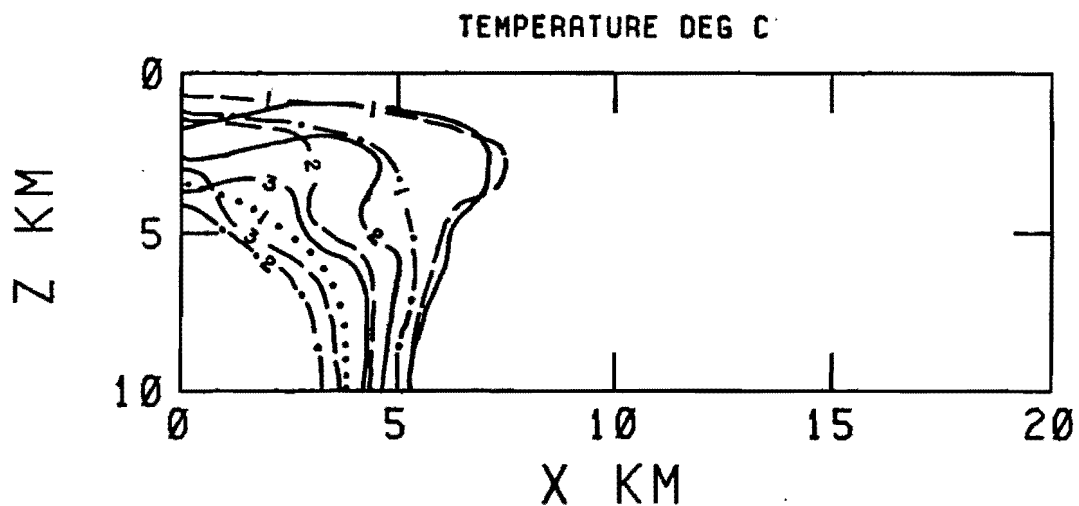
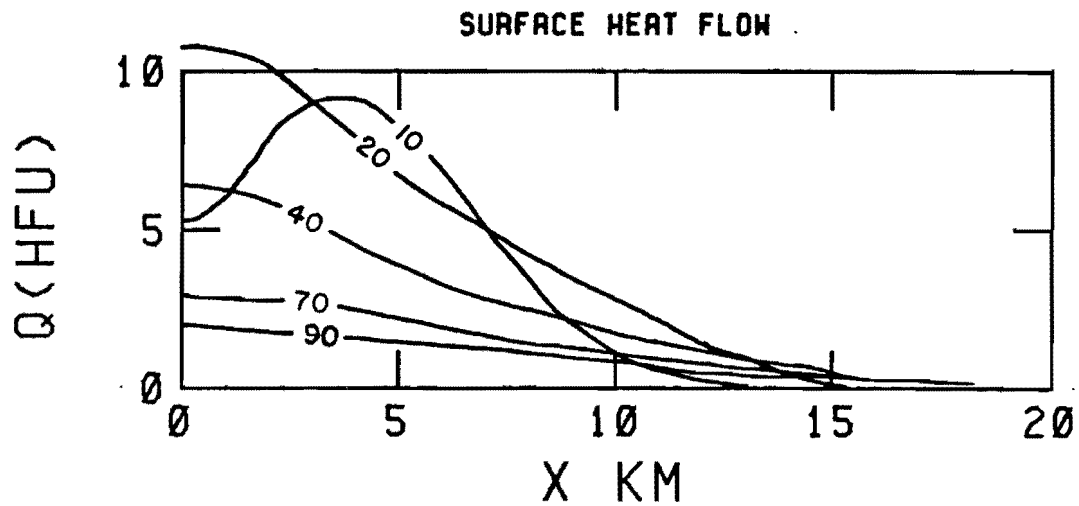


Figure 8.15. Surface heat flow and subsurface temperatures for a two-dimensional rectangular magma chamber 10 km wide, buried 5 km deep, cooling convectively. The initial temperature is 800°C , the Rayleigh number is 200, and the ratio of horizontal to vertical permeability is 2.0. 1 HFU = $10^{-6}\text{cal/cm}^2 \text{ sec}$. The numbers shown on the surface heat-flow figure are thousands of years. Numbers shown on the temperature cross sections are hundreds of degrees C. The isotherms on the subsurface cross section are for cooling ages of 10,000 years (solid line), 20,000 years (dashed line), 40,000 years (dot-dash), and 70,000 years (dotted line).

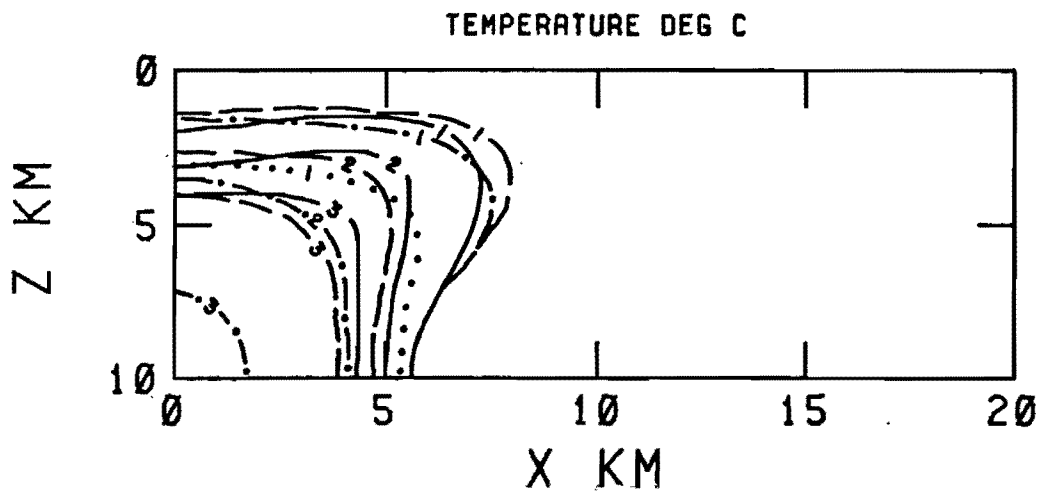
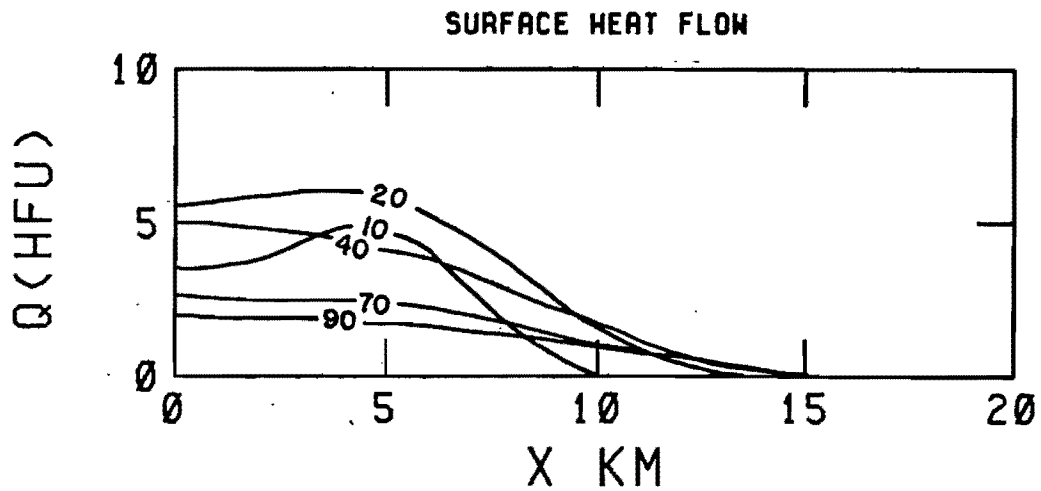


Figure 8.16. Surface heat flow and subsurface temperatures for a two-dimensional rectangular magma chamber 10 km wide, buried 5 km deep, cooling convectively. The initial temperature is 800°C , the Rayleigh number is 200, and the ratio of horizontal to vertical permeability is 0.5. 1 HFU = $10^{-6}\text{cal/cm}^2\text{ sec}$. The numbers shown on the surface heat-flow figure are thousands of years. Numbers shown on the temperature cross sections are hundreds of degrees C. The isotherms on the subsurface cross section are for cooling ages of 10,000 years (solid line), 20,000 years (dashed line), 40,000 years (dot-dash line), and 70,000 years (dotted line).

Topographic effects above the magma chamber will also be of major importance.

The model shown in Figure 8.17 is a 15-km-wide model buried at a depth of 4 km. Again, the vertical margin generates very high heat flow early in the history of cooling the body, and a very strong overturn develops. The velocity and stream-function patterns (see Appendix C) become very complicated, and as the magma chamber cools, several different cells develop on the top of the magma chamber in addition to the main cell associated with vertical flow up the margin of the chamber.

Discussion

The various models presented in the previous section are not intended to be an exhaustive and perhaps not even a representative set of models reflecting the Newberry volcano magma chamber. Since at the moment we know so little of the details of the magma chamber, attempts to model it are speculative at best. Some of the results of most significant interest can be summarized, however. Even the model with the shallowest and smallest magma chamber should have a significant geothermal system associated with it for a period of 20,000 to 40,000 years following emplacement. Therefore, if a magma chamber of that size has been associated with the active silicic volcanism in the past 6,000 to 7,000 years, then certainly such a system should still be present and active. If the chamber has behaved as a continuous heat source with recurrent activity at intervals of a few tens of thousands of years or is larger than the minimum size assumed, then the situation will be even more favorable for existence of a large convective system.

Actual presence of very high temperatures (265° C) at shallow depth in the caldera clearly indicates that a magma chamber forcing a convective system is present. The details of the hydrologic conditions will dominate the actual geometry of the convective system. The large numbers of dikes presumably present at depth north and south of the volcano, as indicated by the alignment of vent areas and faults, probably complicate the permeability distribution there. Sheetlike lateral leakage might exist to the east and the west, however. Thus, even if the heat source is small, hot water is likely to be encountered outside of the caldera.

The drill hole on the northeast side of the volcano would seem to suggest that the 400-m aquifer in the caldera does not exist at that location or is

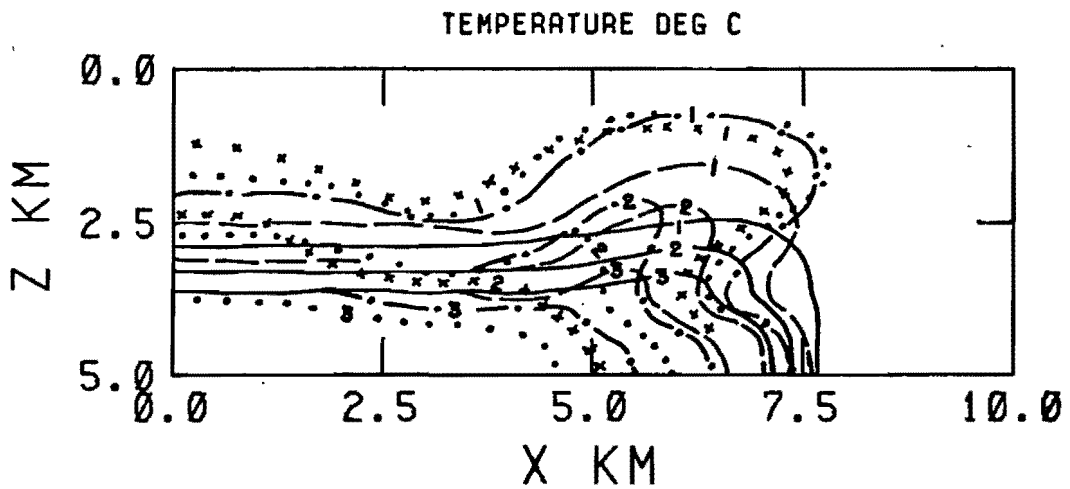
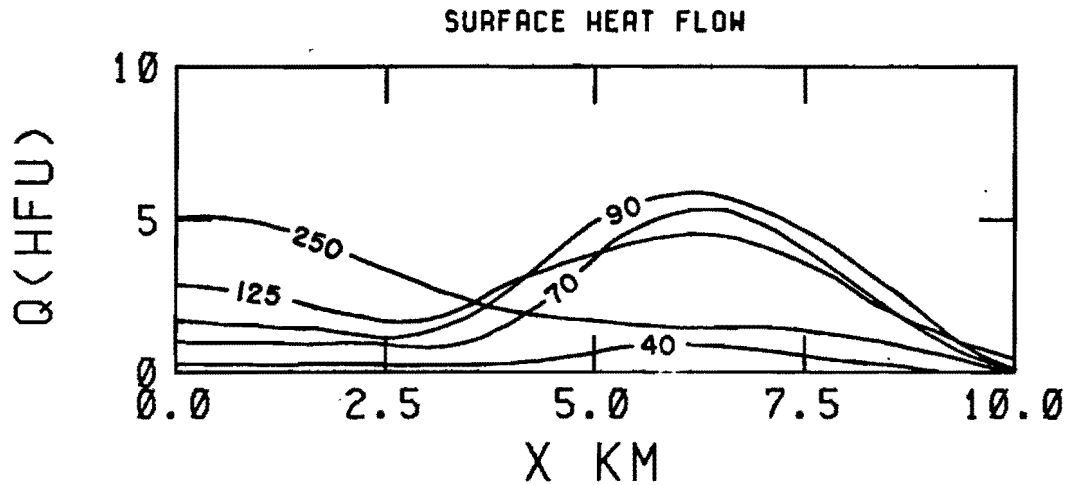


Figure 8.17. Surface heat flow and subsurface temperatures for a two-dimensional rectangular magma chamber 15 km wide, buried 3 km deep, cooling convectively. The initial temperature is 800°C , the Rayleigh number is 200, and the ratio of horizontal to vertical permeability is 2.0. $1\text{ HFU} = 10^{-6}\text{ cal/cm}^2\text{ sec}$. The numbers shown on the surface heat-flow figure are thousands of years. Numbers shown on the temperature cross sections are hundreds of degrees C. The isotherms on the subsurface cross section are for cooling ages of 20,000 years (solid line), 40,000 years (dashed line), 70,000 years (dot-dash line), and 90,000 years (dotted line). In addition, the 100° isotherm for the 125,000-year solution is shown by the X's.

much subdued. The hole is not deep enough to test whether or not the deep hot aquifer encountered beneath the caldera (~ 900 m) is present. Because of the rapid vertical variations in gradient, it is difficult, if not impossible, to attempt to extrapolate observed gradients to deeper depths.

All of these models have assumed relatively shallow magma chambers. If the depth to the top of the magma chamber is 7 to 10 km, then it is more difficult to estimate what the geothermal systems might be like. The existence of a relatively shallow geothermal system in the caldera is an argument for a shallow magma chamber. A possibility not considered in the model presented here is that the shallow high temperatures are related to shallow dikes feeding the young silicic flows. In this case, the actual volume of hot rock might be small and the geothermal systems short lived. However, if the geothermal system is of typical size and $\geq 265^{\circ}$ C, there would be no problem in sustaining electrical energy production for 30 to 50 years. It is quite clear that further drilling is required to evaluate the geothermal potential of the Newberry volcano.

CHAPTER 9
LAND USE AND REGULATION OF NEWBERRY VOLCANO
by
Neil M. Woller,
Oregon Department of Geology and Mineral Industries

Introduction

Newberry volcano is located in southern Deschutes County and is administered by the Deschutes National Forest. It is the central geographic feature in the Fort Rock Ranger District, which has local authority over the area.

National Forest Land Use Planning

The geothermal, timber, mineral, and recreational resources of Newberry volcano are managed in accordance with the U.S. Forest Service (USFS) objective of multiple-use resource management, as set forth in the Deschutes National Forest Land Management Plan (LMP). The LMP provides a mix of resource utilizations that protects forest resources, fulfills legislative requirements, and serves the needs of local and regional residents. It identifies mineral and energy needs; yields for timber harvests; and acreage to be set aside for recreation, wildlife habitat, forage lands, watershed, and other possibly competing uses.

The LMP is periodically updated to reappraise the management direction and the associated outputs of the forest's renewable resources in view of changes in technology, demographics, output schedules, past performance, and newly recognized factors and needs. The current LMP, approved in 1978, deferred consideration of geothermal leasing both within and outside the Newberry Crater Known Geothermal Resource Area (KGRA) (Plate 8). A revised, more inclusive plan, the Land and Resource Management Plan (LRMP), was proposed and submitted for public review in 1982. The proposed LRMP acknowledges the goal of providing "for exploration, development, and production of energy resources within portions of the Newberry Crater KGRA where development of the geothermal resource is compatible with other resource values."

Newberry Crater KGRA

The LRMP proposes that the Newberry Crater KGRA be divided into three zones, shown in Plate 8 and described below.

Zone 1: This area is composed of the crater floor and the inward-facing slopes. It has high recreational and scenic values. Paulina and East Lakes are heavily used by fisherman and campers and are important wildlife habitats. Furthermore, there is concern for stability of some of the steeper slopes. No leasing or surface occupancy would be allowed in this zone.

Zone 2: This area is comprised of the rim of the crater, the major access road, and Paulina Creek. It has high recreational and scenic values. Trails in this zone are used year-round by sportsmen. Competitive leasing would be allowed in this zone, with the stipulation that there be no surface occupancy. Exploration for geothermal resources, if any exist under this zone, would only be via directional drilling from Zone 3 or sites outside the KGRA.

Zone 3: This area lies generally outside the crater but within the KGRA. Visual resources are considered important in these areas, but "other considerations are not as sensitive or critical." Open competitive leasing would be allowed in this area. Surface occupancy would be allowed as well. However, coordination with regulatory agencies would be required to maintain overall visual quality.

Some areas classified by the USFS as "no surface occupancy" contain provisions for limited exploration, providing the exploration proposed is compatible with other resources or the adverse effects can be mitigated. Such exploration may be permitted even though the particular area may not be environmentally suited for power plant siting. Generally, exploration approved within no-surface-occupancy areas would not be expected to go beyond a temperature-gradient hole.

Outside the KGRA

In June 1982, the Regional Forester of the Pacific Northwest Region,

USFS, approved the Noncompetitive Geothermal Leasing Environmental Assessment (NGLEA) report for the Fort Rock Ranger District of the Deschutes National Forest. The decision notice, accompanied by a final modification of the report, institutes the NGLA (with modification) as the policy on geothermal exploration for the district. It declares that an environmental impact statement for district-wide leasing will not be needed because the exploration would not significantly affect the quality of the human environment.

The NGLA inventories district resources, including geology, soil materials, vegetation, habitat, recreation, and demographics, and assesses the effects of geothermal development on each. Various options, ranging from "lease all" to "lease no areas, business as usual" are considered. The decision notice concludes: "(a) no issues, major concerns, or questions have been raised by other Government agencies which cannot be answered on the effects mitigated by the 'existing controls,' the proposed special lease stipulations, and through adequate coordination between the State and Federal agencies involved; and (b) assuming the 'highest level of impact' involving a large land occupancy and some reduction of other resource outputs, the potential benefits of geothermal development outweigh the projected level of environmental impacts."

The NGLA divides Fort Rock Ranger District (excluding the KGRA) into four categories, described below:

Zone 4. No surface occupancy will be allowed on the lands leased in this zone. The lands included in this zone include geologic special-interest areas, research natural areas, developed recreation sites, special-use permit areas, Forest Service administrative sites, critical wildlife habitat, cinder buttes and unstable soil areas, Paulina Creek Management Zone, and old-growth area. Resources that may underlie these areas will be accessible by directional drilling from outside the zone. Zone 4 is analogous to Zone 2 inside the KGRA but differs in that leasing will be by standard (noncompetitive) leasing procedures.

Zone 5. This is a visual and game species management classification zone. Surface occupancy will be permitted, but additional stipulations and environmental analyses and approved plans of operation will be utilized by the government to control leasing operations.

- Zone 6. Standard leasing and exploration procedures will be allowed in this zone. Surface occupancy will be permitted. This zone is roughly equivalent to zone 3 within the KGRA.
- Zone 7. (not shown): No leasing will be allowed in this zone. The zone is very small, involving only the Lavacicle Cave Geologic Special Interest Area.
- The acreage involved in each zone is summarized in Table 9.1.

Table 9.1. Summary of acreage by USFS leasing category (as modified)
(Source: Decision notice, June 11, 1982)

Zone no.	Type of zone	Acreage	Percent of area
Zone 4	Restricted occupancy (no surface occupancy)	62,272	11.6
Zone 5	Visual and game species management	209,490	38.8
Zone 6	Standard leasing	267,290	49.5
Zone 7	Deny leasing	<u>548</u>	<u>0.1</u>
	Total acreage	539,600	100.0

Energy Facility Siting Council (Oregon Department of Energy)

The Energy Facility Siting Council (EFSC) is charged with the responsibility of evaluating individual geographic areas of the state for the siting of thermal power plants. A thermal power plant is defined in ORS-469.300 as a facility capable of generating 25,000 KW (25 MW) or more of electrical power.

EFSC ruled in 1975 that Newberry Crater, North Paulina Roadless Area, South Paulina Roadless Area, and the Lava Cast Forest are unsuitable for use as sites for geothermal power plants. The area declared unsuitable is shown in Plate 8. Much of the area corresponds to USFS zones 1 (no leasing), 2 (leasing, no surface occupancy), and 4 (leasing, no surface occupancy), and therefore there is no disagreement between State and Federal authorities over most of the area. However, portions of USFS zones 3, 5, and 6 are

included within the EFSC boundaries (Plate 8). Unless EFSC modifies its boundaries, it will be possible to develop only less than 25 MW of power within those portions of zones 3, 5, 6, except by directional drilling from outside the EFSC boundary.

Lease Applications

The LRMP reports that 141 lease applications have been filed on the Fort Rock Ranger District by a total of 37 applicants. The lease applications were filed on a total of 285,529 acres. Plate 8 shows areas for which lease applications have been filed around Newberry crater, as of November, 1982 (source: Delores Yates, Greater Columbia Energy, Inc.). The KGRA is completely encircled by a solid block of lands with pending lease applications. Only in the northeast corner of the map area, corresponding to the extreme northeast flank of the volcano, are there lands for which no applications have yet been filed.

Private Lands

Private lands occur as islands within the publicly owned lands on the volcano. These lands are not directly subject to USFS regulation, but they are subject to State and County jurisdiction. Private lands, where surrounded by USFS lands, are subject to Federal access restrictions. The EFSC restrictions apply to the island of private land on the southwest shore of East Lake, within the KGRA (see Plate 8). The EFSC regulations, combined with the distance from lands upon which the USFS will permit surface occupancy, effectively preclude the siting of a large (25 MW or greater) electrical-generation facility on this privately owned parcel. It is, however, unclear whether a small electrical power facility with minimal environmental impact could be sited on this parcel. Its impact on surrounding USFS lands would be a critical factor.

No other private land is affected by the EFSC-restricted boundaries. All other uses of private lands are governed only by Deschutes County zoning regulations.

CHAPTER 10
RECOMMENDATIONS FOR GEOTHERMAL EXPLORATION
by
George R. Priest, Gerald L. Black, and Neil M. Woller,
Oregon Department of Geology and Mineral Industries

Introduction

The preceding papers have presented the available geophysical and geological data base and land use restrictions for Newberry volcano. This section utilizes this information to make recommendations for geothermal exploration of the volcano.

Exploration Strategy

An exploration program should proceed in a series of steps, each increasingly informative and expensive, which lead to the maximum amount of information at minimum capital risk for each stage. This gives the investor the option of suspending operations at any stage, should results be discouraging. Hopefully, one of the number of possible geothermal models--either good or bad--emerges as the most probable.

The relatively cheap, low-risk exploration steps have already been completed at Newberry (i.e., the literature search and surface surveys), and some drilling has begun (i.e., the two USGS wells and some wells by Union Oil Company). If significant new data are to be gathered, additional drilling will be required. The questions are (1) how deep should these exploration wells be, and (2) where are the best locations?

In order to answer these questions, it is first necessary to decide what sorts of information are required from these wells. Reliable information on the temperature regime and hydrology, particularly the presence or absence of thermal fluids, is the most important goal. The holes should thus be deep enough to escape the effects of the rapid lateral flow of cold ground water which characterizes much of the volcanic edifice, and they should be drilled where there is a maximum chance of encountering high permeability and heat flow at relatively shallow depths.

An additional constraint should be the likelihood that the drill site will be developable within the constraints of current land use planning for the area. This, however, is of secondary concern if the information gained in a nondevelopable site is applicable to developable sites and if, in addition, the information can be obtained more cheaply at a nondevelopable site. Some areas classified by the USFS as "no surface occupancy" can be drilled within USFS guidelines, even though they may not be environmentally suitable for siting of a power plant. An example is the Newberry 2 drill hole.

Constraints on Possible Geothermal Models

In order to design a drilling program, it is first necessary to evaluate the currently known constraints on possible models of the geothermal circulation system. The drill holes should then be sited where they will best constrain the possible models in order to yield maximum amounts of information for capital spent.

The constraints on potential Newberry models are as follows:

1. According to the gravity data, the area may be underlain by a shallow silicic plutonic body. The body has a poorly constrained estimated diameter of between 11.7 and 22 km and may lie as much as 6 km to less than 2 km beneath the caldera, depending on which assumptions are made. Regional geophysical studies indicate that the maximum depth to partially molten rock is probably about 10 km.
2. Silicic domes with compositions identical to one another have been found separated by as much as 17 km. The youngest silicic domes are, however, clustered in the southeastern part of the caldera in an area 3 to 4 km in diameter.
3. According to the teleseismic data, individual molten bodies within the larger pluton probably do not exceed 3 km in diameter, but the magnetic data indicate that much of the larger plutonic body may exceed 580° C (the Curie point). This temperature constraint is tentative because it is based on the assumption that, because the pluton lacks a magnetic signature, it is above the Curie temperature. Extensive hydrothermal alteration could also decrease the magnetic signature, and the low-iron silicic rocks commonly have little or no magnetic susceptibility (e.g., Paulina Peak). The regional Curie-point isotherm lies at a depth of about 6 km.

4. A plutonic body has definitely generated a temperature of 265° C at a depth of 932 m in the caldera. The temperature gradient in the lower part of the Newberry 2 well was about 600° C/km, indicating that higher temperatures probably are present below 932 m. The high gradient could be caused by heat from a small local feeder dike or from a large shallow intrusive.
5. The heat from this shallow pluton is additive to the background heat flow. The background heat flow is probably a very small percentage of total heat flow near the pluton, but, in areas farther from the apex of plutonic activity, the background heat flow is an important component of total heat flow. The background heat flow is about 1.9 to 2.5 HFU, with an average gradient of about 40° to 65° C/km (Blackwell and Steele, Chapter 8).
6. Conductive heat flow from individual silicic plutonic bodies of 800° C temperature and between 3-km and 10-km diameter would increase surface heat flow above the pluton between 1.8 and 2.7 HFU in 60,000 to 200,000 years. Heat flow in areas one plutonic radius away from the edge of the bodies would be raised about 0.25 to 0.5 HFU for periods in excess of 250,000 years after intrusion. It is highly probable that injections of magma into a composite pluton beneath the caldera have occurred much more often than one per 250,000 years. If injections have occurred often enough, a steady-state heat-flow anomaly could be present which reaches at least a few kilometers outside of the largely crystallized composite pluton.
7. Convective heat flow will cool an intrusive body much more rapidly than simple conductive heat flow. As a result of the higher heat transfer rate, it will cause much higher surface heat flow than the peak heat flow predicted by purely conductive models. If hydrothermal circulation is taking place, then plutons only a few thousand years old could strongly affect surface heat over relatively large areas. This is especially true if there is significant lateral circulation of thermal fluids.
8. The rapid vertical and lateral movement of ground water in perched aquifers "washes away" heat flow from deeper in the crust and makes the measurement of accurate temperature gradients in shallow holes impossible. The regional ground-water table, which lies at an

elevation of between 1,250 and 1,295 m, must be penetrated before temperature gradients undisturbed by perched aquifers can be obtained. Water-saturated zones below the water table may, of course, also contain thermal fluids.

9. Although there is probably at least some lateral permeability throughout most of the Newberry volcanic pile, deep vertical permeability is probably limited to areas of faulting and fracturing caused by regional tectonics, volcanic eruption, and igneous intrusion. Areas which probably have high deep vertical permeability are
 - a. Ring faults and fractures around the caldera margin.
 - b. The Tumalo-Walker Rim fault zone, and, to a lesser extent, the older Brothers fault zone.
 - c. Areas characterized by intense intrusion such as pre-Newberry rocks near and in the caldera.
 - d. Combinations of the above.
10. Thermal fluids may occur at relatively shallow levels where brought toward the surface in the rising portion of a hydrothermal convection cell.
11. Thermal fluids in vertical convection cells can probably spread laterally along the strike of steeply dipping faults and highly jointed dikes, as well as along subhorizontal volcanic interbeds with high permeability. Highly permeable interbeds of this type were common in the Newberry 1 and 2 drill holes (except between 758 and 930 m in Newberry 2).
12. Hydrothermal circulation can cause alteration and partial or complete sealing of permeability due to the precipitation of dissolved minerals during temperature and pressure changes. This factor can be partially offset by continued fracturing of the rocks by tectonic and volcanic activity. The most recently active structures are probably the Tumalo-Walker Rim fault zones and the caldera ring fractures and faults.
13. Soil-mercury anomalies in areas underlain by Mazama ash probably indicate that vertical permeability has been present in the underlying rock within the last 7,500 years. Soil-mercury anomalies in areas underlain by the young rhyolitic ash fall on the east flank of the volcano may indicate that vertical permeability was

present within the last 1,700 to 1,500 years. Mercury anomalies are highly positive indications, but not proof, that hydrothermal circulation has taken place.

14. Extensive reservoirs of thermal water have yet to be confirmed. Although the Newberry 2 drill hole did encounter formation fluids at 265° C, the large pressure drop which occurred during a 20-hour flow test indicates that the particular reservoir tested may be limited. The nature and extent of deeper reservoirs are not known.

Models That Meet the Constraints

It is possible, within the limits established by the above constraints, to assume a very negative or very positive exploration model for the volcano. The most negative hypothesis assumes that the gravity high associated with the volcano is caused by sealing of the volcanic rocks by hydrothermal alteration. In this hypothesis, only small dikes and plugs have intruded at shallow levels, and no large, shallow plutonic complex underlies the volcano. In the areas with young rhyolitic domes and flows, there must be considerable residual heat from local dikes and plugs. Eruptions have occurred within the last 10,000 years in the southeast part of the caldera and adjacent rim, and the Newberry 2 drill hole encountered temperatures of 265° C near the vent of the Big Obsidian Flow. If hydrothermal circulation has sealed most of the permeability, except locally in faults and fractures (e.g., under the mercury anomalies), there may be little hydrothermal fluid capable of sustained electrical generation anywhere in the volcanic complex.

The most optimistic model assumes that a silicic plutonic complex 12 km in diameter at its top lies at a depth of about 2 km. The body slopes outward and reaches a maximum diameter of about 22 km at a depth of about 4 km. This pluton could be hotter than 580° C but cooler than the solidus of silicic magma over most of its area. Although cool ground water could wash away the thermal effects of this heat source at shallow levels above the regional ground-water table, vertical hydrothermal circulation probably takes place in the regional fault and fracture systems and spreads laterally in numerous strata. Deep circulation systems in pre-Newberry rocks could be very common where intrusive brecciation and faulting have occurred. In this most optimistic model, high-temperature hydrothermal systems might occur at

depths of 1 to 2 km at distances as much as 10 km outside the caldera.

The actual geothermal system is probably an intermediate case between these two extreme cases, but the above exercise serves to show how poorly the current data base constrains the geothermal model.

General Considerations for a Drilling Program

Although the refinement of current geophysical and petrologic models for the caldera would be a worthwhile exercise, this section is limited to a discussion of the most reliable method of testing the resource base--namely drilling. Drilling provides a means of directly testing the main physical parameters that constrain the various theoretical models, which include the following:

1. Temperature.
2. Thermal conductivity (for heat-flow analysis).
3. Permeability.
4. Fluid saturation.
5. Density (for gravity analysis).
6. Magnetic susceptibility (for analysis of magnetic data).
7. Lithology (for structural and stratigraphic analysis).
8. Fluid and gas chemistry (for geothermometry).

Drill sites should be picked to do more than simply test the previously discussed minimum or maximum models. Drilling should be aimed at testing the most important constraints on the size of the potential hydrothermal system. These constraints include the following:

1. The size of the presumed high-level heat source.
2. The extent of lateral hydrothermal circulation through high-angle faults, dike zones, and subhorizontal strata.
3. The reservoir characteristics of the pre-Newberry rocks.

In testing the first constraint, it is important that the drilling not take place so far from the focus of plutonic activity (assumed to be the summit caldera) that only the most optimistic model is tested. The most optimistic model assumes a diameter of 12 km at the top of a still-hot pluton and a diameter of about 22 km at its center. A drill hole located approximately 3 km from the caldera rim wall would lie at a distance of approximately 6 to 7 km from the center of the caldera, a distance which provides an adequate test of the lateral extent of the high-level heat source

but which also provides a considerable safety margin should the most optimistic model prove to be seriously in error.

Wells designed to test the first constraint should also be located so that local effects from the potentially still-hot feeder dikes to the youngest silicic intrusions are avoided. The distances should be such that there would be no significant elevation of temperatures by simple heat conduction except from the potentially more important deeper sources. In the evaluation of the entire geothermal field, data on the overall thermal regime are initially more important than local small-scale heat sources.

In light of the above considerations, it may be necessary to drill holes on both the north and south flanks of the volcano. Recent silicic activity has been most frequent within the summit caldera and on the upper south-southeast flank and has been absent on the northern flank. A hole on the north flank would thus test the nature of the deeper heat source, in particular the hypothesis that much of the large, composite plutonic body may lie above the Curie temperature for magnetite (580° C). Holes on the southern flank where the most recent silicic volcanism has occurred would provide both an estimate of the addition to the total heat flow produced by the young silicic intrusions and the amount of permeability produced by long-term silicic intrusive activity.

Testing of the reservoir characteristics of intruded pre-Newberry rocks (constraint 3) would be best accomplished where the probability of intrusion is high, but where the thickness of overlying younger Newberry rocks is low. Although gravity data indicate that a (probably) complex subvolcanic intrusive extends for a distance of up to 11 km from the center of the volcano, it is safest to assume that the probability of intrusion increases toward the caldera center. However, as the center of the caldera is approached, the thickness of overlying younger Newberry rocks also increases. A sharp increase in the thickness of younger Newberry rocks occurs in the caldera because of thick intracaldera fill. Outside the caldera, the frequency of intrusion by both silicic and mafic magmas, as evidenced by surface volcanic activity, is highest in an area within about 3 km of the southern margin of the caldera. A hole in a deep drainage about 3 km from the southern caldera rim wall would thus penetrate a minimum thickness of Newberry rocks and have a good chance of reaching intruded portions of the pre-Newberry sequence (Figure 10.1). As previously mentioned, this hole must be sited

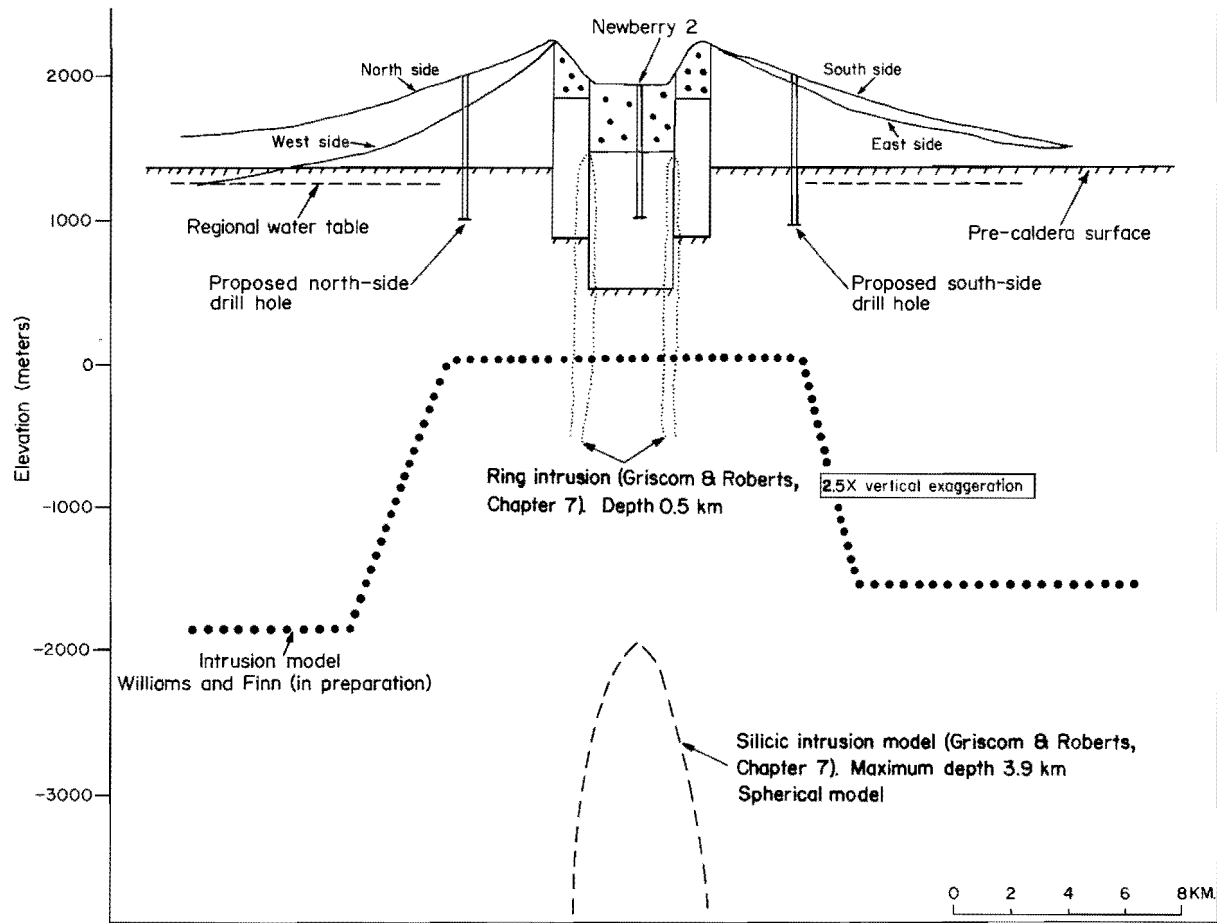


Figure 10.1. Schematic cross section through Newberry volcano (taken from Priest, Chapter 2, and Blackwell and Steele, Chapter 8). Shows location of proposed exploration wells on the north and south flanks of the volcano.

where the local effects from still-hot feeder dikes on the southeast flank are avoided.

Constraint 2 can best be tested by drilling holes a significant lateral distance away from known heat sources which are in contact with potentially permeable zones, such as faults, dikes, and flow contacts. The holes should initially be sited on greater-than-90-ppb mercury anomalies, which are good indications of high vertical permeability. A "significant" distance is the same as was discussed with respect to constraint 1 (i.e., there be no significant elevation of temperatures by simple heat conduction). This obviously requires some assumptions regarding the most probable size and temperature of the heat source, so that at least initially, it would be best to place holes designed to test such resources near more well-known sources, such as the Big Obsidian Flow or the young silicic domes on the upper southeast flank of the volcano. Testing of these types of resources has already begun with completion of a Union Oil drill hole (results unknown) near the young silicic domes on the upper southeast flank and the completion of the USGS Newberry 2 hole near the Big Obsidian Flow. It is possible that the fluids recovered from the bottom 2 m of the Newberry 2 hole represent lateral convective flow from the feeder dike to the Big Obsidian Flow.

Wells drilled to test the nature of the deeper resource should penetrate at least 150 m into the regional ground-water table in order to obtain a reliable temperature gradient. They should also penetrate a significant distance into the pre-Newberry rocks, so that the reservoir characteristics of those rocks can be adequately determined. At a distance of about 3 km from the southern caldera margin, a drill hole would have to penetrate about 560 m of younger Newberry rocks to reach pre-Newberry rocks. The hole would then have to be drilled another 280 m to reach the regional ground-water table and another 150 m to ensure the measurement of an adequate temperature gradient below the ground-water table. The total minimum depth would be about 990 m. A hole of this depth should provide a good heat-flow measurement and intercept about 430 m of pre-Newberry rocks.

Owing to the north-northeast slope of the regional ground-water table, a hole collared at a distance of about 3 km from the northern caldera margin would have to penetrate (roughly) 30 m farther to reach the regional water table. Thus the minimum depth would be 1,020 m. Access to a north-side site

may be a problem, because of the lack of roads in most areas (see Plate 8).

A drill hole should also be completed on the east flank of the volcano to evaluate the significance of the mercury anomalies there. Drilling to about 900 m would adequately test for the presence of hydrothermal circulation systems.

Specific Drilling Recommendations

Inasmuch as the Bonneville Power Administration's (BPA's) primary interest in Newberry volcano is in the theoretical electrical-generation potential of the volcano, it is recommended that they concentrate their investigations on determining the nature and extent of the resource associated with the deeper subvolcanic intrusions. The shallower hydrothermal systems associated with the youngest silicic domes and feeder dikes are also attractive targets, and, where they are adjacent to fault and fissure systems, they can yield information on the lateral dispersion of thermal water in the faults. The northeast-trending mercury anomaly on the south flank coincides with many fissure systems and may be the best area to test.

Therefore, it is recommended that initially four holes be drilled, two approximately 3 km south of the caldera, another approximately 3 km north of the caldera, and one on the east flank of the caldera. The holes should be about 1,000 m deep and should be core drilled to maximize the amount of data recovered. Furthermore, the holes should be outside of EFSC- and USFS-restricted lands and adjacent to one of the many existing roads in order to minimize road construction costs and provide data on the most easily developable areas. The general areas for drilling these four holes are shown on Figure 10.2. The suggested sequence of drilling is summarized in Figure 10.3.

A southern hole should be drilled first because (1) it will encounter the regional ground-water table at a slightly shallower depth than the northern hole, and (2) there has been more recent silicic volcanic activity south of the caldera. A hole which encountered only background temperature gradients (40° to 65° C/km) in the south would therefore essentially eliminate the need for the more northerly hole. A "failure" at a northern drill site would not necessarily eliminate the need for the southern or eastern holes.

Of the two southern holes, the hole sited within the area of high silicic volcanism but away from the youngest silicic intrusions should be

drilled first. This hole would yield valuable information on the extent of both the deep heat-flow anomaly and possible large-scale hydrothermal circulation from deeper, long-lived heat sources. If the drilling program were limited to one hole, this hole would be the most important. If high heat flow but low permeability and fluid flow were encountered in this hole, the next logical step would be to test for enhanced permeability at one of the areas with high soil mercury and a fault or fissure. If, however, both high permeability and high fluid flow were encountered in this first hole, then the next step would be to drill the northern hole to test for the same conditions on that side of the volcano. A hole on one of the southern mercury anomalies could then be drilled to see how much flow rates are augmented in areas of high vertical permeability.

If the second southern hole is successful in demonstrating active hydrothermal circulation at a mercury anomaly, then the mercury anomalies on the east flank should be tested. The east-flank anomalies are considered a higher risk target, because fewer silicic centers and young structures occur there than on the south flank, and they are farther from the apex of the volcano.

Ideally, a number of holes up to 3 km in depth should be drilled in order to fully evaluate all of the constraints on the hydrothermal reservoir, but the drilling program outlined above should provide an important, highly cost-effective next step. Confirmation of a significant hydrothermal reservoir outside of the restricted area of the caldera is a critical constraint on the development of electrical power production at Newberry volcano.

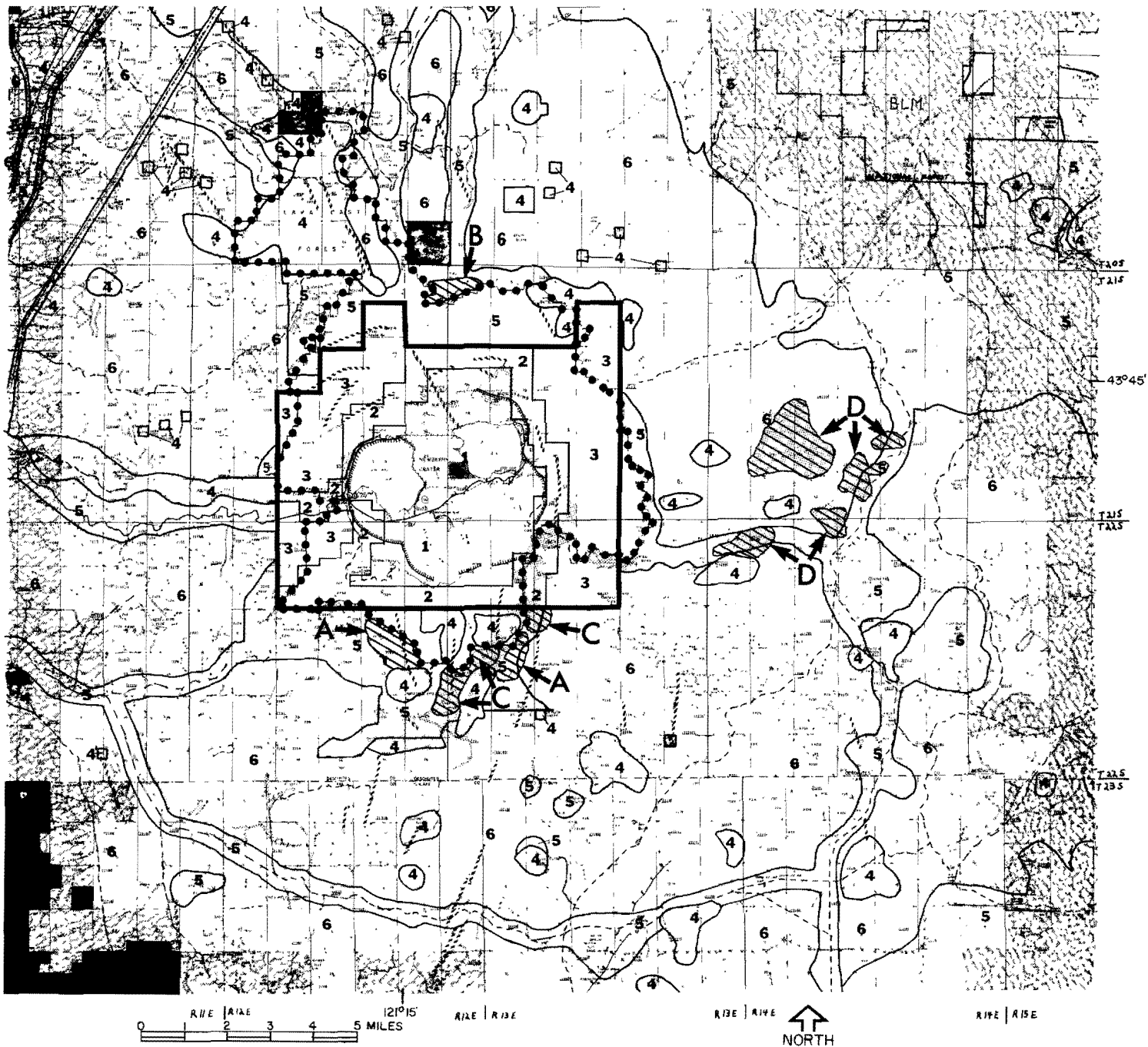
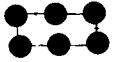


Figure 10.2. Suggested areas for drilling four sites (A, B, C, and D). See Figure 10.3 for drilling sequence.

EXPLANATION



Newberry Caldera Known Geothermal Resource Area



Area considered unsuitable for the siting of geothermal power plants by the Energy Facility Siting Council (EFSC)

Zones defined and delineated by the Deschutes National Forest Land and Resource Plan (proposed), and Land and Resource Plan Environmental Impact Statement (draft) for the Newberry Caldera Known Geothermal Resource Area:

- 1 Area within the crater with high visual and recreational values. No leasing or surface occupancy would be allowed under the proposed plan. Exploratory drilling would be allowed on a case by case basis.
- 2 Area consisting of the rim of the crater, the main road into the crater, and Paulina Creek. This area has high recreational value. Visual quality is also considered important. Leasing would be allowed but surface occupancy will be restricted under the proposed plan. Exploratory drilling would be allowed on a case by case basis.
- 3 Area within the KGRA but outside the crater. Visual resources are important but other resources are not as sensitive or critical. Both leasing and surface occupancy would be allowed under the proposed plan.

Zones defined and delineated by the Deschutes National Forest Noncompetitive Geothermal Leasing Environmental Assessment report (1982) for Newberry Volcano, exclusive of the Known Geothermal Resource Area:

- 4 Areas in which leasing will be allowed but surface occupancy will be restricted. These areas include the following: geologic interest areas, research natural areas, special use permit areas, administrative sites, developed recreation areas, critical wildlife habitat, Paulina Creek Management Zone, old growth management areas, cinder buttes and unstable soil areas.
- 5 Areas in which visual and game species management concerns will be considered in determining leasing policies. Additional regulations, stipulations, environmental analyses and approval of plans and operations will be utilized by the government to control leasing activities.
- 6 Areas in which standard leasing procedures will be used.



Public lands outside of the Newberry KGRA for which no lease applications have yet been filed (source: Dolores Yates Greater Columbia Energy Inc.)



Privately owned land



Mercury anomaly (greater than 90 ppb)



Fissure (source: MacLeod and others, 1982)



Fault, ball and bar on downthrown side (source: MacLeod and others, 1982)



Ring fault (hachures on downthrown side)(source: MacLeod and others, 1982)



Suggested area for drill sites



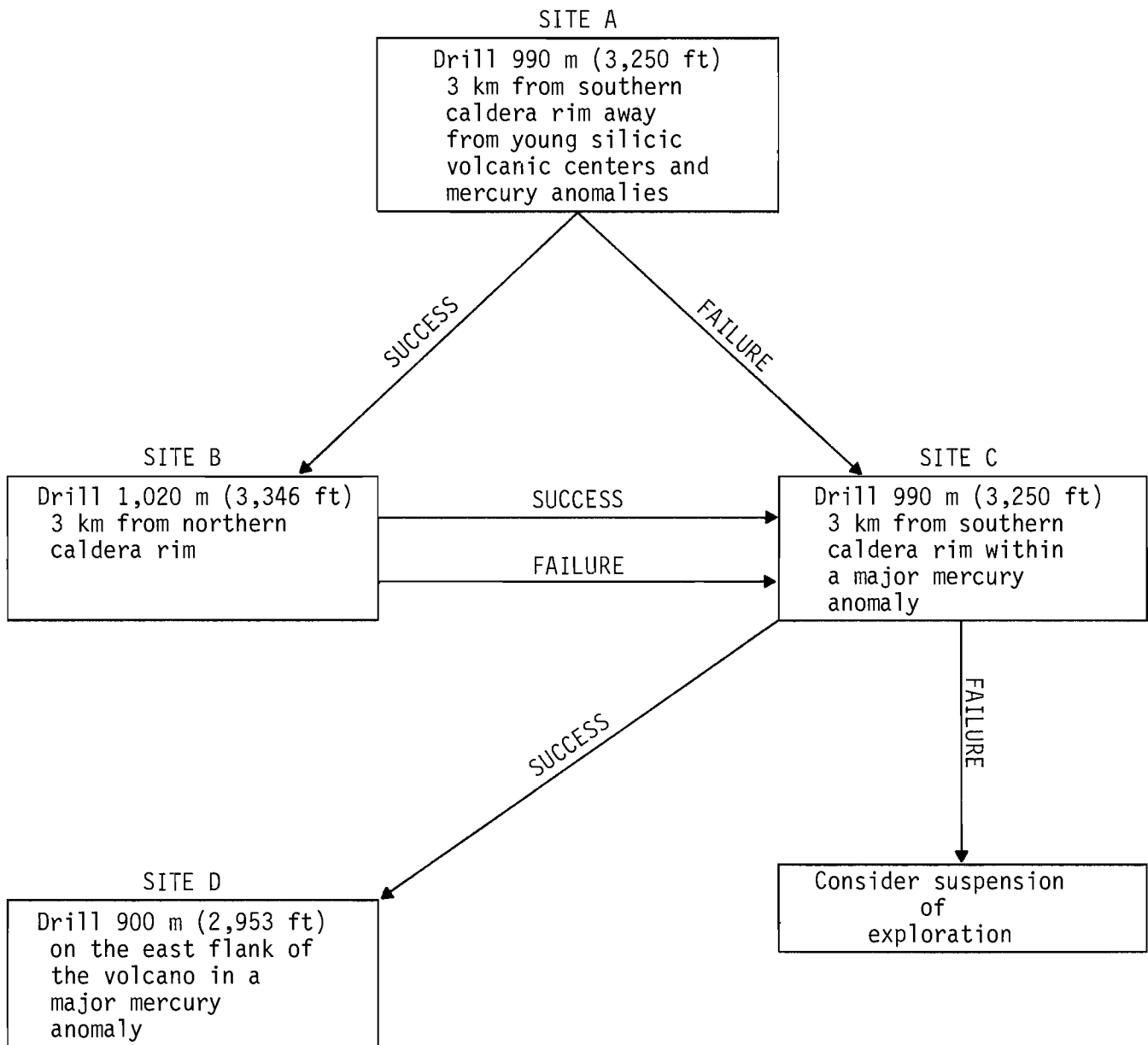


Figure 10.3. Suggested sequence of drilling at four sites. See Figure 10.2 for proposed locations of the sites.

SELECTED REFERENCES

- Anderson, E.M., 1936, The dynamics of the formation of cone sheets, ring dikes, and cauldron subsidences: Royal Society of Edinburgh Proceedings, v. 56, pt. 2, p. 128-157.
- Bacon, C.R., 1981, Geology and geophysics in the Cascade Range [abs.]: Society of Exploration Geophysicists, 51st Annual International Meeting, Los Angeles, Calif., 1981, Geothermal Special Session 3, Technical Program Abstracts, G3.1.
- 1983, Eruptive history of Mount Mazama and Crater Lake caldera, Cascade Range, U.S.A., *in* Aramaki, S., and Kushiro, I., eds., Arc volcanism: Journal of Volcanology and Geothermal Research, v. 18, p. 57-115.
- Bailey, R.A., Dalrymple, G.B., and Lanphere, M.A., 1976, Volcanism, structure, and geochronology of Long Valley Caldera, Mono County, California: Journal of Geophysical Research, v. 81, no. 5, p. 725-744.
- Barnes, H.L., 1979, Solubilities of ore minerals, *in* Barnes, H.L., ed., Geochemistry of hydrothermal ore deposits: New York, N.Y., Wiley and Sons, p. 404-460.
- Beaulieu, J.D., 1972, Geologic formations of eastern Oregon: Oregon Department of Geology and Mineral Industries Bulletin 73, 80 p.
- Berry, G.W., Grim, P.J., and Ikelman, J.A., 1980, Thermal springs list for the United States: National Oceanic and Atmospheric Administration Key to Geophysical Records Documentation No. 12, 59 p.
- Bhattacharyya, B.K., and Leu, L.-K., 1975, Analysis of magnetic anomalies over Yellowstone National Park: Mapping of Curie point isothermal surface for geothermal reconnaissance: Journal of Geophysical Research, v. 80, p. 4461-4465.
- Black, G.L., 1982, An estimate of the geothermal potential of Newberry volcano: Oregon Department of Geology and Mineral Industries, Oregon Geology, v. 44, no. 4, p. 44-46; no. 5, p. 57.
- Blackwell, D.D., Black, G.L., and Priest, G.R., 1982a, Geothermal gradient data (1981): Oregon Department of Geology and Mineral Industries Open-File Report O-82-4, 429 p.

- Blackwell, D.D., Bowen, R.G., Hull, D.A., Riccio, J.F., and Steele, J.L., 1982b, Heat flow, arc volcanism, and subduction in northern Oregon: Journal of Geophysical Research, v. 87, p. 8735-8754.
- Blackwell, D.D., Hull, D.A., Bowen, R.G., and Steele, J.L., 1978, Heat flow in Oregon: Oregon Department of Geology and Mineral Industries Special Paper 4, 42 p.
- Blakely, R.J., 1981, A program for rapidly computing the magnetic anomaly over digital topography: U.S. Geological Survey Open-File Report 81-298, 46 p.
- Bowen, R.G., Peterson, N.V., and Riccio, J.F., compilers, 1978, Low- to intermediate-temperature thermal springs and wells in Oregon: Oregon Department of Geology and Mineral Industries Geological Map Series GMS-10.
- Bowman, J.F., 1940, The geology of the north half of the Hampton quadrangle, Oregon: Corvallis, Oreg., Oregon State College master's thesis, 71 p.
- Brook, C.A., Mariner, R.H., Mabey, D.R., Swanson, J.R., Guffanti, M., and Muffler, L.J.P., 1979, Hydrothermal convection systems with reservoir temperatures $>90^{\circ}$ C, *in* Muffler, L.J.P., ed., Assessment of geothermal resources of the United States--1978: U.S. Geological Survey Circular 790, p. 18-85.
- Capuano, R.M., and Bamford, R.W., 1978, Initial investigation of soil-mercury geochemistry as an aid to drill site selection in geothermal systems: Salt Lake City, Earth Science Laboratory, University of Utah Research Institute report for USDOE, ID0/78-1701.b.3.3.1, 32 p.
- Cathles, L.M., 1977, An analysis of the cooling of intrusives by ground-water convection which includes boiling: Economic Geology, v. 72, p. 804-826.
- Century West Engineering Corporation, 1982, La Pine aquifer managment plan: Bend, Oreg., Century West Engineering Corporation.
- Chapman, R.H., 1966, Gravity base station network: California Division of Mines and Geology Special Report 90, 49 p.
- Christiansen, R.L., and Blank, H.R., 1972, Volcanic stratigraphy of the Quaternary rhyolite plateau in Yellowstone National Park: U.S. Geological Survey Professional Paper 729-B, 18 p.
- Christopherson, K.R., and Hoover, D.B., 1981, Reconnaissance resistivity mapping of geothermal regions using multicoil airborne electromagnetic systems [abs.]: Society of Exploration Geophysicists, 51st Annual International Meeting, Los Angeles, Calif., 1981, Geothermal Special Session 3, Technical Program Abstracts, G3.6.

- Connard, G.G., 1979, Analysis of aeromagnetic measurements from the central Oregon Cascades: Corvallis, Oreg., Oregon State University master's thesis, 101 p.
- Connard, G.G., Couch, R.W., and Gemperle, M., 1983, Analysis of aeromagnetic measurements from the Cascade Range in central Oregon: Geophysics, v. 48, no. 3, p. 376-390.
- Couch, R.W., 1978, Total field aeromagnetic anomaly map, Cascade Mountain Range, central Oregon: Oregon Department of Geology and Mineral Industries Geological Map Series GMS-9.
- 1979, Geophysical investigations of the Cascade Range in central Oregon: U.S. Geological Survey Extramural Geothermal Research Program, Final Report, 95 p.
- Couch, R.W., Gemperle, M., Connard, G.G., and Pitts, G.S., 1981, Structural and thermal implications of gravity and aeromagnetic measurements made in the Cascade volcanic arc [abs.]: Society of Exploration Geophysicists, 51st Annual International Meeting, Los Angeles, Calif., 1981, Geothermal Special Session 3, Technical Program Abstracts, G3.3.
- Cox, M.E., 1981, An approach to problems of a geothermal mercury survey, Puna, Hawaii: Geothermal Resources Council Transactions, v. 5, p. 67-70.
- Dole, H.M., ed., 1968, Andesite conference guidebook (International Upper Mantle Project science report 16-S): Oregon Department of Geology and Mineral Industries Bulletin 62, 107 p.
- Eaton, G.P., Christiansen, R.L., Iyer, N.M., Andrew, M.P., Mabey, D.R., Blank, H.R., Jr., Zietz, I., and Gettings, M.E., 1975, Magma beneath Yellowstone National Park: Science, v. 188, p. 787-796.
- Eshelman, A., Siegel, S.M., and Siegel, B.Z., 1971, Is mercury from Hawaiian volcanoes a natural source of pollution: Nature, v. 233, p. 471-472.
- Fang, S.C., 1978, Sorption and transformation of mercury vapor by dry soil: Environmental Science Technology, v. 12, no. 3, p. 285-288.
- Fiebelkorn, R.B., Walker, G.W., MacLeod, N.S., McKee, E.H., and Smith, J.G., 1982, Index to K-Ar age determinations for the State of Oregon: U.S. Geological Survey Open-File Report 82-596, 40 p.
- Finn, C., and Williams, D.L., 1982, Gravity evidence for a shallow intrusion under Medicine Lake volcano, California: Geology, v. 10, p. 503-507.

- Fournier, R.O., White, D.E., and Truesdell, A.H., 1976, Convective heat flow in Yellowstone National Park: Second United Nations Symposium on the Development and Use of Geothermal Resources, San Francisco, Calif., 1975, Proceedings: Washington, D.C., U.S. Government Printing Office, v. 1, p. 731-739.
- Friedman, I., 1968, Hydration rind dates rhyolite flows: Science, v. 159, no. 3817, p. 878-880.
- 1977, Hydration rind dating of volcanism at Newberry crater, Oregon: U.S. Geological Survey Journal of Research, v. 5, no. 3, p. 337-342.
- Friedman, I., and Peterson, N.V., 1971, Obsidian hydration dating applied to dating volcanic activity: Science, v. 72, p. 1028.
- Ganoe, S.J., 1983, Investigation of P_n -wave propagation in Oregon: Corvallis, Oreg., Oregon State University master's thesis, 97 p.
- Gebhard, C., 1982, Geothermal development issues, in Shay, B., ed., Recommendations to Deschutes County: Bend, Oreg., Central Oregon Project Energy, 163 p.
- Grdenic, D., Tunell, G., and Rytuba, J.J., 1969, Mercury-80, in Wedepohl, K.H., ed., Handbook of geochemistry: New York, N.Y., Springer, Chapter 80A, 8 p.
- Griscom, A., and Roberts, C.W., 1982, Principal facts for 397 gravity stations in the vicinity of Newberry volcano, Oregon: U.S. Geological Survey Open-File Report 82-0652, 12 p.
- Hampton, E.R., 1964, Geologic factors that control the occurrence and availability of ground water in the Fort Rock Basin, Lake County, Oregon: U.S. Geological Survey Professional Paper 383-B, 29 p.
- Hanaoka, H., 1980, Numerical model experiment of hydrothermal system: Bulletin of the Geological Survey of Japan, v. 31, p. 321-332.
- Hawkes, H.E., and Williston, S.H., 1962, Mercury vapor as a guide to lead-zinc-silver deposits: Mining Congress Journal, v. 48, p. 30-32.
- Higgins, M.W., 1969, Airfall ash and pumice lapilli deposits from central pumice cone, Newberry caldera, Oregon, in Geological Survey Research 1969: U.S. Geological Survey Professional Paper 650-D, p. D26-D32.
- 1973, Petrology of Newberry volcano, central Oregon: Geological Society of America Bulletin, v. 84, no. 2, p. 455-487.

- Higgins, M.W., and Waters, A.C., 1967, Newberry caldera, Oregon: A preliminary report: Oregon Department of Geology and Mineral Industries, Ore Bin, v. 29, no. 3, p. 37-60.
- Hildreth, W., 1981, Gradients in silicic magma chambers: Implications for lithospheric magmatism: *Journal of Geophysical Research*, v. 86, no. B11, p. 10153-10192.
- Hildreth, W., and Spera, F. 1974, Magma chamber of the Bishop Tuff: Gradients in T, P_{total} , and P_{H_2O} : *Geological Society of America Abstracts with Programs*, v. 6, no. 7, p. 795.
- Hill, D.P., Mooney, W.D., Fuis, G.S., and Healy, J.H., 1981, Evidence on the structure and tectonic environment of the volcanoes in the Cascade Range, Oregon and Washington, from seismic-refraction/reflection measurements [abs.]: *Society of Exploration Geophysicists, 51st Annual International Meeting, Los Angeles, Calif., 1981, Geothermal Special Session 3, Technical Program Abstracts*, G3.2.
- Horsnail, R.F., Nichol, I., and Webb, J.S., 1969, Influence of variations in secondary environment on the metal content of drainage sediments: *Quarterly of the Colorado School of Mines*, v. 64, p. 307-322.
- Hull, D.A., Bowen, R.G., Blackwell, D.D., and Peterson, N.V., 1977, Geothermal gradient data, Brothers fault zone, Oregon: Oregon Department of Geology and Mineral Industries Open-File Report O-76-2, 25 p.
- Iyer, H.M., Evans, J.R., Zandt, G., Stewart, R.M., Coakley, J.M., and Roloff, J.N., 1981, A deep low-velocity body under the Yellowstone caldera, Wyoming: Delineation using teleseismic P -wave residuals and tectonic interpretation: *Summary: Geological Society of America Bulletin*, v. 92, no. 11, p. 792-798.
- Iyer, H.M., Rite, A., and Green, S.M., 1982, Search for geothermal heat sources in the Oregon Cascades by means of teleseismic P -residual technique: *Society of Exploration Geophysicists, Technical Program Abstracts and Bibliography 1982*, p. 479-482.
- Jepson, A.F., 1973, Measurements of mercury vapor in the atmosphere, in Kothny, E.L., ed., *Trace elements in the environment (Advances in Chemistry Series 123)*, Washington, D.C., American Chemical Society Publications.
- Jerome Instrument Corporation, 1978, Applications manual for the Jerome model 301 gold-film mercury detector: Jerome, Ariz., Jerome Instrument Corporation, 25 p.

- Juncal, R.W., 1980, Mercury and arsenic soil geochemistry, in Geothermal reservoir assessment case study, northern Basin and Range province, northern Dixie Valley, Nevada: Reno, Nev., University of Nevada, Mackay Minerals Research Institute report, 117 p.
- Klusman, R.W., Cowling, S., Culvey, B., Roberts, C., and Schwab, A.P., 1977, Preliminary evaluation of secondary controls on mercury in soils of geothermal districts: *Geothermics*, v. 6, p. 1-8.
- Klusman, R.W., and Landress, R.A., 1978, Secondary controls on mercury in soils of geothermal areas: *Journal of Geochemical Exploration*, v. 9, no. 1, p. 75-92.
- Knapp, R.B., and Norton, D., 1981, Preliminary numerical analysis of processes related to magma crystallization and stress evolution in cooling pluton environments: *American Journal of Science*, v. 281, p. 35-68.
- Koksoy, M., and Bradshaw, P.M.D., 1969, Secondary dispersion of mercury from cinnabar and stibnite deposits, West Turkey: *Quarterly of the Colorado School of Mines*, v. 64, p. 333-356.
- Koksoy, M., Bradshaw, P.M.D., and Tooms, J.S., 1967, Notes on the determination of mercury in geological samples: *Institute of Mining and Metallurgy Bulletin*, v. 726, p. B121-124.
- Lachenbruch, A.H., Sass, J.H., Munroe, R.J., and Moses, T.H., Jr., 1976, Geothermal setting and simple heat conduction models for the Long Valley caldera: *Journal of Geophysical Research*, v. 81, p. 769-784.
- Landa, E.R., 1978, The retention of metallic mercury vapor by soils: *Geochimica et Cosmochimica Acta*, v. 42, no. 9, p. 1407-1411.
- Larsen, D.M., 1976, Soil resource inventory, Deschutes National Forest: U.S. Forest Service, Deschutes National Forest report, 381 p.
- Lau, K.H., 1980, Effect of permeability on cooling of a magma intrusion in a geothermal reservoir: Lawrence Livermore Laboratory Report UCRL-52888, 37 p.
- Lawrence, R.D., 1974, Large-scale tear faulting at the northern termination of the Basin and Range province in Oregon, in The comparative evaluation of ERTS-1 imagery for resource inventory in land use planning: A multidiscipline research investigation, final report: Corvallis, Oreg., Oregon State University, in cooperation with Goddard Space Flight Center, p. 214-224.

- Lowry, W.D., 1940, The geology of the Bear Creek area, Crook and Deschutes Counties, Oregon: Corvallis, Oreg., Oregon State College master's thesis, 78 p.
- Loy, W.G., Stuart, A., Patton, C.P., and Plank, R.D., 1976, Atlas of Oregon: Eugene, Oreg., University of Oregon Bookstore, 215 p.
- McCarthy, J.H., Jr., Meuschke, J.L., Ficklin, W.H., and Learned, R.E., 1970, Mercury in the atmosphere, in Mercury in the environment: U.S. Geological Survey Professional Paper 713, 67 p.
- McCarthy, J.H., Jr., Vaughn, W.W., Learned, R.E., and Meuschke, J.L., 1969, Mercury in soil gas and air--a potential tool in mineral exploration: U.S. Geological Survey Circular 609, 16 p.
- MacLeod, N.S., and Sammel, E.A., 1982, Newberry volcano, Oregon: A Cascade Range geothermal prospect: Oregon Department of Geology and Mineral Industries, Oregon Geology, v. 44, no. 11, p. 123-131.
- MacLeod, N.S., Sherrod, D.R., and Chitwood, L.A., 1982, Geologic map of Newberry volcano, Deschutes, Klamath and Lake Counties, Oregon: U.S. Geological Survey Open-File Report 82-847.
- MacLeod, N.S., Sherrod, D.R., Chitwood, L.A., and McKee, E.H., 1981, Newberry volcano, Oregon, in Johnston, D.A, and Donnelly-Nolan, J., eds., Guides to some volcanic terranes in Washington, Idaho, Oregon, and northern California: U.S. Geological Survey Circular 838, p. 85-103.
- MacLeod, N.S., Walker, G.W., and McKee, E.H., 1975, Geothermal significance of eastward increase in age of upper Cenozoic rhyolitic domes in southeastern Oregon, in Second United Nations Symposium on the Development and Use of Geothermal Resources, San Francisco, California, 1975, Proceedings: Washington, D.C., U.S. Government Printing Office, v. 1, p. 465-474.
- Mariner, R.H., Swanson, J.R., Orris, G.J., Presser, J.S., and Evans, W.C., 1980, Chemical and isotopic data for water from thermal springs and wells of Oregon: U.S. Geological Survey Open-File Report 80-737, 50 p.
- Matlick, J.S., III, and Buseck, P.R., 1976: Exploration for geothermal areas using mercury: A new geochemical technique, in Second United Nations Symposium on the Development and Use of Geothermal Resources, San Francisco, California, 1975, Proceedings: Washington, D.C., U.S. Government Printing Office, v. 1, p. 785-792.

- Matlick, J.S., III, and Shiraki, M., 1981, Evaluation of the mercury soil mapping geothermal exploration techniques: Geothermal Resources Council Transactions, v. 5, p. 95-98.
- Murphey, C.F., 1982, Investigations of the Cascade Range of Oregon through the use of gravity, topography, and heat flow: Dallas, Tex., Southern Methodist University master's thesis, 86 p.
- Nakamura, K., 1977, Volcanoes as possible indicators of tectonic stress orientation--principle and proposal: Journal of Volcanology and Geothermal Research, v. 2, no. 1, p. 1-16.
- Nichols, R.L., 1938, Fissure eruptions near Bend, Oregon [abs.]: Geological Society of America Bulletin, v. 49, no. 12, pt. 2, p. 1894.
- Norton, D., and Taylor, H.P., Jr., 1979, Quantitative simulation of the hydrothermal systems of crystallizing magmas on the basis of transport theory and oxygen-isotope data: An analysis of the Skaergaard intrusion: Journal of Petrology, v. 20, p. 421-486.
- Peterson, N.V., and Groh, E.A., 1963a, Maars of the south-central Oregon: Oregon Department of Geology and Mineral Industries, Ore Bin, v. 25, no. 5, p. 73-88.
- 1963b, Recent volcanic landforms in central Oregon: Oregon Department of Geology and Mineral Industries, Ore Bin, v. 25, no. 3, p. 33-45.
- 1972, Geology and origin of the Metolius Springs, Jefferson County, Oregon: Oregon Department of Geology and Mineral Industries, Ore Bin, v. 34, no. 3, p. 41-51.
- Peterson, N.V., Groh, E.A., Taylor, E.M., and Stensland, D.E., 1976, Geology and mineral resources of Deschutes County, Oregon: Oregon Department of Geology and Mineral Industries Bulletin 89, 66 p.
- PheTps, D.W., and Buseck, P.R., 1978, Natural concentrations of Hg in the Yellowstone and Coso geothermal fields: Geothermal Resources Council Transactions, v. 2, p. 521-522.
- 1980, Distribution of soil mercury and the development of soil-mercury anomalies in the Yellowstone geothermal area, Wyoming: Economic Geology, v. 75, p. 730-741.
- Phillips, K.N., and Van Denburgh, A.S., 1968, Hydrology of Crater, East, and Davis Lakes, Oregon: U.S. Geological Survey Water-Supply Paper 1859-E, 60 p.

- Pitts, G.S., 1979, Interpretation of gravity measurements made in the Cascade Mountains and adjoining Basin and Range province in central Oregon: Corvallis, Oreg., Oregon State University master's thesis, 186 p.
- Pitts, G.S., and Couch, R., 1978, Complete Bouguer gravity anomaly map, Cascade Mountain Range, central Oregon: Oregon Department of Geology and Mineral Industries Geological Map Series GMS-8.
- Plouff, D., 1977, Preliminary documentation for a FORTRAN program to compute gravity terrain corrections based on topography digitized on a geographic grid: U.S. Geological Survey Open-File Report 77-535, 45 p.
- Ribando, R.J., Torrance, R.E., and Turcotte, D.L., 1978, Numerical calculation of the convective cooling of an infinite sill: *Tectonophysics*, v. 50, p. 337-347.
- Robertson, D.E., Fruchter, J.S., Ludwick, J.D., Wilerson, C.L., Crecelius, E.A., and Evans, J.C., 1978, Chemical characterization of gases and volatile heavy metals in geothermal effluents: *Geothermal Resources Council Transactions*, v. 2, p. 579-582.
- Robinson, J.W., and Price, D., 1963, Ground water in the Prineville area, Crook County, Oregon: U.S. Geological Survey Water-Supply Paper 1619-P, 49 p.
- Rogers, R.D., and McFarlane, J.C., 1978, Factors influencing the volatilization of Hg from soil: Environmental Protection Agency Report 600/3-78-054, 13 p.
- Ryan, M.P., Blevins, J.Y.K., Okamura, A.T., and Koyyanagi, R.T., 1983, Magma reservoir subsidence mechanics: Theoretical summary and application to Kilauea volcano, Hawaii: *Journal of Geophysical Research*, v. 88, no. B5, p. 4147-4181.
- Sammel, E.A., 1981, Results of test drilling at Newberry volcano, Oregon: *Geothermal Resources Council Bulletin*, v. 10, no. 11, p. 3-8.
- Sherrod, D.R., and MacLeod, N.S., 1979, The last eruptions at Newberry volcano, central Oregon [abs.]: *Geological Society of America Abstracts with Programs*, v. 11, no. 3, p. 127.
- Smith, R.L., and Shaw, H.R., 1975, Igneous-related geothermal systems, in White, D.R., and Williams, D.L., eds., *Assessment of geothermal resources of the United States-1975*: U.S. Geological Survey Circular 726, p. 58-83.

- Stanley, W.D., 1981, Magnetotelluric survey of the Cascade volcanoes region, Pacific Northwest [abs.]: Society of Exploration Geophysicists, 51st Annual International Meeting, Los Angeles, Calif., 1981, Geothermal Special Session 3, Technical Program Abstracts, G3.7.
- 1982, A regional magnetotelluric survey of the Cascade Mountains region: U.S. Geological Survey Open-File Report 82-126, 16 p.
- Stearns, H.T., 1931, Geology and water resources of the middle Deschutes River basin, Oregon, in Grover, N.C., Chief Hydraulic Engineer, Contributions to the hydrology of the United States 1930: U.S. Geological Survey Water-Supply Paper 637, p. 125-212.
- Steeple, D.W., and Iyer, H.M., 1976, Low-velocity zone under Long Valley caldera as determined from teleseismic events: Journal of Geophysical Research, v. 81, p. 849-860.
- Stensland, D.E., 1970, Geology of part of the northern half of the Bend quadrangle, Jefferson and Deschutes Counties, Oregon: Corvallis, Oreg., Oregon State University master's thesis, 118 p.
- Stewart, J.H., Walker, G.W., and Kleinhample, F.J., 1975, Oregon-Nevada lineament: Geology, v. 3, no. 5, p. 265-268.
- Swanson, D.A., 1969, Reconnaissance geologic map of the east half of the Bend quadrangle, Crook, Wheeler, Jefferson, Wasco, and Deschutes Counties, Oregon: U.S. Geological Survey Miscellaneous Geologic Investigations Map I-568.
- Taylor, E.M., 1965, Recent lava flows of the Three Sisters area, Oregon: Oregon Department of Geology and Mineral Industries, Ore Bin, v. 27, no. 7, p. 121-142.
- Trost, P.B., and Bisque, R.E., 1971, Differentiation of vaporous and ionic mercury in soils: International Geochemical Exploration Symposium, 3rd, Toronto, 1970, Proceedings: Canadian Institute of Mining and Metallurgy Special Volume 11, p. 276-278.
- 1972, Distribution of mercury in residual soils, in Hartung, R., and Dinman, D.B., eds., Environmental mercury contamination: Ann Arbor, Mich., Ann Arbor Science Publications, p. 178-196.
- Truesdell, A.H., and Fournier, R.O., 1976, Conditions in the deeper parts of the hot spring systems of Yellowstone National Park, Wyoming: U.S. Geological Survey Open-File Report 76-428, 22 p.

- Tucker, E.R., 1975, Geology and structure of the Brothers fault zone in the central part of the Millican SE quadrangle, Deschutes County, Oregon: Corvallis, Oreg., Oregon State University master's thesis, 88 p.
- Turner, F.J., and Weiss, L.E., 1963, Structural geology of metamorphic tectonites: New York, N.Y., McGraw-Hill, 545 p.
- U.S. Forest Service, 1980, Environmental assessment report, noncompetitive geothermal leasing, Fort Rock Ranger District, Deschutes National Forest: U.S. Forest Service, Pacific Northwest Region Deschutes National Forest, 140 p.
- U.S. Geological Survey, 1979, Aeromagnetic map of the Newberry area, Oregon: U.S. Geological Survey Open-File Report 79-1366.
- Walker, G.W., 1969, Geology of the High Lava Plains province, in Mineral and water resources of Oregon: Oregon Department of Geology and Mineral Industries Bulletin 64, p. 77-79.
- 1970, Cenozoic ash-flow tuffs of Oregon: Oregon Department of Geology and Mineral Industries, Ore Bin, v. 32, no. 6, p. 97-105.
- 1974, Some implications of late Cenozoic volcanism to geothermal potential in the High Lava Plains of south-central Oregon: Oregon Department of Geology and Mineral Industries, Ore Bin, v. 36, no. 7, p. 109-119.
- 1977, Geologic map of Oregon east of the 121st meridian: U.S. Geological Survey Miscellaneous Investigations Series Map I-902.
- Walker, G.W., Dalrymple, G.B., and Lanphere, M.A., 1974, Compilation of potassium-argon ages of Cenozoic volcanic rocks of Oregon: U.S. Geological Survey Miscellaneous Field Studies Map MF-569.
- Walker, G.W., Peterson, N.V., and Greene, R.C., 1967, Reconnaissance geologic map of the east half of the Crescent quadrangle, Lake, Deschutes, and Crook Counties, Oregon: U.S. Geological Survey Miscellaneous Geologic Investigations Map I-493.
- Weast, R.C., Samuel, M.S., and Hodgman, C.D., 1965, Handbook of chemistry and physics: Cleveland, Ohio, Chemical Rubber Company, 1696 p.
- Wells, F.G., and Peck, D.L., 1961, Geologic map of Oregon west of the 121st meridian: U.S. Geological Survey Miscellaneous Geologic Investigations Map I-325.
- White, D.D., Fournier, R.D., Muffler, L.J.P., and Truesdell, A.H., 1975, Physical results of research drilling in thermal areas of Yellowstone National Park, Wyoming: U.S. Geological Survey Professional Paper 892, 70 p.

- White, D.E., Muffler, L.J.P., and Truesdell, A.H., 1971, Vapor-dominated hydrothermal systems compared with hot-water systems: *Economic Geology*, v. 66, p. 75-97.
- Williams, D.L., and Finn, C., 1981a, Evidence from gravity data on the location and size of subvolcanic intrusions [abs.]: Society of Exploration Geophysicists, 51st Annual Meeting, Los Angeles, Calif., Geothermal Special Session 3, 1981, Technical Program Abstracts, G3.5.
- 1981b, Gravity anomalies and subvolcanic intrusions in the Cascade Range and at other selected volcanoes: Preliminary results: In preparation.
- 1982, Gravity studies in volcanic terranes: Society of Exploration Geophysicists, Technical Program Abstracts and Bibliography 1982, p. 303-305.
- Williams, H., 1935, Newberry volcano of central Oregon: *Geological Society of America Bulletin*, v. 46, no. 2, p. 253-304.
- Ziagos, J.P., and Blackwell, D.D., 1980a, A model for the effect of horizontal flow in a thin aquifer on temperature-depth profiles: *Geothermal Resources Council Transactions*, v. 5, p. 221-224.
- 1980b, The role of convective heat transfer in the cooling of shallow crustal magma chambers, *EOS (American Geophysical Union Transactions)*, v. 61, p. 1146.

APPENDIX A

ANALYTICAL LABORATORY PROCEDURE FOR THE NEWBERRY MERCURY SURVEY

by

R. Mark Hadden,

Oregon Department of Geology and Mineral Industries

Introduction

The Jerome Model 301 Gold Film Mercury Detector and the low-temperature method was used to analyze soil samples for the Newberry project. This method was found to give good results, reproducibility, and ease in sample testing. The data produced are of relative value and not absolute value; however, the data are easily sufficient to establish the mercury anomalies. The following pages contain comments, an account of the analytical laboratory procedure (Figure A.1), and a description of the materials used. This procedure should be used in conjunction with the Jerome Instrument Corporation instruction manual for the Model 301 Mercury Detector. If this procedure is followed with the same detector, then future workers in the Newberry volcano area should be able to add data directly comparable to the data of this survey.

Initial Assembly

Prepare mercury vessel by placing two drops of fresh mercury into it. Place vessel into a styrofoam or insulated container. This helps stabilize air temperature for more constant readings. Place digital thermometer probe into mercury vessel and set aside for one hour. In one hour the mercury-saturated vapor in the vessel will reach equilibrium at room temperature. The ideal temperature range is between 17° and 22° C. Turn hot plate to maximum setting (700° F) and allow to obtain full temperature (approximately 10 minutes). Heat glassware on hot plate during this time to volatilize any mercury in tubes.

Connect filters, glassware, and tubing in the proper air-flow direction to the Jerome 301 (see manual). Upon correct hookup, turn power on, turn "Gain" to middle position, turn "Mode" selector right to "Collector," adjust

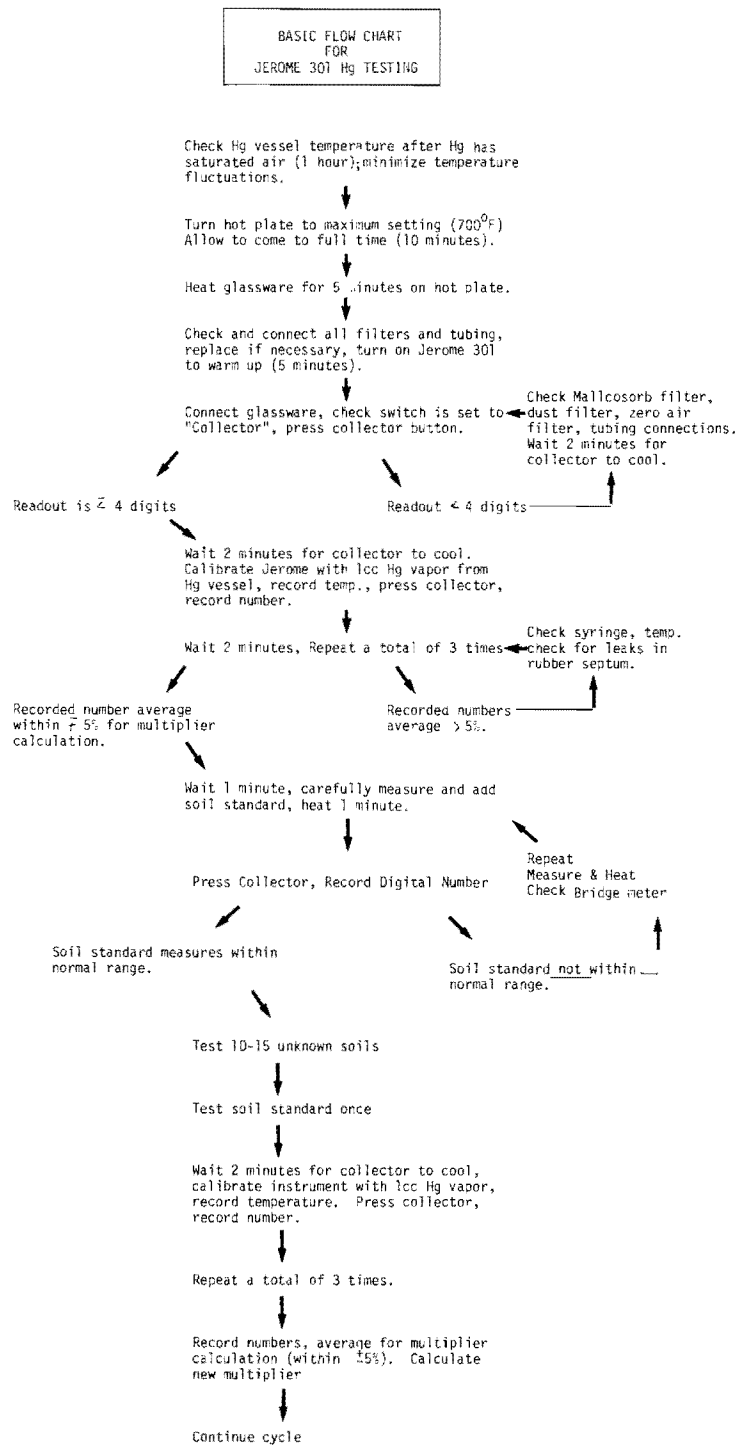


Figure A.1. Basic flow chart for Jerome 301 Hg testing.

"Bridge/Balance" to center. Allow approximately 5 minutes for instrument to warm up, press "Timer" firmly, and release. The indicator to the right of "Collector" will light up for 12 seconds. Wait 2 minutes and press "Timer" again. The collector takes 2 minutes to cool down. If, after pressing the timer, the readout is more than 4 digits, wait the required 2 minutes and press the timer again. Repeat until readout is only 3 or 4 digits.

Calibration

To calibrate the Jerome 301, record the temperature in the mercury vessel and place the syringe needle into the small hole in the top of the mercury vessel. Pump the syringe plungers up and down a few times to mix the mercury vapor. Withdraw 1 cc mercury vapor from the vessel, and inject the vapor into the rubber septum located near the pyrex wool duct filter. Wait 5 seconds for the meter to read 0 ± 2 , and press the timer; record the peak reading from the digital meter. Wait 2 minutes and repeat these steps until three consecutive readings within ± 5 percent of each other are obtained. Compute the average, and use the temperature-conversion chart and formula to calculate the "C factor" (calibration factor).

Soil Analysis

Once the Jerome 301 has been calibrated and a "C factor" has been established, unknown soil samples can be analyzed. Rotate the glass vial containing the unknown soil samples to mix the soil. Carefully fill the calibrated sample scoop or use an analytical balance to determine sample weight. Use the 0.25-gram scoop for soil samples greater than 50 ppb and a 1.0-gram scoop for soil samples less than 50 ppb.

Empty the soil sample completely into the first hot test tube, gently tapping the scoop against the bulb so all soil is removed. Immediately cap the test tube with combustion top and wait 1 minute. Remove the combustion top from the test tube and place on a clean bulb. Set the hot test tube on a heat-resistant pad with a test-tube clamp. Wait for the digital meter to stabilize, if needed, and then press the timer to heat the collector. Record the peak reading on the digital meter. Wait at least 1 minute for the collector to cool, then measure and add the next unknown soil sample,

and heat for the required 1 minute.

Clean the calibrated scoop before filling the next soil sample by using a paper tissue to eliminate any contamination between samples. Once the test tube has cooled on the heat-resistant pad, gently tap it upside down on a paper towel to remove any soil, and use a nylon test-tube brush to clean the tube.

Careful arrangement of the sample vials in an order during testing and an order after testing was used to keep a tight check of the samples. The procedure that was used for this project was to place 10 vials in order against the Jerome 301, and, after use, the vials were placed back in an empty vial carton.

Ten to 15 unknown samples were tested, depending on instrument function and whether the total accumulated digits recorded were below 1,000 digits. Upon reaching either of these limits, a soil standard was checked once, and then the instrument was recalibrated. Approximately 70 to 100 soil samples were analyzed using this procedure in one day's time.

Clean-Up Procedure

Mercury has collected on the gold films and must be removed before the instrument is turned off. Turn mode selector to "Films" and press "Timer." This heats the gold film to volatilize the absorbed mercury for a period of 20 minutes. During this time the hot plate can be turned off and all glassware must be removed or it will shatter. It is recommended that the zero air filter be placed onto a tube at the "in" part of the collector to eliminate any mercury from entering the instrument. After 20 minutes, turn the mode selector to "Collector" and turn off the instrument.

If the soil vials are not to be retested, empty soil and wash along with the test tubes in a mild detergent and rinse well.

Material and Supplies

The mallcosorb filter utilizes mallcosorb (magnesium perchlorate), a material commercially prepared by the Mallenchrordt Company. It is used to remove any H₂O, HCl, CO₂, and sulfur gases which may be present in the air stream. An indicator causes the mallcosorb to change from white to a medium violet when exposed to moisture and gases. The change in color is normal

during testing due to the moisture and gases in the air stream. However, if the mallcosorb is too contaminated, it will not change back to its original white color. Jerome Instrument Corporation states that there is a 200 to 400 sample range that can be tested before the mallcosorb should be changed. Use a 20 to 50 mesh size, mix thoroughly, and sieve out the fines before using. Use pyrex wool on the ends of the filter to keep the mallcosorb from entering the tygon tubing.

APPENDIX B

SOIL-MERCURY SURVEY ERROR ANALYSIS

by

George R. Priest,

Oregon Department of Geology and Mineral Industries

Comparison of the Low-Temperature Technique to Other Techniques

The low-temperature technique does not measure absolute mercury concentrations, because not all mercury is driven off by the heat source. Fifty samples were analyzed by complete-digestion atomic absorption (AA) at Bondar-Clegg and Company, North Vancouver, B.C., and by the high-temperature (800° C) gold-film technique at the University of Utah Research Institute in order to calibrate the low-temperature data to that determined by other techniques (Table B.1). Figure B.1 shows the three data sets, and Table B.2 gives calibration equations. The low-temperature method measures about 54 percent of the mercury, assuming the AA technique is a good absolute value. The low-temperature method measures about 42 percent of the mercury if the high-temperature gold-film technique is used as a standard. This compares well with the results obtained by the Jerome Instrument Corporation, who obtained about 40 to 60 percent of the high-T values when using a hot plate at 290° C (see the Model 301 gold-film mercury-detector manual).

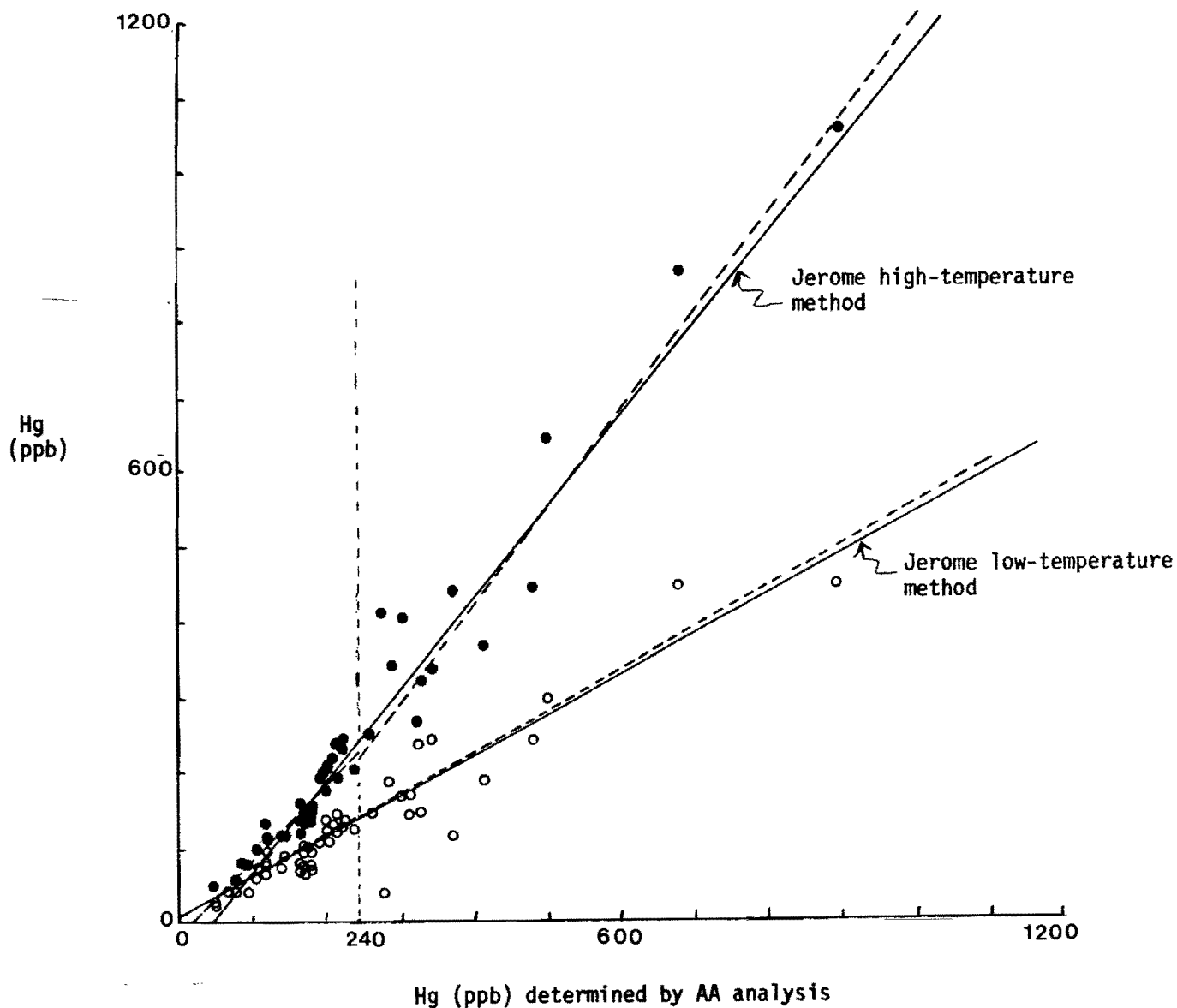


Figure B.1. Comparison of the low-temperature (open circles) and high-temperature (dots) gold film mercury measurements to atomic-absorption (AA) determinations on the same samples (see Table B.1). Least-squares regression lines (solid) were fitted to each data set. Dashed lines are regressions through values corresponding to AA values above and below 240 ppb. The linear equations for all regressions are given in Table B.2.

Table B.1. Duplicate analyses of 50 Newberry volcano soil samples analyzed by atomic absorption spectrometry (AA), utilizing total sample decomposition, by low-temperature (low-T) volatilization gold film method and by high-temperature (high-T) volatilization gold-film method. See mercury-contour map for exact locations of these samples.

Sample no.	Location T.(N.)-R.(E.) sec.	Primary material*	AA Hg (ppb)	Low-T Hg (ppb)	High-T Hg (ppb)
P5	21-13-31	NA+palagonitic sands	275	40	415
P20	21-12-31	MA	180	80	138
P21	21-12-31	MA	140	77	120
P161	21-12-31	NA or MA	120	75	120
P163	21-12-30	NA or MA	95	45	80
P200	21-12-30	Glacial outwash	315	170	150
P215	23-11-12	MA	325	150	323
P216	23-11-12	MA	500	300	645
P220	23-12-17	MA + basalt	185	95	143
P295	21-12-5	MA + basalt	180	100	160
P380	22-12-20	MA	680	450	868
P806	21-13-27	Palagonite sands	305	170	410
P819	21-12-31	Glacial outwash(?)	110	56	100
P870	23-13-16	MA	80	42	60
P874	23-13-20	MA	120	65	120
P915	22-14-3	NA	325	240	270
P919	21-14-34	NA	285	190	345
P924	21-14-26	NA	240	124	207
P925	21-14-27	NA	205	110	215
P1013	23-12-2	MA	195	110	195
P1015	22-12-36	MA	190	102	150
P1017	22-12-36	MA	165	69	140
P1018	23-12-2	MA	165	80	120
P1020	22-13-31	MA	180	73	150
P1021	22-13-31	MA	200	124	180
P1022	22-13-31	MA	200	139	205
P1023	22-13-31	MA	175	94	135
P1025	22-13-31	MA	260	143	255

Table B.1. Duplicate analyses of 50 samples.--Continued

Sample no.	Location T.(N.)-R.(E.) sec.	Primary material*	AA Hg (ppb)	Low-T Hg (ppb)	High-T Hg (ppb)
P1032	22-12-25	Cinders + MA	215	126	195
P1034	22-12-25	Cinders + MA	415	191	368
P1036	22-12-24	MA	220	131	235
P1038	22-12-24	MA	170	68	110
P1050	22-13-26	MA	70	42	65
P1066	22-13-26	MA	120	81	115
P1078	22-13-21	MA	95	84	82
P1081	22-13-16	Cinders	170	106	145
P1082	22-13-16	Cinders	480	244	453
P1088	22-13-20	NA	225	140	250
P1093	21-13-31	NA	105	60	70
P1095	21-13-31	NA	55	25	35
P1099	21-13-31	Cinders	55	34	55
P1115	22-12-3	MA or NA	145	93	120
P1128	22-13-6	MA or NA	120	98	135
P1201	22-13-8	Cinders	165	111	160
P1205	22-13-8	Cinders	345	246	340
P1210	22-13-5	Cinders + NA or MA	205	136	225
P1218	22-13-3	Cinders + NA or MA	215	148	240
PTP-1-24	21-13-25	Cinders	370	115	445
PTP-9-9	21-13-6	Cinders	900	450	1060
1028	22-12-25	Cinders	---	211	350

*NA = Ash from Newberry volcano

MA = Mazama ash

Table B.2. Regression data for linear equation $y=bx+a$. Regression intervals were picked relative to the 240-ppb AA level. R^2 =coefficient of determination. Syx=standard error of estimate. See Table 2 for explanation of high-T, low-T, and AA.

<u>x</u>	<u>y</u>	<u>Interval (ppb)</u>	<u>R²</u>	<u>a(ppb)</u>	<u>b(ppb)</u>	<u>Syx(ppb)</u>
AA	Low-T	All	0.88	4.17	0.54	3.15
AA	Low-T	0-240	0.78	1.92	0.56	15.13
AA	Low-T	240+	0.78	-12.96	0.57	52.58
AA	High-T	All	0.94	-51.08	1.22	49.36
AA	High-T	0-240	0.86	-17.76	1.02	21.01
AA	High-T	240+	0.88	-96.02	1.31	82.80
Low-T	AA	All	0.88	21.62	1.63	54.35
Low-T	AA	0-240	0.78	32.02	1.39	23.75
Low-T	AA	240+	0.78	109.17	1.37	81.74
Low-T	High-T	All	0.81	-23.35	1.98	84.62
Low-T	High-T	0-240	0.76	16.78	1.35	25.97
Low-T	High-T	240+	0.66	81.81	1.69	136.67
High-T	AA	All	0.94	53.95	0.77	39.15
High-T	AA	0-240	0.69	36.30	0.88	31.29
High-T	AA	240+	0.92	76.76	0.73	52.06
High-T	Low-T	All	0.81	33.61	0.41	38.47
High-T	Low-T	0-240	0.76	12.76	0.56	16.71
High-T	Low-T	240+	0.66	41.99	0.39	65.63

Analytical Error

The moderate scatter of the data in Figure 6.3 shows that the precision of the low-temperature (low-T) and high-temperature (high-T) methods is not as high as might be desired, although much of the scatter occurs in samples with absolute mercury over 240 ppb (AA method). Samples in this range of absolute concentration yield values greater than about 90-ppb mercury when analyzed by the low-T method. Samples in this range correspond to less than 9 percent of the data points plotted on the contour map (Figures B.1 and B.2). If these data were excluded, the correlation between analytical methods would be somewhat higher (Figure B.1, Table B.2). This is further suggested by the tendency for the high-T points to follow an upward-sloping curve relative to the AA data at high mercury concentrations (Figure B.1). The regression through high-T mercury values below 240 ppb (AA method) has a slope much closer to the ideal 1:1 slope (i.e., close to $b = 1.0$ in Table B.2) than the regression through values above 240 ppb (Figure B.1; Table B.2). This upward-sloping tendency is not, however, apparent in the low-T data, and all of the linear regression lines pass near the origin (Figure B.1). A significant conclusion is that the gold-film technique may not be accurate or precise at high concentrations of mercury.

A single sample of the most common soil type--the Mazama ash--was analyzed 50 times by the low-T method to evaluate precision. The range of the data is from 69 to 55 ppb about a mean of 71 ppb. The standard deviation at one sigma is 5 ppb (7 percent). This is a relatively low deviation compared to the standard error estimated for the regression analyses of Figure B.1 (see Table B.2). This deviation is a measure of the uniformity with which the samples are scooped and run through the detector with the low-T method. It is apparent that only about 14 to 34 percent of the standard error (Table B.2) could be from the sampling procedure (e.g., scooping versus weighing samples) and other repetitious techniques associated with the low-T analysis itself--at least for concentrations near 71 ppb (123 ppb by the AA method) in Mazama ash.

The rest of the scatter in Figure B.1 is probably due to other sources of error such as the following:

1. Inhomogeneity of the sample aliquots split for duplicate analysis.
2. Random errors caused by contaminants which affected the samples after splitting.

3. Differing mercury retention of various sample types when subjected to the two gold-film analytical techniques. Differences in the mineralogy and texture of the soils could affect the amount of mercury vapor released during heating in the gold-film techniques.
4. Contamination of the gold-film detectors from previous high-mercury samples or from inadequately filtered air (e.g., dirty filters).
5. Unknown systematic errors inherent in the electronics and gas-circulation systems of the various detection devices.

Errors 1, 2, and 4 are probably small, because the samples were carefully split, placed in sealed containers, and run with numerous check runs on standards.

Error number 5 may be a problem with any of the methods. There is no other obvious explanation for high-T values consistently higher at high absolute mercury than total-decomposition AA values. Theoretically, the data from the two methods should give a regression with a 1.0 slope, because both should be measuring 100 percent of the mercury. If the high-T method yielded lower mercury values than the AA, then an argument could be made that not all of the mercury was liberated during heating. But the high-T method yields higher mercury values than the AA method at high mercury concentrations; it follows that these systematic variances at high mercury concentrations are due not to variances in the mercury retentiveness of samples but to variances associated with either the high-T or AA instrumentation. Because the AA technique is a well-established method, it is probably less likely to be the source of error than the newly developed high-T gold-film method. The AA values are assumed to represent absolute mercury contents in the following discussions.

Error number 3 is the most obvious source of error for the low-T gold-film method, because the mercury is incompletely removed. If the mineralogy of the sample is a significant source of error for the gold-film detector, then there should be some correlation between sample composition and the variance of the samples which depart from the regression line the most strongly, namely the soils and beach sands developed on palagonitic deposits within the caldera. Sample P5 is the most extraordinary example of this type of variation (Table B.1). The low-T gold-film measurement for P5 is 40 ppb, whereas the high-T measurement is 415 ppb and the AA measurement is 275 ppb. The low-T value plots well below the low-T regression lines, and the high-T

value plots well above the high-T regressions. Another palagonitic sample, P806, has a low-T value of 170 ppb, a high-T value of 410 ppb, and an AA value of 305 ppb. Whereas the low-T value plots on the regression line through other low-T samples, the high-T value is far above the high-T regression line. Assuming that the total decomposition AA method gives a reasonable measure for absolute Hg, high-T values that are 34 percent (P806) to 51 percent (P5) higher than the AA method are difficult to explain. These results again cast doubt on the absolute accuracy of the high-T technique for samples with relatively high mercury concentrations. The low value obtained by the low-T method for the P5 sample may possibly be due to incomplete degassing of mercury from the sample. Perhaps some of the mercury is tied up in sulfides or oxides which were not decomposed in the P5 sample during heating to 327° C. The P5 sample is from the caldera near areas of known thermal spring and fumarole activity, where mercury sulfides or oxides may be present. Koksoy and others (1967) found that samples with mercuric sulfide and oxide did not show complete mercury volatilization until temperatures of 340° and 535° C, respectively, were reached, although they found some volatilization at temperatures of 210° to 270° C.

The net effect of the above errors on the anomaly patterns displayed in the mercury-contour map should be small. Palagonitic soils and hot springs are uncommon over most of the survey area, except within the caldera. The vast majority of samples were taken from the Mazama ash layer (carbon-14 date = 6,845 yr B.P. = actual date of about 7,500 yr B.P.) which blankets much of the area (see MacLeod and others, 1982). Other Quaternary ash deposits cover most of the remainder of the map area. One of the largest of these other ash-fall layers is an upper Holocene rhyolitic pumice fall deposit which is isopached by MacLeod and others (1982). This pumice fall was vented from the same vent as the intracaldera Big Obsidian Flow and has yielded carbon 14 dates of 1,720±250 yr B.P. (Higgins, 1969) and 1,550 yr B.P. (S.W. Robinson, written communication, 1979, to MacLeod and others, 1982). It is unlikely that soils developed on this youthful Holocene ash fall and underlying post-Mazama ash falls have significant hydrothermal sulfides or secondary oxides, unless the soils were developed within the orifice of an active hot spring or fumarole. Anomalous amounts of mercury that are locally present in these young deposits are more likely

in the form of easily degassed metallic mercury volatilized from underlying heat sources, although some primary mercury may be present in unknown form in the young rhyolitic pumice fall (see the section on background concentrations of mercury in igneous rocks).

Temporal Changes in Mercury

Variations of mercury content with time in most areas are probably small. Juncal (1980) noted that temporal variability over an eight-week period in the northern Dixie Valley area was similar to the variability observed in replicate analyses using the high-temperature gold-film method. Matlick and Buseck (1976) found little mercury variation in four sites periodically resampled over a two-month period. While Capuano and Bamford (1978) reported significant temporal variations in one area over a two-week period, the relative position of anomalies did not change.

Although no concerned effort was made to evaluate temporal changes in soil mercury at Newberry, one area near Paulina Lake was sampled at the beginning and near the end of the survey. Mercury in samples collected on July 31, 1982, were within 6 percent (2 ppb) to 11 percent (4 ppb) of mercury measured in samples on September 23, 1983 (see test pit TP-10, Table 6.1).

APPENDIX C

DETAILED PLOTS OF CONVECTIVE HEAT-FLOW MODELS

by

David D. Blackwell and John L. Steele,

Southern Methodist University

Detailed plots showing the evolution of flow patterns, isotherm distribution, and surface heat flow for the convective cooling models of possible Newberry volcano magma chambers discussed in the text are included in this appendix. Results are included for five combinations of magma chamber geometries, reservoir thickness, and ratio of horizontal to vertical permeability. For each model, figures giving results at a number of times are presented. The times are chosen to illustrate the evolution of various types of phenomena associated with the cooling. For all models for each time there are temperature-depth maps at contour intervals of 50° or 100° C, stream-function contour maps, velocity plots, and surface heat-flow cross sections. Stream-function plots are nondimensionalized by the maximum stream-function value. The velocity plots have line segments showing by length and direction the flow and normalized velocity. Arrowheads are not included to indicate the actual direction of the flow, but in most cases it is obvious from the pattern of isotherms and surface heat flow. Without exception, water is drawn in toward the magma chamber along the bottom of the circulation system and moves up along the side of the magma chamber. It then moves vertically up or laterally across the top of the magma chamber. At the top of the system, the flow moves away from the magma chamber. In one or two cases, separate cells develop on top of the magma chamber for certain periods of time. A summary of the model geometry and the times for which results are shown is listed in Table C.1. The surface heat flow is plotted in terms of HFU, where 1 HFU = 10^{-6} cal/cm²sec.

Table C.1. Parameters and ages for convective model results.
 In all cases the initial temperatures are 800° C, Rayleigh numbers are 200, and diffusivities are 0.01cm²/sec.

Magma chamber width (km)	Magma chamber depth to top (km)	Reservoir depth	Horizontal to vertical permeability ratio	Cooling time (years)	Figure numbers
3	3	5	2	10,000	C1
				20,000	C2
				40,000	C3
				70,000	C4
				125,000	C5
				250,000	C6
6	3	5	2	10,000	C7
				20,000	C8
				40,000	C9
				70,000	C10
				125,000	C11
				250,000	C12
10	5	10	2	10,000	C13
				20,000	C14
				40,000	C15
				70,000	C16
				90,000	C17
				10,000	C18
10	5	10	0.5	20,000	C19
				40,000	C20
				70,000	C21
				90,000	C22
				10,000	C23
				20,000	C24
15	4	5	2.0	40,000	C25
				70,000	C26
				125,000	C27
				250,000	C28

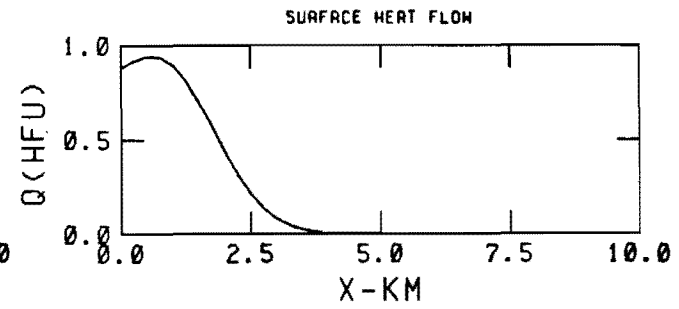
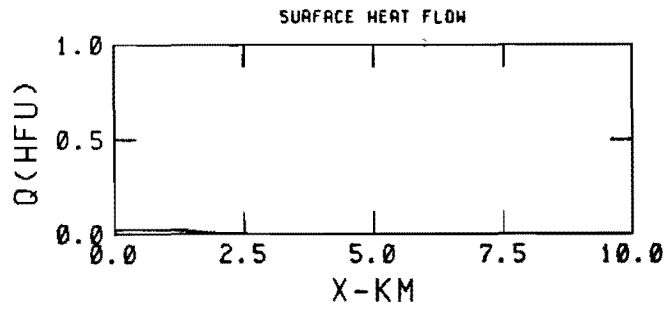
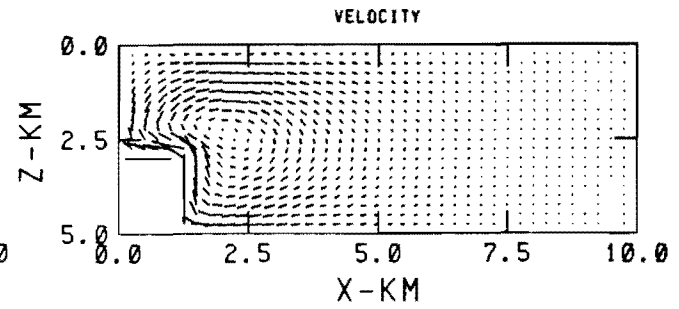
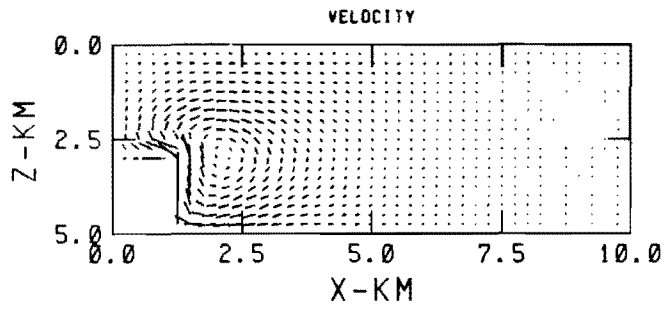
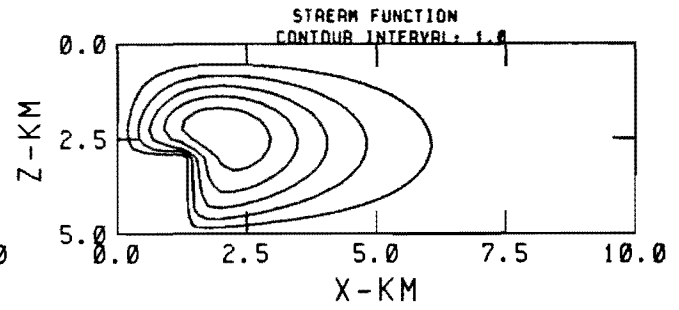
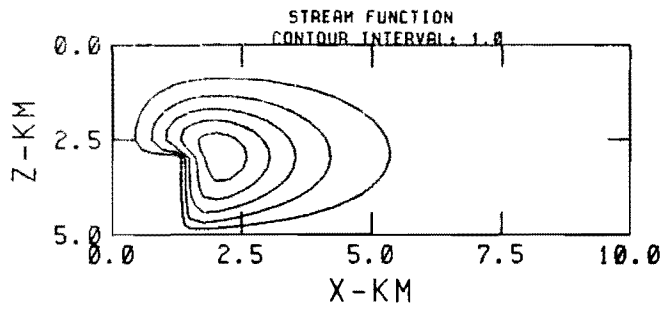
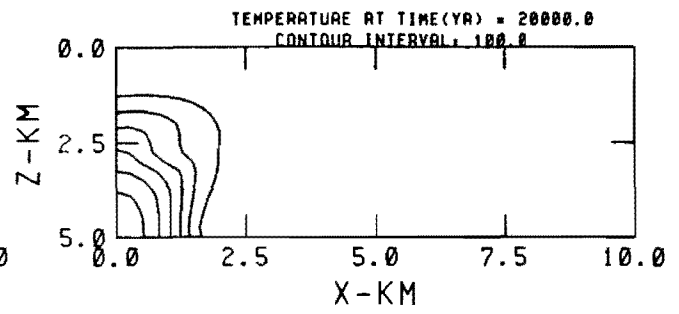
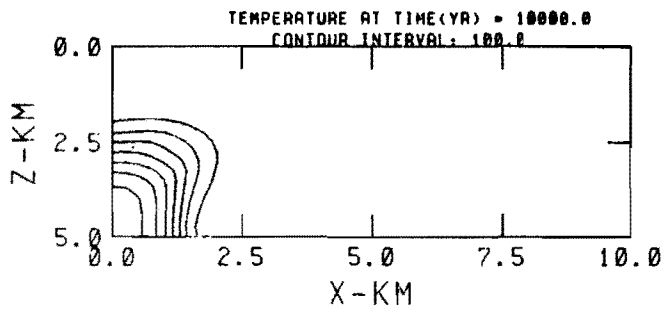


Figure C.1.

Figure C.2.

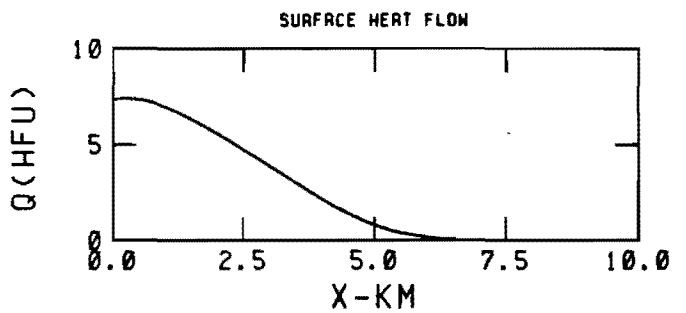
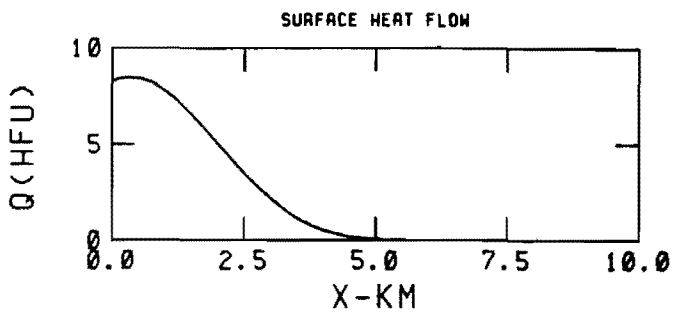
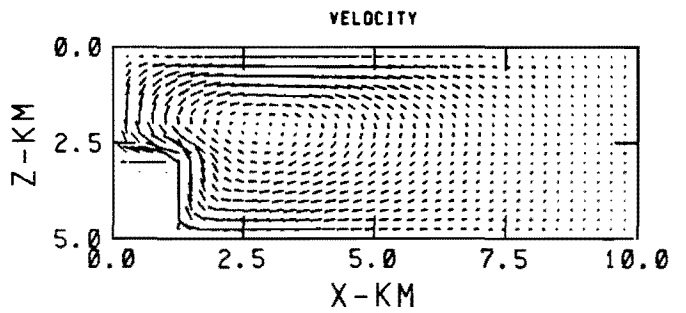
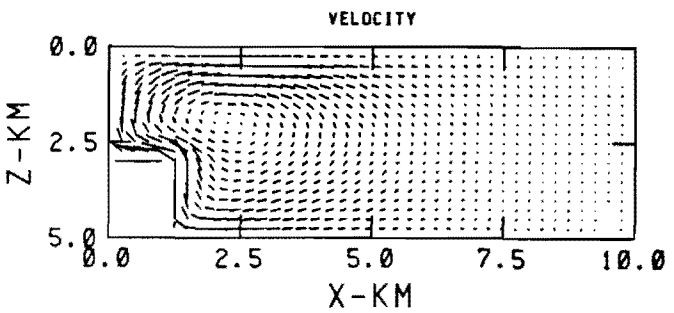
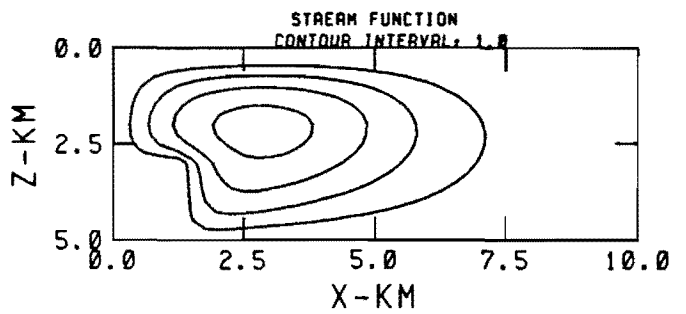
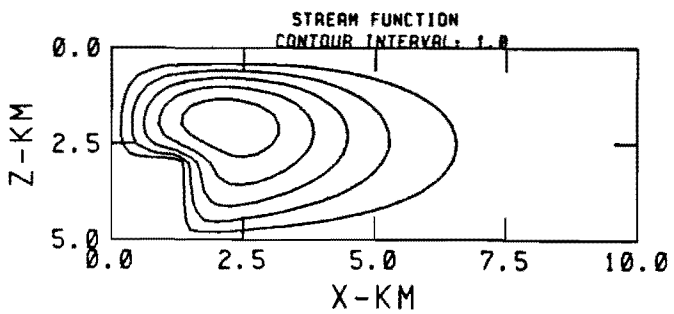
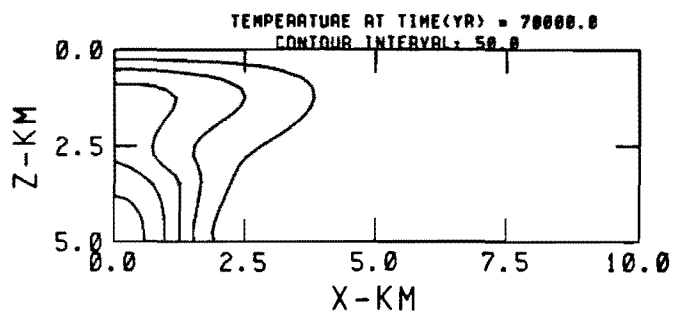
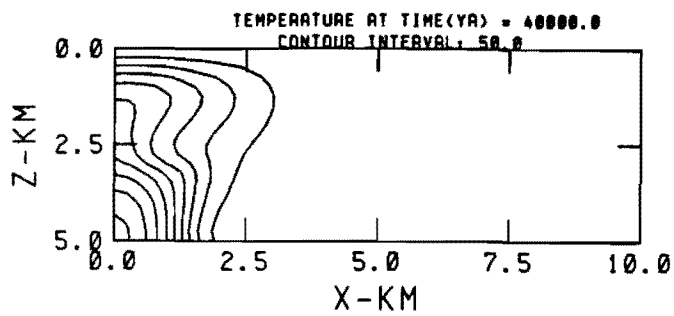


Figure C.3.

Figure C.4.

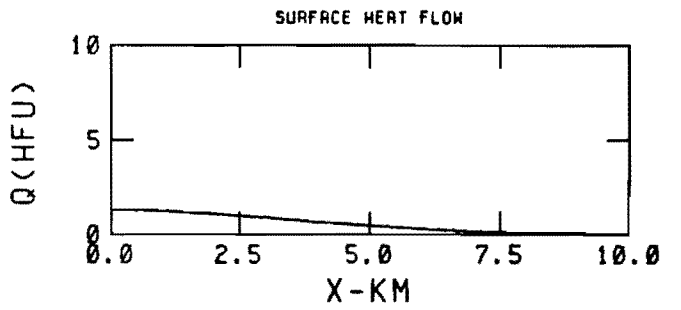
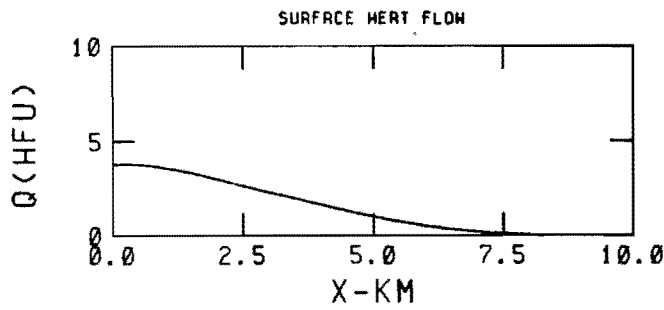
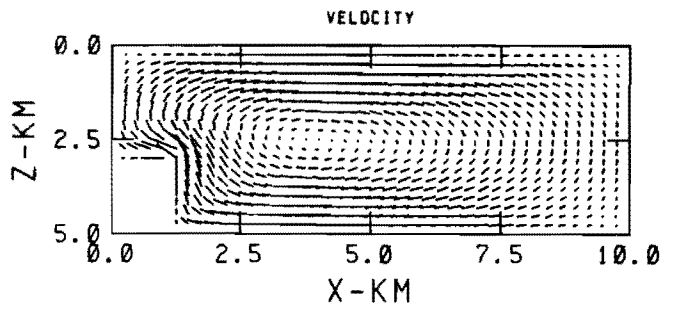
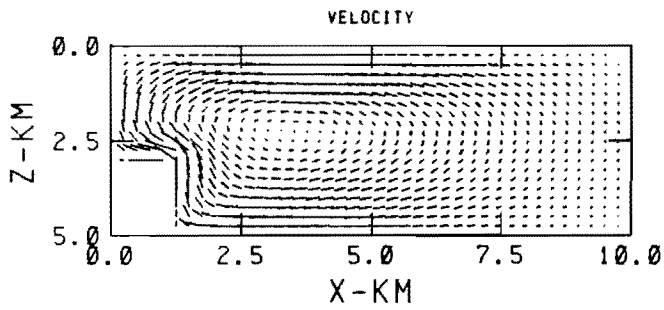
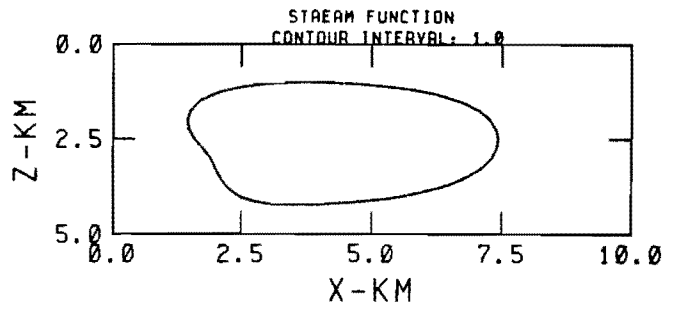
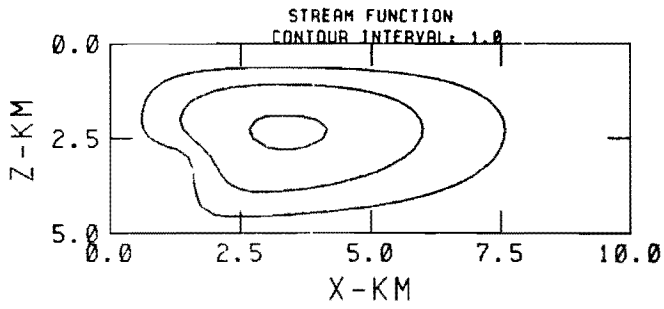
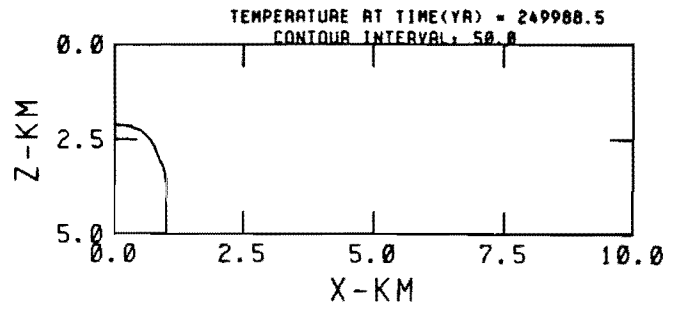
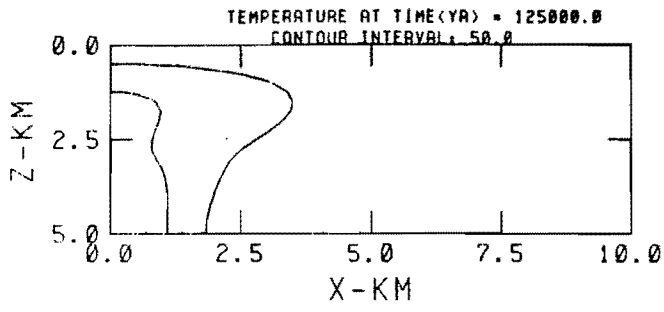


Figure C.5.

Figure C.6.

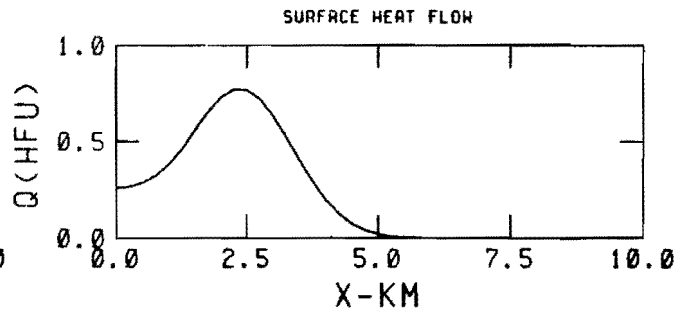
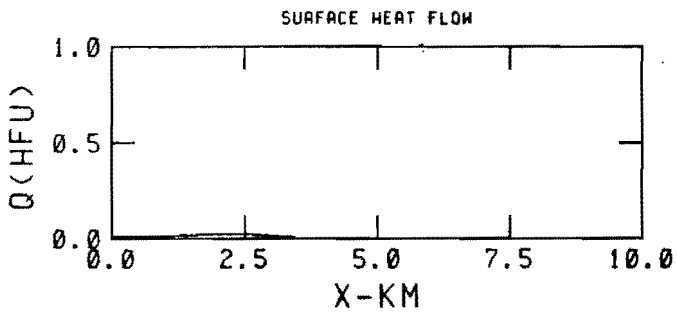
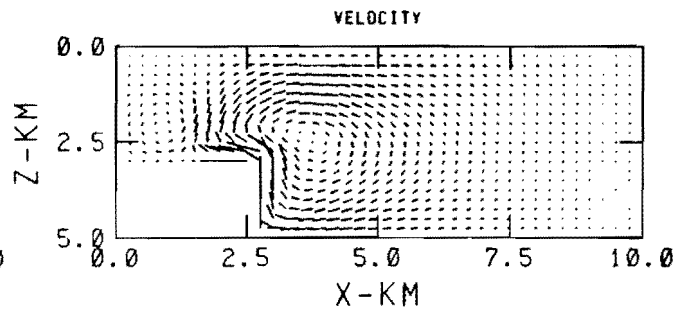
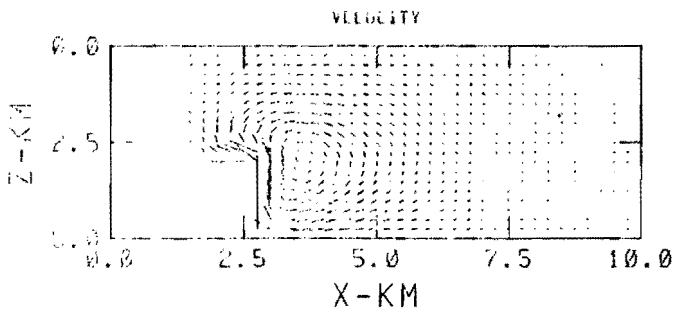
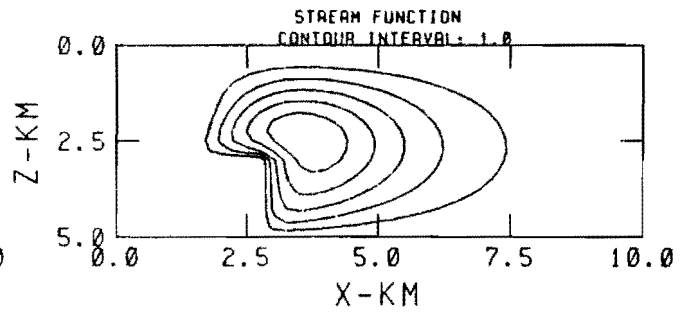
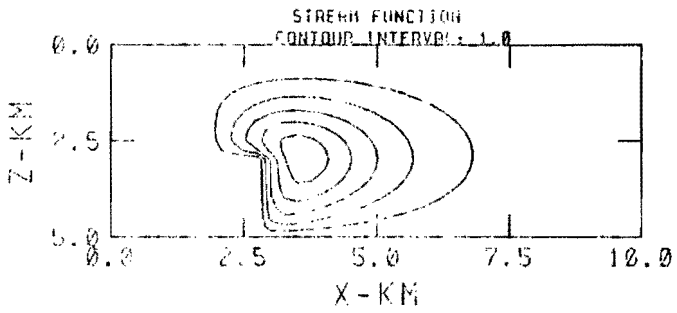
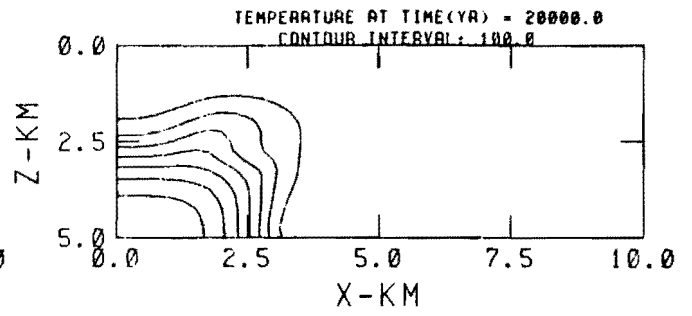
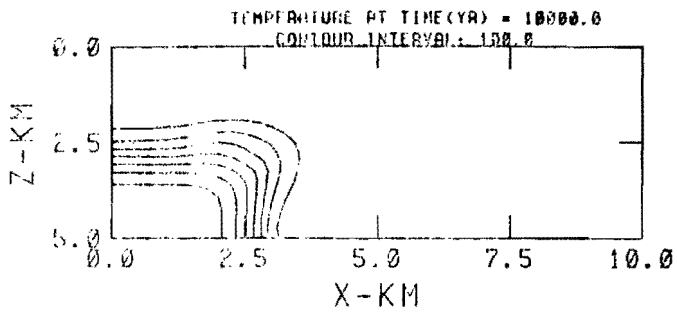


Figure C.7.

Figure C.8.

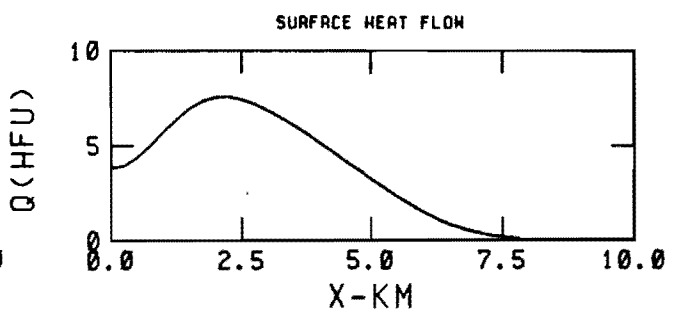
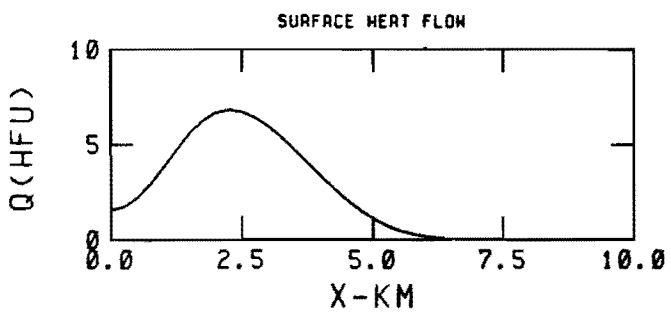
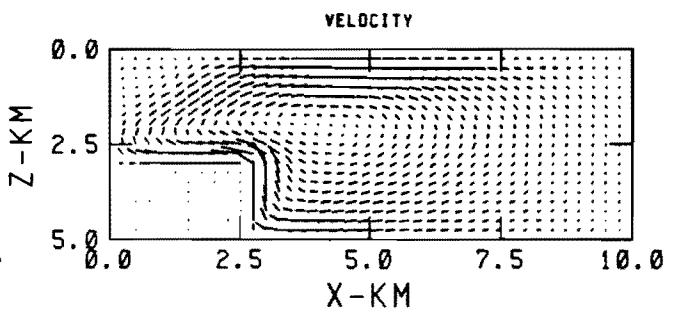
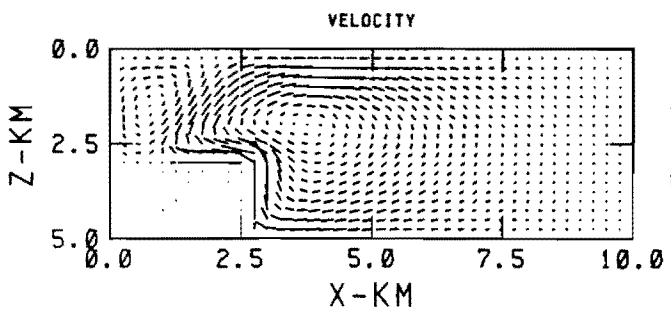
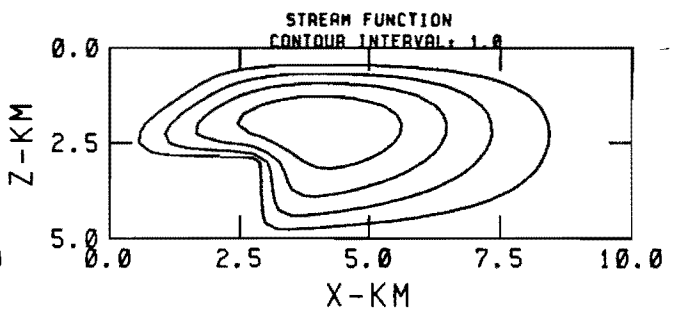
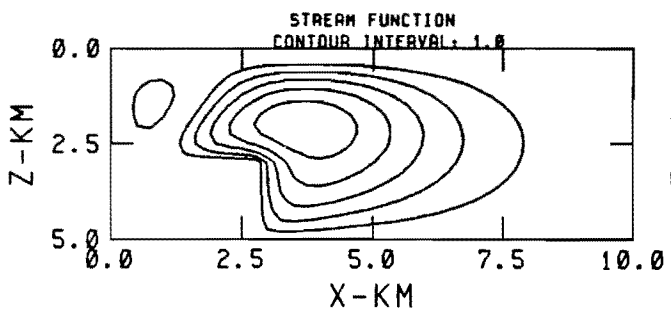
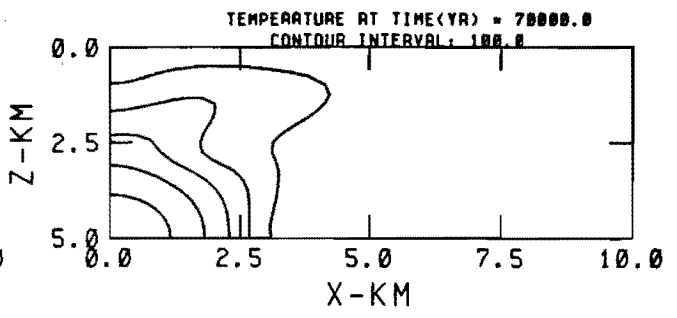
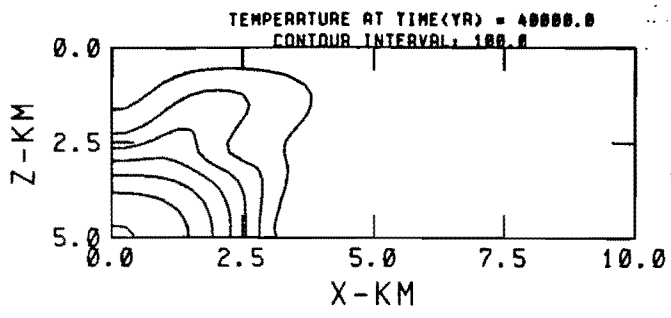


Figure C.9.

Figure C.10.

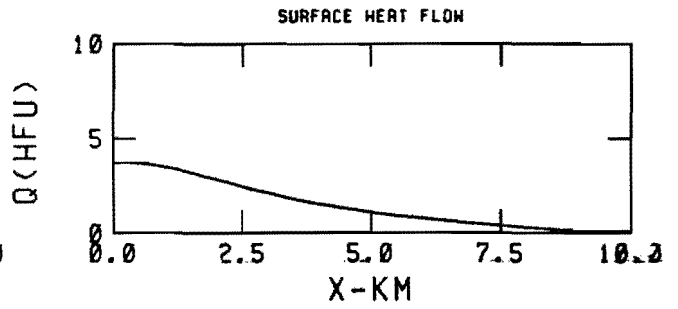
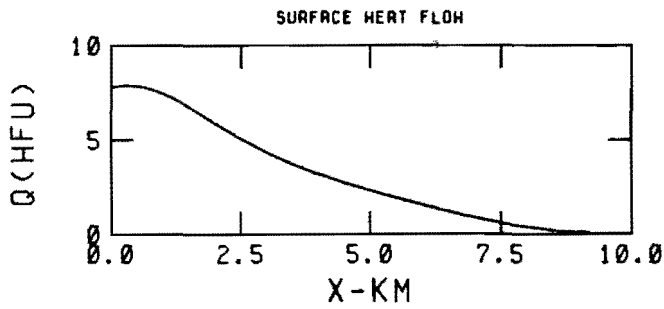
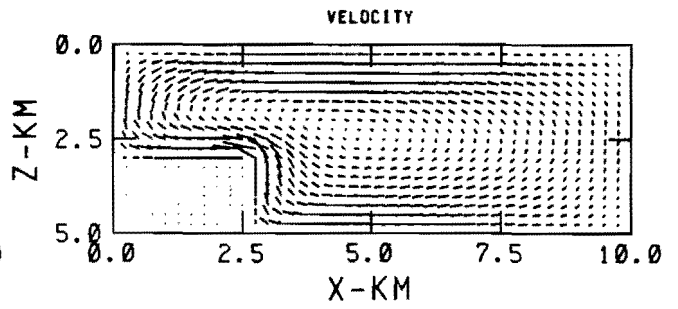
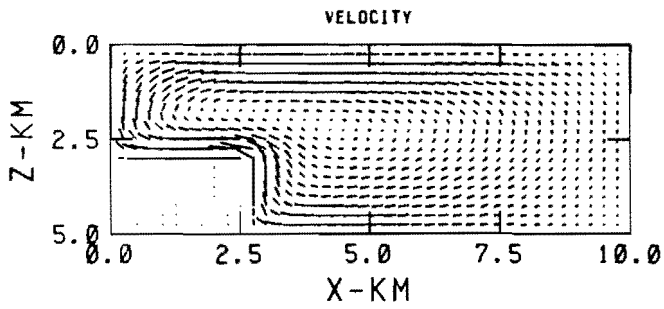
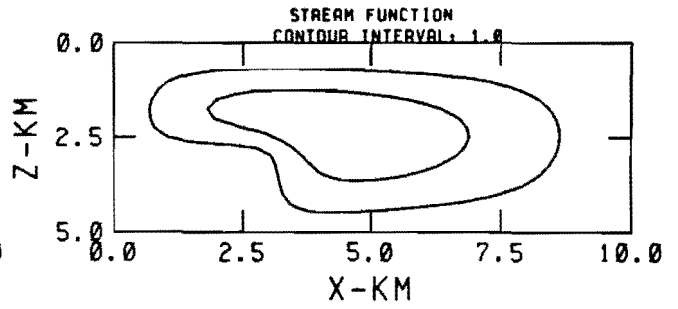
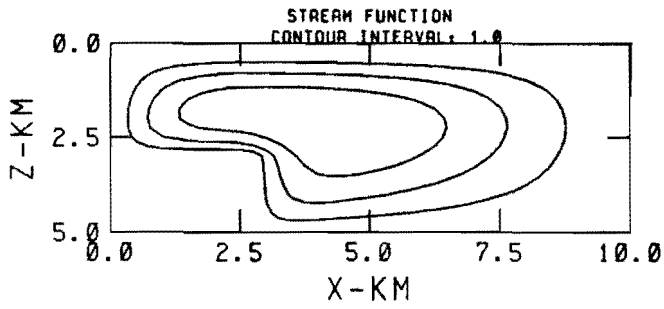
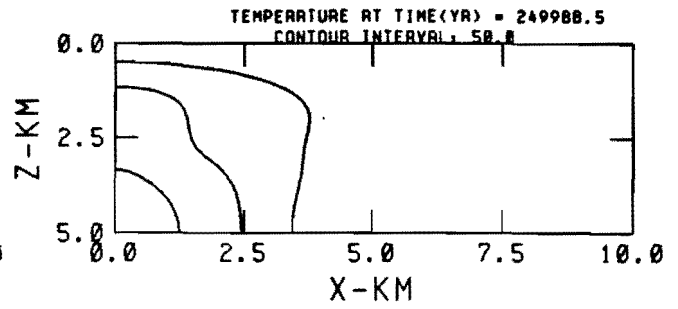
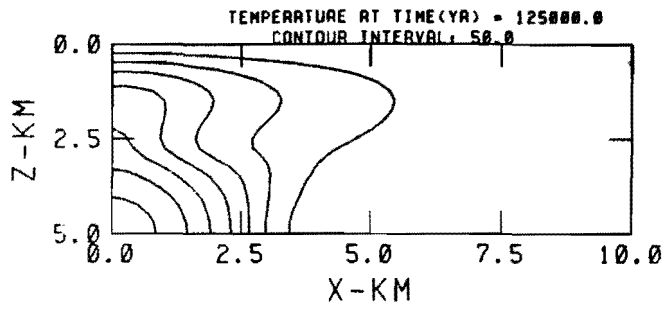


Figure C.11.

Figure C.12.

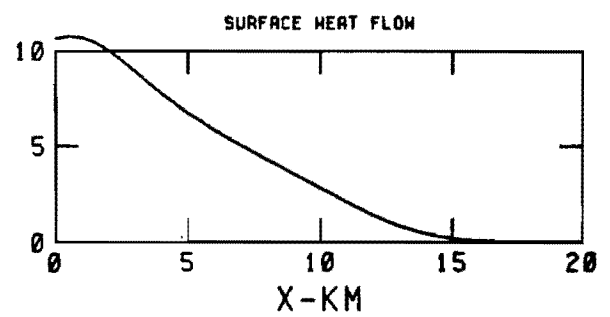
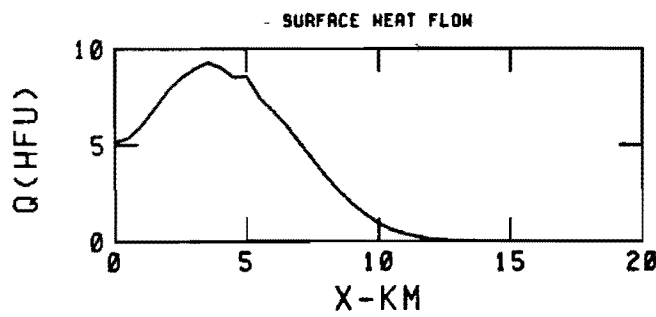
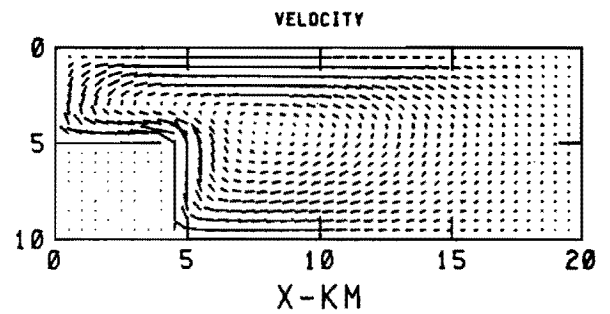
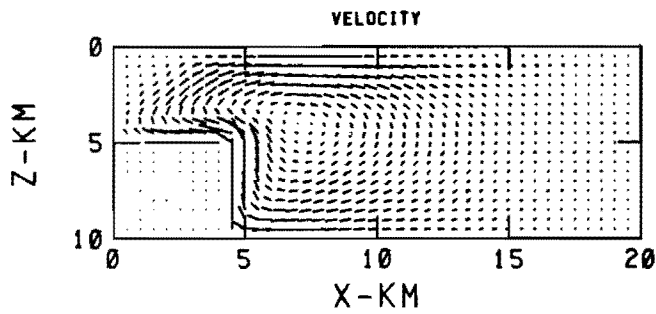
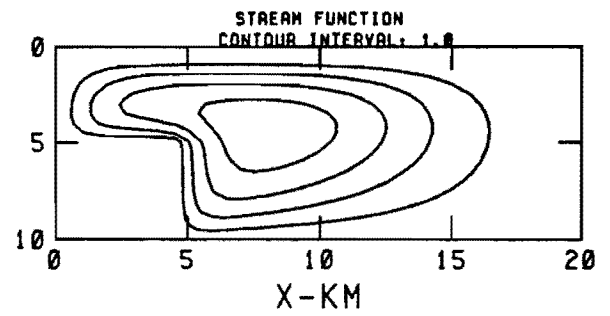
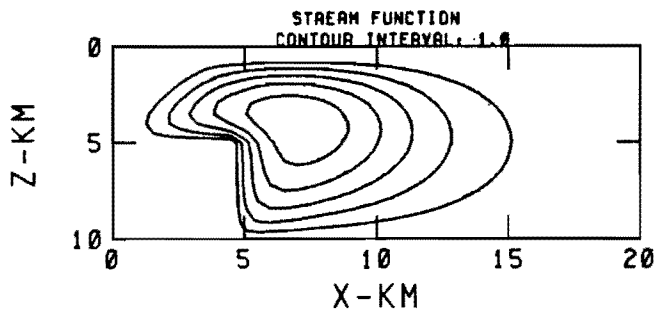
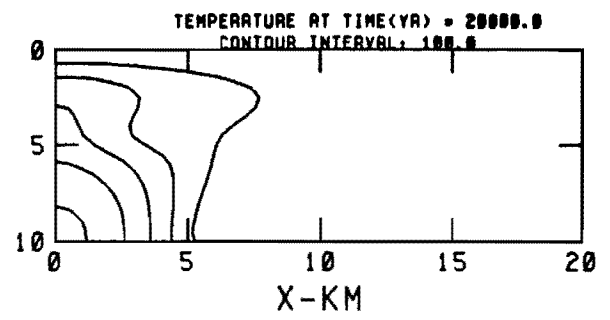
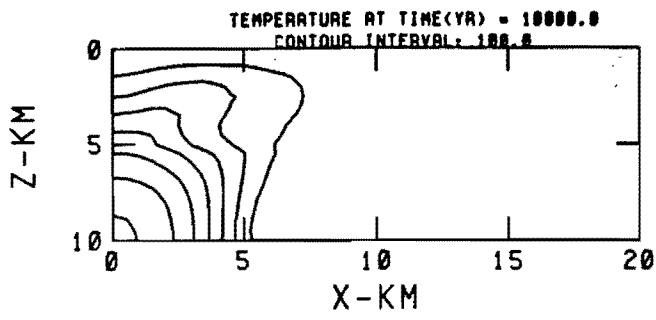


Figure C.13.

Figure C.14.

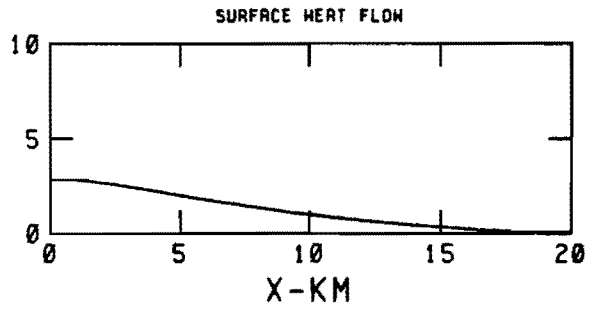
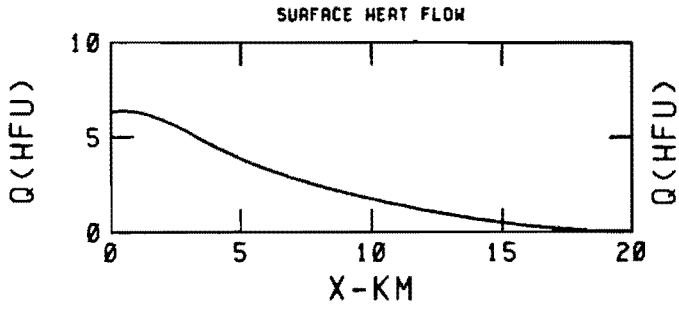
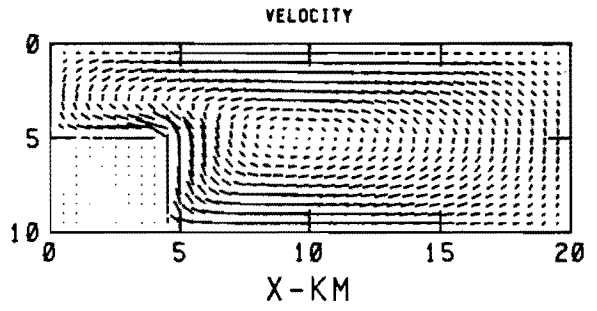
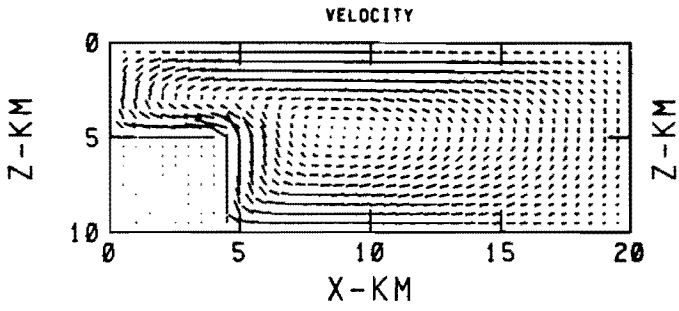
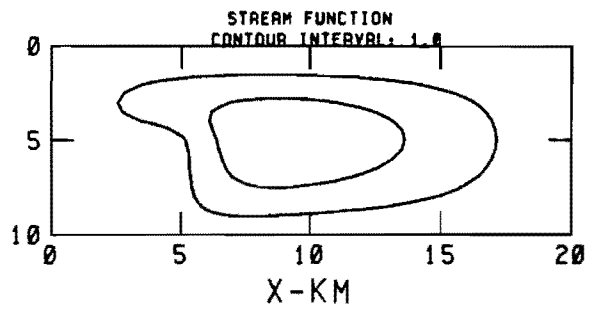
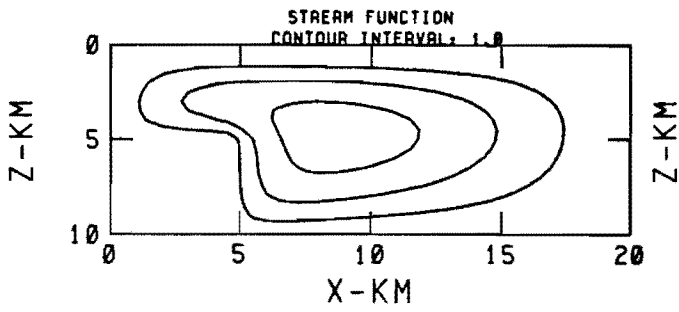
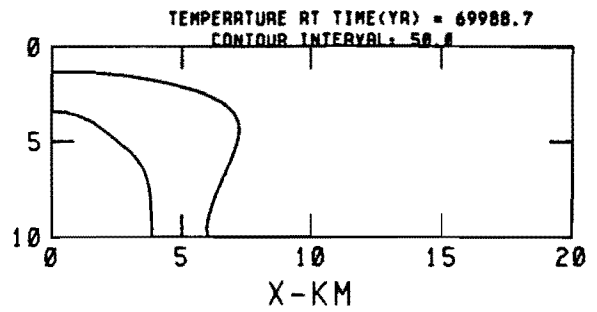
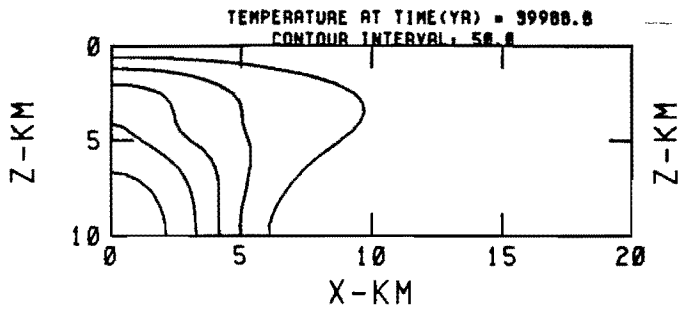


Figure C.15.

Figure C.16.

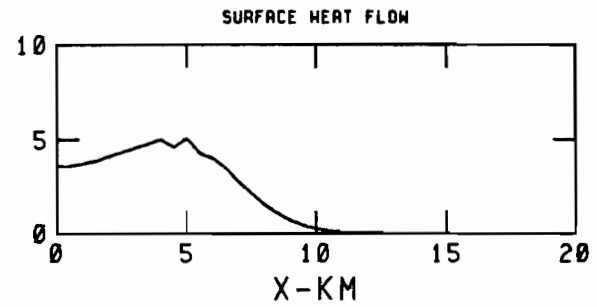
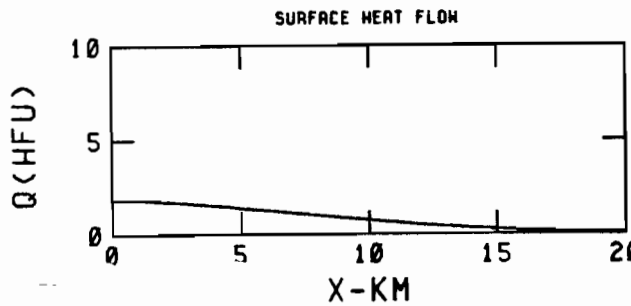
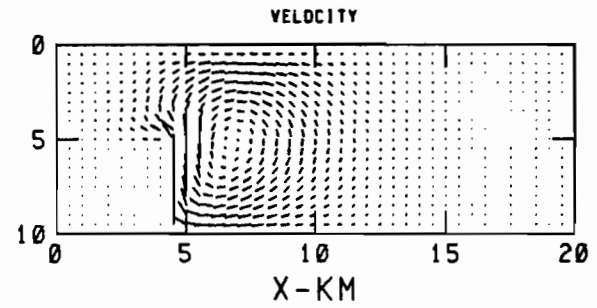
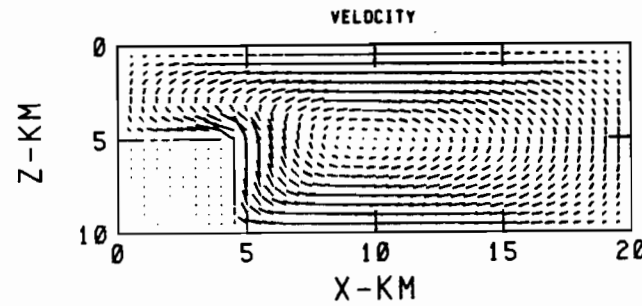
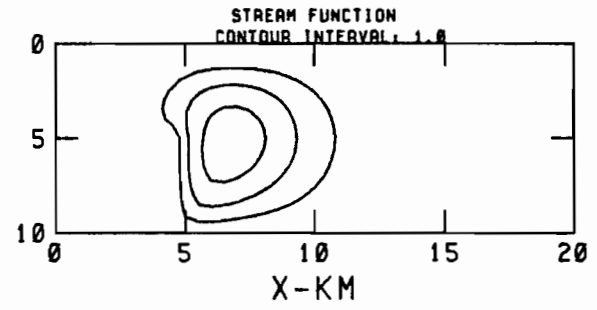
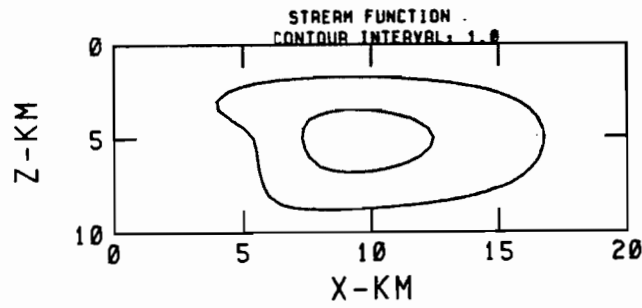
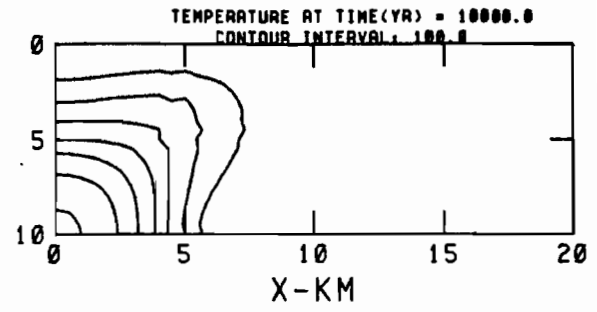
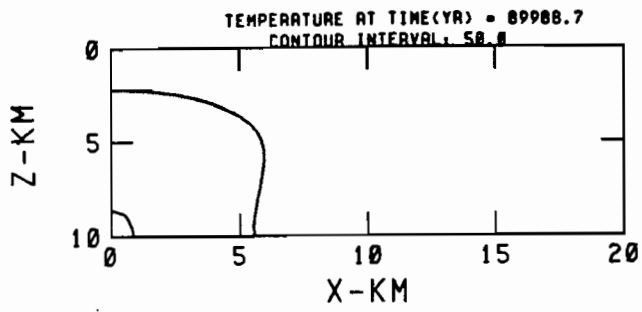


Figure C.17.

Figure C.18.

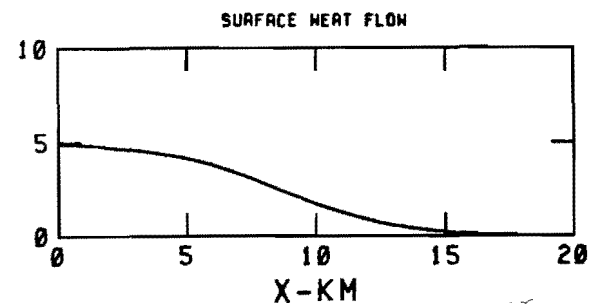
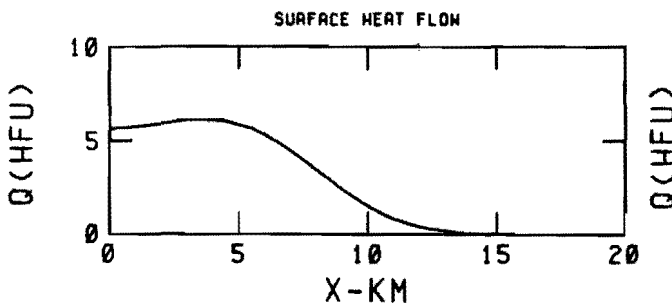
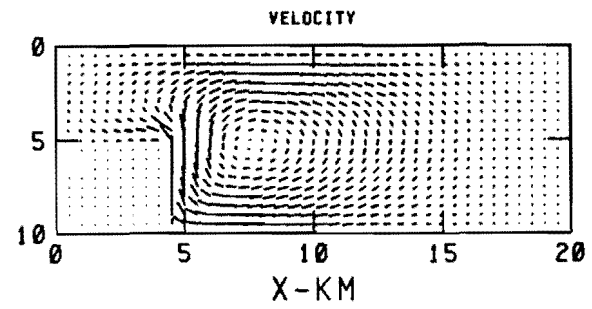
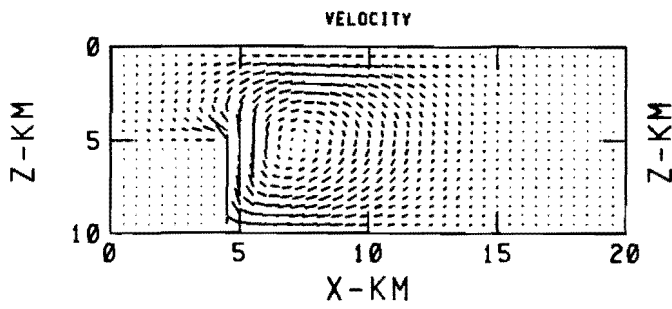
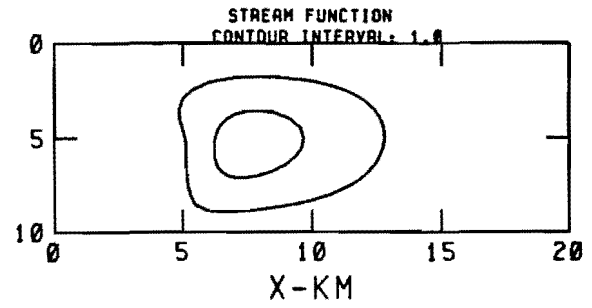
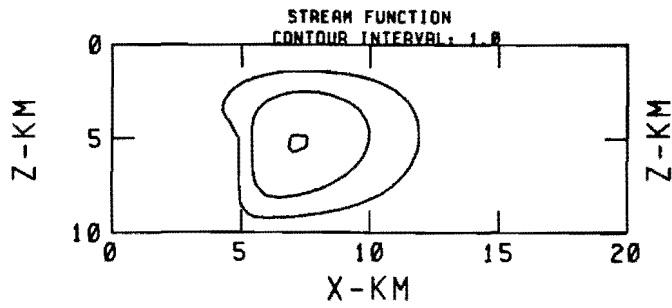
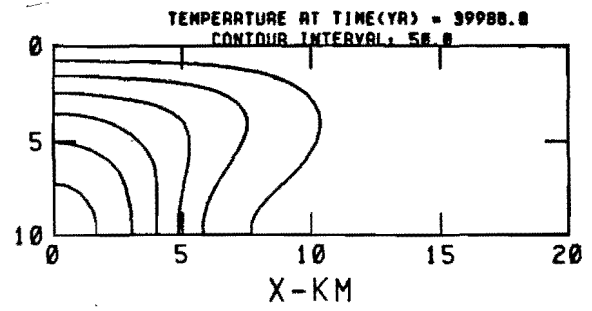
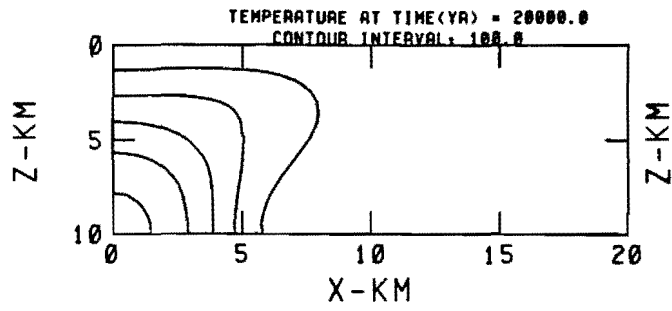


Figure C.19.

Figure C.20.

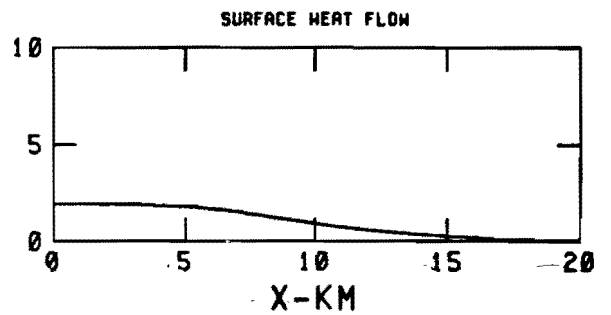
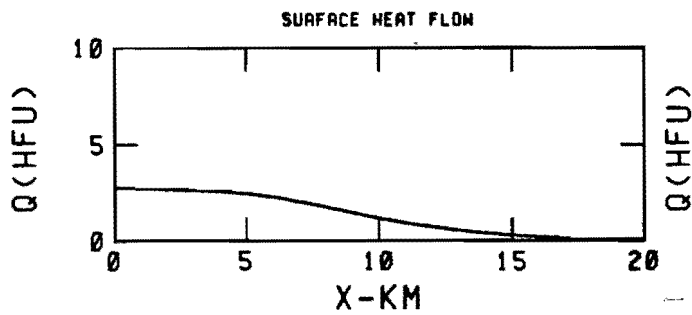
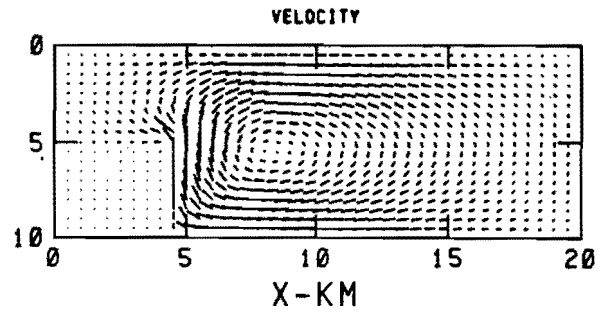
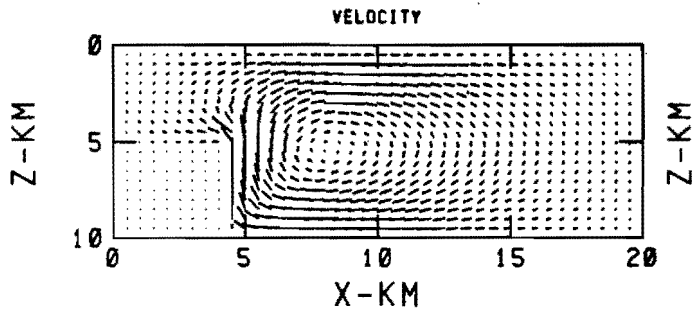
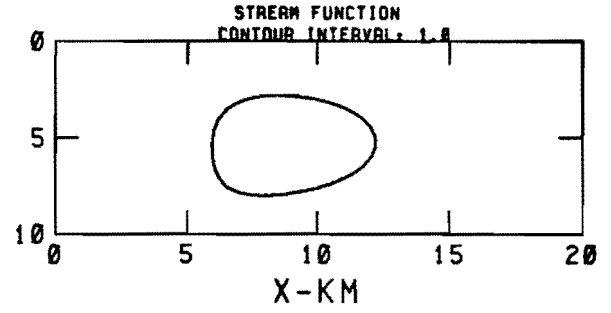
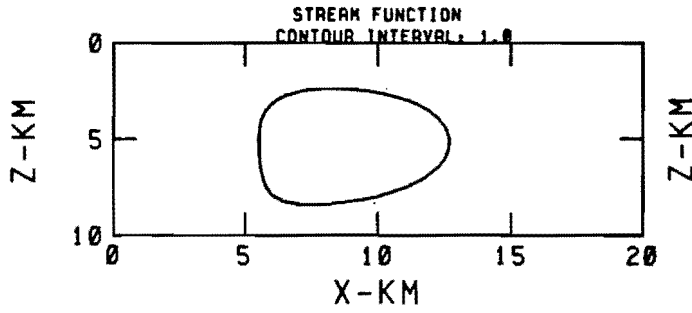
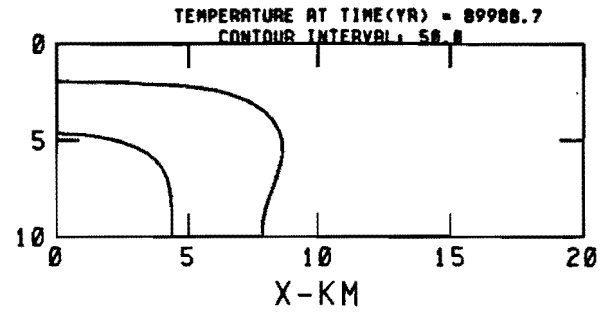
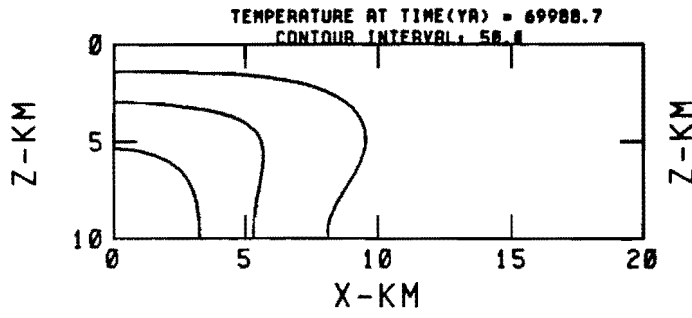


Figure C.21.

Figure C.22.

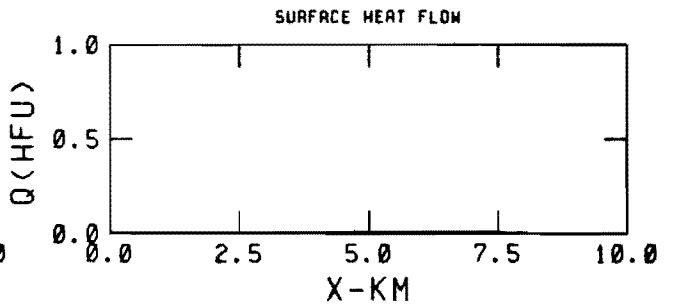
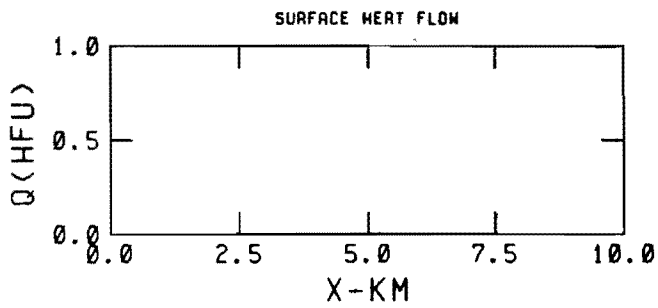
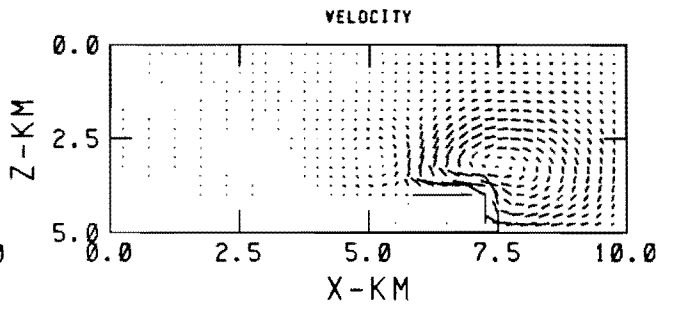
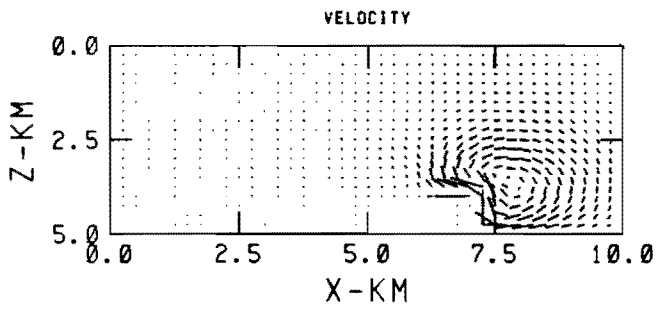
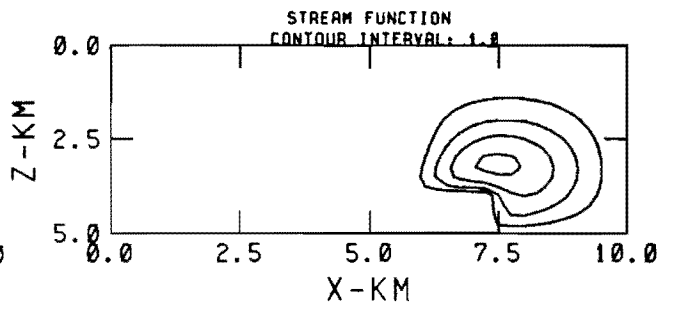
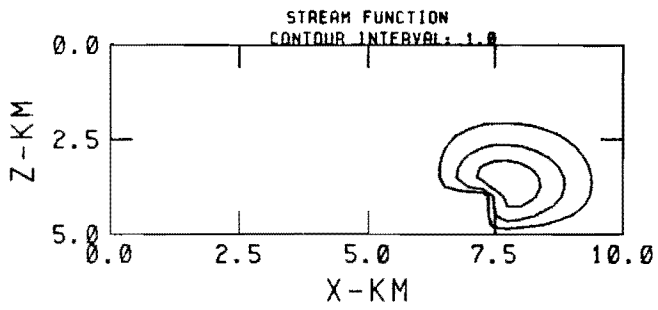
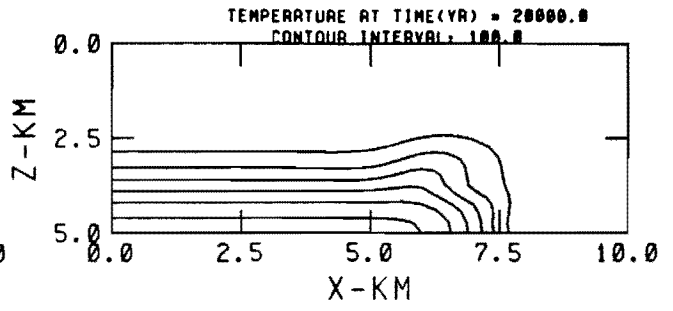
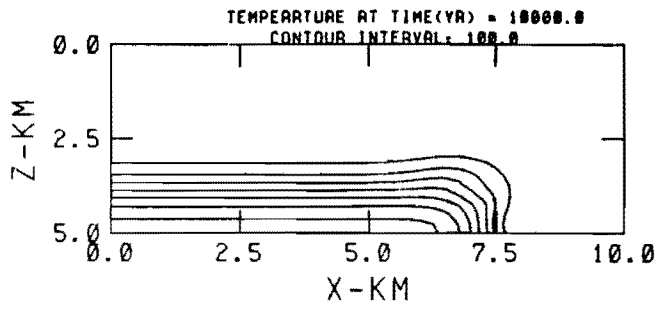


Figure C.23.

Figure C.24.

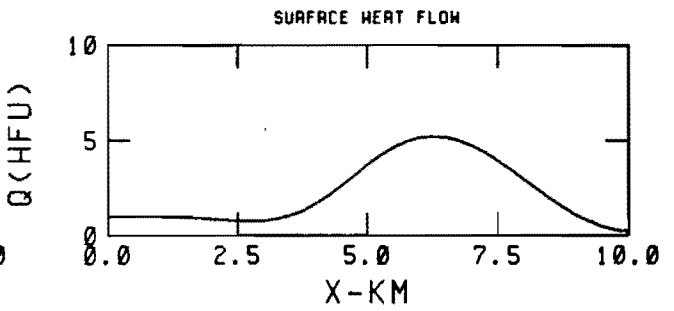
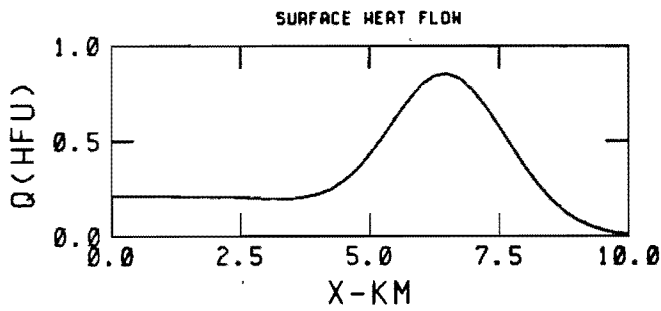
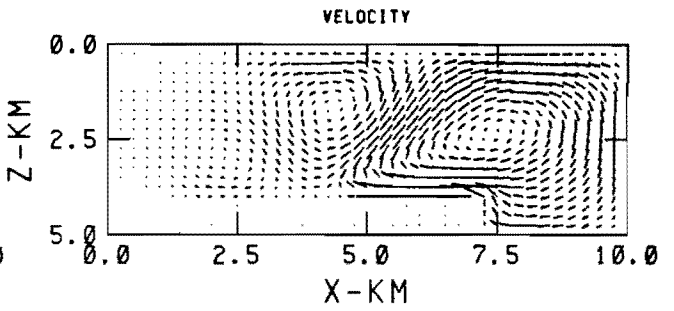
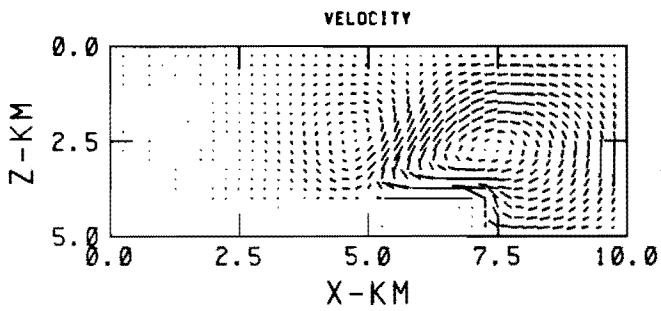
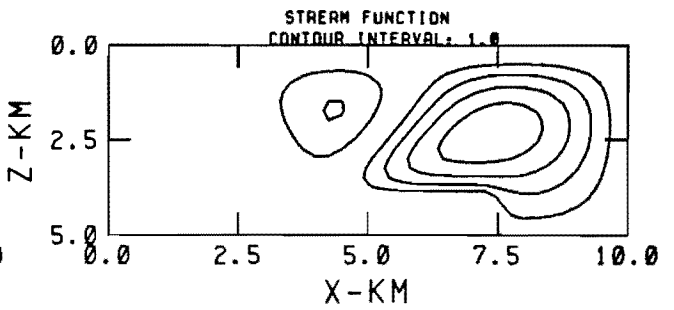
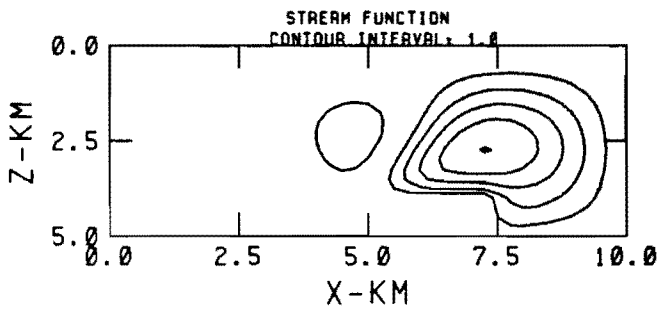
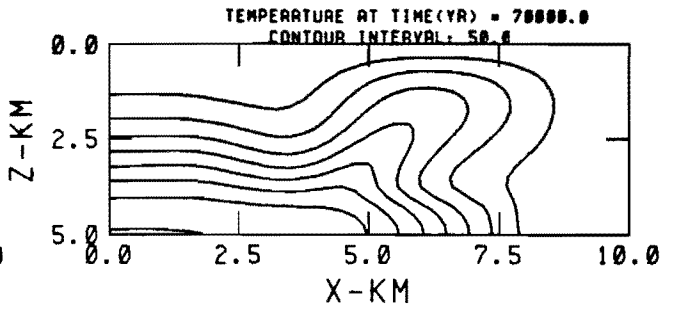
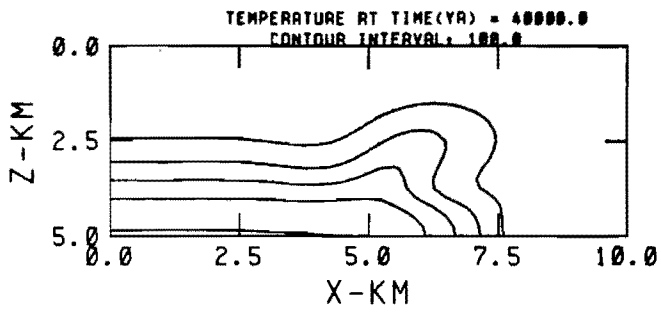


Figure C.25.

Figure C.26.

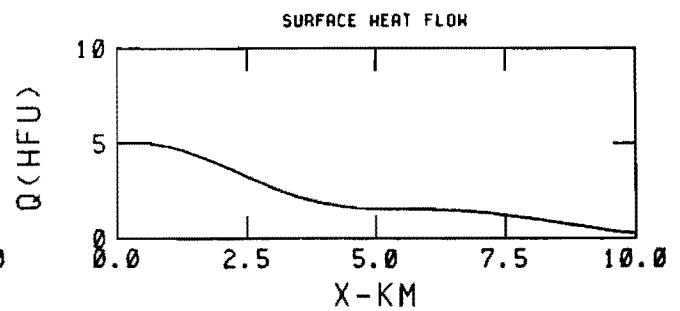
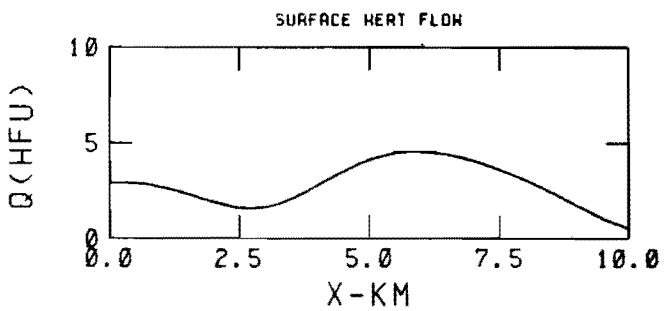
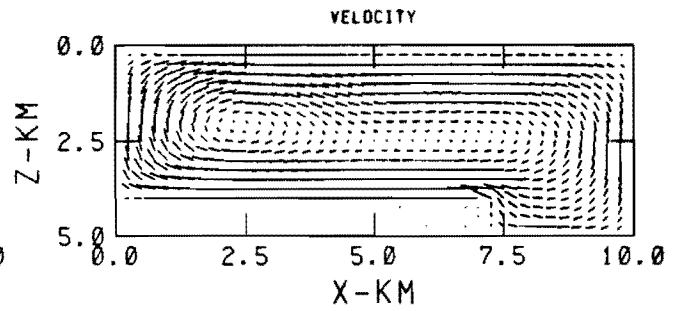
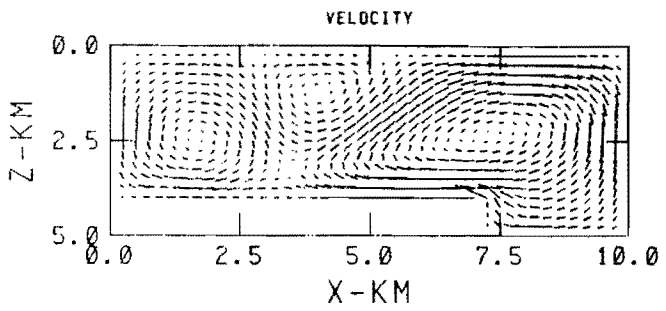
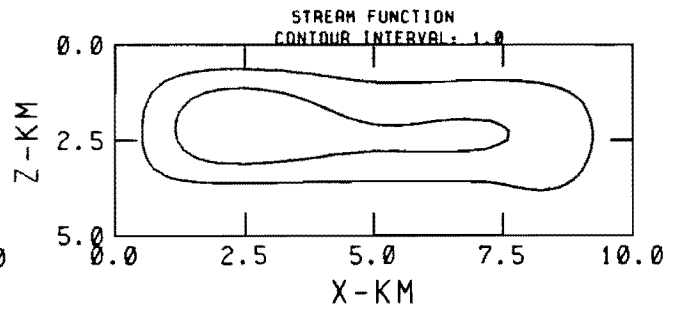
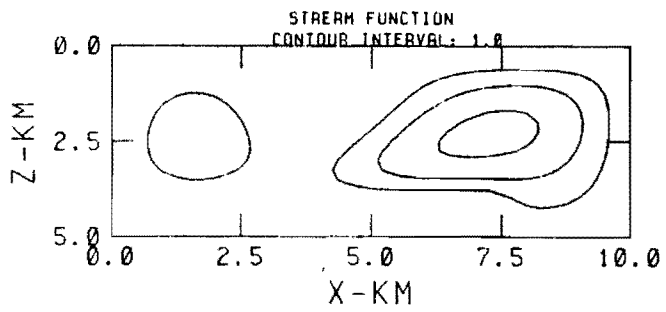
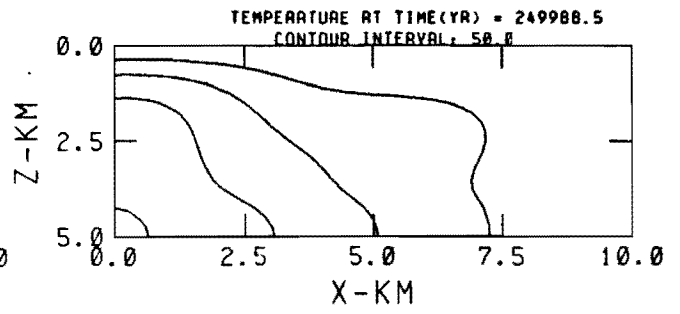
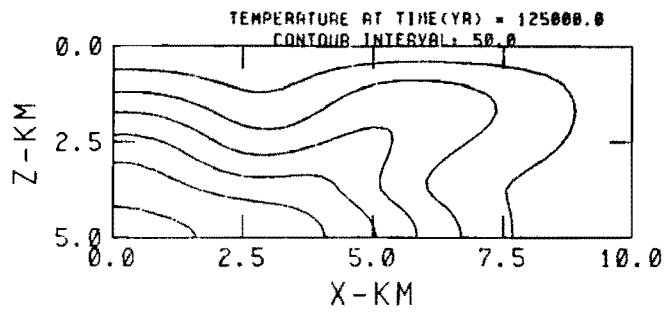


Figure C.27.

Figure C.28.

O-83-3
 SURVEY OF POTENTIAL GEOTHERMAL EXPLORATION SITES
 AT NEWBERRY VOLCANO, DESCHUTES COUNTY, OREGON
 By Priest and others
 1983

MAP OF THE DISTRIBUTION OF VOLCANIC CENTERS,
 NEWBERRY VOLCANO, DESCHUTES COUNTY, OREGON

Legend

-  Contours indicate numbers of volcanic centers per 1% area (of geologic map, MacLeod (1982))
-  Sillic volcanic centers
-  Mafic volcanic centers
-  Faults
-  Buried ring faults
-  Fissure vents

Prepared by Gerald L. Black, Neil M. Woller, and Chase B. Brand.
 Data base MacLeod and others (1982)

REFERENCES

MacLeod, N.S., Sherrod, D.R., and Chitwood, L.A., 1982, Geologic Map of Newberry Volcano, Deschutes, Klamath and Lake Counties, Oregon: U.S. Geological Survey Open-File Report, 82-847, 1:62,500 scale map. 25 p. text

Map Base: Reduced U.S. Geological Survey Topographic quadrangles from U.S.G.S. Open-File Report 82-847

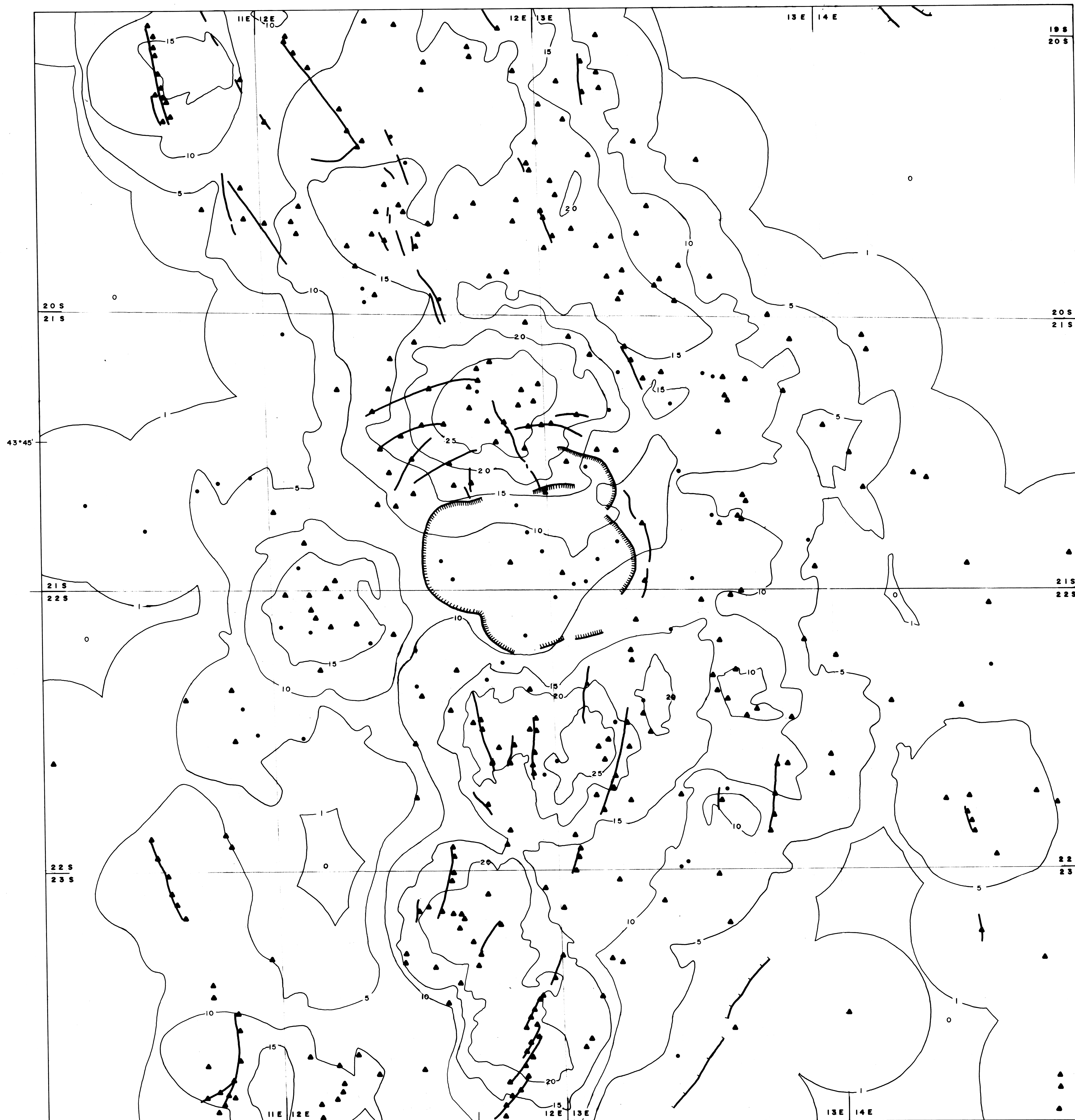
The project was supported by funds from the Bonneville Power Administration (Cooperative Agreement No. DE-AC-79-82-BP36734).

DISCLAIMER

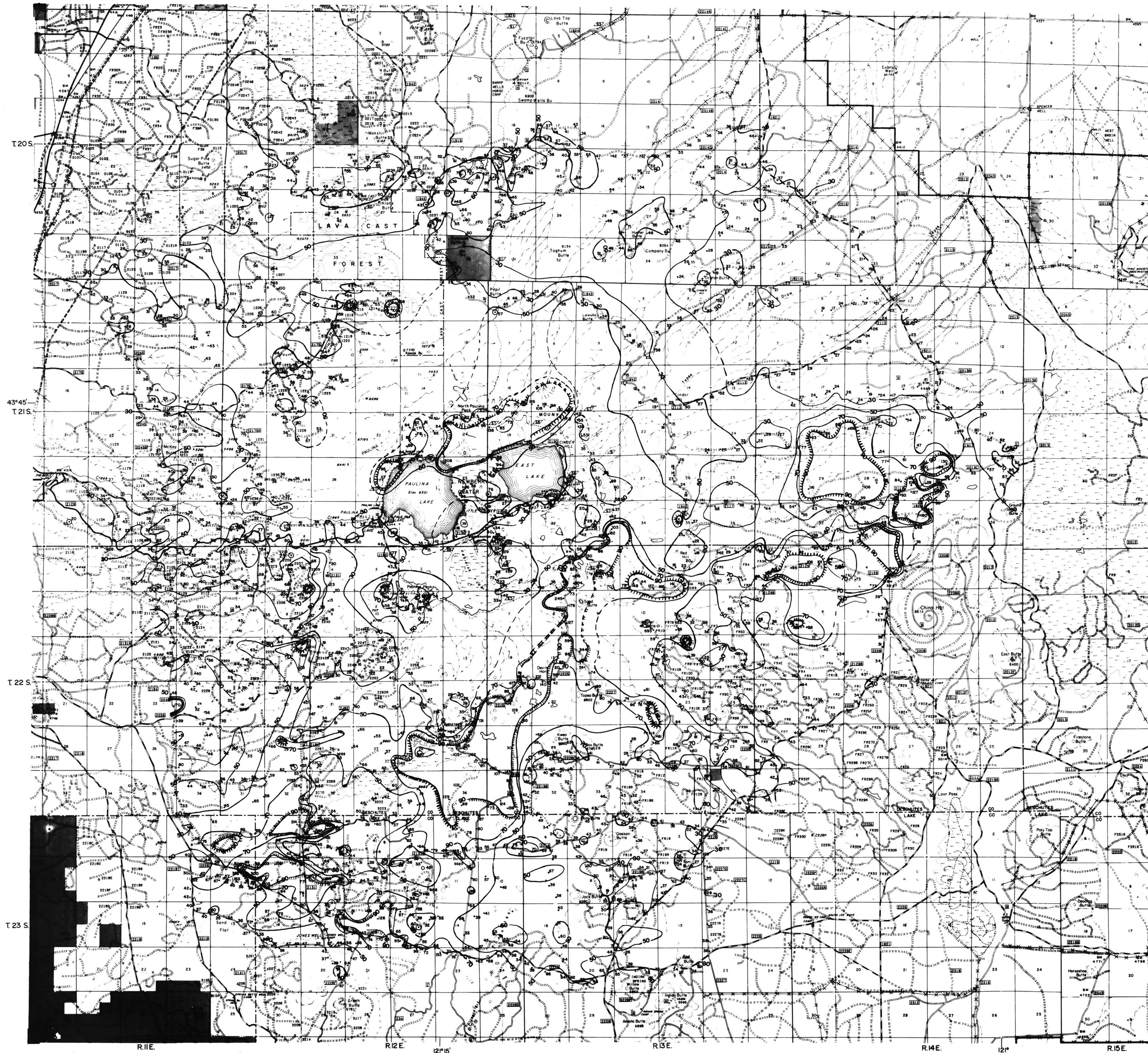
This work is preliminary and has not been edited or reviewed to conform with either the Oregon Department of Geology and Mineral Industries or the Bonneville Power Administration standards.

SCALE: 1"=1 MILE


N

The project was supported by funds from the
Bonneville Power Administration (Cooperative
Agreement No. DE-AC-79-BP36734)



EXPLANATION

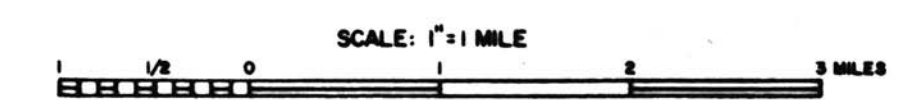
--- Iso-concentration contour line for Hg levels measured by the low-temperature volatilization technique utilizing the Jerome Gold Film Detector, Model 301. Contours are dashed where inferred.

--- 90 ppb contour line with hachures on the low-concentration side. Samples with levels above 90 ppb define a statistically anomalous population (see accompanying text).

• Sample point with Hg content in ppb.

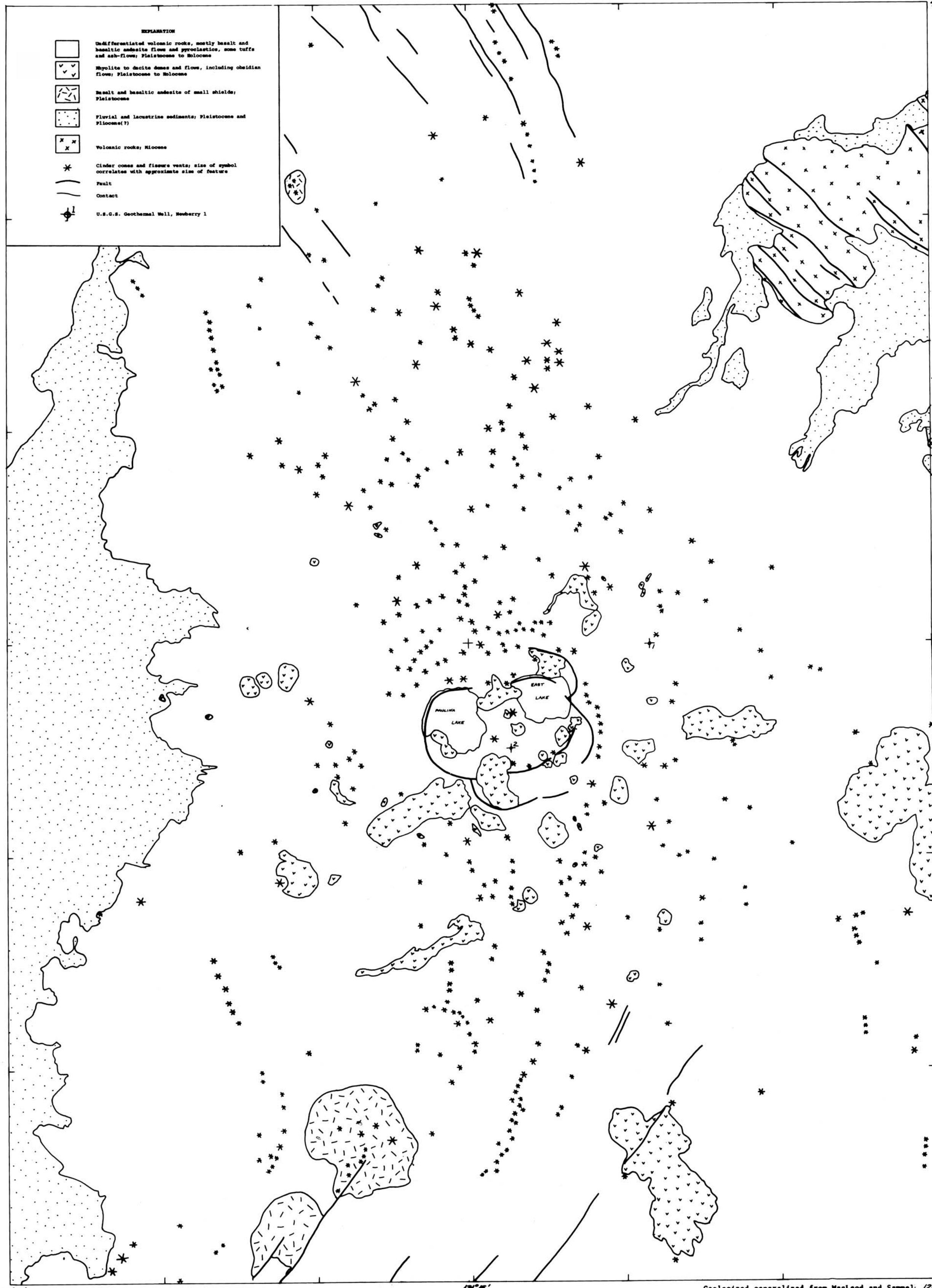
○ Test pit

Hg contour interval = 20 ppb



Disclaimer

This work is preliminary and has not been edited or reviewed to conform with either Oregon Department of Geology and Mineral Industries or Bonneville Power Administration standards.



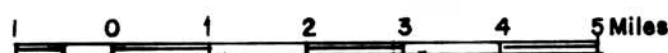
Disclaimer

This work is preliminary and has not been edited or reviewed to conform with either Oregon Department of Geology and Mineral Industries or Bonneville Power Administration standards.

Geologized generalized from MacLeod and Sammel, 12/00', 1982, and from MacLeod, Sherrod, and Chitwood, 1982



STATE OF OREGON
DEPARTMENT OF GEOLOGY AND MINERAL INDUSTRIES



0-83-3

SURVEY OF POTENTIAL GEOTHERMAL EXPLORATION SITES
AT NEWBERRY VOLCANO, DESCHUTES COUNTY, OREGON

By Priest and others

STATE OF OREGON
DEPARTMENT OF GEOLOGY AND MINERAL INDUSTRIES
DONALD A. HULL, STATE GEOLOGIST

COMPLETE BOUGUER GRAVITY ANOMALY MAP OF NEWBERRY VOLCANO, OREGON

121° 00' 44" 00" 1983

EXPLANATION

+ Gravity station

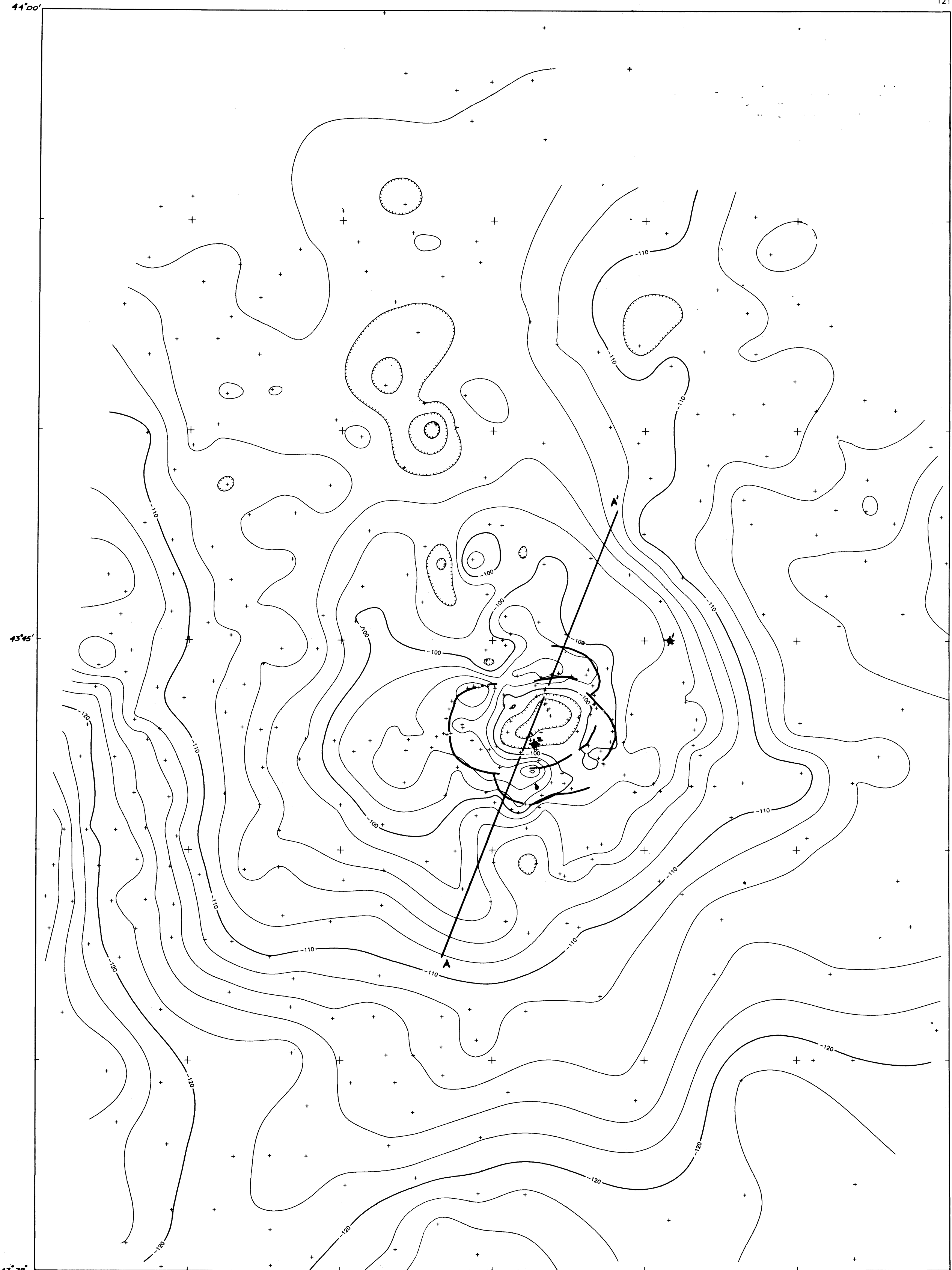
Contours of equal Bouguer gravity anomaly in milligals; hachures indicate closed lows; reduction density is 2.20 g/cm³. Contour interval 2 mgal

Inferred caldera ring fault (MacLeod and others, 1982)

U.S.G.S. geothermal well, Newberry 1

Disclaimer

This work is preliminary and has not been edited or reviewed to conform with either Oregon Department of Geology and Mineral Industries or Bonneville Power Administration standards.



43° 30' 121° 30'

121° 15'

121° 00'



Data collected by U.S. Geological Survey between 1965 and 1979

Map prepared by Andrew Griscom and Carter W. Roberts, U.S. Geological Survey, 1983

STATE OF OREGON
DEPARTMENT OF GEOLOGY AND MINERAL INDUSTRIES



LOCATION

STATE OF OREGON
DEPARTMENT OF GEOLOGY AND MINERAL INDUSTRIES
DONALD A. HULL, STATE GEOLOGIST

AEROMAGNETIC MAP OF NEWBERRY VOLCANO, OREGON

0-83-3
SURVEY OF POTENTIAL GEOTHERMAL EXPLORATION SITES
AT NEWBERRY VOLCANO, DESCHUTES COUNTY, OREGON

By Priest and others
1983

EXPLANATION


Inferred caldera ring fault
(MacLeod and others, 1982)


U.S.G.S. geothermal well,
Newberry 1

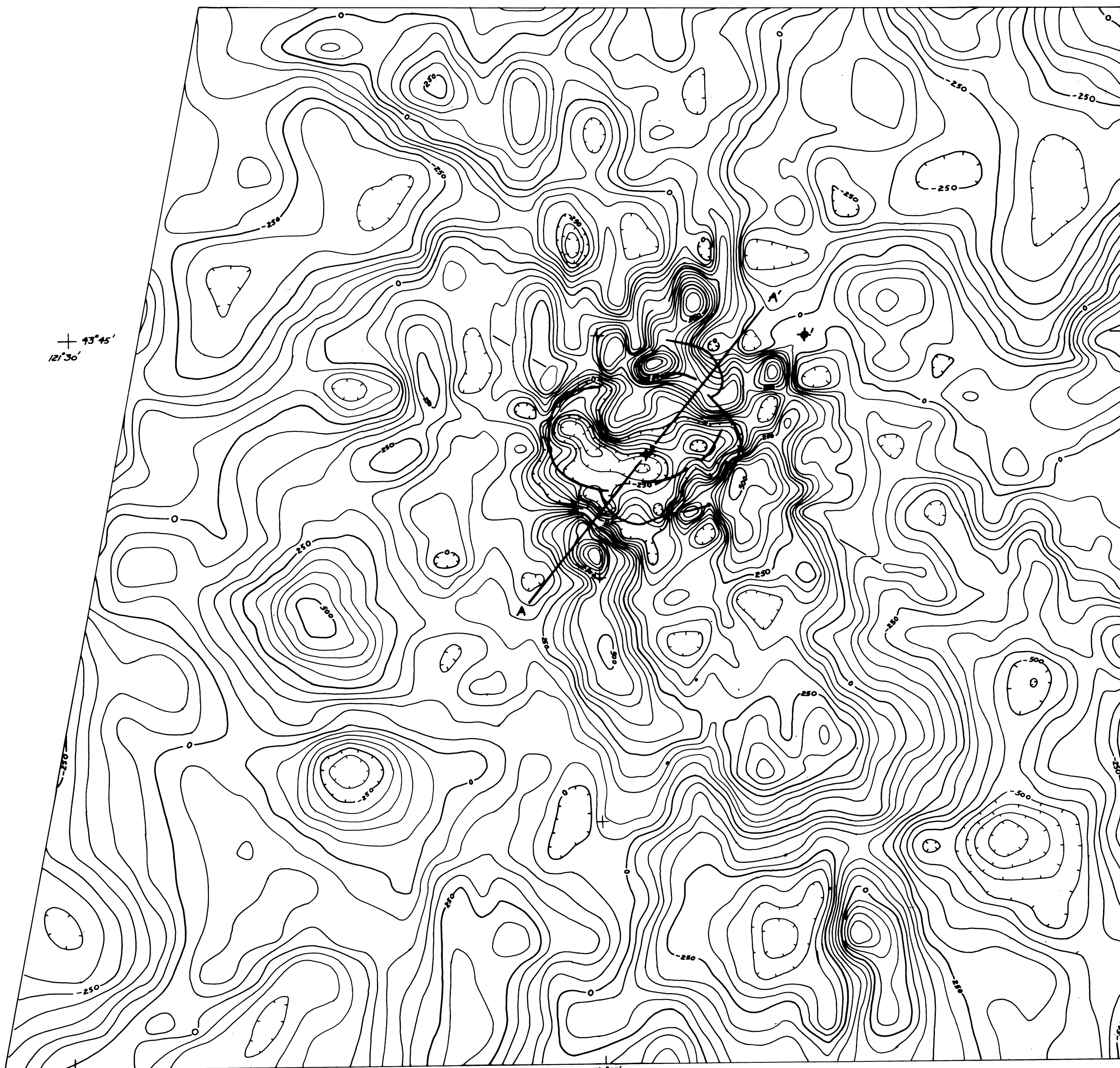


Magnetic contours
Showing residual total intensity magnetic
field of the earth (in gammas) at a flight
altitude of 8,000 ft. Contour interval is
50 and 250 gammas

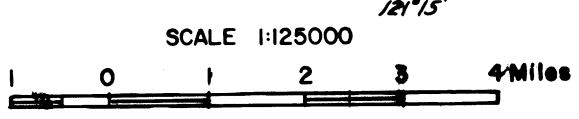
Flight lines are east-west and spaced
either 0.5 mi apart (between lat 43°38' N
and lat 43°45' N) or 1.0 mi apart (else-
where). Magnetic lows are hachured in the
closed contours

Disclaimer

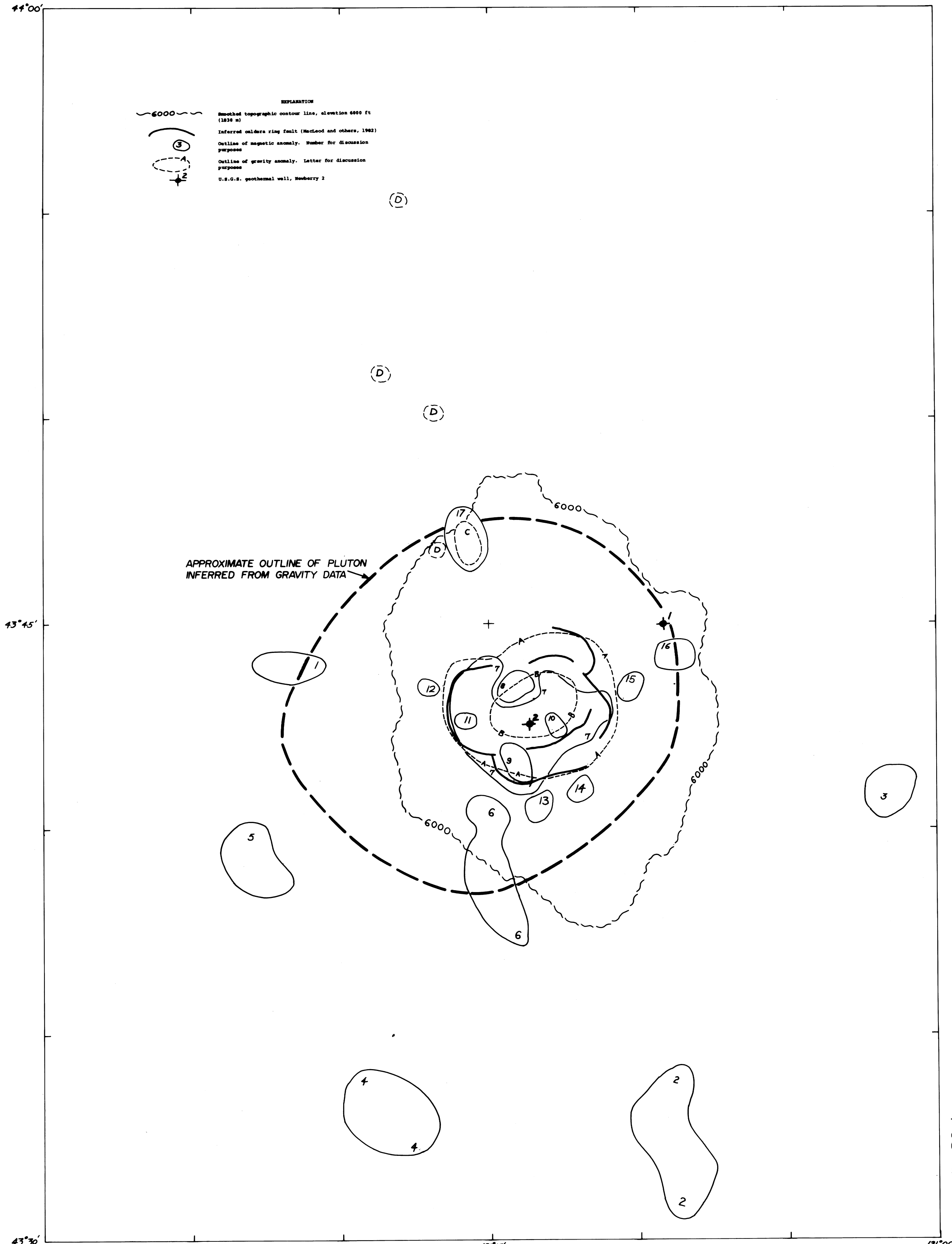
This work is preliminary and has not
been edited or reviewed to conform
with either Oregon Department of
Geology and Mineral Industries or
Bonneville Power Administration
standards.



43°45'
121°30'



Aeromagnetic intensity data flown by
Aerial Surveys, Salt Lake City, Utah,
in April 1975. Map generalized from
U.S. Geological Survey, 1979



EXPLANATION

6000 Smoothed topographic contour line, elevation 6000 ft (1830 m)

() Inferred caldera ring fault (MacLeod and others, 1982)

() Outline of magnetic anomaly. Number for discussion purposes

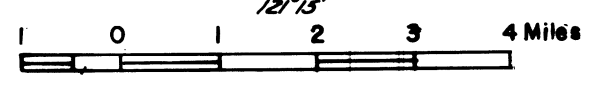
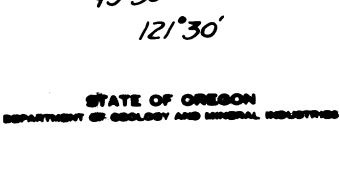
() Outline of gravity anomaly. Letter for discussion purposes

* U.S.G.S. geothermal well, Newberry 2

APPROXIMATE OUTLINE OF PLUTON INFERRED FROM GRAVITY DATA

Disclaimer

This work is preliminary and has not been edited or reviewed to conform with either Oregon Department of Geology and Mineral Industries or Bonneville Power Administration standards.



Map prepared by Andrew Griscom,
U.S. Geological Survey, 1983

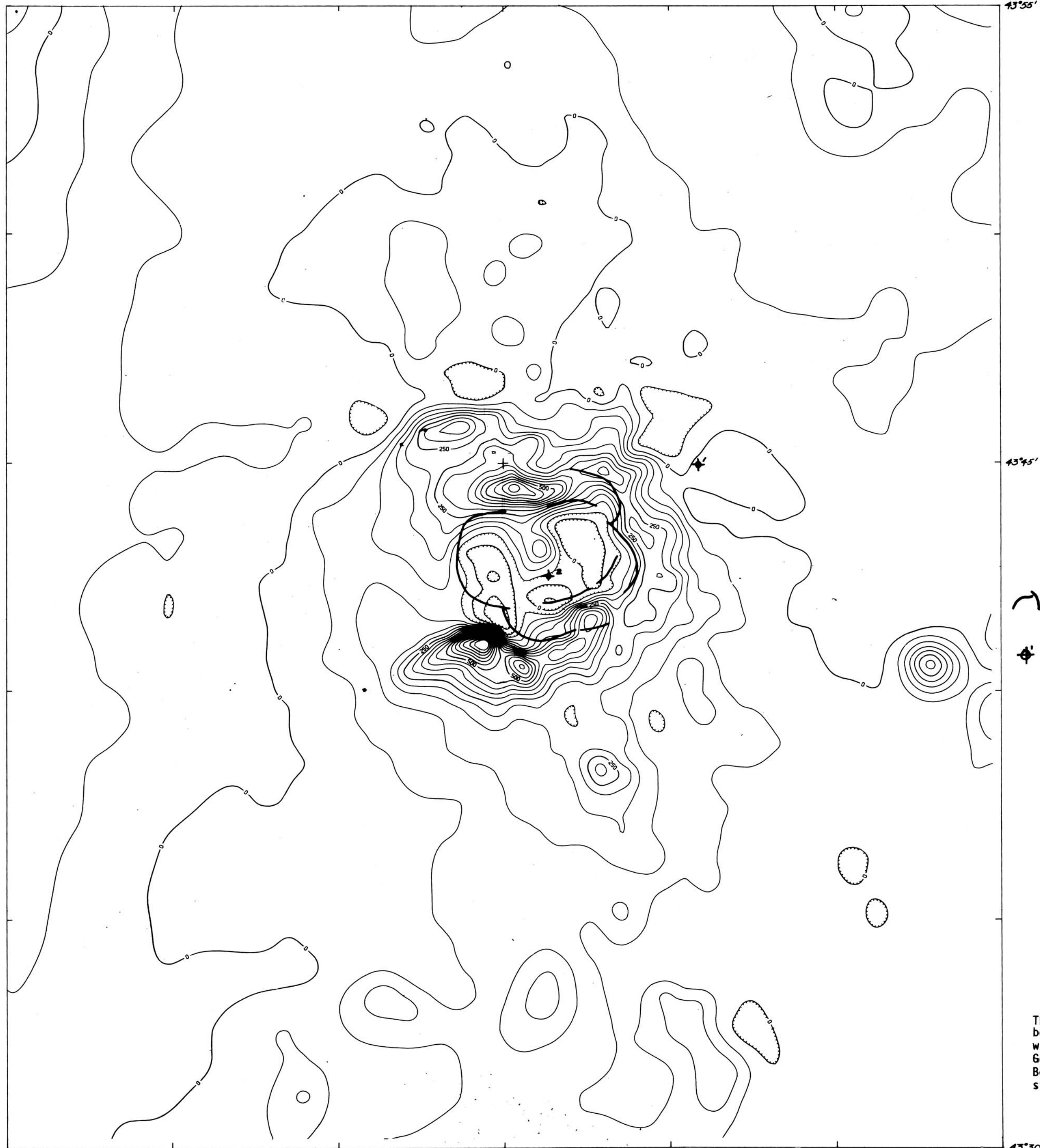
PLATE VII

STATE OF OREGON
DEPARTMENT OF GEOLOGY AND MINERAL INDUSTRIES
DONALD A. HULL, STATE GEOLOGIST

CALCULATED MAGNETIC MAP OF DIGITAL TOPOGRAPHIC MODEL OF NEWBERRY VOLCANO, OREGON

0-83-3
SURVEY OF POTENTIAL GEOTHERMAL EXPLORATION SITES
AT NEWBERRY VOLCANO, DESCHUTES COUNTY, OREGON

By Priest and others
1983



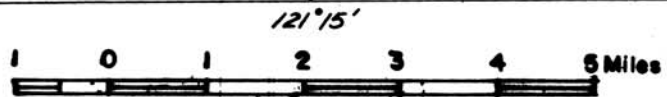
EXPLANATION

-  Inferred caldera ring fault (MacLeod and others, 1982)
-  U.S.G.S. geothermal well, Newberry 1

Disclaimer

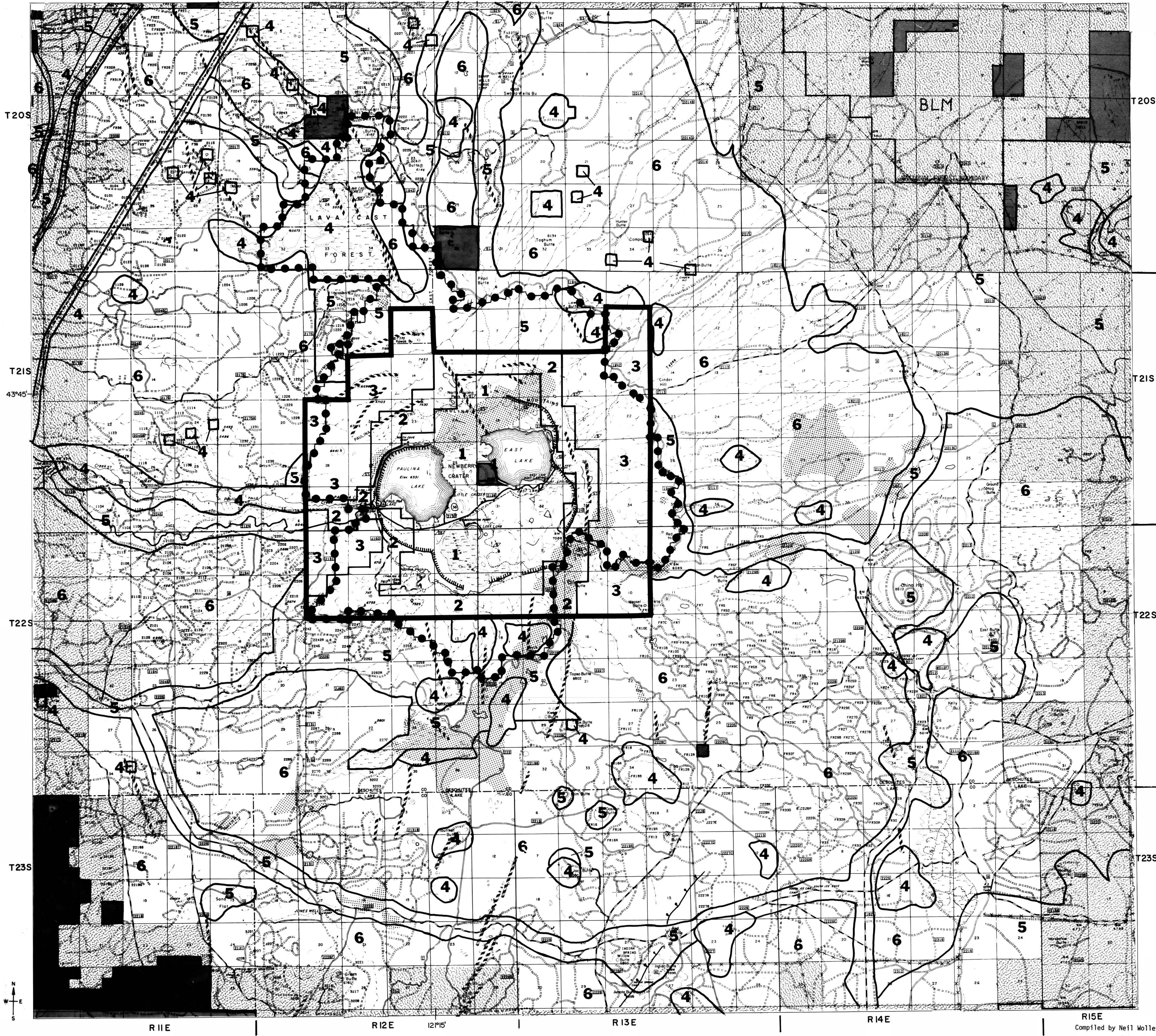
This work is preliminary and has not been edited or reviewed to conform with either Oregon Department of Geology and Mineral Industries or Bonneville Power Administration standards.

STATE OF OREGON
DEPARTMENT OF GEOLOGY AND MINERAL INDUSTRIES



Map prepared by Carter M. Roberts,
U.S. Geological Survey, 1981

Digitization interval 4 minute
Contour interval 50 gamma
Magnetization 3.004 emu/cm³



EXPLANATION

- Newberry Caldera Known Geothermal Resource Area
- Area considered unsuitable for the siting of geothermal power plants by the Energy Facility Siting Council (EFSC)

Zones defined and delineated by the Deschutes National Forest Land and Resource Plan (proposed), and Land and Resource Plan Environmental Impact Statement (draft) for the Newberry Caldera Known Geothermal Resource Area:

- 1 Area within the crater with high visual and recreational values. No leasing or surface occupancy would be allowed under the proposed plan. Exploratory drilling would be allowed on a case by case basis.
- 2 Area consisting of the rim of the crater, the main road into the crater, and Paulina Creek. This area has high recreational value. Visual quality is also considered important. Leasing would be allowed but surface occupancy will be restricted under the proposed plan. Exploratory drilling would be allowed on a case by case basis.
- 3 Area within the KGRA but outside the crater. Visual resources are important but other resources are not as sensitive or critical. Both leasing and surface occupancy would be allowed under the proposed plan.

Zones defined and delineated by the Deschutes National Forest Noncompetitive Geothermal Leasing Environmental Assessment report (1982) for Newberry Volcano, exclusive of the Known Geothermal Resource Area:

- 4 Areas in which leasing will be allowed but surface occupancy will be restricted. These areas include the following: geologic interest areas, research natural areas, special use permit areas, administrative sites, developed recreation areas, critical wildlife habitat, Paulina Creek Management Zone, old growth management areas, cinder buttes and unstable soil areas.
- 5 Areas in which visual and game species management concerns will be considered in determining leasing policies. Additional regulations, stipulations, environmental analyses and approval of plans and operations will be utilized by the government to control leasing activities.
- 6 Areas in which standard leasing procedures will be used.

- Public lands outside of the Newberry KGRA for which no lease applications have yet been filed (source: Dolores Yates Greater Columbia Energy Inc.)
- Privately owned land
- Mercury anomaly (greater than 90 ppb)
- Fissure (source: MacLeod and others, 1982)
- Fault, ball and bar on downthrown side (source: MacLeod and others, 1982)
- Ring fault (hachures on downthrown side)(source: MacLeod and others, 1982)



Disclaimer

This work is preliminary and has not been edited or reviewed to conform with either Oregon Department of Geology and Mineral Industries or Bonneville Power Administration standards.